SPAWAR
Systems Center
San Diego

TECHNICAL DOCUMENT 3124
September 2001

Electrode and Electric Field Sensor Evaluation

Applied Physics Laboratory,
University of Washington

Science Applications International
Corporation

SSC San Diego

TECHNICAL DOCUMENT 3124
September 2001

Electrode and Electric Field Sensor Evaluation

Applied Physics Laboratory,
University of Washington

Science Applications International
Corporation

SSC San Diego
San Diego, CA 92152-5001

SSC SAN DIEGO
San Diego, California 92152-5001

E. L. Valdes, CAPT, USN
Commanding Officer

R. C. Kolb
Executive Director

ADMINISTRATIVE INFORMATION

This report was prepared by Applied Physics Laboratory, The University of Washington for Space and Naval Warfare Systems Center, San Diego (SSC San Diego), under CDRL A0001BA, Delivery Order 33 Contract No. N66001-92-D0004.

Released by
M. J. Hoernemann, Head
Operations Office

Under authority of
G. L. Davis , Head
Maritime Surveillance
Division

LH

TABLE OF CONTENTS

1. EXECUTIVE SUMMARY

Self-noise was measured for a sample of silver-silver chloride (Ag-AgCl) electrodes and electric field sensors commonly used in ocean electric field measurements. First, electrodes from the Naval Surface Warfare Center (NSWC), Science Applications International, Inc. (SAIC), and the Applied Physics Laboratory of the University of Washington (APL-UW) were evaluated in a constant temperature bath operated at 4°C, 10°C, 15°C, and while drifting in temperature between 17 and 19°C. Second, pairs of electrodes, configured to measure a voltage difference in sea water between two spaced points attached to low-noise amplifiers, were evaluated in a large sea water filled tank over a period of more than 30 days. While the SAIC and NSWC systems provided their own preamplifier, the APL system used a commercial preamplifier, the Keithley 1801.

Over the entire measurement bandwidth from 1 mHz to 1 kHz, the SAIC electrodes exhibited the lowest noise performance. Above 10 mHz, SAIC electrode measurements show only measurement noise, about 2 $nV/\sqrt{Hz}$. The APL electrodes reach the noise floor at 40 mHz and 2 $nV/\sqrt{Hz}$. At frequencies higher than 40 mHz, the SAIC and APL electrodes dropped into the measurement noise of about 1.8 $nV/\sqrt{Hz}$ in the low-frequency band and 2 to 2.5 $nV/\sqrt{Hz}$ in the high-frequency band. The NSWC electrodes are much noisier than the SAIC and APL electrodes below 1 Hz, especially at frequencies less than 100 mHz, but achieve a noise level of 3 $nV/\sqrt{Hz}$ above 1 Hz. The higher noise floor of the NSWC electrodes is probably because of their higher resistances.

The relative performances of the sensors and systems depend on frequency. Over some frequency band, each unit showed superior performance. For example, the SAIC system is better than the APL sensors with the Keithley amplifier for frequencies below 10 mHz. Above 1 Hz, and between the spurious response frequency lines (spurs), the APL system with the Keithley 1801 preamplifier is quieter than the SAIC system. As expected from the electrode tests, NSWC system is much noisier than the SAIC and APL systems below 1 Hz, but it equals the performance of the SAIC system from 1 Hz to about 50 Hz. In this band, the spurious tones produced by the SAIC and Keithley amplifiers are very noticeable, while there the NSWC system provides the best overall performance.

One of the principal conclusions of the electrode tests is that the inherent noise of some electrode pairs is not much greater than the noise of the measurement system. Only at frequencies less than 10 mHz do the best of the electrode pairs exhibit noise significantly greater than expected for their equivalent resistances plus system contributions. This means that electric field performance is not limited by noise processes that are inherent to these Ag-AgCl electrodes, such as random electrochemical reactions, but is controlled mostly by random Johnson noise, deterministic temperature and salinity variations at the electrodes, interference from external EM fields (EMI), and amplifier noise (current and voltage noise). No significant changes in electrode noise were observed as a function of bath temperature, but self-noise did decrease with electrode aging.

2. INTRODUCTION

The measurement of ocean electric fields depends on electrodes to interface electronics to sea water and amplifiers to boost the weak signals to useful levels. An electric field sensor consists of a pair of electrodes in an enclosure such that the potential differences between two points in the ocean can be sensed and amplified. Each aspect of the implementation of ocean electric field sensing requires scrutiny to be sure that electrodes and amplifiers are providing the optimum performance.

There are a variety of internal and external noise sources which can often dominate the measurement and interpretation of ocean electric fields. External sources include signals arising from ionospheric influences, motional induction in ocean currents and waves, man-made sources (e.g., 60 Hz power and vessel fields), and geological and biological sources. Internal sources include contributions, often large, from electrode and amplifier noise sources, and consequences of the measurement implementation. Electrode noise can be caused by random influences, such as Johnson noise (also known as thermal noise), and by more deterministic causes, such as temperature and salinity variations between electrodes. Other sources include motionally induced voltages resulting from vibration and motion of the sensor. Amplifier noise sources include thermal and electronic noises in the low-level stages (e.g., preamplifiers) and interference from external sources, such as EMI (Electro-Magnetic Interference), and internal sources, such as switching noise from power regulators.

In order to understand better the performance of certain commonly used electrodes and amplifiers, an evaluation project was undertaken. The objectives of the project were to establish the inherent noise of electrodes at various temperatures with a minimum of amplifier-caused noise and to establish the performances of several electric field sensors and amplifiers.

The electrode and electric field sensor evaluations were undertaken at APL-UW because of its extensive experience and instrumentation in low-noise measurements and ocean electric field observations. In particular, a suite of computer-controlled signal sources and measurement instruments were available for operation using dedicated computers operating with automated measurement software. Specialized environmental control facilities, such as a constant temperature bath and a large salt water tank (in which variable ambient electric fields could be impressed), were available.

The work consisted of evaluations of electrodes in a constant temperature bath, where thermal effects on electrodes were reduced, and of electric field sensors in a large tank, where thermal and salinity effects were larger and external signals could be applied to verify system operation.

In the constant temperature bath, the self-noise was measured of three groups of four electrodes each from the Naval Surface Warfare Center, Science Applications International, Inc., and the Applied Physics Laboratory of the University of Washington (hereafter known as NSWC, SAIC, and APL, respectively). For comparison, a group of four resistors of different values were measured. The electrodes were immersed in salt

water inside sealed jars, while the resistors were inside the same type of jars with no water. The jars were put under the surface of the fresh water in the stirred bath. The measurements were taken at four different temperatures, 4, 10, and 15°C, and one that drifted from 17 to 19°C in two days with the bath controller turned off. Two overlapping frequency ranges were used, a low-frequency (LF) band spanning the range 1 mHz to 0.7 Hz and a high-frequency (HF) one spanning 0.15 Hz to 1 kHz.

These tests were followed by a month-long series of measurements of electric field sensors and, where appropriate, low-noise amplifiers. Two electric field sensors had amplifiers (NSWC and SAIC). The APL-UW sensor did not have a low-noise amplifier and was observed using a commercial amplifier. It was intended that use of the commercial amplifier would provide a commonly available standard for comparison of the custom system and any future evaluations.

This report discusses the constant temperature bath and salt water tank measurements and interpretations. The next section is a discussion of the methods, including the performance of measurement instrumentation and the physical and electronic arrangements of equipment. This section includes a discussion of spectral methods. The next section presents a summary of the measurements and a commentary about what was done and why. Section 7 is a summary of results and conclusions. Appendices are used to provide records of the original observations and selected spectra.

3. ELECTRODE TEST SETUP

Three different types of electrode assemblies were tested in a constant temperature bath. SAIC provided electrodes as manufactured by Subspection, Ltd. They were removed from their normal underwater sensor housing and repackaged in amber glass bottles. The electrodes were left in their small PVC mounting block and electrode housing. New heavy-gauge insulated copper wires were attached to the electrodes, and a waterproof seal was provided at the exit of the wires from the jar. Figure 3.1 shows the SAIC electrode assembly.

NSWC provided Ag-AgCl electrodes manufactured by In Vivo Metric Systems. These electrodes were IVM type E211-X having a diameter of about 8 mm and a thickness of 1 mm. NSWC constructed a custom assembly which held the electrode as well as lagging material to buffer the electrode from temperature and salinity variations. Figure 3.2 shows the NSWC electrode assembly. The lagging consists of five layers of fiberglass cloth held in place by a perforated disk of printed circuit board material.

APL-UW provided electrodes of their own manufacture. They are a thermally fired type of Ag-AgCl electrode having a diameter of 12 mm and a thickness of 4 mm. Pure silver wire (1/32" diameter) is embedded in the Ag-AgCl matrix and provides the electrical connection between the electrode material and the copper wires leading to the measurement equipment. Figure 3.3 shows the APL-UW electric field sensor assembly.

SAIC Electrodes

The SAIC electrodes were provided already sealed in amber glass jars approximately 3 inches in diameter by 6.5 inches tall. The jars were provided with a metal screw cap which had been sealed and waterproofed by SAIC. Large, #16 AWG, plastic-insulated twisted stranded copper wires without shielding were used to bring the electrode signals out of the jar. A hole cut in the metal screw lid provided the exit for the wires and was sealed with a generous layer of silicone RTV adhesive sealant. The electrodes were operated in a 35 ppt (parts per thousand) solution of pure NaCl and deionized water. The wires provided by SAIC were long enough to reach from the isothermal bath to the input multiplexer, so no extensions were required.

NSWC Electrodes

The NSWC electrode assemblies were placed in clear glass 16 oz. laboratory specimen jars. The original pairing of the electrodes was retained. The NSWC electrodes came preassembled with a neoprene-jacketed cable. The electrodes were hung from their cables which passed through the lid and were glued to it. The hanging electrodes were spaced so that they were nearly touching the bottom of the jar. The electrodes were spaced apart from each other about 1.5 inches.

The NSWC jars were three quarters filled with approximately 35 ppt synthetic sea water. This "sea water" was made using 820.2 g "Sea Salt" from Lake Products Co. and 19.06 liters of distilled water.

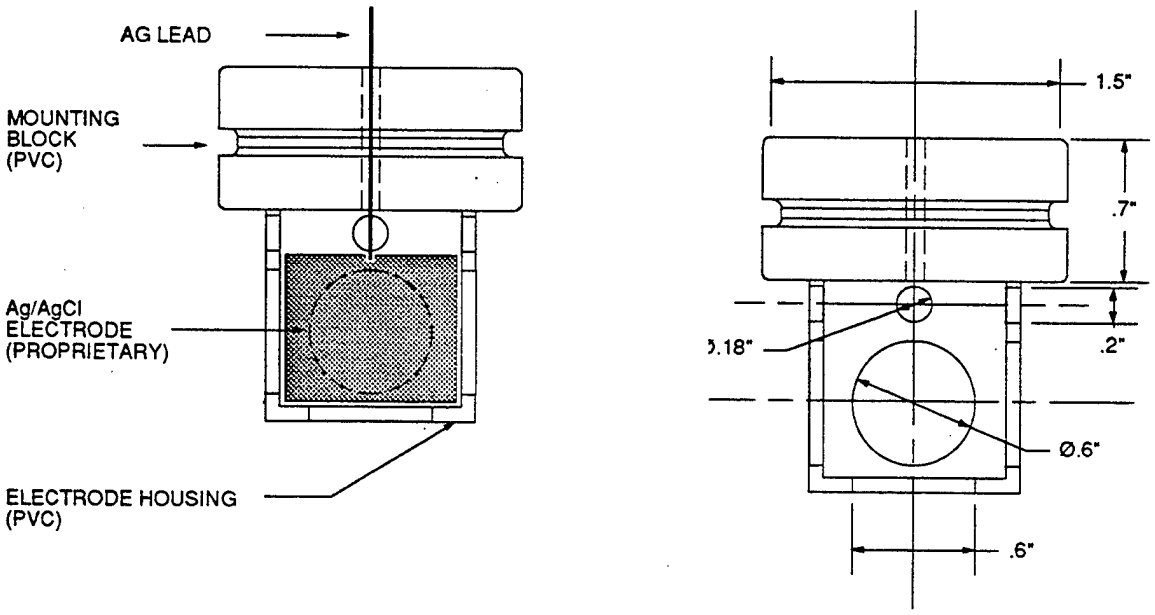

Figure 3.1 Electrode assemblies used by SAIC for the constant temperature bath tests. Two assemblies were used in each amber jar and operated in pure 35 ppt NaCl and water solution.

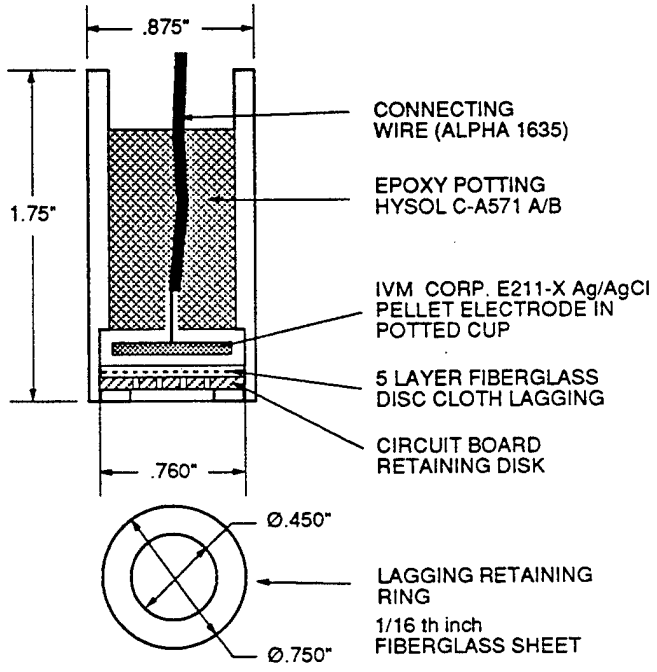

Figure 3.2 NSWC electrode assembly construction details. Lagging is a thermal insulation barrier applied to improve low frequency performance.

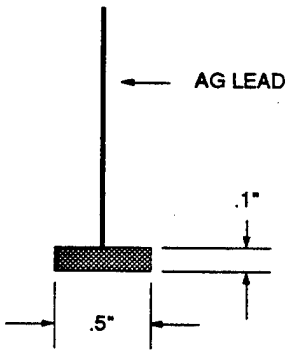

Figure 3.3 APL-UW electrode assembly construction details.

APL-UW Electrodes

The electrodes were paired, and the self-potentials for these pairs were measured over a several week period prior to being installed in the bath. The APL-UW electrodes were placed in clear 16 oz. glass laboratory specimen jars. The jars for the APL electrodes were filled about three-quarters full with synthetic sea water. The synthetic sea water was taken from the same batch described in the NSWC electrode section.

The electrodes were hung from their silver wires which passed through the lid. The hanging electrodes were spaced so that they were about 1 inch above the bottom of the jar. The electrodes were spaced apart from each other about 1.5 inches.

For both the NSWC and APL-UW electrode jars, the plastic lids were sealed to prevent intrusion of fresh water from the isothermal bath.

Isothermal Bath and Controller

The isothermal bath has an insulated container of fresh water that is temperature controlled. The candidate electrodes were enclosed in salt-water-filled containers immersed in the bath water. It was hoped that the constant temperatures would minimize temperature-induced electrode noise. This was not quite the case. When the bath controller was turned off, the electrode noise at frequencies less than 10 mHz was reduced.

A constant temperature test facility was constructed utilizing a stirred water bath with internal dimensions of 29 inches in diameter by 31 inches in height. A heat exchanger coil was located concentrically with and adjacent to the inner wall of the bath. Automotive antifreeze was circulated through the heat exchanger coil and a bath temperature controller unit which was previously constructed and used at APL-UW for instrument calibrations. A refrigeration unit constantly cooled the circulating fluid. Two electrical heating elements totaling 1.5 kW were driven by a commercial bath controller unit. These heaters opposed the cooling unit to provide a constant temperature.

Figure 3.4 shows the layout of the constant temperature facility. A set of electromagnet coils surrounded the constant temperature bath and were used to provide small test signals to all data channels via electromagnetic induction. The top of the bath was thermally insulated from the room air with a 3-inch layer of rigid foam insulation. Small openings for the electrode cabling were provided at the outer edge of the rigid foam lid. A rack with receptacles for 16 oz. glass laboratory specimen jars was provided in the bath at a level which allowed the jars to be submerged with about 4 inches of water above them. The bath temperature was measured with a SeaBird Electronics electronic thermometer. Figure 3.5 is a view into the bath from the top showing the rack and electrode jars.

Scanner, Amplifier, Voltmeter

A block diagram of the electronic test setup for electrode testing in the isothermal bath is shown in Figure 3.6. A 16-channel scanner (Keithley 705) alternately connected sources to a low-noise preamplifier (Keithley 1801) which was attached to a digital voltmeter (Keithley 2001). A total of 16 pairs of electrodes could thus be accommodated. Several of the channels were dedicated to monitoring the performance of the

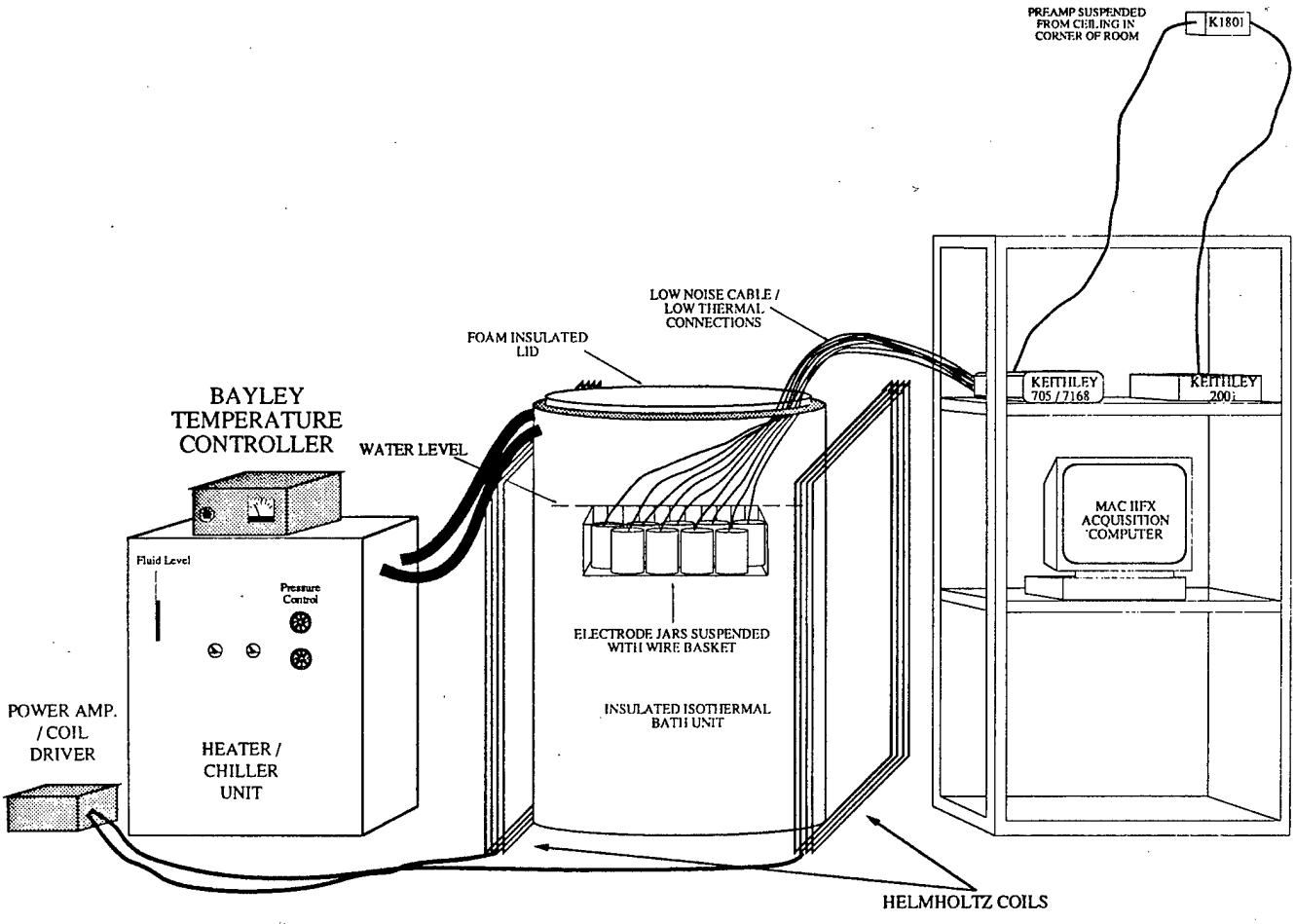

Figure 3.4 Layout of the isothermal bath and electrode test setup. The Helmholtz coils were periodically energized with a 1 Hz signal to provide small induced voltages used to verify proper system operation. The bath remained stable to within ±2 m°C.

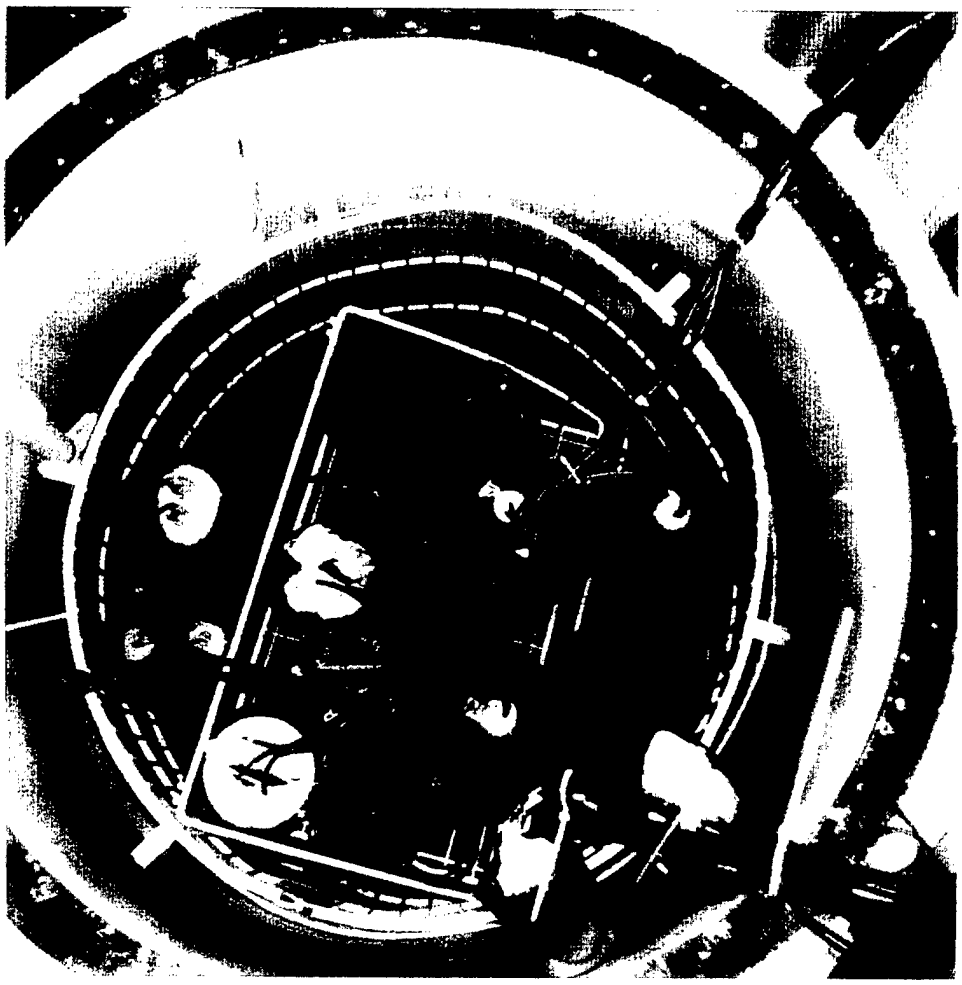

Figure 3.5 View into top of constant temperature bath. SAIC electrode assemblies have heavy gauge twisted pair wires which exit the tank to the upper right. The NSWC and APL-UW electrode are in jars that have low noise cables bundled together and exit to the lower right. The small cylindrical object at the left against the wire basket is the platinum RTD used by the bath controller to monitor the bath temperature.

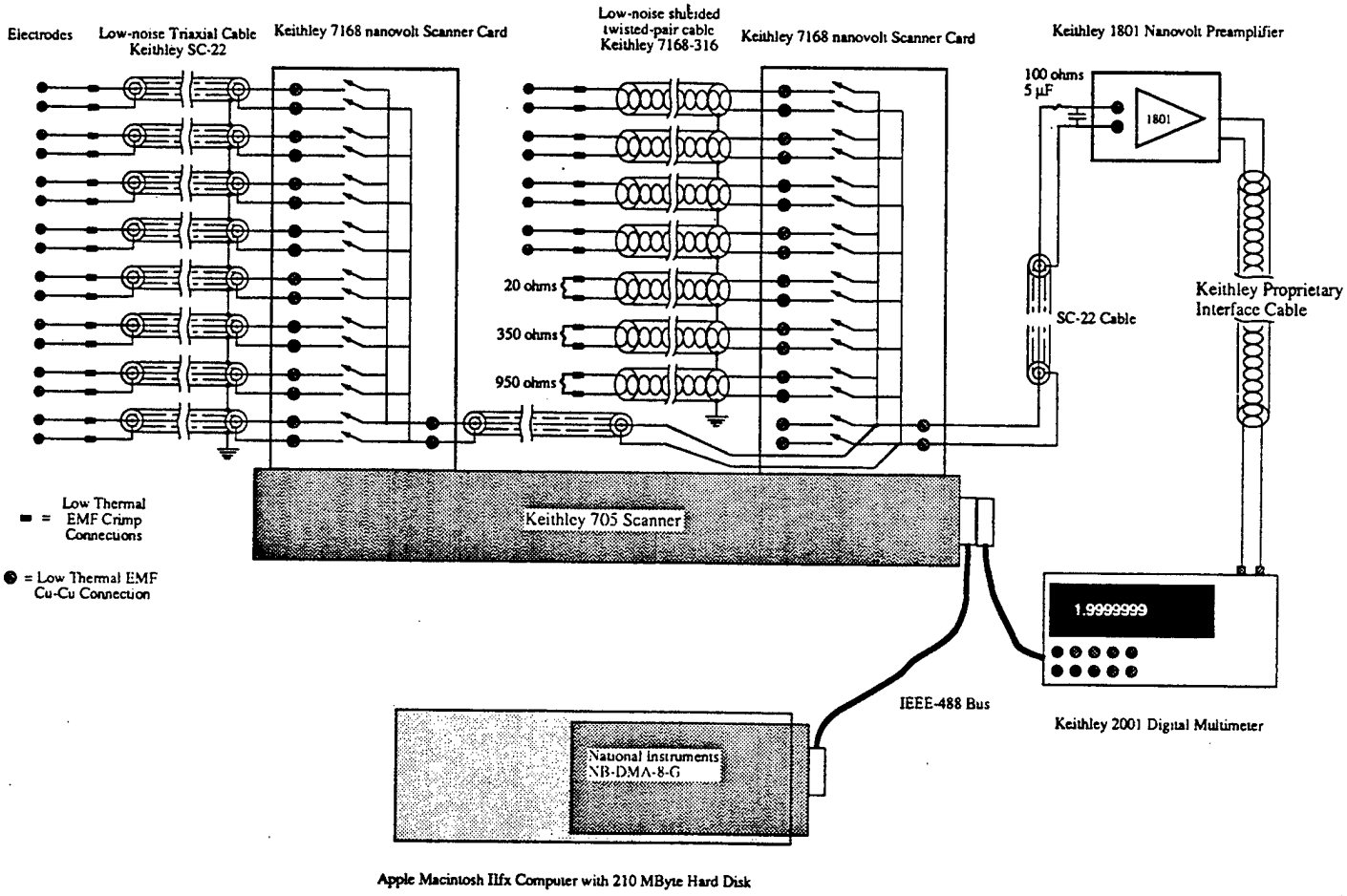

Figure 3.6 Schematic representation of electrical wiring for isothermal bath tests of electrodes. The digital data from the 2001 DMM was logged by an Apple Macintosh IIfx computer. The Macintosh IIfx computer utilized an NB-DMA-8-G interface board from National Instruments for communications with the Keithley 2001 digital multimeter.

scanner switches and the low-noise amplifier and were not connected to electrode pairs.

Low-noise, Vishay Inc. precision metal film resistors were used to quantify the instrumentation noise. As the resistor values are increased the noise increases. This is a direct result of Johnson noise, the theoretical thermal noise. The root mean square (rms) noise voltage of a resistor, V_n, is

$$V_n = (4\,k\,T\,R\,B)^{-0.5}\ ,$$

where k is Boltzmann's constant ($1.38\times10^{-23}\ J\ K^{-1}$), T is absolute temperature (K), R is resistance (Ω), and B is bandwidth (Hz). For a resistor of 120 Ω at 300 K, the Johnson noise is 1.4 nV/$\sqrt{\text{Hz}}$ for a 1-Hz bandwidth. Figure 3.7 shows the Johnson noise for a 1-Hz bandwidth as a function of resistance along with K-1801 specifications and some measured data.

We estimate our instrumentation noise to be about 2 nV/$\sqrt{\text{Hz}}$ for electrode resistances of about 20 Ω and about 3 nV/$\sqrt{\text{Hz}}$ for electrode resistances of about 200 Ω. (This is higher than Figure 3.7 would indicate because of a 100 Ω filter resistor in series.)

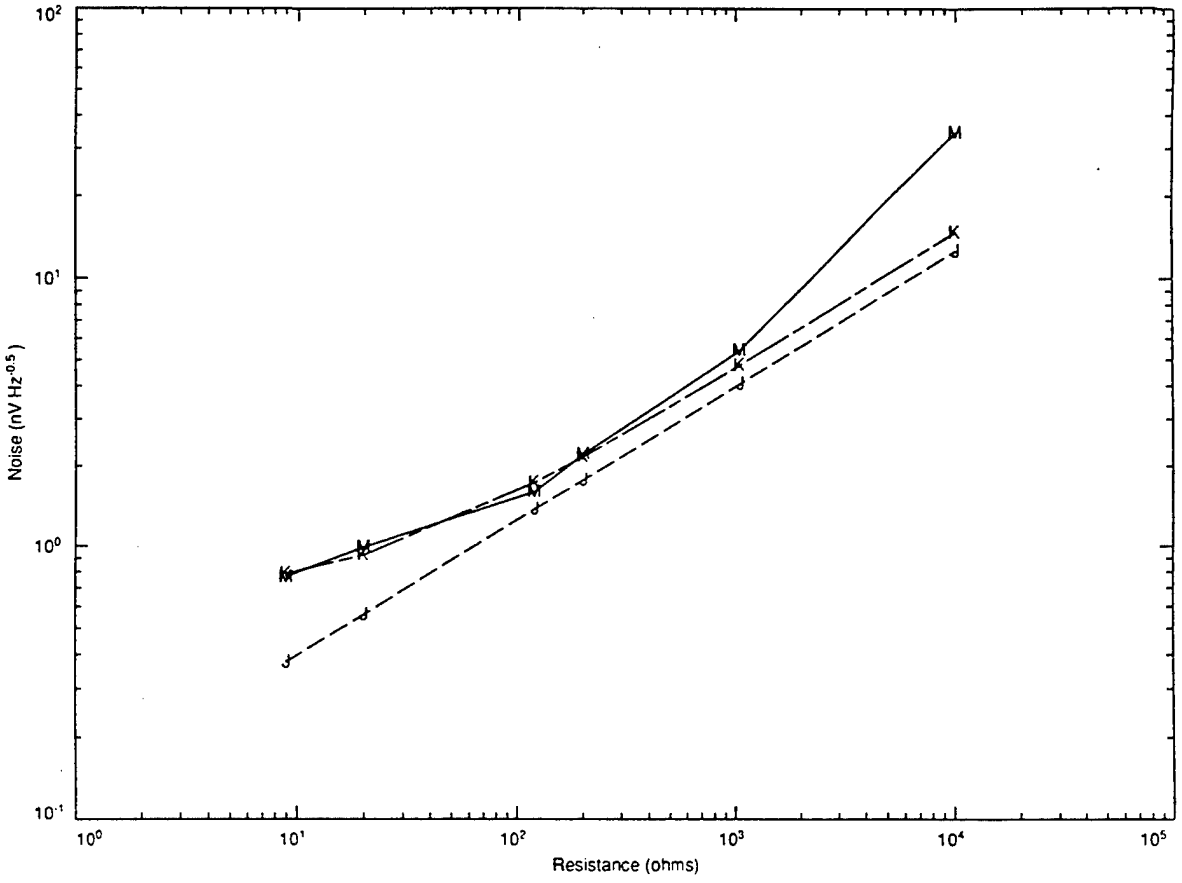

Figure 3.7 The root mean square noise voltage of a resistor increases as the square root of its resistance. The three graphs shown indicate the square root of the variance density for theoretical Johnson noise (J), the Keithley 1801 preamp specification (K), and the measured value of the preamp (M).

Computer and Peripherals

The voltage and temperature readings were transferred to an Apple Macintosh IIfx computer via an IEEE-488 (GPIB, General Purpose Interface Bus) connection. The Keithley 2001 voltmeter provides its own built-in IEEE-488 interface, and the Macintosh was provided with a National Instruments NB-GPIB interface board. The Macintosh IIfx was configured with 16 MB of RAM, a 210 MB hard disk, and Operating System 7.0 as well as LabVIEW 3.0.1. The Macintosh included a 16-inch color monitor which provided a real-time display of the acquired data. The Macintosh was also equipped with an IEEE 802.3 LAN (local area network) connection so that data could be transferred via FTP (Internet File Transfer Protocol) to an HP-9000 model 385 computer system running HP-UX, HP's Unix, where further data analysis was performed. The data were stored temporarily on the 210 MB hard disk attached to the Macintosh and archived on writable magneto-optical 650 Mbyte disks mounted on the HP-9000 system.

Data Acquisition Software

The LabVIEW programming language was used to construct the data acquisition and display program which was resident on the Macintosh computer. LabVIEW is a programming environment based on visual cues and icons. It is highly integrated with interface boards for instruments that have an IEEE-488 bus interface.

The acquisition program provided three main functions. First, the program used the IEEE-488 bus to control and read data from the measurement instrumentation. Second, the program displayed the data with appropriate scaling on the color monitor just after they had been acquired. Third, the data were written to a hard disk for access by the HP computer.

LabVIEW provided a number of color chart types and we have chosen to use a "strip chart" type to display the data. As the main loop cycled around to other scanner channels, the data from each was overlaid onto the same strip chart. This overlaying allowed for a rapid comparison of the various electrode pairs in real time.

Three basic sampling programs were used: low frequency (LF), medium frequency (MF), and high frequency (HF). The "LF" program was for monitoring all the electrode pairs for reasonable behavior. It sampled too slowly for low-noise spectra, however. The "MF" program was used for collecting data specifically for determining the 1 mHz to 1 Hz section of the spectrum. The "HF" program was used specifically for determining the 1 Hz to 1 kHz section of the spectrum.

The low-frequency program sampled each electrode pair in turn 10 times in 5 seconds and repeated this every 2 minutes. The long interval was to allow time to sample all the other electrode pairs and temperature, write these data to the disk, and update the graph.

The medium-frequency program sampled 7200 measurements about every 0.5 second from each scanner channel for about an hour. All 16 channels on the scanner were used. Thus, every 16 hours another 1-hour segment of data was obtained for any

particular channel. The K-1801 preamplifier filter was set to roll off at 3.2 Hz. The K-2001 averaged for 0.5 second. In order to increase the sample rate, and thus decrease the spectral noise, every data point was not plotted on the screen; only the last value of each hour is displayed. Thus this program is not good for monitoring the data in real time. It is used after watching the data with the "LF" or "LFF" (a faster version of LF) or "NS" (no scanner) programs to see that the systems are all working properly.

For the 1 Hz to 1 kHz band spectra, data were sampled at 2 kHz for about 15 seconds. This was repeated five times at 2-minute intervals to allow spectra to be averaged. The maximum allowable number of measurements, 29500, were stored in the K-2001 and downloaded to the Mac after the sampling was complete. The "HF" program was used for this.

Data were transferred via the LAN to a Unix work station for processing.

4. ELECTRODE TEST MEASUREMENTS AND RESULTS

This section describes the equipment, procedures, measurements, and results of the electrode noise tests.

Constant Temperature Bath

The measured temperature was constant within 2 m°C with the controller operating. Occasionally we turned off the controller for lowest noise tests. There are two aspects to the noise. One is that the spectrum of temperature while the bath is slowly drifting with the controller off is lower in much of the frequency range of interest. The other noise is electrical from the heater controller. It uses SCRs (silicon-controlled rectifiers) which are electrically noisy devices.

The temperature controller was turned off for the high-frequency runs to eliminate the noise from the SCRs. The high-frequency runs took a couple of hours, during which time the bath warmed slightly.

Low-Frequency Keithley 2001 and 1801 Validation

Performance and validation tests were conducted on the instrumentation. Some tests involved a single piece of equipment while others tested combinations. In addition, the most extensive test was performed nearly continuously: namely, measurements of resistors which were installed as much like electrodes as possible to be able to separate electrode noise from other environmental and instrumentation noise. Any extraneous signals that could get onto the cables from the electrodes would also get onto the resistor cables.

The Keithley 2001 voltmeter in combination with the K-1801 preamplifier meets the specification for the low-frequency configuration used. Figure 4.1 shows a time series taken using the 2 mV range with the K-1801's slow filter, 3.2 Hz, and with a pure copper short on the input of the 1801. The data have noise with an amplitude of 6 nV peak to peak. This is just as the specifications indicate. The rms of the time series is 0.9 nV. Figure 4.2 shows that the spectrum is roughly flat with a level between 1 and 2 $nV/\sqrt{Hz}$.

High-Frequency Keithley 2001 and 1801 Validation

The high-frequency check of the Keithley 2001 and 1801 also showed that it met the specifications. A 20 Ω resistor was used on the input of the K-1801. The K-1801 filter was set to fast, (i.e., 700 Hz). The K-2001 "burst mode" was used to sample at 2000 Hz. Up to 29500 samples were stored in the K-2001 until the sampling was finished and then downloaded to the Mac. Figure 4.3 shows the average spectra of five successive 15-second time series.

Scanner Tests

We checked that the scanner had insignificant cross talk between channels. This was done by connecting the same large signal to seven of the eight scanner channels and

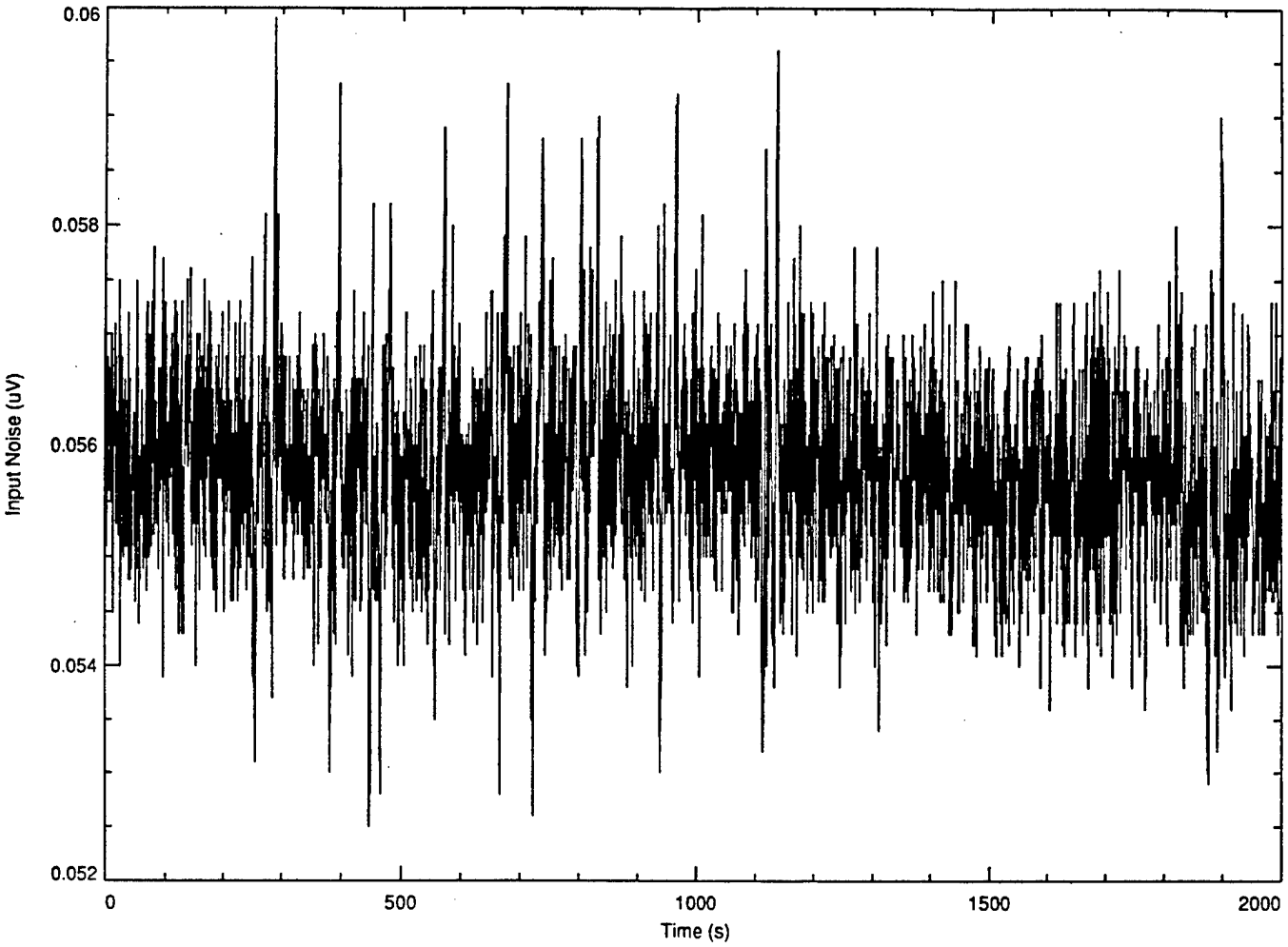

Figure 4.1 Time series of about 4000 measurements of the Keithley 1801 preamp and 2001 multimeter. The 1801 has a pure copper short on its input for lowest possible noise. The 2001 averaging is set to 12 measurements of one power line cycle per measurement. The sample interval is about 0.5 s. The peak to peak noise is about 6 nV as the specification indicates.

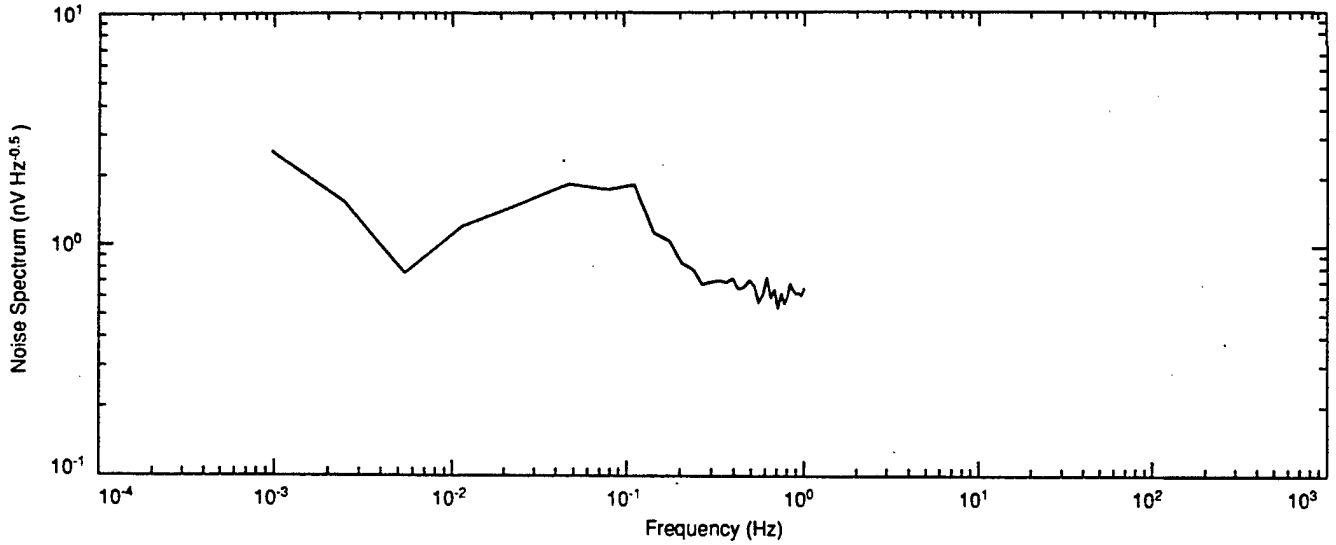

Figure 4.2 Spectrum of the time series of the previous figure, 4.1, which has about 6 nV peak to peak noise. The maximum variance density is 2 nV/$\sqrt{\text{Hz}}$. The spectrum is roughly flat as expected for a resistor.

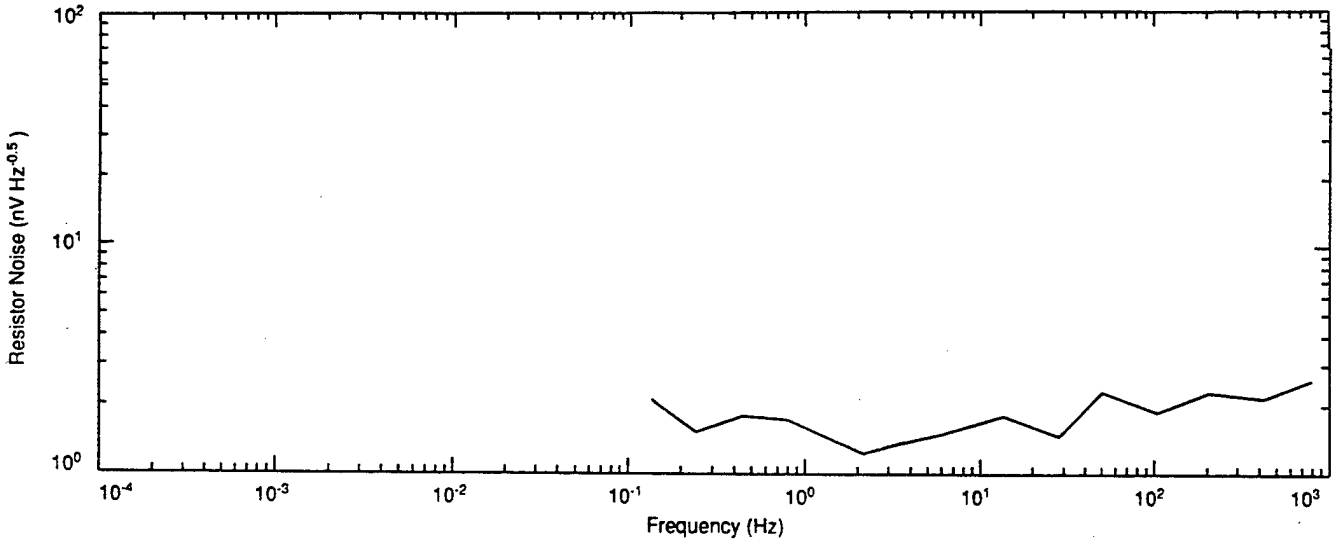

Figure 4.3 Spectrum of test time series of a 20 Ω resistor in the isothermal tank. The variance density about 2 nV $\sqrt{\text{Hz}}$. The spectrum is roughly flat as expected.

a resistor to the remaining eighth channel. The seven were programmed to be open and the eighth to be closed. In other words, only the eighth channel should be connected to the output while none of the signal on the other seven should be present on the output. The output was examined for indications of the signal on the seven channels that were driven.

A Keithley 230 Programmable Voltage Source was connected to the seven driven channels. The resistor used on the eighth channel was 950 Ω. More crosstalk might be expected at the higher resistance. Some of the electrodes were about 20 Ω and some had resistances of a few hundred ohms. The output channel was examined with the Keithley 1801 and 2001 and a simple LabVIEW display program.

With the 950 Ω resistor on the eighth channel, the drive signal was increased until we could just barely see a change in the output for a step change in the input. For both configurations of driven channels this occurred when ±10 mV was applied to the seven driven channels. An electrode offset of 10 mV is very large but not out of the question. Thus, to use the scanner without fear of crosstalk, we monitored the electrode potentials to ensure they remained below 10 mV. None needed to be removed. All electrode potentials except one remained below 2 mV for the isothermal tests, and that one was removed. Thus, we verified that the scanner was good enough for the electrode tests.

Electrode Tests Conducted

The carboys of mixed synthetic sea water were made on September 12, 1994. The first APL electrode pairing tests were made on September 14. Daily measurements of these pairs were made using a Keithley 155 null detector/microvoltmeter and recorded. The APL electrode pairs to be used in the electrode tests were selected from a batch of about 35 electrodes. Electrodes were paired that had low DC offset potentials with respect to each other. APL electrode pairs were selected by September 29.

The SAIC electrodes were delivered October 11. RTV was added to their jar tops between the cables to prevent fresh water from entering the jars.

The NSWC electrode cables were sealed with RTV into jar tops on October 11.

By October 12, all the electrodes except one NSWC pair were in their jars and installed in the bath and cabled to the scanner. The bath temperature had been at 4°C for some time, since that system had been giving some trouble and needed repair. A new heater element had to be obtained and installed. The last NSWC electrode pair was added on October 14, 1994.

The "LF" program was used with all 16 scanner channels sampled as well as temperature. The first 12 channels were electrodes and the last 4 were resistors. Initially the overall sample rate was 50 seconds, but we were concerned that 5 samples per scanner channel were insufficient and increased the number of samples to 10, resulting in a sample interval of 120 seconds.

Electrode Summary Plots

An example of an hour of reading on each electrode or resistor is presented in Figures 4.4a and 4.4b. The medium frequency (MF) sampling was used to collect electrode time series from which spectral estimates were made. So as to be able to see the noise for frequencies above 1 mHz, all the MF raw data have been filtered with a high-pass filter with a 1-mHz corner frequency. This one-pole digital recursive Butterworth filter was implemented in software. All MF time series are presented in Appendix A.

There are four MF runs in the isothermal tank. Data from the files "oct28h", "nov18a", "nov26a", and "nov30b" were taken at 4, 10, 15, and 17–19°C, respectively. Most scales are ±0.05 μV, but some have a wider range to allow for noisier data. The figures are labeled with their file name followed by the segment number. Each segment took about 16 hours to complete, during which time each of the 16 scanner channels was sampled continuously for about 1 hour. Although the data are depicted concurrently for convenience, they are not concurrent. In order to organize the graphs, the order of display is not exactly the order of sampling.

Note that while most of the graphs have a common scale for easy comparison, several electrode pairs and resistors required different scaling to display them. The NSWC 7-8 pair is obviously almost 10 times noisier than the others. The NSWC 1-2 pair is off scale and thus did not produce any digital data. The 950 Ω and 10 kΩ resistors have elevated noise as is to be expected.

The SAIC electrodes are quietest. Two pairs of APL electrodes show significant wandering while the other two are considerably quieter. The two quietest NSWC electrodes are noisier than any of the SAIC and APL electrodes. The low-value resistors show low noise levels, confirming that the measurement system continued to perform well.

Electrode Spectra

Spectra from APL, NSWC, and SAIC electrodes as well as from resistors are presented in Figures B.1 through B.16 in Appendix B. Figure 4.5 is a summary plot of typical electrode performance.

The first four figures in Appendix B show the APL electrode noise during the three isothermal tests at 4°C, 10°C, and 15°C and the final test from 17 to 19°C with the bath controller off. The next two groups of four figures are for the NSWC and SAIC electrodes for the same temperatures. The last group of four plots shows spectra of resistors to demonstrate that noise of the measurement system is less than the electrodes.

The better APL pairs at 4°C have about 100 nV/$\sqrt{\text{Hz}}$ noise at 1 mHz and reach the instrumentation noise floor of 2 to 3 nV $\sqrt{\text{Hz}}$ at about 30 mHz. At 10°C the noise floor is reached at a slightly lower frequency and all pairs are quieter at 100 mHz. The APL electrode spectrum at 15°C shows no real difference from that at 10°C.

For the test at 17 to 19°C with the bath controller off, the two best pairs of APL electrodes from the previous isothermal tests were removed from the bath to be installed in sensors. The best remaining pair has half the noise it did in the 15°C test; at 1 mHz it had about 150 nV/$\sqrt{\text{Hz}}$ while here it has 70 nV/$\sqrt{\text{Hz}}$.

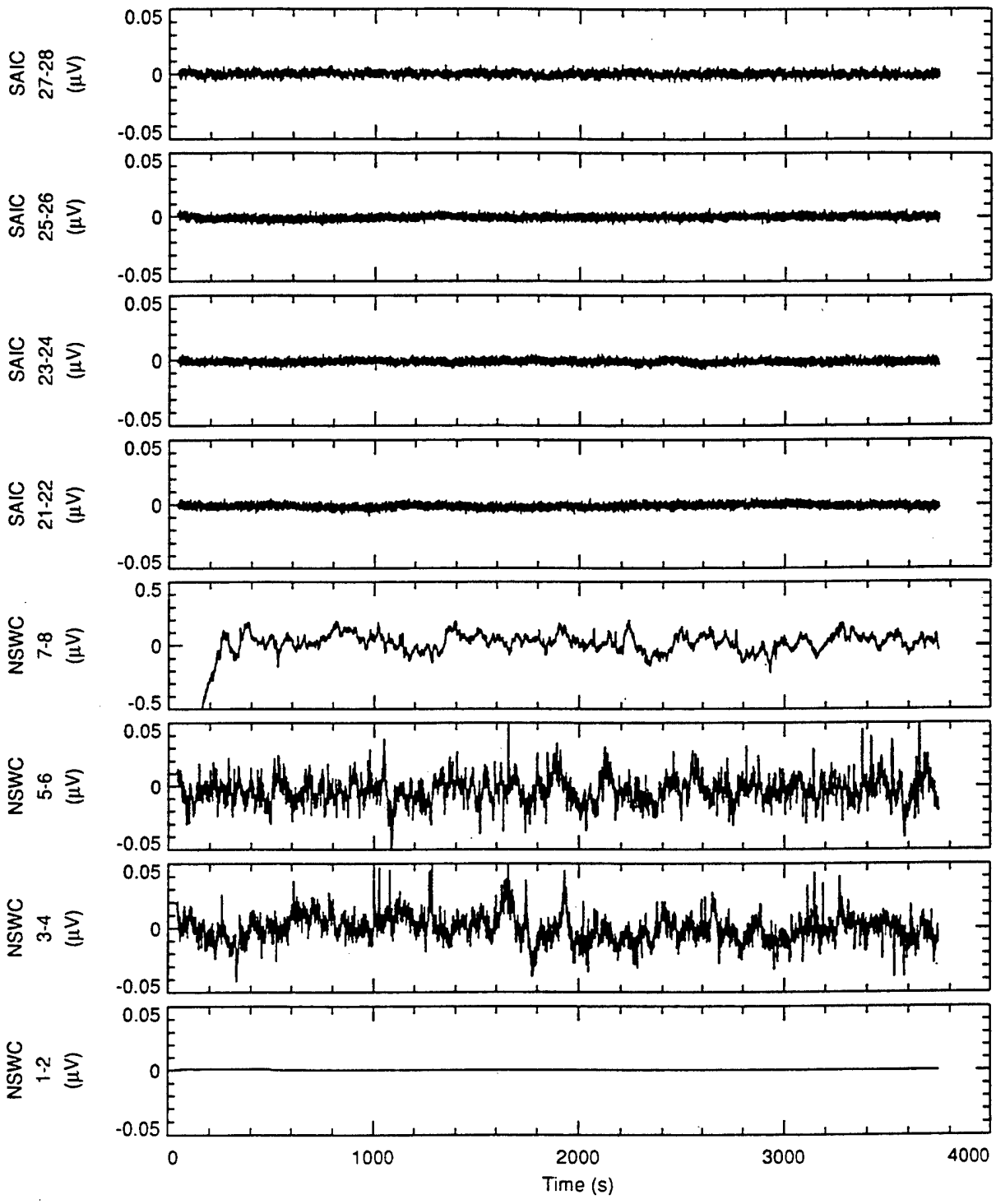

Figure 4.4a The first hour of the time series of the NSWC and SAIC electrodes during the first isothermal MF sampling run at 4°C. All are high pass filtered in software with a one pole Butterworth filter with a corner frequency of 1 mHz. See appendix A for a complete set of time series. One NSWC electrode pair, 7-8, is noisier so has a different scale.

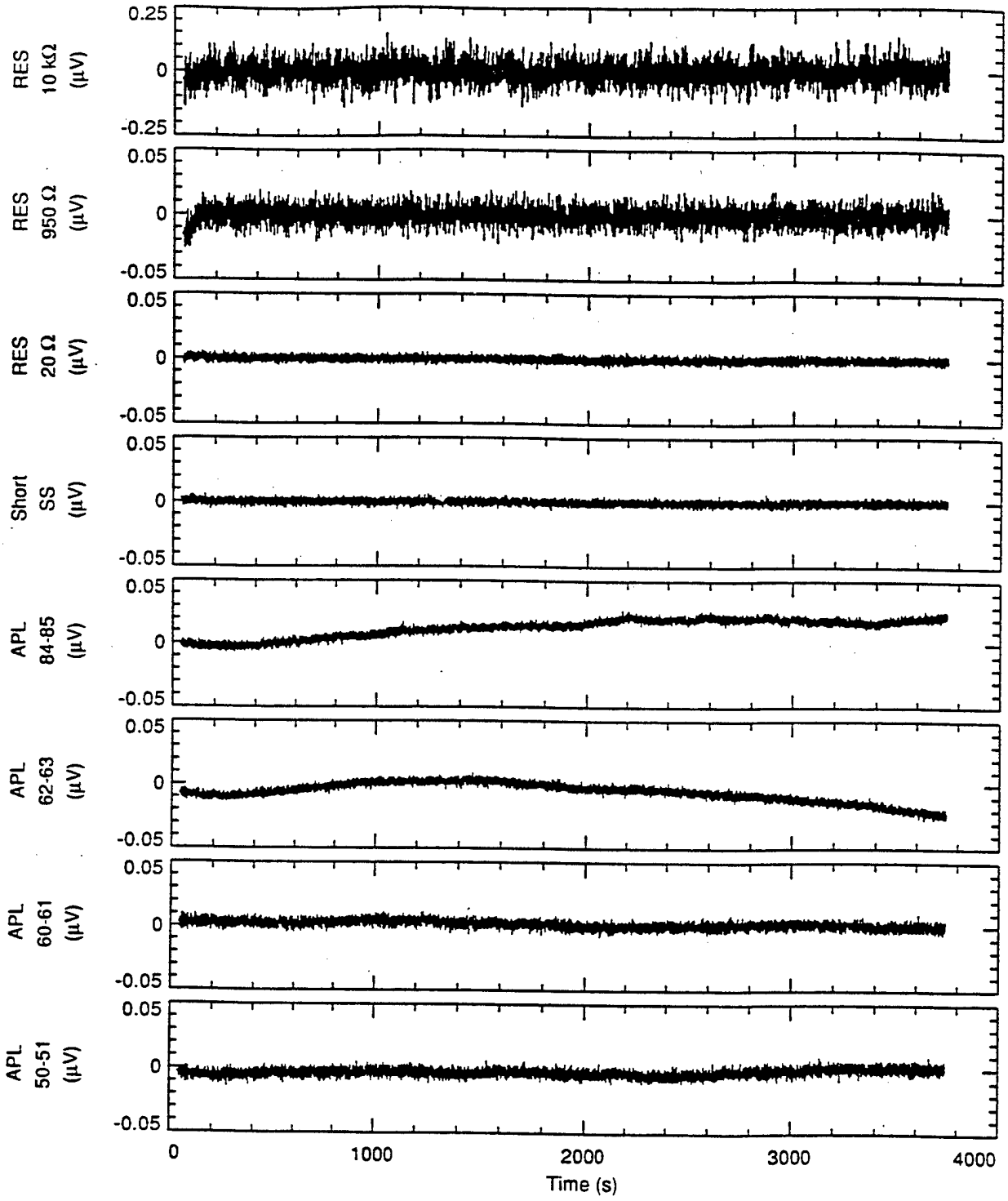

Figure 4.4b The first hour of the time series of the APL electrodes and resistors during the first isothermal MF sampling run at 4°C. All are high pass filtered in software with a one pole Butterworth filter with a corner frequency of 1 mHz. See appendix A for a complete set of time series. The high value resistor, 10 kΩ, is noisier so has a different scale.

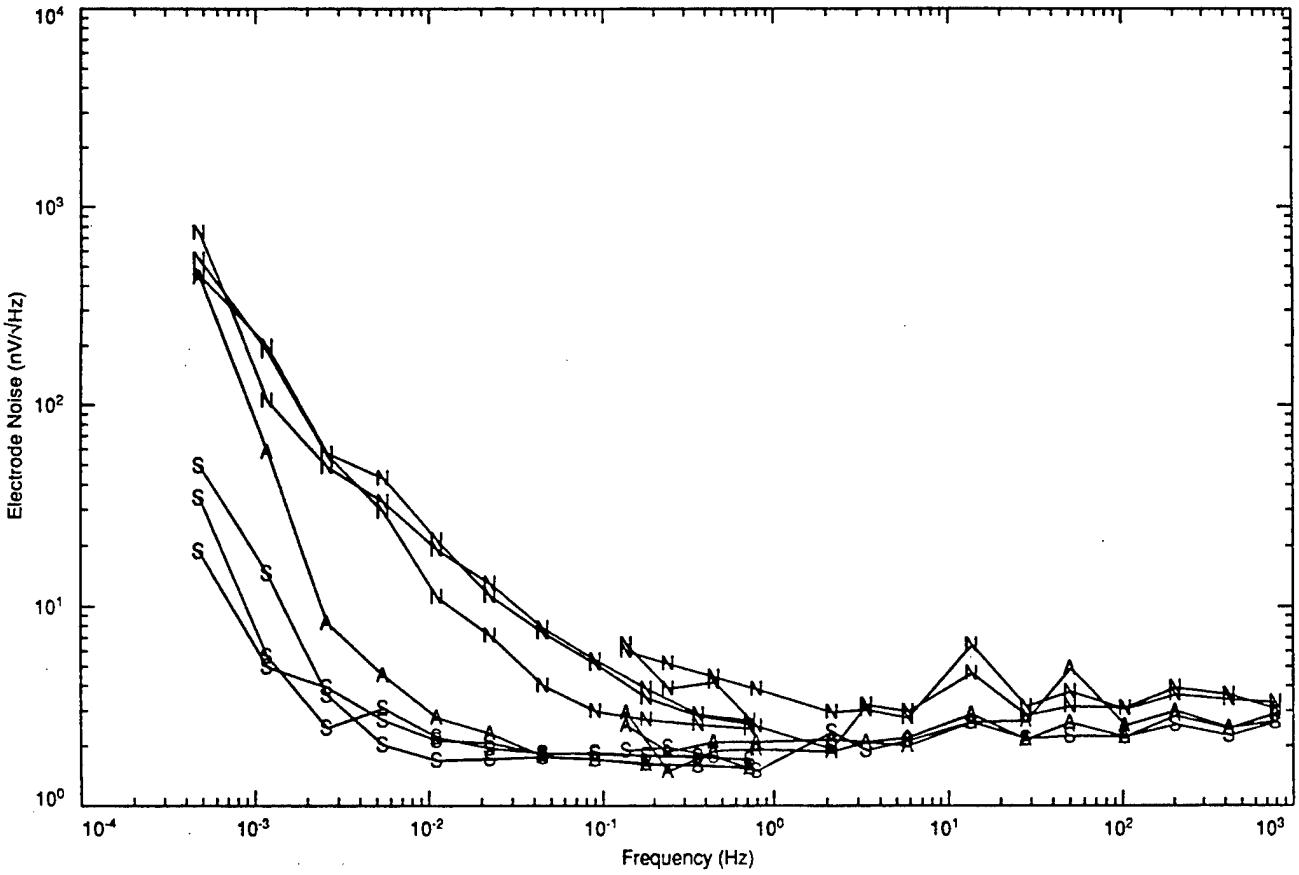

Figure 4.5 Electrode noise in 17–19°C bath. N denotes NSWC electrode pairs, A is a single APL-UW electrode pair (the other two APL pairs were by this time removed to install into sensor configurations as in Figure 5.1), and S denotes SAIC electrode pairs.

The NSWC electrode spectra at all temperatures are obviously noisier than the SAIC and APL spectra. The slope of the spectrum is much less than for the APL and SAIC electrodes. All three pairs reach the instrument noise floor at about 1 Hz. One pair not shown exceeded the full-scale range of the Keithley 1801 preamplifier. At 1 mHz, the noise of the best electrodes is about 30 to 40 $nV/\sqrt{Hz}$. The noise floor for the NSWC electrodes, 3–4 $nV/\sqrt{Hz}$, is somewhat higher than for the APL and SAIC electrodes. This is probably because of higher electrode resistance.

At 10°C, 15°C, and 17–19°C, four NSWC electrode pairs are shown. The pair that was not shown at 4°C is replaced with a new pair which is much better. The new electrodes reach the noise floor at about 50 mHz, about a decade and a half lower than the other three pairs. Even though the new pair is much quieter at 50 mHz, it has the same noise at 1 mHz as the others.

The SAIC electrode spectra at 4°C are shown in Figure B.9. These electrodes are the quietest of the three manufacturers, with the exception of one pair has with elevated noise from 5 mHz to 0.2 Hz. Note that this pair has mended its ways and falls in with the rest in the 15 and 17–19°C runs, Figures B.11 and B.12. The quietest have noise of 40 $nV/\sqrt{Hz}$ at 1 mHz and reach the instrumentation noise floor at 10 mHz. The noise of the SAIC electrodes at 1 mHz is significantly less than that of the APL electrodes, but both reach the same noise floor at the same frequency.

The SAIC electrode spectra at 10°C have somewhat lower noise, 25 $nV/\sqrt{Hz}$, at 1 mHz than at 4°C. At 15°C, the best have 30 $nV/\sqrt{Hz}$ noise at 1 mHz. The noise floor is reached at a slightly lower frequency than at 4 and 10°C.

SAIC electrode spectra at 17–19°C (Figure B.12) with the bath controller off show a very dramatic decrease in noise at 1 mHz. The average noise at 1 mHz is 7 $nV/\sqrt{Hz}$; the best is 5 $nV/\sqrt{Hz}$. The electrode noise is only slightly above the resistor noises shown in the following four figures.

Figures B.13 to B.16 show resistor spectra at 4, 10, 15, and 17–19°C. In the first two figures, the three groups of measured spectra less than 1 Hz correspond to three values of resistance, 10 kΩ, 950 kΩ, and 20 Ω. The single high-frequency spectrum is measured with a 20 Ω resistor. These measured spectra have the same noise at all frequencies above 10 mHz, and the noise decreases as resistance decreases. We feel that the rise in noise below 10 mHz is due to the thermal noise of the scanner. Figures B.15 and B.16 do not include the 10 kΩ resistor spectra. Figure 4.6 shows resistor noise spectra during the 17–19°C tests.

The capabilities of our instrumentation have almost been exceeded for most of the spectral range in the case of the SAIC electrodes. Recall that the best pair of the other figures had been removed for use in preparation for the system tests. Also, note that while the SAIC electrodes show marked improvement when the bath controller was off, the APL show only moderate improvement, and the NSWC electrodes show none.

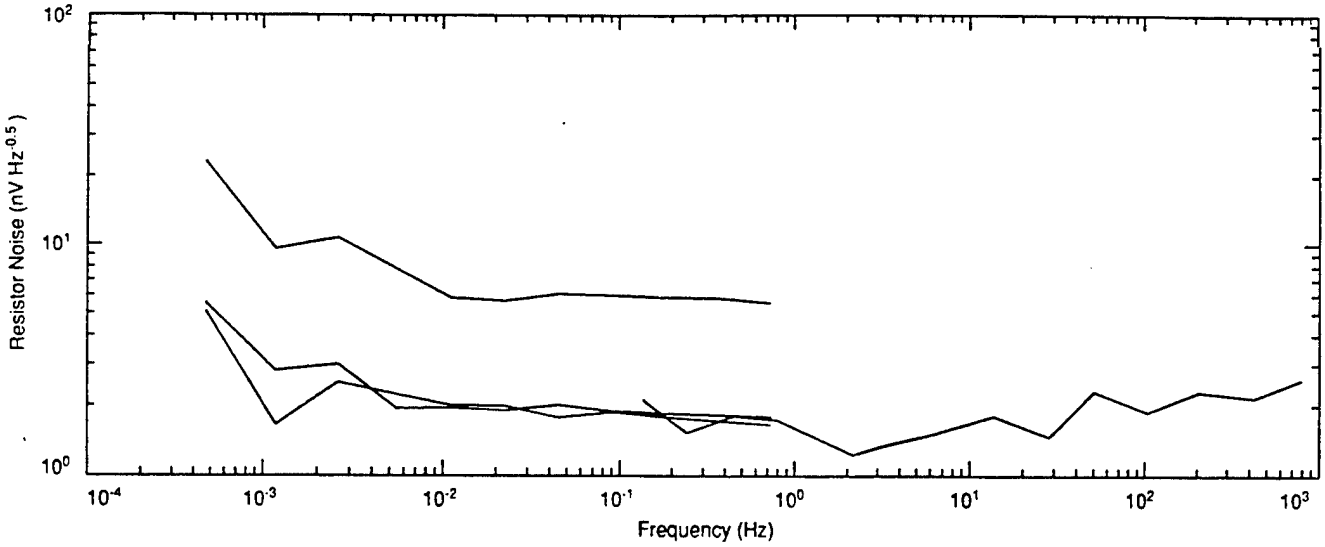

Figure 4.6 Spectra of resistors from 0.5 mHz to 1 kHz showing measurement noise during the last test in the isothermal tank. The spectra are nearly flat at about 2 nV/$\sqrt{\text{Hz}}$ except below 2 mHz. The rise at low frequencies is less than that of the electrodes, indicating that the rise of electrode noise at low frequency is real. The lower noise graphs are from 20 Ω resistors. The elevated graph from 0.5 mHz to 1 Hz is from a 950 Ω resistor, showing that it is important to keep the resistance low for low-noise measurements.

5. ELECTRIC FIELD SENSOR TEST SETUP

APL Sensors

The APL sensor blocks were manufactured using standard white PVC plastic household drain-pipe fittings. Each sensor block consists of two electrode chambers formed by cutting a tee fitting and gluing it back together with two flat plates of grey PVC as described below. Ag-AgCl electrodes are installed in these chambers. The reason for this configuration is to provide an assembly with very small thermal gradients between the two electrode chambers. Figure 5.1 shows the sensor block assembly.

Two of these new APL sensor block assemblies (labeled A1 and A2) were modified to include a thick membrane or plug composed of synthetic sea water mixed with agarose. The gelled agarose provides a barrier between the synthetic sea water in the electrode chamber and that in the salt bridges and the rest of the tank. The plugs don't touch the electrodes. The electrode chambers are filled with synthetic sea water while the plugs are spaced about 35 mm away from the electrodes.

One of the sensor assemblies (labeled A3) was produced more simply. The molten agarose gel was poured directly over the electrodes themselves, completely filling the ell-shaped portion of the chambers with agarose gel. This is the sensor that was sampled after January 17 during the 30-day test. This test was of particular interest because it was speculated that placing the agarose gell completely around the electrode would lead to large offsets. It was thought that the gell would prevent the proper exchanges of chemical species needed at the electrode/water interface. This effect did not appear important, at least for the small bias currents required of the scanner/preamplifier.

SAIC System

The SAIC system used in the salt water tank tests consists of two underwater units, a data receiver above water and an electrical cable harness. The larger underwater unit contains a preamplifier, filters, line drivers, and batteries for powering these electronics as well as an integral electrode assembly. The smaller unit contains only the second electrode assembly.

The electrodes are not visible. They are in an inner chamber with a solution of pure NaCl and pure deionized water. Electrical connection to the sea water is via a porous membrane. The membrane is kept wet when in storage by putting sea water in the outer chamber just inside a coarse plastic screen. Removable covers hold sea water in the outer chamber for storage. The NaCl solution is replaced periodically to prevent contaminants from reaching the electrodes. The membranes are sensitive to oil fouling.

A short cable connected the two underwater units. When these units were arranged with the electrode ends farthest apart, the electrode port spacing was 2 m. A longer data cable connected the larger underwater unit to the data receiver. This cable would be much longer in an actual field operation. The underwater unit required two lithium batteries which were soldered in place.

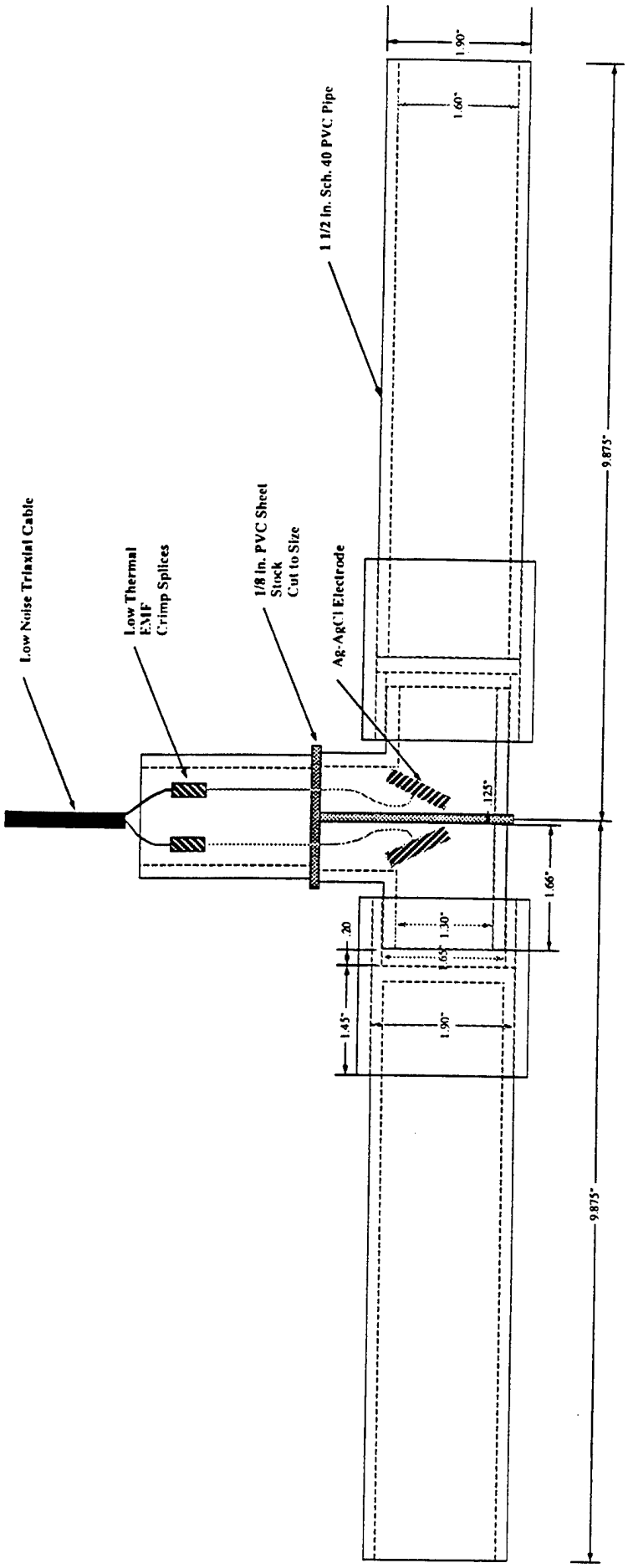

Figure 5.1 Side view of APL-UW sensor assembly showing internal arrangement of parts and dimensions. A piece of 1 in. PVC pipe was cemented to the stub end of the tee and used to support the sensor in the saltwater tank.

The potential difference between the electrodes was amplified by a single preamplifier in the large underwater unit. The resulting signal was filtered into two frequency bands, 0.1 mHz to 1 Hz and 1 Hz to 1 kHz. After more amplification, these two signals were transmitted up the data cable as currents proportional to the electrode potential difference.

The SAIC system specifications for electric field noise are shown as a function of frequency in the following table. In the second column a 2-meter separation is assumed. The third column is multiplied by 2 meters to show the combined electrode and amplifier noise.

Table 5.1

Frequency (Hz)	Electric Field Noise ($nV\ m^{-1}/\sqrt{Hz}$)	Electrode and Amplifier Noise ($nV/\sqrt{Hz}$)
0.01	50	100
0.1	10	20
1	2	4
1	2	4
1000	2	4

NSWC System

The NSWC system consists of a pair of electrodes, each with about 4 feet of neoprene-jacketed underwater cable and an amplifier suitable for a laboratory environment. The amplifier has a gain of 6000 and a low-pass filter with a 3-dB corner frequency of 17 Hz. We did not seek permission from NSWC to modify the passband to allow a wider band of frequencies. However, as discussed later in this report, we applied data processing corrections to flatten the response. Power for the amplifier is furnished with a standard adjustable laboratory power supply set to ±15 V.

Description of Salt Water Tank

All the systems were installed in a single salt water tank measuring about 8 feet east-west, 6 feet north-south, and 3.5 feet deep. See Figure 5.2 for tank details. Plenums just inside the north and south walls of the tank provided a means of impressing electric signals in the tank. The tank is constructed from 4 x 4 lumber and plywood which was waterproofed with a laid-up fiberglass and polyester resin lining. The tank is insulated from the floor with rubber matting and a 1/4-inch-thick plastic sheet. The capacitance to ground is reduced somewhat by having the bottom of the tank raised about 4 inches above the floor on 4 x 4 lumber.

Before the electric field distribution measurements, the tank had been filled with tap water and 424 lb of the same shipment of synthetic sea salt that was used in the

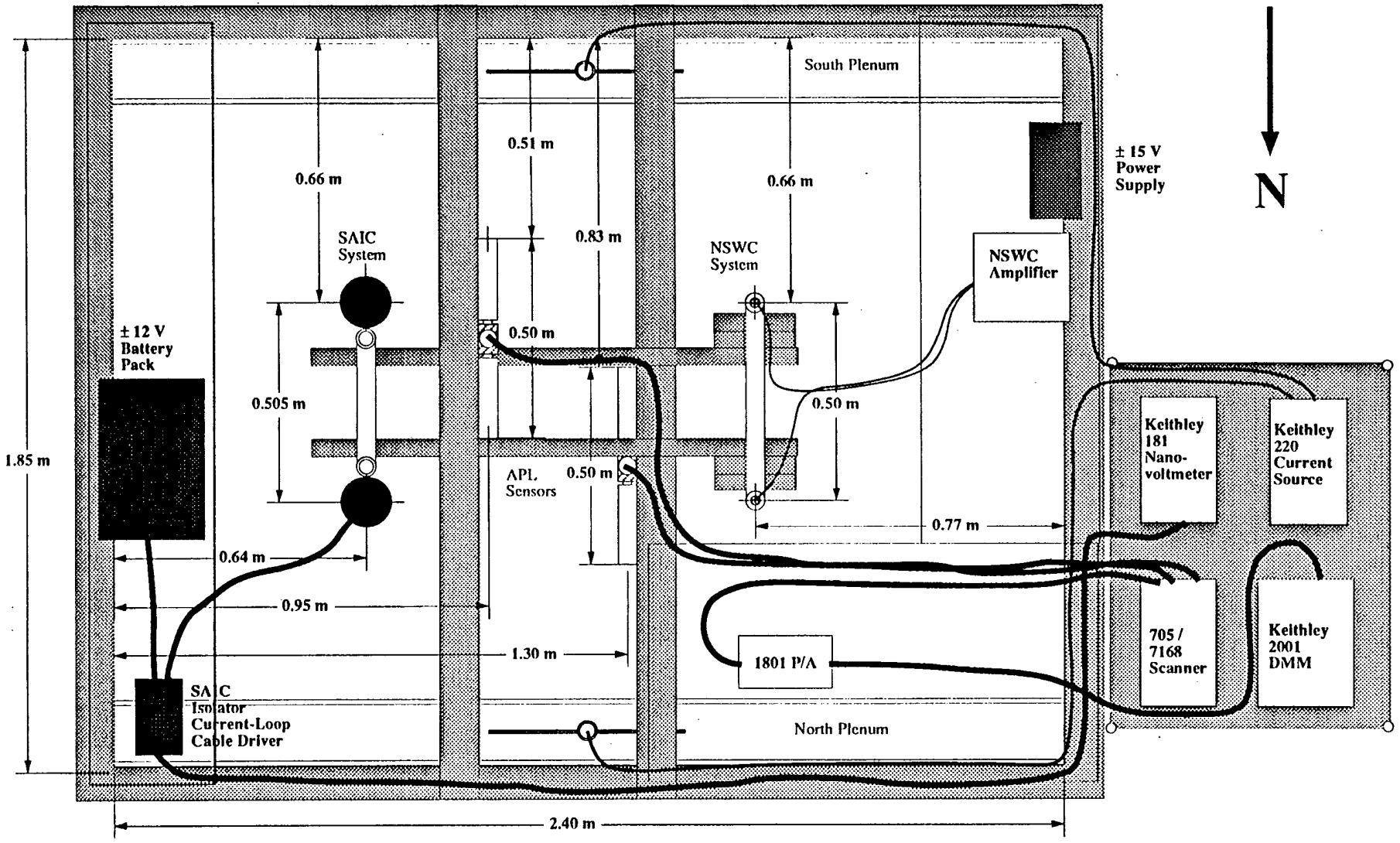

Figure 5.2 View from above APL-UW salt-water test tank. Diagram shows placement of sensor systems and cabling to data acquisition electronics. The NSWC amplifier was surrounded with rigid foam insulation and mu-metal shielding to reduce noise. Likewise the 1801 preamplifier was surrounded with mu-metal to reduce noise. The data acquisition computer's monitor (CRT) was turned off at times to provide the lowest noise environment.

isothermal test jars. The salinity of the tank is about 35 psu (practical salinity units). No water was added to compensate for evaporation during the test.

The north and south sides of the tank each have a plenum about 5 inches thick and covering the whole side of the tank. The plenums have holes to the main bulk of the tank interior. The plenums enclose electrodes which are used drive current in the tank. A fairly uniform electric field in the bulk of the tank is obtained. This is because the holes in the plenum are intentionally of higher resistance than along any path from the electrode to the holes in the plenum. Because there is a small voltage drop between the electrodes and the holes inside the plenum, each hole is at nearly the same potential as its associated electrode and thus the potential across the surface of the plenum is roughly uniform. The spacing of the holes is about 8 inches, so one needs to get away from the plenum somewhat to allow the field to recover from the discreet hole effects.

A Keithley 220 programmable current source is used to drive the electrodes in the plenums in order to provide signals for verifying functionality of the systems. A current of 10 μA produces an electric field of about 1 μV per meter.

Installation of SAIC System in Tank

The best SAIC electrode pair as determined from the previous electrode tests was installed in SAIC unit labeled with a large "#4", S/N 3. The SAIC system was installed about 2 feet from the east end of the tank and equidistant from the north and south plenums. Its car batteries and data receiver were mounted 8 inches above the water at the northeast corner of the tank on a shelf which spanned the tank north-south at the east end. The electrodes were positioned 0.505 meter apart (center to center) and about half way to the bottom of the tank. The electrodes ports faced down. The cylindrical axes of both sensor units were vertical.

There was considerable initial difficulty obtaining quiet operation from the SAIC system. Both the low- and high-frequency outputs showed inexplicable enhanced levels of noise from time to time. The low-frequency output had 100 and 200 nV spikes which were very frequent at times and every 10 minutes in other cases. The noise level was sensitive to people moving around the tank. Certain cable placements were much worse than others. The noise was isolated to the underwater unit. Fortunately, at one point in trying to cure the noise problem a fortuitous placement of a cable caused the noise to decrease markedly. This discovery allowed the tests to proceed. The SAIC noise level was variable. This is probably because at some times the cable placement was not optimum for the low-noise condition.

The placement of the cable between the SAIC underwater electronics package and the separate electrode was critical to keeping the 60 Hz pickup from exceeding the dynamic range of the high-frequency amplifier in the system.

Installation of NSWC System in Tank

The best NSWC electrode pair as determined from the isothermal tests was taped to the bottom of a frame made of PVC pipe. They were spaced 0.5 meter apart. The pipe frame was screwed to the wood frame above the tank. The remaining sections of electrode wires were twisted together to minimize magnetically induced noise pickup.

The NSWC electrode array was mounted about 2.5 feet from the west end of the tank and roughly equidistant from the north and south plenums. The depth of the electrodes is roughly half way from top to bottom of the water.

The NSWC amplifier box was determined to be very temperature sensitive. An insulated air-tight foam box for it was made. The NSWC amplifier in its foam box is mounted along with a ±15 VDC laboratory power supply on a platform over the tank at the southwest corner of the tank. It was also noted that the amplifier was subject to radio frequency interference (RFI). RFI suppressors did not cure the problem, which occurred only when the metal roll-up doors to the laboratory were open (a rare event).

Installation of APL System in Tank

The APL system uses an APL sensor connected to the Keithley 705/6178 scanner which is connected to the K-1801 preamplifier which in turn is connected to the Keithley 2001 multimeter.

Several APL sensors were installed in the tank between the NSWC and SAIC systems. Several old sensors and three new sensors with lower salt bridge resistances were mounted. One of the old units failed (Ab). One of the new units (A3) was used for most of the duration of the 30-day test. These sensors were mounted in staggered positions with the center of each arm about a foot north or south of the tank's east-west centerline. The closest proximity was about 9 inches. All the salt bridge arms were aligned north-south and were about mid-depth in the tank.

The scanner and multimeter were mounted on the computer cart since they had GPIB data and control cabling from the computer which was required to be short.

Computer and Software

The existing software as described in Section 3 was slightly modified to operate with the modified equipment setup in the salt water tank. For the low-frequency and medium-frequency sampling programs, this meant reading two separate Keithley 181 nanovoltmeters instead of the K-2001 for the NSWC and SAIC system outputs. The K-2001 and K-1801 were used for the APL sensors.

"LFF," a faster version of "LF," the low-frequency program, was used occasionally to monitor the quality of all the sensors and systems in the tank. The predecessor LF program had a flaw that slowed it artificially. "LFF" took about 20 seconds to complete the main loop with five samples taken on each channel. The "MF," medium frequency, program was used occasionally to obtain 1 hour records of 0.5 second sampling of each sensor or system in tank. This program was used to provide the 1 mHz to 1 Hz spectra.

A new program, designated "NS" for "no scanner," was written to be able to sample the three voltmeters quickly without driving the scanner. The scanner was manually set to a particular APL sensor and the program started. This program was the main one used to monitor the operation of the three systems in the tank.

The "HF," high frequency, burst mode sampling program which was used in the isothermal tests was modified slightly for use with all three systems in the salt water tank. The Keithley 2001 multimeter was used for all high-frequency sampling. Controls were added to set the voltmeter and preamplifier to the special settings required for each system. The SAIC system used a 20 V full-scale range, the NSWC system used a 2 V range, and the APL system used the K-1801 preamplifier on the 2 mV range. This program provided all the 0.1 to 1 kHz spectra.

Sampling Rate, Multiplexing, and Spectral Noise

The "MF" sampling is the best to show the spectral noise for frequencies below 1 Hz. This is for two reasons: 1) the multiplexing of the "NS" sampling raises the spectral noise level, and 2) the averaging of the input signal is different between the Keithley 181 and the Keithley 2001/1801 combination. Because of the above noise of the "NS" sampling, the "MF" sampling was used once to obtain a better measure of the noise of each system.

Round robin "NS" sampling was used to be able to monitor all systems in real time. But, there are short, about 0.5 second, gaps while the other systems are being measured. Because of these gaps, the spectral noise floor of each system using the "NS" data is not as low as if the systems were sampled continuously. One way of thinking about this is that a more accurate average value can be computed if more statistically independent samples are used. More accurate values have lower noise. More independent samples can be collected if no multiplexing gaps occur.

Another reason the "NS" sampling is not optimum for comparing systems is that the averaging time for each system using the "NS" sampling is different and thus shows different rms noise levels which are not truly representative of the system noises. The SAIC and NSWC systems used a Keithley 181 on the 2 V range. The averaging interval for them is 0.125 second. The APL system used the Keithley 1801 and 2001 with the averaging interval set to four measurements, or about 0.2 second.

Spectral Processing

The spectra in this report are the square root of the variance density spectra. This is the same quantity manufacturers use in operational amplifier specification sheets. The spectra are computed so the integrals over frequency of the squares of the ordinate values are equal to the variance of the input signals. In other words, the variance of a frequency spectrum is equal to the variance of its input time series.

The spectral processing consists of several steps. First, it extracts pieces from the time series that overlap each other by 50%. Then, the mean of each piece is removed. Next, the data in each piece may be first-differenced. The low-frequency time series are first-differenced twice while the high-frequency time series are not first-differenced at all. First-differencing prevents spectral leakage from energetic lower frequencies to higher frequencies. The rule of thumb is to first-difference as many times as is required to have the spectral slope of the resulting variance density as a function of frequency be between -2 and 0. The low-frequency data have a very steep spectral slope requiring

two stages of first-differencing. Next, each piece is multiplied by a Hanning window (cosine squared). Then the actual FFT (fast Fourier transform) is performed on each piece and manipulated to form a variance density spectrum which is recolored to correct for the first-differencing and Hanning operations that were applied to the time series. The variance density spectra for the individual pieces are averaged together.

The high-frequency spectra are contaminated with many very narrow frequency lines. These lines all seem to be instrumental, that is, they come from known sources other than the electrodes. When a few fundamental frequencies, their harmonics and aliases of their harmonics are suppressed, we find the remaining spectrum quite clean. We feel this cleaned spectrum is representative of the true spectrum of the electrodes. We don't expect electrodes to have narrow frequency emissions.

The fundamentals of the spurious frequencies are 60 Hz from the power line, 67 Hz from the magnetic field of the computer monitor's vertical sweep, and 288 Hz from the chopper stabilizing frequency K-1801 preamplifier. All the harmonics and aliases of the harmonics (up to 7000 Hz) of the basic contaminating frequencies have been removed. In addition, there are some spurious emissions at 288 Hz plus and minus 60 Hz. These intermodulation products of 60 Hz and 288 Hz were caused by the instrumentation and were removed.

Finally, to obtain more stability, the variance density estimates are band averaged with bandwidth proportional to the exponential of frequency.

In all cases, the square root of the averaged variance density spectra is plotted.

6. ELECTRIC FIELD SENSOR TEST MEASUREMENT RESULTS

Electric Field Distribution in Tank

Before installing equipment in the salt water tank, the electric field distribution was characterized. This tank was built for the testing of instruments that measure electric fields in the ocean, is kept filled with salt water approximating the composition of sea water, and is equipped with electrodes to impose ambient electric currents. The tank is rectangular, as shown in Figure 5.2, with the two electrodes inside two large perforated polyethylene plenums along the two longest sides of the tank, in order to produce the most uniform field possible in the tank interior. The unobstructed interior region of the tank measures about 8 feet east-west by 5 feet north-south by 3.5 feet deep.

For these measurements, the tank was filled with city tap water and 424 lb of a synthetic compound called "Sea Salt" manufactured by Lake Products, Inc., which contains the most common elements in sea water. The volume of water in the tank computed from the linear measurements is estimated to be 4.590 m^3 when the level is filled to the "line" which is 4 inches above the top row of plenum holes. Although a detailed chemical analysis has not been performed, the density of the solution was measured to be approximately 1,026 kg m^{-3}, which is close to that of average sea water. The electrodes were driven to provide current in both directions by a Keithley 220 programmable current source running at ±20 mA. The potentials at the current source were measured by a hand-held Fluke current meter to be producing 1.44 V and −1.34 V, respectively. All instruments involved in taking the measurements were controlled, via GPIB, through LabVIEW on a Macintosh IIfx computer.

The measurements were made using two APL-made Ag-AgCl electrodes installed in a machined electrode block and attached to salt bridges, long tubes extending to the points of measurement within the tank. One tube, the reference, was fixed into position, terminating at the approximate center of the tank, and the other, the probe, was attached to a rigid rod on a movable stage above the tank, so that its end could be positioned anywhere. The stage was labeled with measurements in all three dimensions to provide positioning information about the probe. The voltage measured between the electrodes, then, is the summation of a) electrode offset and b) the potential of the probe salt-bridge with respect to the reference. To subtract the electrode offset, the tank was driven with currents in both directions, reversing the sign of the probe potential but not the electrode offset. The commands to reverse the voltage, as well as the calculation of offset and potential, were all automated within a LabVIEW program, X-PROFILE. Electrode voltages were measured by a Keithley 181 nanovoltmeter.

Measurements were carried out on two grid spacings. The entire tank was mapped out by a rough 7 by 6 by 4 foot grid, spaced at 10 inches. This appeared sufficient for all large-scale features observed. In order to determine the local effects of the small perforations in the polyethylene plenums, a set of fine grid measurements was carried out in the vicinity of one plate. These measurements were not spaced entirely uniformly, to allow some flexibility in the presence of variable gradients, but the spacing ranged from 0.5 inch to 2 inches, in three horizontal planes, 2 inches apart.

Somewhat arbitrarily, the coordinates for these grids were chosen as follows: the longest dimension of the tank is x, as measured by a metal tape on the side. Positive x is to the west. The shorter dimension is measured using another tape on the rolling stage over the tank, but to preserve a right-handed coordinate system these measurements were subtracted from 80 inches for the y-data as reported in the figures; y is positive to the south. The z-axis is defined by markings on the rod holding the probe salt-bridge. The height of the reference salt-bridge port is $z=0$; z is positive up.

The tank is designed to give a uniform electric field throughout most of its interior, and, indeed, the measurements show a fairly uniform gradient in the potential between the two plenums. A least-squares linear fit in the direction of this gradient yields the equation

$$\phi(y) = 45.1y - 1845.0\,,$$

where ϕ is in μV and y is in inches.

Though the field of 45.1 μV per inch dominates the potential, there are substantial asymmetric residuals after the uniform field has been subtracted. Two features are most obvious: a high-voltage anomaly in the bottom level of the SW corner, and a low-voltage anomaly in the top level of the SE corner. There is also the possibility of a slightly high potential in the NW corner of the top level, but the rest of the residuals appear generally symmetric, low valued (<50 μV), and trapped to the edges of the tank.

The origin of the two major anomalies is a bit puzzling. The high one could be the result of a leak in the polyethylene plate, perhaps at the bottom where there is a small plug, but the low anomaly is a bit more mysterious. Both are almost certainly centered at or near extreme corners of the tank, which makes it appear unlikely that the low could be the result of a plugged hole in the plate, but this is a possibility. It was not explored as to whether anomalies are permanent features of the tank setup or simply artifacts that were present only at the time of measurement.

The fine grid measurements showed no surprises whatsoever. As expected, potentials very close to the plate are high adjacent to holes and low between holes, with a peak-to-peak amplitude of up to 200 μV between the two positions, which are only 4 inches apart. The effect of the holes drops off rapidly with distance from the plate, to an amplitude of less than 10 μV at 3.25 inches, and is undetectable at 5.25 inches.

Validation of Installation in Salt Water Tank

In order to make sure the systems continued to function during the tests, a signal was applied to the tank daily, usually at the beginning of the run started after the daily HF sampling. The signal was a square wave current of $\pm$10 μA with dwell times of 60 seconds. It produced approximately 1 μV peak to peak in all the systems. The systems were always functional.

All the systems were mounted in close proximity in the same tank. This would not be the usual case in the field. We were concerned that various systems would interact. Before conducting the systems tests, we made interference tests. In turn the power to all the systems except the one being checked was turned off and on to see if there were any effects.

We watched the real-time data display as systems were turned on and off. There was no interference or interaction between systems as far we could determine.

Description of Measurements

Just as with the isothermal tests, the salt water tank tests were executed with several sampling schemes. A new data acquisition program, "NS", sampled each of the three systems, APL, SAIC and NSWC, every 0.7 second using separate voltmeters in round-robin fashion. The high-frequency, 2 kHz, sampling using the "HF" program was usually done once every weekday starting on January 18. On January 20, a special run using the "MF" program obtained low-frequency measurements with lower noise than the "NS" sampling by dedicated 0.5-second sampling of each system for about an hour before switching to the next system.

More than 30 days of data from three systems were obtained in the large salt water tank in a 6-week interval. These are summarized in Figure 6.1 and Appendix C. These time series were taken with the "NS" sampling program and have numerous intentional 1 to 2 hour gaps on most weekdays when the high-frequency (HF) sampling occurs. Other gaps occurred when verifying and improving the measurement system setup. The gap in all data starting on January 20 is when special "MF" (medium frequency) sampling was done to obtain a lower system noise floor. Some of the gaps occurred because equipment failed or failed to perform as expected. The APL gap starting January 14 was because that sensor (A1) exceeded the full-scale range of the K-1801 preamplifier. A different sensor (A3) was used starting January 17. The SAIC gaps starting on January 5 and January 13 are when that system was being repaired and tested. The gap in all data on January 5 and January 13 was while the SAIC system noise was being examined. The SAIC gap starting on January 28 was when the sensor batteries failed after exceeding their life expectancy. The 4-hour SAIC gap on February 10 was to charge one of the data receiver car batteries. One gap starting on February 11 was an operator error: the disk filled, so data were not recorded.

The ± 1 μV bidirectional spikes that occur periodically are from the occasional driving of the tank with ± 10 μA holding for 60 seconds in each state. This signal was to ensure that all systems were responding properly. These were usually done at the beginning of an "NS" file just after HF sampling.

Three new APL sensors, labeled A1, A2, and A3, were fabricated in late December. One of these unaged sensors, A1, was used from January 3 to January 13. This sensor drifted out of the Keithley 1801 ± 2 mV range. We switched to sensor "A3" on January 17. By the end of the test, all three of the new APL sensors had aged sufficiently so they had offsets within the K-1801 range and they were quiet.

The SAIC system required equipment repairs to correct noise problems. Several different units were tried. Part of the trouble was from a faulty cable and part seemed to be inherent in the design of the sensor. The faulty cable was discovered on January 13, repaired, and put into service again on January 17. The large amount of variability in the January 17 data is during the testing of the SAIC system. There were 100 to 200 nV unidirectional spikes in the data that would come and go. Finally a cabling arrangement was

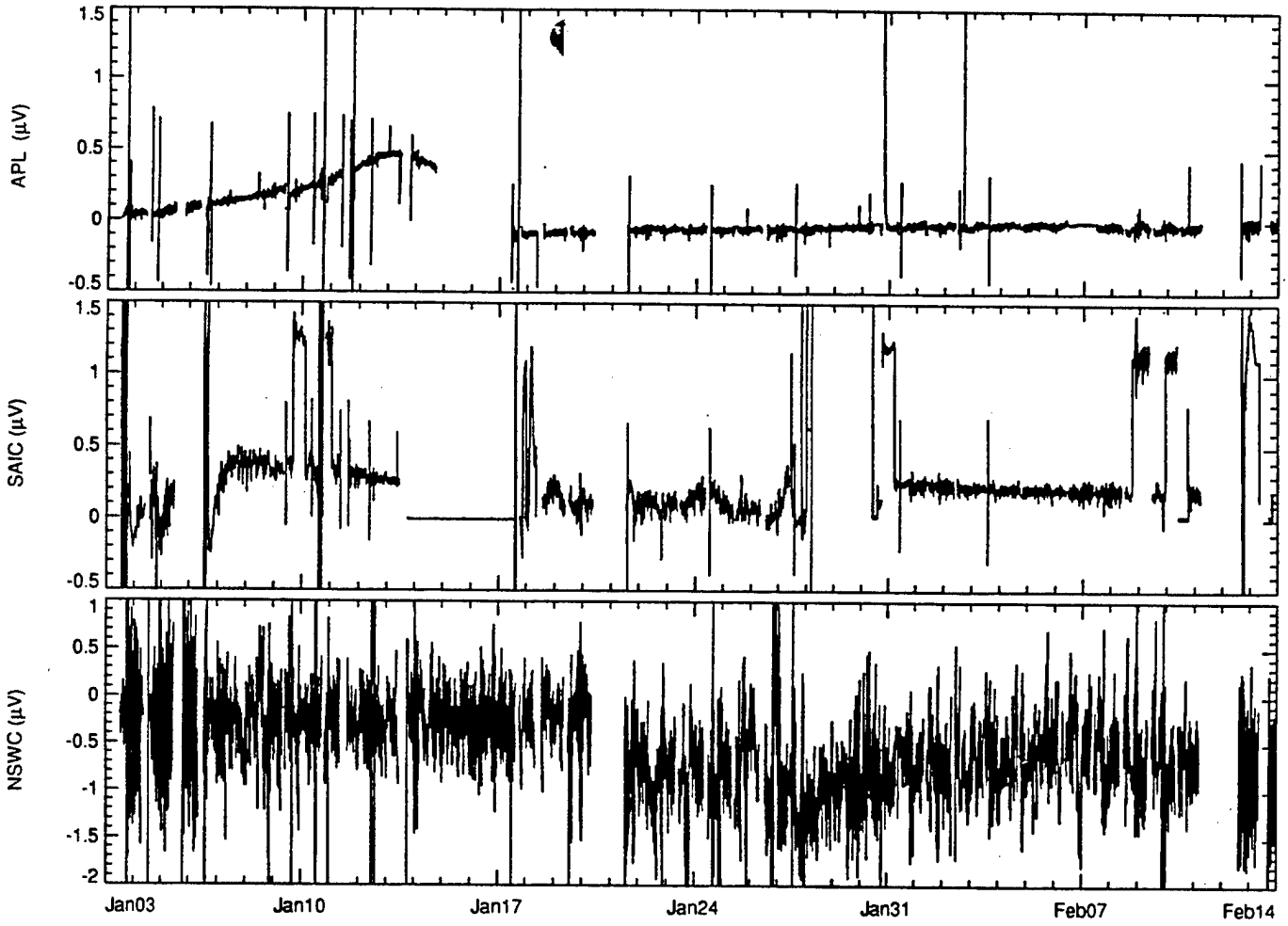

Figure 6.1 Forty-two days of time series from the salt-water tank tests. The APL sensor has been high-pass filtered with a one-pole Butterworth filter with a corner frequency of 1 mHz to match the high-pass filtering in the hardware of the NSWC and SAIC systems. Before January 12 the SAIC system was noisy. It was fixed on January 18. The APL electrode pair in use before January 15 went off scale. A different one was used after January 17.

found that was reasonably satisfactory. The rest of the tests were done with that arrangement. The batteries ran out on January 28 and were replaced on January 30. After that disturbance and rearrangement of the cabling, the system behaved better. For several hours on February 10, one of the car batteries was charged. The internal batteries ran out on February 12. The SAIC system had several unexplained jumps from about 0.2 μV offset to about 1.2 μV offset. Five times the jumps exceeded 4 hours in duration.

The NSWC system was very much affected by having the roll-up door open and by having people move around in the room. The increased noise on January 3 to 6 is during a period when the room was being used as a staging area for a cruise, so the door was open repeatedly and the room had lots of activity. We think that having the roll-up door up allows RF from nearby TV and FM broadcast stations to overload the low-noise front end of the NSWC system. We had seen this problem in the past with previous similar systems of our own.

All the systems are sensitive to ARGOS PTT transmitters with about 1 W at 400 MHz. Portable cellular phones at 800 MHz and hand-held marine radios at about 160 MHz also produce spurious signals in all systems. These radios were being tested from January 3 to 9 in and near this room.

Summary Plots and Examples

Figure 6.1 shows an overview of 6 weeks of "NS" data from the three systems. Higher resolution graphs, one per day, of this same data are shown in Appendix C.

Appendix C also contains plots of the time series of the "MF" sampling from January 20 and February 16.

The data in the "NS" figures have been subsampled by 100 and thus are shown about every 70 seconds. All three panels are processed with comparable high-pass filtering. The APL data are filtered with a software one-pole Butterworth high-pass filter with a corner frequency of 0.001 Hz. The SAIC and NSWC systems have similar high-pass filters in their hardware.

Examples of Spectra

Seven figures in Appendix D show electric field sensor system noise. Three of the figures, D.1, D.5, and D.6, provide example spectra from the APL, NSWC, and SAIC systems, respectively. Each covers 0.5 mHz to 1 kHz. The "MF" sampling as well as selected "HF" sampling is shown. Figure 6.2 characterizes the spectral shapes of the NSWC (N), SAIC (S), and APL-UW (A) electric field sensors.

Two figures in the appendix are tests. Figure D.3 shows 20 Ω resistor spectra to show the instrumentation noise for the APL spectra above. Figure D.7 shows the spectra of the SAIC system with the underwater unit turned off. The first test shows that only below about 10 mHz do the APL sensors have more noise than the instrumentation system. The second test shows that the SAIC front-end noise dominates as it should.

Six figures in Appendix D show all the high-frequency spectra for the three systems in various configurations. The first three figures, D.8–D.10, show the APL sensors in the

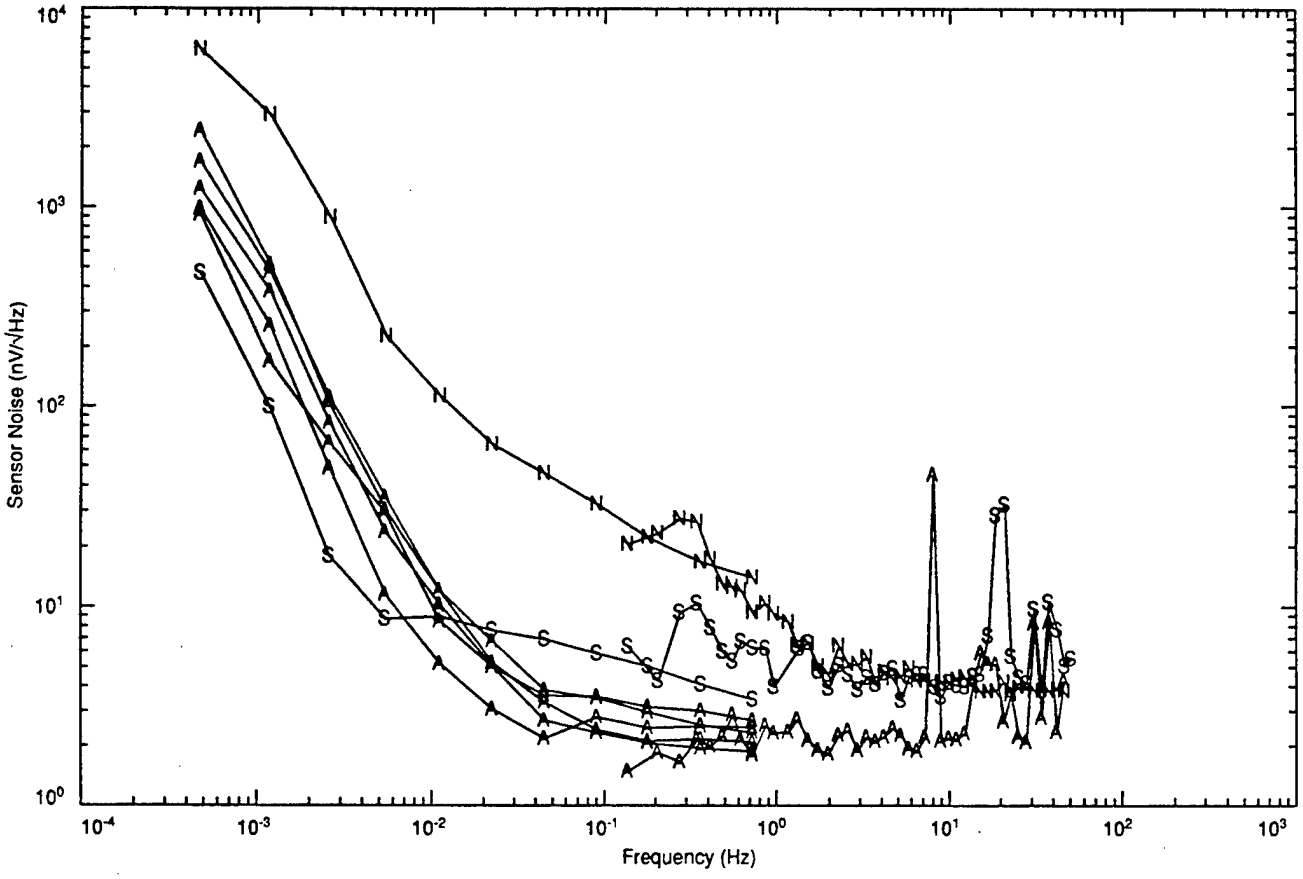

Figure 6.2 Electric field sensor noise in tank. N denotes the NSWC sensor, A denotes several APL-UW sensors, and S denotes the SAIC sensor.

salt water tank with three different filters at the K-1801 input. Figures D.11 and D.12 show the NSWC system spectra with the big and small loop areas. Figure D.13 shows the SAIC system spectra.

Three figures in Appendix D show spectra of the three systems, APL, NSWC and SAIC respectively, when a signal is impressed in the tank. A 14.71 Hz square wave ±10 μA current drive from the Keithley 220 programmable current source was impressed.

The rolloff in frequency for the harmonics of the signals is very close to the predicted values for a square wave.

7. CONCLUSIONS AND RECOMMENDATIONS

A measurement system was developed around a suite of Keithley Instruments devices, environmental baths, computers, and data acquisition software. Typically, an electrode pair or electric field sensor was periodically connected to a preamplifier/voltmeter which provided the reading(s) to a computer operating custom acquisition software.

The measurement system performed very well, being only a few decibels more noisy than the theoretical limit set by Johnson noise for source impedances of 100 Ω. Considering the multitude of noise sources present in a typical laboratory setting, it is remarkable that the evaluations were conducted with such low noise interference. Measurement system performance was typically better than 2 nV/$\sqrt{\text{Hz}}$. Many of the electrodes exhibited noise levels less than this value at some frequency, often a few tens of millihertz for the best ones. The systems tested attained 2 to 4 nV/$\sqrt{\text{Hz}}$ at some part of their spectrum. In order to achieve this performance in the bands of interest, it was necessary to install a one-pole, RC filter on the input to the Keithley 1801 preamplifier. It was observed that out-of-band interference was contaminating the band of interest. This filter added 100 Ω to the series resistance of the sources, the electrode pairs in salt water.

Performance tests of the instrumentation demonstrated the system noise level. To ensure high-quality measurements throughout the observational period, resistor voltages were measured along with electrodes and electric field sensors. Periodically, resistors were used in place of electrodes in the measurement schemes to determine measurement noise exclusive of electrode noise.

All electrodes were tested for inherent noise, and selected electrodes were combined with a preamplifier to evaluate electric field sensor noise. Electrodes were provided by the Naval Surface Warfare Center (NSWC), Science Applications International, Inc. (SAIC), and the Applied Physics Laboratory of the University of Washington (APL-UW). While the SAIC and NSWC systems provided their own preamplifiers, the APL system used a commercial preamplifier, the Keithley 1801. The APL electrodes/electric field sensor served as a reference for the NSWC and SAIC electrodes and systems.

The isothermal electrode tests exhibited noise levels of about 2 nV/$\sqrt{\text{Hz}}$ for SAIC and APL electrodes and 3 nV/$\sqrt{\text{Hz}}$ for NSWC electrodes. Although each of the different systems tested in the salt water tank had different characteristics, the noise in all the systems was less than 4 nV/$\sqrt{\text{Hz}}$ in *some* frequency band.

Evaluation of Electrode Tests

Pairs of electrodes were installed in glass jars containing salt water, submerged in an isothermal bath, and monitored with a low-noise preamplifier/voltmeter. The electrodes were usually attached to a 16-channel, differential scanner which periodically connected pairs of electrodes to the preamplifier/voltmeter. High-frequency measurements were conducted while the scanner remained on a given channel.

In order to assess measurement noise, we had installed four resistors in a jar identical to that used for the APL electrodes and put them in the bath along with the electrode

jars. The intention was to have the same wire lengths and routing and, thus, the same amount of pickup from interference sources in order to assess the quality of the electrode measurements. Spectra from these resistors at each of the above temperatures are shown in Figures B.13 to B.16. Between 1 mHz and 1 Hz, the lowest graph in each of these four figures is that of the 20 Ω resistor in the jar. Between 1 Hz and 1 kHz, only a 20 Ω resistor spectra is shown.

The 20 Ω resistor spectra are a bit below 2 nV/$\sqrt{\text{Hz}}$ for most of the frequency range. Recalling that there is a 100 Ω resistor in the 320 Hz low-pass filter added to the 1801 input, this is virtually the same as the 1801 specification of 1.8 nV/$\sqrt{\text{Hz}}$. This confirms that the experimental setup was operating at its expected performance. A comparison of system performance vs theoretical Johnson noise is shown in Figure 3.7.

The electrode measurements are only slightly above the theoretical Johnson noise, which varies among electrode assemblies according to their resistances. We were told that the SAIC electrode assembly has a resistance of about 80 Ω. This resistance has Johnson noise of about 1.2 nV/Hz. The APL electrodes are about 10 Ω, which corresponds to 0.4 nV/$\sqrt{\text{Hz}}$. We were told the NSWC electrodes are about 150 Ω, which corresponds to 1.7 nV/$\sqrt{\text{Hz}}$. Each electrode pair had a effective impedance that was over 100 Ω greater because of the series resistances of the scanner (about 20 Ω) and the input filter we added to suppress noise (100 Ω).

One of the principal conclusions of the electrode tests is that the inherent noise of some electrode pairs is not much greater than the noise of the measurement system. Only at lower frequencies do the best of the electrode pairs exhibit noise significantly greater than expected for their equivalent resistances plus system contributions. That is, above a certain frequency each electrode pair produce signals about equivalent to their Johnson noise and measurement system noise. This means that electric field performance is not limited by noise processes that are inherent to the electrodes, such as random electrochemical reactions, but is controlled mostly by stochastic Johnson noise, deterministic temperature and salinity variations at the electrode, and amplifier noise (current and voltage noise).

A summary of electrode performance must be stated in terms of the energy observed above that expected system noise. Over the entire measurement bandwidth from 1 mHz to 1 kHz, the SAIC electrodes exhibited the lowest noise performance. At 1 mHz, the SAIC electrodes are more than 20 dB quieter than the APL and NSWC electrodes. Above 10 mHz, SAIC electrode measurements show only measurement noise, about 2 nV/$\sqrt{\text{Hz}}$. The APL electrodes reach the noise floor at 40 mHz and 2 nV/$\sqrt{\text{Hz}}$. The NSWC electrodes measure about 3 nV/$\sqrt{\text{Hz}}$ above 1 Hz. The NSWC electrodes are much noisier than SAIC electrodes below 1 Hz. Between 1 mHz and 1 Hz, the APL electrodes are quieter than the NSWC electrodes. The higher noise floor of the NSWC electrodes is probably because of their higher resistances.

Frequency spectra of the isothermal electrode noise tests are shown in Figures D.1 to D.12. The first four show the APL electrode noise during the three isothermal tests, 4°C, 10°C, and 15°C, and the final test from 17 to 19°C with the bath controller off. The next two groups of four are for the NSWC and SAIC electrodes for the same temperatures.

All the electrodes show a highly red spectrum at low frequencies: there is much more variance at lower frequencies than at higher frequencies. The level at which the measured spectra level out is the instrumentation noise exclusive of the electrodes.

The NSWC electrodes have a much shallower sloped spectrum than the APL and SAIC electrodes. They reach the instrumentation noise level two decades higher in frequency than the SAIC electrodes and a decade and a half above the APL electrodes. The spectral slopes of the electrodes are curious. The APL electrodes have very steep spectral slopes, SAIC less so, and NSWC even less so.

We find it surprising that the NSWC electrode measurements show spectra so different from the APL electrodes. The NSWC electrode assemblies are made using In Vivo Metric electrodes. Previous APL tests have used IVM electrodes and found them to be noiser than the APL electrodes but not so much so as shown here. This difference could be caused by the electrical conditioning that NSWC performs on their electrodes or by the drying of the electrodes after matching pairs for low offset voltage.

As the experiment progressed, there was a slight decrease in noise levels of the NSWC and APL electrodes. This is an expected result that occurs as electrodes age. The SAIC electrodes did not show this behavior since they were aged already. The NSWC electrodes arrived dry on the outside. They may have been wet on the inside, but we did not have any means for checking that. The SAIC electrodes arrived in their bottles of NaCl solution. They had been kept in this solution for months prior to this. Many of the APL electrodes had been stored wet. Some had not. Some were recently manufactured. Within each electrode group (i.e., NSWC, APL, and SAIC), the performances of individual electrode pairs are similar.

The following table presents the noise level and frequency at the point where the electrode spectra merge with system noise. This is the frequency at which the electrode noise becomes less than the measurement system noise. Above these frequencies, the electrode noise is equal to or less than the measurement noise.

Table 7.1. Electrode Noise Floor Frequencies

Type	Noise ($nV/\sqrt{Hz}$)	Frequency
SAIC	1.8-2.5	10 mHz
APL	2-3	40 mHz
NSWC	3-4	1 Hz

We cannot explain the very different behavior of the NSWC electrodes. We do not know what factors in construction, treatment, and maintenance contribute to the different spectral slope of these electrodes.

One NSWC electrode pair is much worse than the others, and after the first test at 4°C, another one is much better. The better one is an electrode pair that was provided by NSWC after the experiment began. It is the NSWC electrode pair used later in the tests in the large sea water tank.

For the last test with the bath controller turned off, the best electrodes had been removed from the bath to be installed in the sensors that were to be put in the large tank for the second part of the experiment. The spectral levels of the remaining electrodes while slowly warming are less than the removed good ones were when "isothermal." This indicates that the "isothermal" tests may not have had temperature regulated tightly enough. The electrodes are very sensitive to temperature. We had not anticipated that the electrodes would be so quiet and sensitive below 10 mHz that we could see the temperature noise of the bath. Also, turning the controller off stopped a known source of EMI.

Spectral values of data taken in the last bath test while it was slowly warming with the controller off are tabulated below. For the low-frequency band, this condition was found to provide low temperature noise and, thus, low electrode noise. For the high-frequency band, it provided relief from the temperature controller electrical noise. The data for high-frequency and low-frequency bands were taken on two different dates (hence the break in the table). Data from 1 mHz to 1 Hz were taken on November 30. Data from 1 Hz to 1 kHz were taken on November 10. One NSWC and one APL electrode pair were obviously much noisier than their mates and are not included in Table 7.2. At this stage of the tests, the best SAIC electrode pair and the best two APL electrode pairs had been removed from the bath in preparation for the system tests.

Table 7.2. Electrode Noise Levels ($nV/\sqrt{Hz}$)

Frequency	NSWC	APL	SAIC
1 mHz	100-200	40	6-15
2 mHz	60	12	2.5-4
10 mHz	30	3	2
100 mHz	3-5	1.8	1.8
0.7 Hz	2.7	1.7	1.7
1 Hz	3	2	2
10 Hz	3	2	2
100 Hz	3	2-3	2.5
1000 Hz	3	2.5	2.5

The SAIC electrodes were the quietest. They were quieter than APL electrodes from 1 mHz to 40 mHz. At frequencies higher than 40 mHz, the SAIC and APL electrodes dropped into the measurement noise of about 1.8 $nV\sqrt{Hz}$ in the low-frequency

band and 2 to 2.5 nV/$\sqrt{\text{Hz}}$ in the high-frequency band. The NSWC were much noisier, especially at frequencies less than 100 mHz.

As the tests progressed, the electrode noise levels decreased somewhat. We attribute this to electrode aging since that has been the case in previous tests. Although the electrode tests were performed at different temperatures, colder to warmer, the results do not indicate a significant dependence of electrode noise on absolute temperature.

Evaluation of System Tests

Electric field sensors and amplifiers were installed and operated in a salt water tank at the end of the electrode testing. Sections 5 and 6 present information about the installation and operation of the sensors and systems. Systems or sensors from SAIC, NSWC, and APL-UW were operated for more than 30 days. The salt water tank was not temperature or salinity controlled.

The relative performances of the sensors and systems depend on frequency. Over some frequency band, each unit showed superior performance. For example, the SAIC system is better than the APL sensors with the Keithley amplifier for frequencies below 0.1 Hz. Above 1 Hz, and between the spurious response frequency lines (spurs), the APL system with the Keithley 1801 preamplifier is quieter than the SAIC system. As expected, the NSWC system is much noisier than the SAIC and APL systems below 1 Hz, but it equals the performance of the SAIC system from 1 Hz to about 50 Hz. In this band, the spurious tones produced by the SAIC and Keithley amplifiers are very noticeable, and there the NSWC system provides the best overall performance.

It is interesting that the NSWC system is so quiet between 1 and 50 Hz. This would not be expected from the specifications of the parts used in the NSWC amplifier. However, we are told that critical parts of the NSWC amplifier are individually selected for low noise.

Table 7.3 summarizes the noise levels of the systems as a function of frequency. It is shown in the same format and for the same frequencies as the electrode noise table, Table 7.2. Contributions from spurious emissions are not included in this table, but they are significant for the APL and SAIC systems, as explained below.

Table 7.3. System Noise Levels (nV/$\sqrt{\text{Hz}}$)

Frequency	NSWC	APL	SAIC
1 mHz	500–5000	60–400	50–100
2 mHz	400–2000	40–80	25
10 mHz	100–150	5–15	8
100 mHz	30–40	2.5–4	6
0.7 Hz	15	2–3	3.5
1 Hz	6-9	2.5	4–15
10 Hz	4	2.5	3–8
100 Hz	4	2.5	3–5
1000 Hz	n/a	2.5	2.5–4

At frequencies above 1 Hz, the system noise is comparable to the electrode noise in the isothermal tests. On the other hand, below 1 Hz each system is noisier. Part of the increased noise in the large salt water tank could be caused by the SAIC and NSWC amplifiers used and part of could be caused by the environment acting on the electrodes. The amplifier for the APL system is the same Keithley 1801 used for the isothermal tests.

Some of the noise increase is the electrode response to temperature fluctuations. The amplifier for the APL system is the same as that for the isothermal tests, so any increase in noise for the APL system can be attributed to environmental effects on the electrodes, probably mostly temperature fluctuations. It could be that motional induction from tank water slowly circulating through the earth's magnetic field is a contributor. Salinity variations have been highly reduced in all systems by restricting the water exchange at the electrodes: APL uses agarose plugs, NSWC uses fiberglass lagging, and SAIC uses porous plugs.

Electrodes are known to have higher noise levels with increased temperature variability. This effect shows up mostly at low frequency because the thermal mass of the tank slows the temperature fluctuations, allowing only low-frequency temperature forcing to be applied to the electrodes. The electrode tests showed that the APL electrodes had a higher sensitivity to temperature than the SAIC electrodes. This could explain the higher noise level for the APL electrodes than for the SAIC electrodes in the salt water tank.

Another obvious noise producer is the amplifier. Amplifiers that are not chopper stabilized exhibit "one over f" noise at low frequencies. The noise increases with decreasing frequency. The NSWC amplifier is such an amplifier. Its noise increases dramatically at low frequencies. At low frequencies the NSWC system is much noisier than the NSWC electrodes were in the isothermal tests. From the electrode tests, the noise of the APL electrodes and that of the NSWC electrodes are about the same at 1 mHz, so elevated noise of the NSWC system is certainly due to the amplifier.

One of the first things that one notices about the system spectra, in Appendix D, is that there are many spurious responses (spurs) in the high-frequency band. These are a result of the amplifiers being used. The electrodes don't have such emissions.

Two of the amplifiers have many spurious responses (spurs) below 180 Hz. The Keithley 1801 amplifier used in the APL system is the most obnoxious, with with about five spurs below 50 Hz. The first is at about 7 Hz. The SAIC system is somewhat better in this respect. There are fewer spurs and the first is at a higher frequency, about 20 Hz. The NSWC system is excellent in this respect, having no spurs below 180 Hz.

Excluding the spurious tones, the Keithley 1801 preamplifier as used in the APL system is quite a bit quieter and less variable than the SAIC system. Offsetting this is the fact that the SAIC system is the only one that operates at low power on internal batteries. There is a tendency for low-noise devices to require high power, thus the SAIC system is quite remarkable.

The NSWC system is much noisier than the other systems for frequencies below 1 Hz. However, between 1 Hz and 100 its noise level is comparable to the SAIC system's noise between spurious tones. The NSWC system has a distinct advantage in this regime, since its first spurious tone is at about 180 Hz.

Overall, the SAIC system is a bit better than the APL sensor with the K-1801. Its noise at frequencies below 10 mHz is as good as or better than the APL one. At high frequencies, the Keithley 1801 preamplifier used in the APL system contributes many spurious tones between 7 and 60 Hz. The good low-frequency performance of the SAIC system is because of the good SAIC electrodes. The Keithley 1801 preamplifier used in the APL system is much better than either the APL or SAIC system performance, and yet the APL system is noisier at low frequencies.

The only system that can be considered close to operational as provided for these tests is the SAIC system. The SAIC system is the only one with an underwater unit that is capable of being deployed in the ocean. The APL and NSWC systems have amplifiers above water and powered from the AC mains. The SAIC system used batteries, both below and above water. Presumably, there is a version of the NSWC amplifier that has been configured for in-water deployment. It is possible to install the K-1801 preamplifier in an underwater housing, but power and connections to the K-2001 voltmeter would be required.

However, it should be pointed out that we had significant difficulty obtaining quiet operation from the SAIC system. This was discussed earlier in Section 5 in more detail and is apparent in Figure D.13. The result is that the HF spectra from the SAIC system vary quite a bit in amplitude whereas those from the APL and NSWC systems are quite stable.

The SAIC system is not exactly what they use in the field. Their field system has several data receivers, anti-aliasing filters, and analog-to-digital converters in one package. The system we tested was specially built by SAIC for these tests to provide ±5 V outputs so that a commercial digital voltmeter could be used. The method of transmitting the data up the cable uses a current loop. This compensates for changes in the cable resistance as well as allowing a low-resistance load to be used in the data receiver to reduce the crosstalk.

The NSWC system tested appears to be a copy or a sample of part of the operational system. The output of the NSWC amplifier is ±5 V, which we sampled with a commercial digital voltmeter. The actual system would need a method of transmitting the potential over a long cable without significant crosstalk. Unless the signals are loaded significantly at the data receiver, the crosstalk can be severe. The coupling between data cables depends on frequency.

The SAIC system and the APL system showed quite a number of spurious responses in the HF band. Very significant APL system spurs occur at about 7, 14, 20, 30, 35, and 45 Hz and many at higher frequencies. Most of these appear to be aliases of the harmonics of the chopper frequency. The sampling is at 2000 Hz and the chopper runs at 287.2 Hz. The SAIC system has fewer spurs. These occur at 20, 30, and 40 Hz and many at higher frequencies. The NSWC system has far fewer spurs. The lowest-frequency spur occurs at about 180 Hz.

Summary of Results

The tests were successful at determining the inherent noise of electrodes and evaluating the performance of electric field sensors and amplifiers. It was shown that the SAIC electrodes exhibited the lowest broadband noise. The APL electrodes had comparable performance at frequencies above 40 mHz. At lower frequencies, it is thought that the SAIC electrodes benefitted from additional buffering (lagging) provided by their plastic enclosures. The APL electrodes where suspended openly in the glass jar and were subject to small thermal fluctuations at low frequency. The NSWC electrodes were substantially noisier than the others at frequencies lower than about 1 Hz. No explanation is known for this behavior.

System tests confirmed superior performance of the SAIC system, especially at low frequency. This system was, however, difficult to maintain in its lowest noise state. Small changes to cable layout produced large changes in noise performance. Also, the performance changed for no apparent reason from day to day. The NSWC system did not perform well at frequencies below about 1 Hz, but it showed very good and tone-free performance in the 1–50 Hz band. The APL sensor was operated with the K-1801/K-2001 and provided a standard for comparison. The Keithley instruments provided the best broadband amplification but produced a number of spurious tones.

Improvements could be made in the procedures and instrumentation used in these tests. For example, we suggest:

- Arrange the equipment so the K-1801 doesn't need a 100 Ω resistor at the input for a filter.
- Obtain a more tightly controlled bath or use a tank with more insulation so it drifts in temperature more slowly.
- Use anti-alias filters for HF spurs.
- Conduct measurements in a large Faraday cage.
- Dispense with the scanner and use separate preamplifiers and anti-alias filters for each electrode pair.
- Use different sample rates in the HF regime to determine and side-step aliases.
- Use power line cycle integration for sample rates up to 30 Hz.

8. REFERENCE

1. Keithley, J.F., J.R. Yeager, and R.J. Erdman, "Low Level Measurements", Keithley Instruments, Cleveland, Ohio, 1984, third edition.

ELECTRODE AND ELECTRIC FIELD SENSOR EVALUATION

APPENDICES

APPENDIX A: Electrode Time Series

Electrode Test Setup

Three different types of electrode assemblies were tested in a constant temperature bath. SAIC provided electrodes as manufactured by Subspection, Ltd. They were removed from their normal underwater sensor housing and repackaged in amber glass bottles. The electrodes were left in their small PVC mounting block and electrode housing. New heavy-gauge insulated copper wires were attached to the electrodes and a waterproof seal was provided at the exit of the wires from the jar. Figure 3.1 shows the SAIC electrode assembly.

NSWC provided Ag-AgCl electrodes manufactured by In Vivo Metric Systems. These electrodes were IVM type E211-X having a diameter of about 8 mm and a thickness of 1 mm. NSWC constructed a custom assembly which held the electrode as well as lagging material to buffer the electrode from temperature and salinity variations. Figure 3.2 shows the NSWC electrode assembly. The lagging consists of five layers of fiber glass cloth held in place by a perforated disk of printed circuit board material.

APL-UW provided electrodes of their own manufacture. They are a thermally fired type of Ag-AgCl electrode having a diameter of 12 mm and a thickness of 4 mm. Pure silver wire (1/32" diameter) is embedded in the Ag-AgCl matrix and provides the electrical connection between the electrode material and the copper wires leading to the measurement equipment. Figure 3.3 shows the APL-UW electric field sensor assembly.

Gas-free copper-to-copper connections

Most of the connections made by APL-UW personnel in the low level sections of the tests were made with various gas-free copper-to-copper connections. These connections are recommended by Keithley Instruments as providing the lowest noise connections. Keithley [1] states that the copper to copper thermoelectric potential is less than 0.2 μV per °C. They are affected very little by temperature changes. By excluding oxygen from the actual copper-to-copper contact, copper oxide formation was thus prevented. Copper oxide has a very high thermally induced voltage and so is very detrimental to low noise work.

Low thermal coefficient Cd/Sn solder was used in some of the connections between NSWC cables and their extensions. Ordinary Pb/Sn solder to Cu junctions have thermoelectric potentials of 1 to 3 μV per °C while Cd/Sn to Cu junctions are much less, about about 0.3 μV per °C.

The connections between cables used small pure copper crimp splice parts purchased from Keithley by ordering model 1483 "Low Thermal Connection Kit". The inside hole of each splice part was reamed with a small drill bit just before crimping to remove the copper oxide. The wire being attached is burnished with 3M, Inc., Scotch-Brite. In the case of connecting to tinned wire, the tinning was scraped off to expose bright copper and then a copper crimp connector was applied.

The connections between cables and instrumentation used pure copper lugs from the connection kit purchased from Keithley. These were crimped onto the cable and then bolted or screwed to the instrumentation. All the low noise instrumentation had pure copper threaded binding posts with pure copper nuts or pure copper pads and pure copper screws. The copper binding posts and nuts and screws of the instrumentation were burnished until shiny.

As we discovered several times, it pays to be diligent about the oxide removing procedure. A bad connection is very noisy and takes significant time to find and cure. A good connection is very quiet. In addition, reconfiguring the cabling attachments is time consuming because of the burnishing required.

Whenever possible, the copper-to-copper connections were protected from rapid temperature changes by encasing them in thermal insulation. This is an effort to reduce thermally induced noise.

Low noise cabling

Special low-noise cable was purchased from Keithley for all low-level cabling runs except when cables were furnished by the electrode suppliers already attached to their electrodes. Two types of Keithley cable were used: product numbers 7168-316 and SC-22. The former is a shielded twisted pair utilizing solid #22 AWG wire and a vinyl jacket. It can also be ordered as Belden M-YM23112 NM. The latter is a triaxial cable with a center conductor, a coaxial return and finally an outer shield. Both are recommended for low noise applications. The APL electrodes were connected using twisted shielded pairs while the NSWC extension cables were triaxial.

Scanner, amplifier, voltmeter

A block diagram of the electronic test setup for electrode testing in the isothermal bath is shown in Figure 3.6. A 16-channel scanner (Keithley 705) alternately connects sources to a preamplifier (Keithley 1801) which is followed by a voltmeter (Keithley 2001). Hereafter, these two instruments are denoted as K-705, K-1801, and K-2001.

The electrodes were paired and the self-potentials for these pairs were measured over a several week period prior to being installed in the bath. In order to accommodate the twelve pairs of electrodes being measured an input multiplexer (scanner) was used. We chose the K-705 scanner equipped with two Keithley 7168 nanovolt scanner cards for the input multiplexing. Each K-7168 scanner switch card accommodates eight differential sources. A total of 16 pairs of electrodes could thus be accommodated. Several of the channels were dedicated to monitoring the performance of the scanner switches and the low-noise amplifier and were not connected to electrode pairs. The K-705 scanner mainframe has no pertinent specifications and is simply a housing and control panel and IEEE-488 interface for the scanner cards. The most critical piece of the test setup is the input multiplexer switch because any error voltages produced by the switch are added directly to the self potentials being measured. The specifications for the K-7168 nanovolt scanner card are shown in Table A.1. The most important specification is the contact potential and its variability with temperature. The contact potential is a

Table A.1 Specifications for the Keithley 7168 scanner card used to multiplex different electrode pair signals to the low noise Keithley 1801 preamplifier. For our experimental setup the important specification is contact potential and its variability with temperature. With the low impedances presented to this card the specified input leakage current becomes insignificant.

SPECIFICATIONS

MODEL 7168 nV SCANNER CARD

CHANNELS PER CARD: 8

CONTACT CONFIGURATION: 2 poles per channel, input HI and LO.

CONNECTOR TYPE: Screw terminal to bare copper printed circuit pad.

MAXIMUM SIGNAL LEVEL: 10V, 50mA, peak (resistive load)

CHANNEL TO CHANNEL CROSSTALK: −46dB (typical) at 1KHz with 20KΩ terminations.

CONTACT RESISTANCE: <12Ω

CONTACT POTENTIAL (HI to LO) BETWEEN CHANNELS: <30nV when properly zeroed with supplied leads (see manual for recommended procedure). Typically <60nV without zeroing.

Temperature Coefficient: <6nV/°C between channels

CONTACT TYPE: Solid-state JFET switch

ACTUATION TIME: <3ms, exclusive of mainframe

INPUT LEAKAGE: <50pA per channel at 23°C

INPUT ISOLATION: >10⁹Ω, <40pF between any input terminals or between any input terminal and earth.

COMMON MODE VOLTAGE: 30V peak

MAXIMUM VOLTAGE BETWEEN ANY TWO TERMINALS: 10V

GENERAL

WARMUP: 2 hours in mainframe for thermal stability.

ENVIRONMENT,

Operating: 0° to 40°C, up to 35°C at 70% RH

Storage: −25°C to 60°C

DIMENSIONS, WEIGHT: 32mm high × 114mm wide × 272mm long (1¼" × 4½" × 10¾"). Net weight 0.53kg (18.5 oz.)

ACCESSORIES SUPPLIED: 7168-316 Input Cable, Eight supplied
Model 1507 Input Cable

ACCESSORY AVAILABLE: Model 1483 Low Thermal Connection Kit

voltage that is added in series with the signal being measured. The switch contact in this scanner card is a solid-state JFET (Junction Field Effect Transistor) transistor. Since this switch contact is placed in the circuit before any amplification, any error voltages generated in the switch will be amplified along with the electrode signals by the subsequent low-noise preamplifier. The specifications state a maximum static error voltage of 30 nV and a variability of 6 nV per °C. Since the switch runs at ambient room temperature the variability of contact potential (error voltage) will presumably track temperature variations in the laboratory environment. Other scanner performance limitation, such as leakage current and crosstalk were not problems because the source impedances were so low, less than 100 Ω.

After passing through the appropriate scanner switch the electrode signal is amplified by a Keithley 1801 nanovolt preamplifier. Table A.2 shows some of the pertinent specifications of the K-1801 preamplifier. Since many of the electrode pairs had self potentials greater than 200 μV the K-1801 preamplifier was set to its lowest gain which provided a 2 mV full scale range. The K-1801 also provides an analog low pass filter with switchable corner frequencies. When we operated the test facility in the continuous slow scan mode, the 1801 was operated with the filter set to provide a passband of DC to 3.2 Hz. We used the thermally insulating foam box that Keithley furnished for the K-1801 since the K-1801 specifications assume its use.

After switching the scanner channel, we were able to use the output of the preamplifier after waiting about 1 s for the output to settle. At first the preamplifier settling took many seconds, but by adding a 1 MΩ resistor across the preamplifier input the settling time was much reduced. The resistor supplied the input bias current to the preamplifier while the scanner was briefly open circuit while between channels. This prevented the input potential from rising above a point where a long recovery time was required. With this modification, the output of the preamplifier settled within 1 s after a channel change.

The scanner left the unused electrode pairs open circuit when not being sampled. It is our understanding that some electrode systems are designed to short the electrodes when they are not in use. We did not do that.

The noise level of the K-1801 preamplifier was measured by connecting it directly to Vishay Inc. precision low-noise resistors. Several values were used in the range of 10 Ω to 2 kΩ. Low-thermal-EMF crimped copper lugs were attached to the resistors, and these lugs were cleaned and used to attach to the pure copper binding posts used on the K-1801 input. This type of connection provides the lowest noise at frequencies less than 1 Hz.

In order to have the K-1801 equal or better the specified noise in the laboratory environment, additional input filtering was required. It was determined that EMI and RFI noise was upsetting the low noise behavior at low frequencies. A single-pole RC low pass filter was added to the input of the K-1801 using the low thermal EMF connection technique previously described. The filter consisted of a 5 μF metalized polycarbonate film capacitor across the input terminals with a series 100 Ω low-noise resistor. This combination provides a 3-dB corner frequency of about 320 Hz for 10 Ω electrode resistances.

Table A.2 Specifications for the Keithley 1801 low noise nanovolt preamplifier used in this experiment. The pertinent specifications have been highlighted. Only the 2 mV range was used. Measured performance equaled or exceeded the specifications.

GENERAL NOTES:

1. The Model 1801 Nanovolt Preamp consists of a power-supply card that plugs into the Model 2001 scanner slot, the remote nanovolt preamp, and a 3 meter cable to connect the two.
2. The Model 1801 Nanovolt Preamp is specified only for use with the Model 2001 Multimeter. Specifications are based on the published Model 2001 performance and are referenced to the 1801 Nanovolt Preamp input. It is assumed the Model 2001 used with the nanovolt preamp is properly calibrated.
3. 1801 Nanovolt Preamp specified calibration interval is 1 year.
4. The Model 2001 checks for the presence of the nanovolt preamp on power up. If the nanovolt preamp is detected, the front panel menu tree is adjusted accordingly. A subset of the 2001 functions are active with ranges as follows:

FUNCTION	RANGES AVAILABLE
DC Volts	20μV, 200μV, 2mV.
DC Volts Peak Spikes	Not Available.
AC Volts Low Frequency rms	500μV rms.
AC Volts Normal rms Average Peak, Crest Factor	Not Available.
DC Current	Not Available.
DC In-Circuit Current	Not Available.
AC Current	Not Available.
2-Wire Ohms	Not Available.
4-Wire Ohms	2mΩ, 20mΩ, 200mΩ, 2Ω, 20Ω, 200Ω.
Frequency	Available for Limited Frequency Range.
Temperature	Only Differential Thermocouple Temperature is Specified. RTD Not Available.

DC VOLTS

DCV ACCURACY[1]

RANGE	FULL SCALE	7½ DIGIT RESOLUTION	DEFAULT RESOLUTION	ACCURACY[2] ±(ppm of reading + ppm of range) 24 Hours[3]	90 Days[4]	1 Year[4]	2 Years[4]	TEMPERATURE COEFFICIENT ±(ppm of reading + ppm of range)/°C Outside TCAL ±5°C
20 μV	±21.000000	1 pV	10 pV	300 + 60	450 + 60	460 + 60	470 + 60	40 + 13
200 μV	±210.00000	10 pV	100 pV	200 + 20	250 + 20	260 + 20	270 + 20	40 + 2
2 mV	±2.1000000	100 pV	1 nV	200 + 6	250 + 6	260 + 6	270 + 6	40 + 2

DC VOLTAGE UNCERTAINTY = ± [(ppm of reading) × (measured value) + (ppm of range) × (range used)] / 1,000,000.
% ACCURACY = (ppm accuracy) /10,000.
1PPM OF RANGE = 2 counts at 6½ digits.

INPUT CHARACTERISTICS (HI to LO):

Input Bias Current: Adjustable at preamp to <20pA. Temperature drift less than 25pA/°C.

Zero Drift: Typical variation of zero reading with low thermal short (see Instruction Manual) is less than 10nV/5nV/°C. (24 hours, TREF± 1°C, 1 PLC, 10-reading digital filter).

DC Input Resistance: >1GΩ.

Transient Input Resistance: >1kΩ 1ms after step input. >10MΩ 4s after step input.

Linearity: <4 ppm of range non-linearity, exclusive of zero offset and noise.

Isolated Polarity Reversal Error: <4 counts at 6½ digits, exclusive of zero offset and noise.

Maximum Input Levels: 1V or 100 mA peak.

Overload Recovery: 1s for <10mV overload, 1 minute for ≥ 10mV overload.

COMMON MODE ISOLATION (input LO to 2001 chassis ground):

Isolation Impedance: 1GΩ in parallel with 1nF.

Maximum Common Mode Voltage: 41V peak.

Common Mode Current: <15nA p-p at 50 or 60Hz.

NOISE REJECTION (dB):[2]

CMRR:[1] 175dB for DC, 50 or 60 Hz ± 0.1%, common mode signals up to 5V p-p AC. 41V p-p AC+DC.

NMRR (at 50 or 60 Hz ± 0.1%, NPLC ≥ 1, Line Sync OFF):

FILTER:	SLOW	MEDIUM	FAST
20 uV Range	90 dB	80 dB	60 dB
200 uV Range	90 dB	80 dB	60 dB
2 mV Range	90 dB	60 dB	60 dB

Effective noise is reduced by a factor of 10 for every 20dB of noise rejection (60dB reduces effective noise by 1,000:1).

CMRR is rejection of undesirable AC or DC signal between LO and earth. With a 1Ω imbalance in the LO lead.

NMRR is rejection of undesirable AC signal between HI and LO.

PREAMP SETTLING CHARACTERISTICS (nominal, ± 20%):

FILTER:	10% to 90% Rise Time SLOW	MEDIUM	FAST
20 uV Range	10 s	1 s	10 ms
200 uV Range	1 s	100 ms	2 ms
2 mV Range	100 ms	10 ms	500 μs

ZERO SUPPRESSION: Adjustable ± 100μV at preamp. 2001 front panel suppression using REL.

INPUT NOISE (with low thermal short): Equivalent noise resistance of 20Ω. There is no 1/f component, 1PLC integration.[5]

FILTER:	Input Noise SLOW	MEDIUM	FAST
20 uV Range	0.6 nV p-p	2 nV p-p	30 nV p-p
200 uV Range	2 nV p-p	9 nV p-p	40 nV p-p
2 mV Range	6 nV p-p	20 nV p-p	90 nV p-p

MAXIMUM SOURCE RESISTANCE: 10kΩ.

DC VOLTS NOTES:

1. Specifications are for 1 PLC, Auto Zero on, 10-reading digital filter, Preamp on SLOW filter.
2. When properly zeroed (using zero adjustment initially then REL according to procedure in Instruction Manual) every 20 minutes or whenever the ambient temperature changes by more than 1°C.
3. For TCAL ± 1°C, following 15-minute preamp warmup. TCAL is ambient temperature at calibration which is 23°C from factory.
4. For TCAL ± 5°C, following 15-minute preamp warmup. Specifications include factory traceability to US NIST.
5. For source resistance Rs above 1Ω multiply noise by $\sqrt{\frac{20 + Rs}{20}}$

The 1801 is sensitive to AC magnetic fields. The specifications indicated that it should be mounted away from any power transformers and AC magnetic fields. The CRT monitor has a large magnetic field from the deflection coil circuitry. We installed the K-1801 about eight feet above the floor over the computer and instrumentation cart.

The output of the K-1801 preamplifier was applied to the input of a Keithley 2001 digital voltmeter. This digital voltmeter has a special options slot which accommodates the K-1801 preamplifier interface card. This special interface card provides extra power supply isolation and common mode rejection for the preamplifier. It also stores calibration coefficients unique to the K-1801 (e.g., gain and zero offsets). Table A.3 shows some of the pertinent K-2001 specifications for the DC volts function that we were using. The K-1801 preamplifier specifications for DC volts accuracy in Table A.2 are based upon the assumption that a K-2001 DVM will be used to digitize the preamplifier output. The absolute accuracy of the K-1801/K-2001 combination is specified for 90 days as: $\pm 250\times10^{-6}$ times the reading plus or minus 12 nV at constant temperature. As an example, a 200 μV signal has an absolute accuracy of -62 nV. The temperature affects accuracy in the amount of $\pm 40\times10^{-6}$ times the reading plus 2 nV per °C. For our same 200 μV signal the temperature effect on accuracy would be 6 nV per °C. The Keithley 2001 digital voltmeter/K-1801 preamplifier combination provides a resolution of 0.1 nV when operated with a full scale of ±2 millivolts. This resolution is more than adequate to fully evaluate the noise levels of the electrodes.

Low noise, Vishay Inc. precision metal film resistors were used to quantify the instrumentation noise. As the resistor values are increased the noise increases. This is a direct result of Johnson noise, the theoretical thermal noise. Its root mean square (rms) noise voltage of a resistor, V_n, is

$$V_n = (4\,k\,T\,R\,B)^{-0.5}$$

where, k is Boltzmann's constant ($1.38\times10^{-23}\ J\ K^{-1}$), T is absolute temperature (K), R is resistance (Ω), and B is bandwidth (Hz). For a resistor of 120 Ω at 300 K, the Johnson noise is 1.4 nV/$\sqrt{\text{Hz}}$ for a 1 Hz bandwidth. Figure 3.7 shows this effect along with 1801 specifications and some measured data.

The K-1801 specification is 6 nV peak-to-peak (p-p) with a pure copper short on the input while set to the 2 mV range with the slow (i.e., 3.2 Hz) low-pass filter. With the fast (i.e., 700 Hz) low-pass filter, the noise specification is 90 nV p-p. We use the 3.2 Hz filter for the low-frequency sampling and the 700 Hz filter for the high-frequency sampling. Both these filter settings and noise level specifications translate to the same spectral density, 0.67 nV/$\sqrt{\text{Hz}}$. This is computed by assuming the rms value to be one fifth of the peak-to-peak value and dividing the rms. by the square root of the bandwidth. The factor of one fifth is from the K-1801 specifications.

In addition, according to the K-1801 specifications, for source resistances, R_s, greater than 1 Ω the K-1801 noise specification is increased by the factor

Table A.3 Specifications for the Keithley 2001 digital voltmeter. The pertinent specifications have been highlighted. in general, the specifications of the 1801 preamplifier and not those of the 2001 DMM provide the limiting factors with respect to noise and accuracy for our experimental setup.

DC VOLTS

DCV INPUT CHARACTERISTICS AND ACCURACY

RANGE	FULL SCALE	RESOLUTION	DEFAULT RESOLUTION	INPUT RESISTANCE	ACCURACY[1] ± (ppm of reading + ppm of range) 5 Minutes[1,2]	24 Hours[2]	90 Days[3]	1 Year[3]	2 Years[3]	TEMPERATURE COEFFICIENT ± (ppm of reading + ppm of range)/°C Outside TCAL ± 5°C
200 mV[4]	±210.00000	10 nV	100 nV	>10 GΩ	3+3	10+6	25+6	37+6	50+6	3.3+1.5
2 V	±2.1000000	100 nV	1 µV	>10 GΩ	2+1.5	7+2	18+2	25+2	32+2	2.6+0.15
20 V	±21.000000	1 µV	10 µV	>10 GΩ	2+1.5	7+4	18+4	24+4	32+4	2.6+0.7
200 V	±210.00000	10 µV	100 µV	10 MΩ ±1%	2+1.5	13+3	27+3	38+3	52+3	4.3+1
1000 V	±1100.0000	100 µV	1 mV	10 MΩ ±1%	10+1.5	17+6	31+6	41+6	55+6	4.1+1

DC VOLTAGE UNCERTAINTY = ±[(ppm of reading) × (measured value) + (ppm of range) × (range used)] / 1,000,000.

% ACCURACY = (ppm accuracy)/10,000.

1 PPM OF RANGE = 2 counts for ranges up to 200V, 1 count on 1000V range at 6½ digits.

SPEED AND ACCURACY[5] 90 Days

RANGE	ACCURACY ± (ppm of reading + ppm of range + ppm of range rms noise[10]) 1 PLC DFILT On, 10 Readings	1 PLC DFILT Off	0.1 PLC DFILT Off	0.01 PLC[11] DFILT Off
200 mV[4]	25+6+0	25+6+0.6	25+30+10	100+200+15
2 V	18+2+0	18+2+0.2	18+25+1	130+200+3
20 V	18+4+0	18+4+0.3	18+20+0.5	130+200+3
200 V	27+3+0	27+5+0.3	27+20+0.8	130+200+3
1000 V	31+6+0	31+6+0.1	31+21+0.5	90+200+2

PLC = power line cycle; DFILT = digital filter

NOISE REJECTION (dB)

SPEED (Number of Power Line Cycles)	AC and DC CMRR[6] Line Sync On[7]	Internal Trigger[8]	AC NMRR Line Sync On[7] 25-Reading DFILT On	Line Sync On[7] DFILT Off	Internal Trigger[8] DFILT Off
NPLC = 10	140	120	90	80	60
NPLC ≥ 1	140	120	90	80	60
NPLC < 1	60	50	30	20	0

Effective noise is reduced by a factor of 10 for every 20dB of noise rejection (140dB reduces effective noise by 10,000,000:1).

CMRR is rejection of undesirable AC or DC signal between LO and earth. NMRR is rejection of undesirable AC signal between HI and LO.

DCV READING RATES[9,10]

200mV, 2V, 200V Ranges

NPLC	MEASUREMENT APERTURE	BITS	DEFAULT DIGITS	READINGS/SECOND TO MEMORY Auto Zero Off	Auto Zero On	READINGS/SECOND TO IEEE-488 Auto Zero Off	Auto Zero On	READINGS/SECOND WITH TIME STAMP TO IEEE-488 Auto Zero Off	Auto Zero On
10	167 ms (200 ms)	28	7½	6 (5.1)	2 (1.7)	6	2 (1.6)	6 (4.1)	2 (1.6)
2	33.4 ms (40 ms)	26	7½	30 (25)	9 (7.6)	28 (23)	9 (7.3)	27 (22)	8 (7.2)
1	16.7 ms (20 ms)	25	6½	58 (48)	44 (34)	54 (45)	41 (32)	49 (41)	37 (30)
0.2	3.34 ms (4 ms)	22	6½	214 (186)	127 (112)	183 (162)	104 (101)	140 (126)	88 (85)
0.1	1.67 ms (2 ms)	21	5½	272 (272)	150 (148)	228 (225)	129 (123)	156 (153)	100 (96)
0.02	334 µs (400 µs)	19	5½	284 (287)	156 (155)	230 (230)	136 (134)	158 (156)	104 (103)
0.01	167 µs (167 µs)	16	4½	417 (417)	157 (157)	317 (317)	137 (134)	198 (198)	105 (103)
0.01[11]	167 µs (167 µs)	16	4½	2000 (2000)		2000 (2000)			

20V, 1000V Ranges

NPLC	MEASUREMENT APERTURE	BITS	DEFAULT DIGITS	READINGS/SECOND TO MEMORY Auto Zero Off	Auto Zero On	READINGS/SECOND TO IEEE-488 Auto Zero Off	Auto Zero On	READINGS/SECOND WITH TIME STAMP TO IEEE-488 Auto Zero Off	Auto Zero On
10	167 ms (200 ms)	28	7½	6 (5.1)	2 (1.7)	6	2 (1.6)	6	2 (1.6)
2	33.4 ms (40 ms)	26	7½	30 (25)	9 (8.2)	28 (23)	9 (7.8)	27 (22)	9 (7.7)
1	16.7 ms (20 ms)	25	6½	57 (48)	42 (38)	54 (45)	43 (35)	48 (41)	39 (32)
0.2	3.34 ms (4 ms)	22	6½	201 (186)	102 (113)	173 (162)	102 (99)	129 (127)	84 (83)
0.1	1.67 ms (2 ms)	21	5½	201 (201)	126 (116)	175 (173)	105 (105)	129 (128)	86 (86)
0.02	334 µs (400 µs)	19	5½	227 (227)	129 (129)	178 (178)	114 (114)	138 (138)	90 (90)
0.01	167 µs (167 µs)	16	4½	422 (422)	130 (130)	333 (333)	117 (117)	199 (199)	95 (95)
0.01[11]	167 µs (167 µs)	16	4½	2000 (2000)		2000 (2000)			

SETTLING CHARACTERISTICS: <500µs to 10ppm of step size. Reading settling times are affected by source impedance and cable dielectric absorption characteristics. Add 10ppm of range for first reading after range change.

ZERO STABILITY: Typical variation in zero reading, 1 hour. TREF ±1°C, 6½-digit default resolution, 10-reading digital filter:

Range	ZERO STABILITY 1 Power Line Cycle Integration	10 Power Line Cycle Integration
2V – 1000V	±3 counts	±2 counts
200 mV	±5 counts	±3 counts

ISOLATED POLARITY REVERSAL ERROR: This is the portion of the instrument error that is seen when high and low are reversed when driven by an isolated source. This is not an additional error—it is included in the overall instrument accuracy spec. **Reversal Error:** <2 counts at 10V input at 6½ digits, 10 power line cycles, 10-reading digital filter.

INPUT BIAS CURRENT: <100pA at 25°C.

LINEARITY: <1ppm of range typical, <2ppm maximum.

AUTORANGING: Autoranges up at 105% of range, down at 10% of range.

DC VOLTS NOTES

1. Specifications are for 1 power line cycle, Auto Zero on, 10-reading digital filter, except as noted
2. For TCAL ±1°C, following 55-minute warm-up. TCAL is ambient temperature at calibration, which is 23°C from factory.
3. For TCAL ±5°C, following 55-minute warm-up. Specifications include factory traceability to US NIST.
4. When properly zeroed using REL function.
5. For TCAL ±5°C, 90-day accuracy. 1-year or 2-year accuracy can be found by applying the same speed accuracy ppm changes to the 1-year or 2-year base accuracy.
6. Applies for 1kΩ imbalance in the LO lead. For 400Hz operation, subtract 10dB.
7. For noise synchronous to the line frequency.
8. For line frequency ±0.1%.
9. See Operating Speed section for additional detail. For DELAY=0, internal trigger, digital filter off, display off (or display in "hold" mode). Aperture is reciprocal of line frequency. These rates are for 60Hz and (50Hz).
10. Typical values.
11. In burst mode, display off. Burst mode requires Auto Zero refresh (by changing resolution or measurement function) once every 24 hours.
12. DCV Transfer Stability typical applications are standard cell comparisons and relative accuracy measurements. Specs apply for 10 power line cycles, 20-reading digital filter, autozero on with type synchronous, fixed range following 2-hour warm-up at full scale to 10% of full scale, at TREF ± 1°C (TREF is the initial ambient temperature). Specifications on the 1000V range are for measurements within 5% of the initial measurement value and following measurement settling.

$$\left[\frac{R_s + 20}{20}\right]^{0.5}.$$

According to the above, the K-1801 specification is 1.8 nV/$\sqrt{\text{Hz}}$ at 120 Ω. Thus, the K-1801 noise specification is excellent: only about 1.3 times the theoretical rms value at 120 Ω.

In the above 120 Ω value used, the 20 Ω part is approximately the source resistance of the APL electrodes while the 100 Ω is part of a passive single resistor/capacitor low pass filter at the input of the 1801 preamplifier. This is the filter used to reduce interference from the bath's heater controller.

From the above, we estimate our instrumentation noise to be about 2 nV/$\sqrt{\text{Hz}}$ for electrode resistances of about 20 Ω and about 3 nV/$\sqrt{\text{Hz}}$ for electrode resistances of about 200 Ω.

A new program, "HF", to do the high frequency tests was used for the first time on November 07. The definitive HF tests of the electrodes were run on November 10. These were done with the electrodes connected directly to the K-1801 without the use of the scanner in order to prevent contamination from the scanner.

The scanner was recabled on November 11 and a "LF" sampling run was started. It was left running for three days at 4 °C.

On November 14, the bath temperature was changed to 10 °C. Once the controller dial was changed, this temperature changed linearly over about 3 hours. A notable feature during the temperature change was the variability of the APL electrode potentials. The potentials had oscillations with a frequency of about 5 to 7 cycles per hour and peak to peak excursions of 2 to 4 μV.

Some of the channels seemed noisy. On November 15 their scanner connections were examined. Channels 04 and 13 and 17 were disconnected. Some of these copper surfaces were discolored with oxidation. All the ones disconnected were burnished with Scotchbrite and reassembled.

From November 15 to 18 the LF program sampled all the electrodes. From November 18 to 21 the "MF" program was used to determine the noise spectra of the all electrodes. The bath temperature was at 10 °C for these two tests.

On November 21 the bath temperature was driven actively with the controller in order to test the response of the electrodes to temperature changes. Several cycles between 10 and 12.5 °C took 4.5 hours.

A thermal shock test of the electrodes was performed on November 23 while the "LF" sampling program was running. First, we drained about 20 gallons of water from the bath with a siphon hose. Then, 16 gallons of 40°C tap water were added and, several minutes later, 4 more gallons of 40 °C tap water were added. The bath temperature rose from 10 °C to 15 °C and the controller was set to hold it at the final temperature. The LF run continued until November 26.

A two-day MF run at 15 °C was started on November 26.

The best SAIC electrode was removed from the system and returned to SAIC on November 28. At the same time the two best APL electrodes were removed. These electrodes were for installing in the electrode sensors, labeled Ab and As, for use in the subsequent salt water tank tests.

An MF run was started on November 30 with the temperature controller shut off but the bath stirrer still running. The insulating lid was left on the bath to slow the rate of temperature change. The temperature rose from about 17 to 19 °C in 4.5 days.

The isothermal bath tests were terminated on December 5.

A table with medium frequency sampling (MF) filenames and temperatures is shown below. The time series data from these are shown in this appendix.

Table A.4

filename	T (°C)
oct28h	4
nov18a	10
nov26a	15
nov30b	17-19

A table with high frequency (HF) filenames and electrode pairs used in the later discussion is shown below.

Table A.5

filename	electrode pairs
nov10_1.5kHzLPF_nscw_ch02_b	NSWC 5-6
nov10_1.5kHzLPF_nswc5,6_ch01b	NSWC 3-4
nov10_1.5kHzLPF_apl_ch11_b	APL 50-51
nov10_1.5kHzLPF_apl_ch13_b	APL 62-63
nov10_1.5kHzLPF_saic2526_ch07c	SAIC 25-26

Several tables of electrode pair numbers and resistor values versus the scanner connections and variable sequence number in the files are shown below. Differences are noted as we refined the setup.

At first the channels were labeled with the SAIC and APL electrodes reversed. The log book is actually incorrect as we learned later when undoing the scanner connections. Thus the plots made in October are labeled incorrectly. The table below was determined to be correct on November 1.

Note the change in the scanner channel mapping for the last three index numbers. Prior to October 19 at 1600 this mapping was monotonically increasing. After that time, the scanner channels 18 and 16 were interchanged so that the APL NaCl electrode would not be left connected to the scanner for a longer period of time than other electrodes.

Channel 04, NSWC 7-8 was added on October 14. The correct labeling as of October 14:

Table A.6

variable index number	scanner channel number	variable description	
T	-	Temperature	
v01	ch01	NSWC 3-4	
v02	ch02	NSWC 5-6	
v03	ch03	NSWC 1-2	Off scale
v04	ch04	NSWC 7-8	
v05	ch05	SAIC 21-22	
v06	ch06	SAIC 23-24	
v07	ch07	SAIC 25-26	
v08	ch08	SAIC 27-28	
v09	ch11	APL 50-51	
v10	ch12	APL 60-61	
v11	ch13	APL 62-63	
v12	ch14	APL 84-85	
v13	ch15	20 Ω	Jar above water
v14	ch16	95 Ω	
v15	ch17	390 Ω	
v16	ch18	N/C	

On October 17 at 1500 a new set of APL electrodes, 54-55, were put in the bath with an NaCl solution from SAIC. They were attached to the scanner on channel 18. At the same time the resistor bottle was opened and a 6.616 kΩ resistor was installed in place of the 95 Ω resistor. The bottle was resealed and put back partially in the bath. (The leads were too short to get it all in.) After this change the last four table entries are as shown below.

Table A.7

variable index number	scanner channel number	variable description	
v13	ch15	20 Ω	
v14	ch16	6.616 kΩ	
v15	ch17	390 Ω	
v16	ch18	APL 54-55	In NaCl. Not in bath yet.

On October 18 at 1715 the resistor bottle was found to have water. The 6.616 kΩ resistor had a 14 μV offset so was replaced. The log says the 390 Ω resistor was replaced with a 950 Ω resistor and the 6.6 kΩ resistor was replaced by a 10 kΩ one, but from other later notes in the log it appears that the above is reversed. The following table is correct. The new resistors were connected to the wires in the bottle. The last four table entries are now:

Table A.8

variable index number	scanner channel number	variable description	
v13	ch15	20 Ω	
v14	ch16	950 Ω	Reverse of log entry
v15	ch17	10 kΩ	Reverse of log entry
v16	ch18	APL 54-55	In NaCl. Not in bath yet.

On October 19 at 1115 the APL 54-55 pair was removed and cut off inside the jar. Its offset had risen to 400 μV. Later in the day the end of the cable near the bottle was chopped off and crimped connections added and bolted together with a stainless steel bolt.

On October 19 at 1600 the sampling order of channel 16 and 18 was swapped so that the scanner did not sit for a long time on the APL electrode in NaCl solution. Note the swap in the variable order.

And, note the swap between the 10 k and 950 resistors. Somewhere the documentation is fouled up. The state below is correct. The above table is probably incorrect.

The whole table is repeated below for easy reference. It was in this state from October 19 until November 11.

Table A.9

variable index number	scanner channel number	variable description	
T	-	Temperature	
v01	ch01	NSWC 3-4	
v02	ch02	NSWC 5-6	
v03	ch03	NSWC 1-2	Off scale
v04	ch04	NSWC 7-8	
v05	ch05	SAIC 21-22	
v06	ch06	SAIC 23-24	
v07	ch07	SAIC 25-26	
v08	ch08	SAIC 27-28	
v09	ch11	APL 50-51	
v10	ch12	APL 60-61	
v11	ch13	APL 62-63	
v12	ch14	APL 84-85	
v13	ch15	20 Ω	
v14	ch18	Cu-Cu short	Shorted using a SS bolt
v15	ch17	10 kΩ	
v16	ch16	950 Ω	

New NSWC electrodes, the pair we labeled 11-12, arrived during the scanner tests. On November 10, after rewiring after the scanner tests, the state was recorded as above except for the following entry:

Table A.10

variable index number	scanner channel number	variable description	
v03	ch03	NSWC 11-12	These are the new ones

On November 21 a special electrode pair was put in the tank. An EFF electrode block with a 18 inch sea water salt bridge between the electrode ports was attached in place of the 10 kΩ resistor on scanner channel 17. These electrodes have only ever been exposed to one type of synthetic sea water and were quite stable. However, the salt bridge has a resistance of about 3 kΩ so the noise level of these electrodes is more than the others at frequencies above 10 mHz.

Table A.11

variable index number	scanner channel number	variable description
v15	ch17	EFF block

The best SAIC electrode pair, 23-24, was removed on November 28 for installation in a system for the tank tests. The best two APL electrodes, 50-51 and 60-61, were removed at the same time for installation into the APL sensors. The two cables that were cut when the APL electrodes were removed had pure copper lugs attached shorting them together. These were channels 11 and 12. Channel 06 had a 20 ohm resistor attached inside the scanner at the scanner card. The table after November 28 is:

Table A.12

variable index number	scanner channel number	variable description	
T	-	Temperature	
v01	ch01	NSWC 3-4	
v02	ch02	NSWC 5-6	
v03	ch03	NSWC 11-12	
v04	ch04	NSWC 7-8	
v05	ch05	SAIC 21-22	
v06	ch06	20 Ω at scanner	
v07	ch07	SAIC 25-26	
v08	ch08	SAIC 27-28	
v09	ch11	Cu-Cu crimp	At end of cable
v10	ch12	Cu-Cu crimp	At end of cable
v11	ch13	APL 62-63	
v12	ch14	APL 84-85	
v13	ch15	20 Ω	
v14	ch18	Cu-Cu short	Shorted using a SS bolt
v15	ch17	EFF block	
v16	ch16	950 Ω	

Plots of Time Series of the MF Runs in the Isothermal Bath

These figures show all four of the MF (medium frequency) time series taken in the isothermal tank. Data from the files "oct28h", "nov18a", "nov26a" and "nov30b" were taken at bath temperature of 4, 10, 15, and 17–19°C, respectively. Each segment is about 1 hour and the sample rate is about 0.5 second. All data have been high-pass filtered in software with a one-pole Butterworth filter with a corner frequency of 1 mHz. Most scales are -0.05 μV, but a few have wider ranges to allow for noisier data. The figures are labeled with their file name followed by the segment number. Each segment took about 16 hours to complete, during which time each of the 16 scanner channels was sampled continuously for about 1 hour. Although the data are depicted concurrently for convenience, they are not concurrent. In order to organize the graphs, the order of display is not exactly the order of sampling. These data are those used in the spectra shown from 0.5 mHz to 1 Hz in Appendix B.

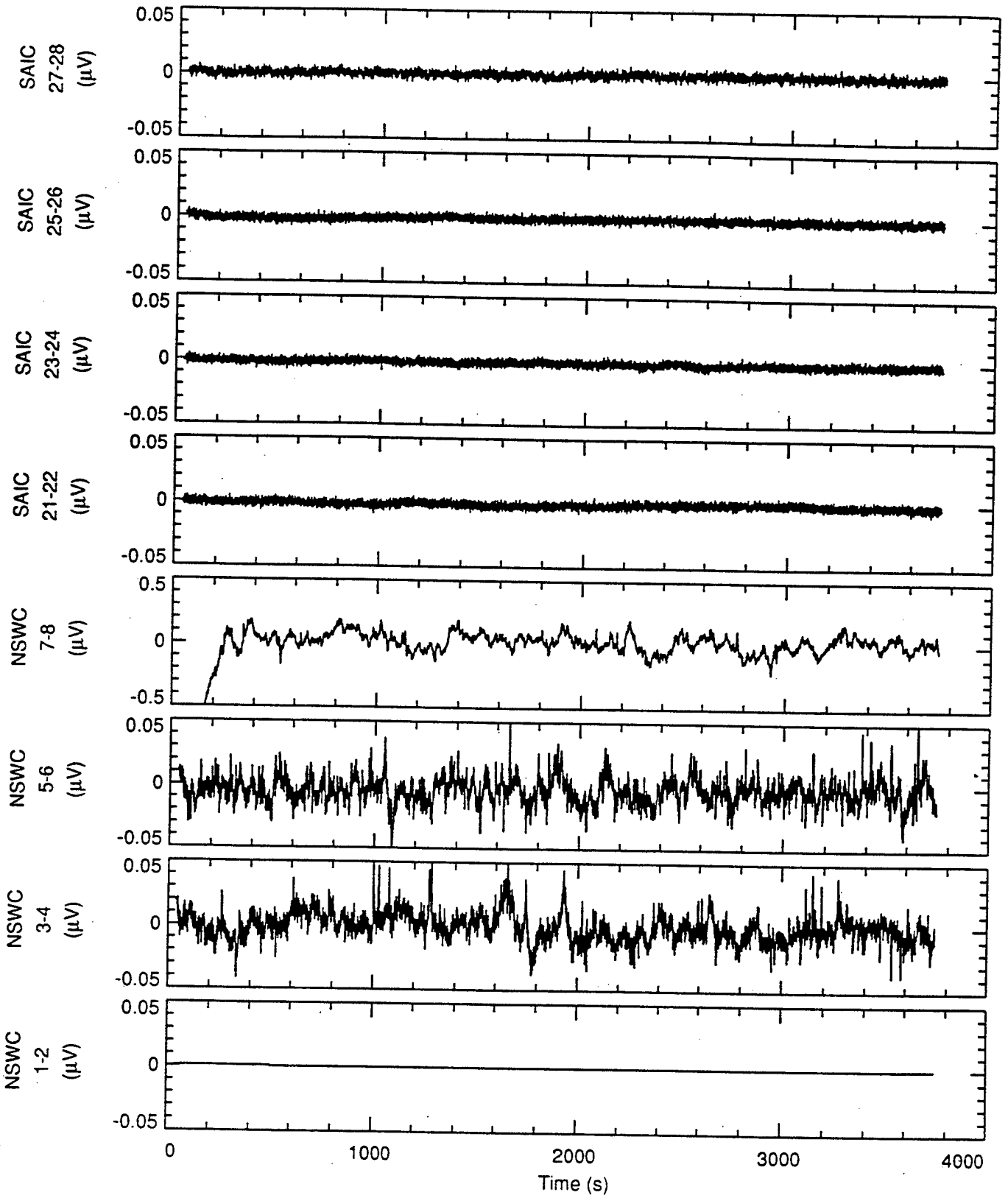
SAIC 27-28 (μV)
SAIC 25-26 (μV)
SAIC 23-24 (μV)
SAIC 21-22 (μV)
NSWC 7-8 (μV)
NSWC 5-6 (μV)
NSWC 3-4 (μV)
NSWC 1-2 (μV)
0.05
0
-0.05
0.5
-0.5
0
1000
2000
3000
4000
Time (s)

Figure A.1a

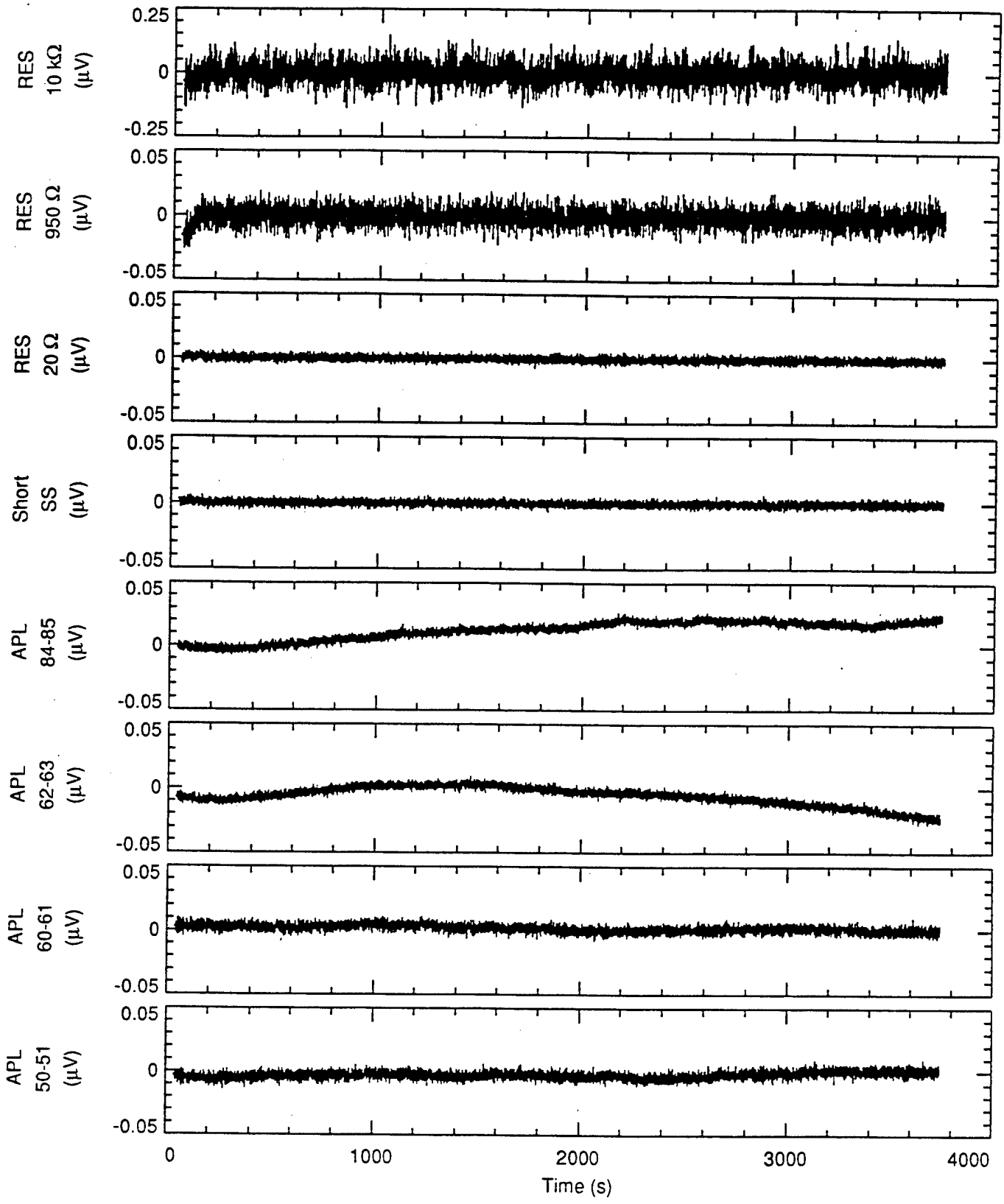
RES 10 kΩ (μV)
RES 950 Ω (μV)
RES 20 Ω (μV)
Short SS (μV)
APL 84-85 (μV)
APL 62-63 (μV)
APL 60-61 (μV)
APL 50-51 (μV)
0.25
0
-0.25
0.05
0
-0.05
0
1000
2000
3000
4000
Time (s)

Figure A.1b

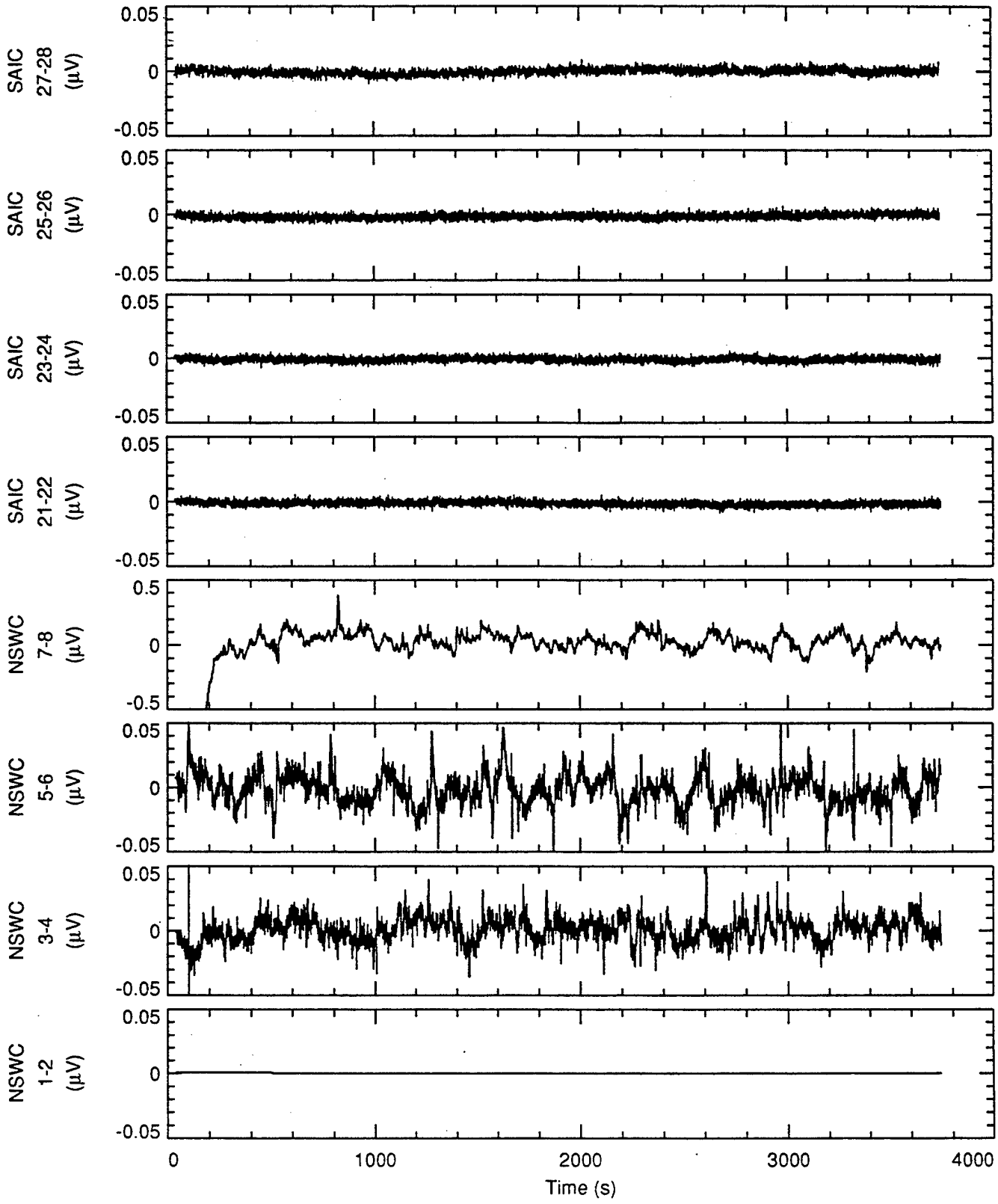
SAIC 27-28 (μV)
SAIC 25-26 (μV)
SAIC 23-24 (μV)
SAIC 21-22 (μV)
NSWC 7-8 (μV)
NSWC 5-6 (μV)
NSWC 3-4 (μV)
NSWC 1-2 (μV)
0.05
0
-0.05
0.5
-0.5
0
1000
2000
3000
4000
Time (s)

Figure A.2a

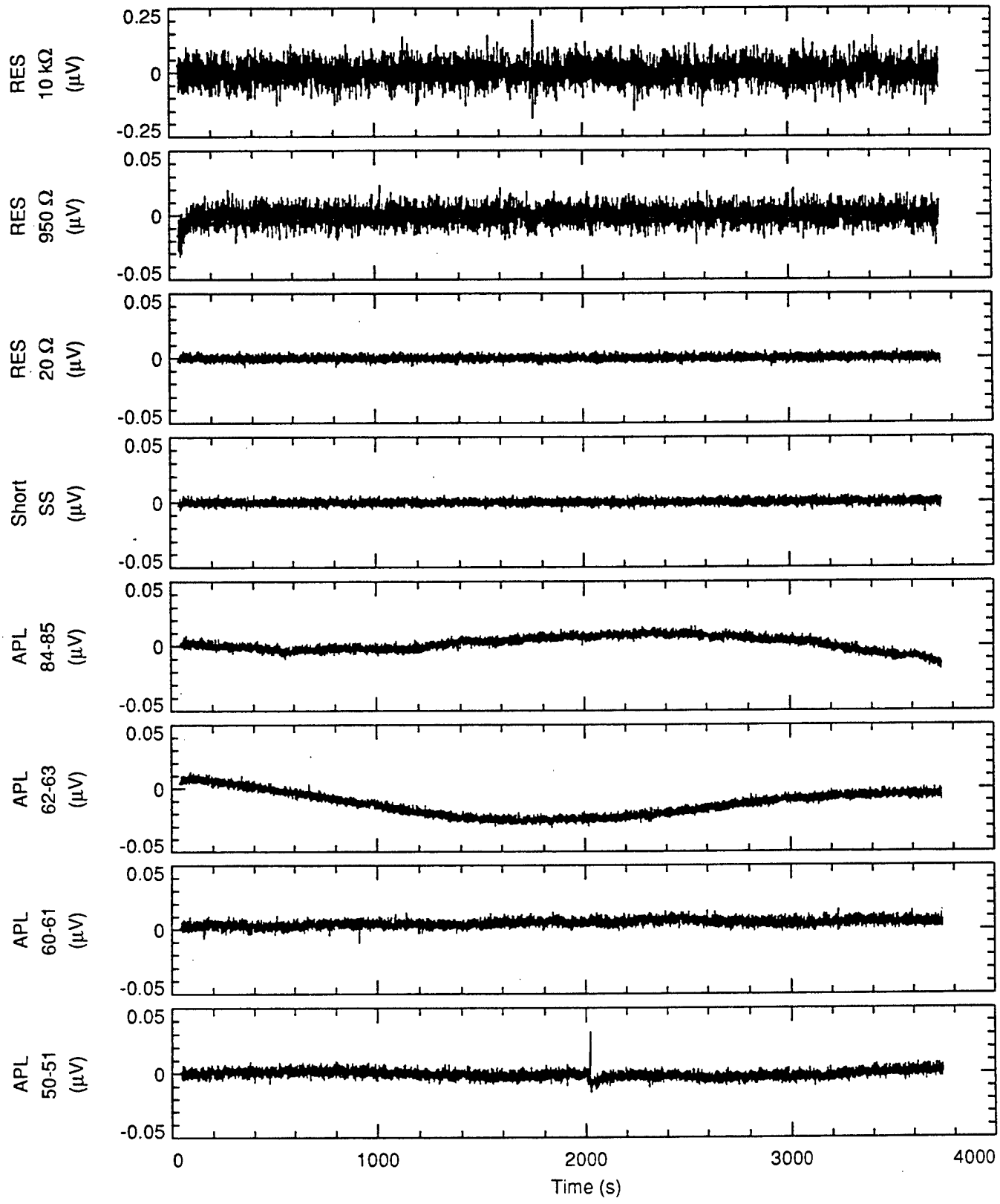
RES 10 kΩ (μV)
RES 950 Ω (μV)
RES 20 Ω (μV)
Short SS (μV)
APL 84-85 (μV)
APL 62-63 (μV)
APL 60-61 (μV)
APL 50-51 (μV)
0.25
0
-0.25
0.05
0
-0.05
0
1000
2000
3000
4000
Time (s)

Figure A.2b

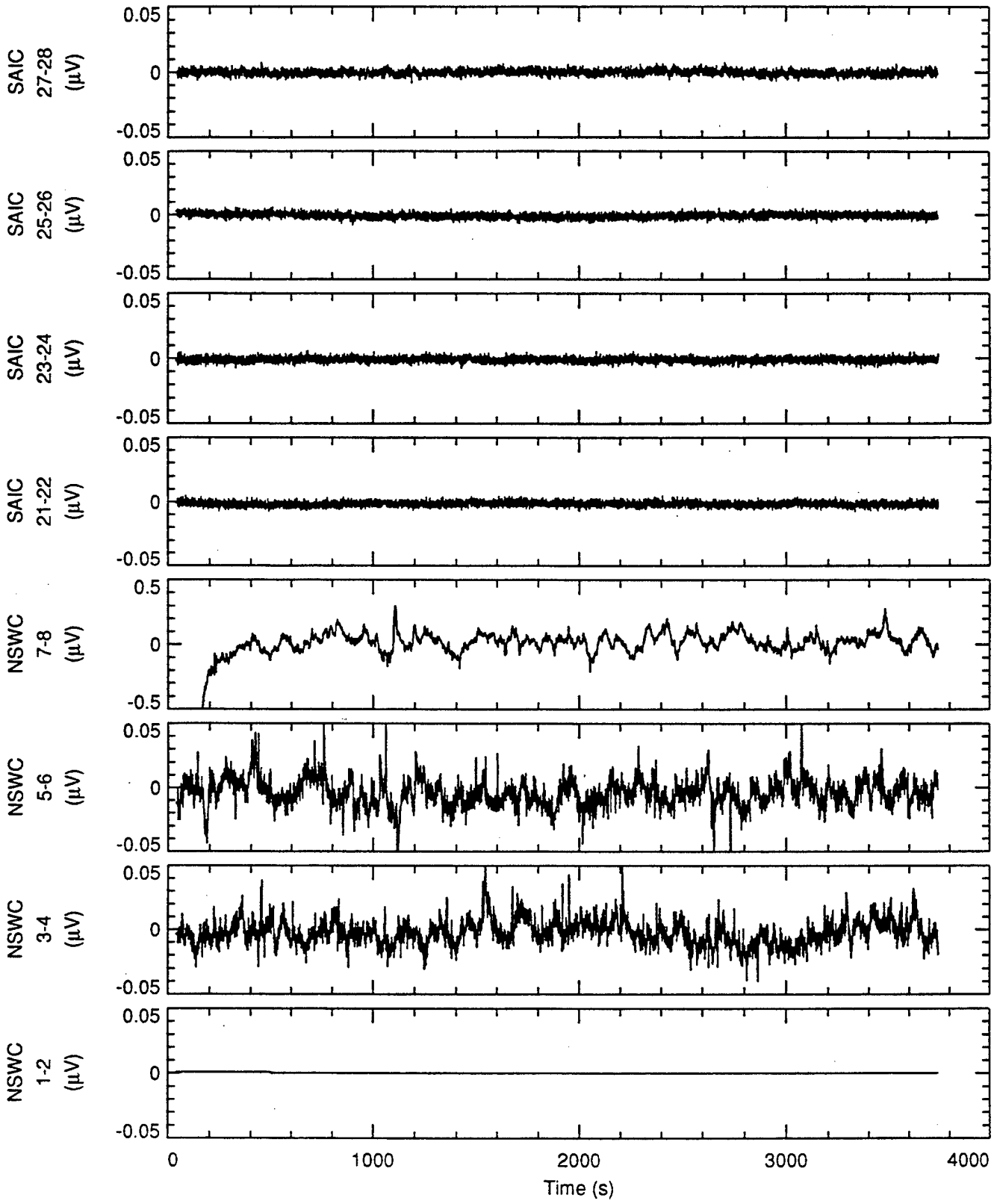
SAIC 27-28 (μV)
SAIC 25-26 (μV)
SAIC 23-24 (μV)
SAIC 21-22 (μV)
NSWC 7-8 (μV)
NSWC 5-6 (μV)
NSWC 3-4 (μV)
NSWC 1-2 (μV)
0.05
0
-0.05
0.5
-0.5
0
1000
2000
3000
4000
Time (s)

Figure A.3a

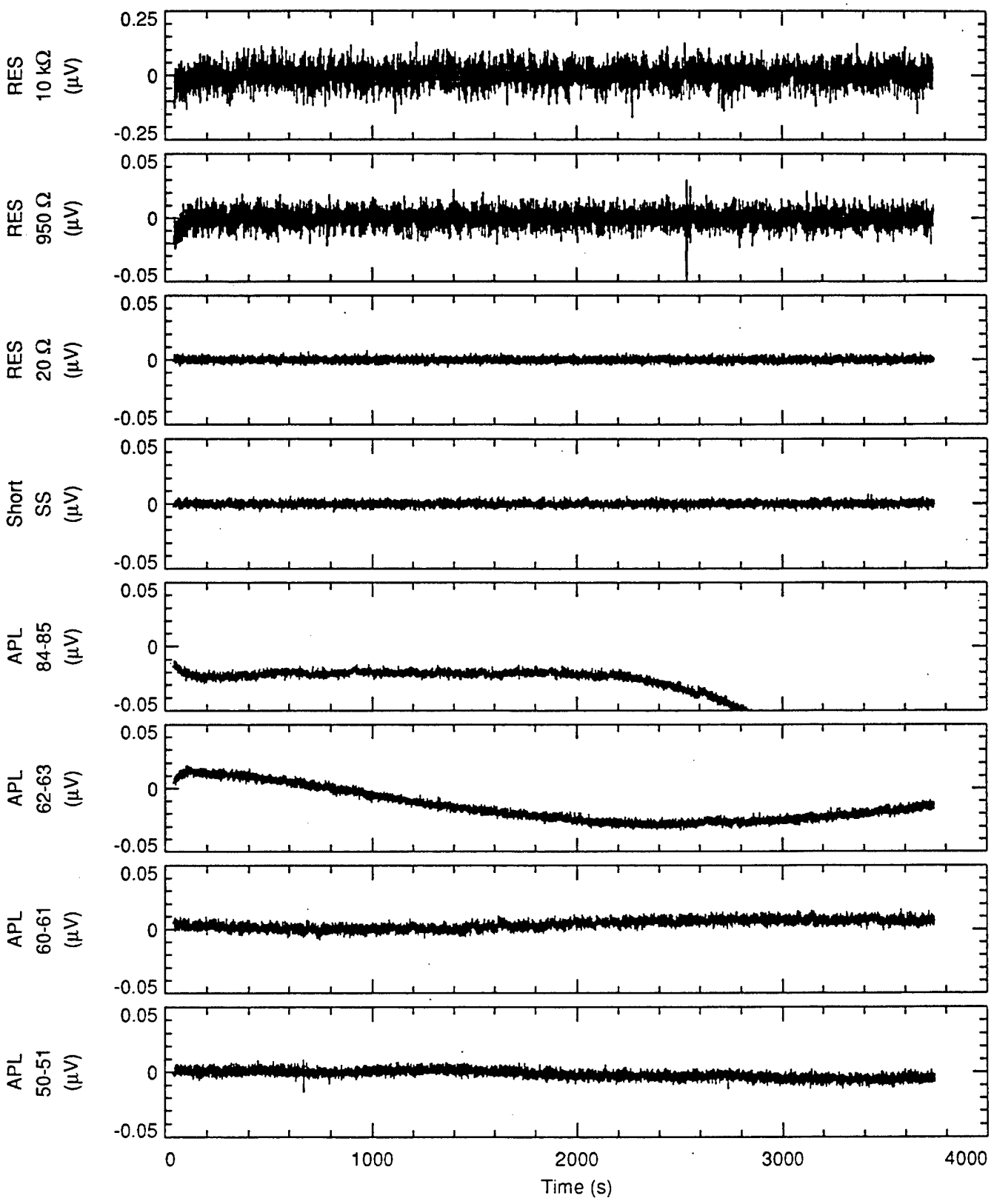
RES 10 kΩ (μV)
RES 950 Ω (μV)
RES 20 Ω (μV)
Short SS (μV)
APL 84-85 (μV)
APL 62-63 (μV)
APL 60-61 (μV)
APL 50-51 (μV)
0.25
0
-0.25
0.05
0
-0.05
0
1000
2000
3000
4000
Time (s)

Figure A.3b

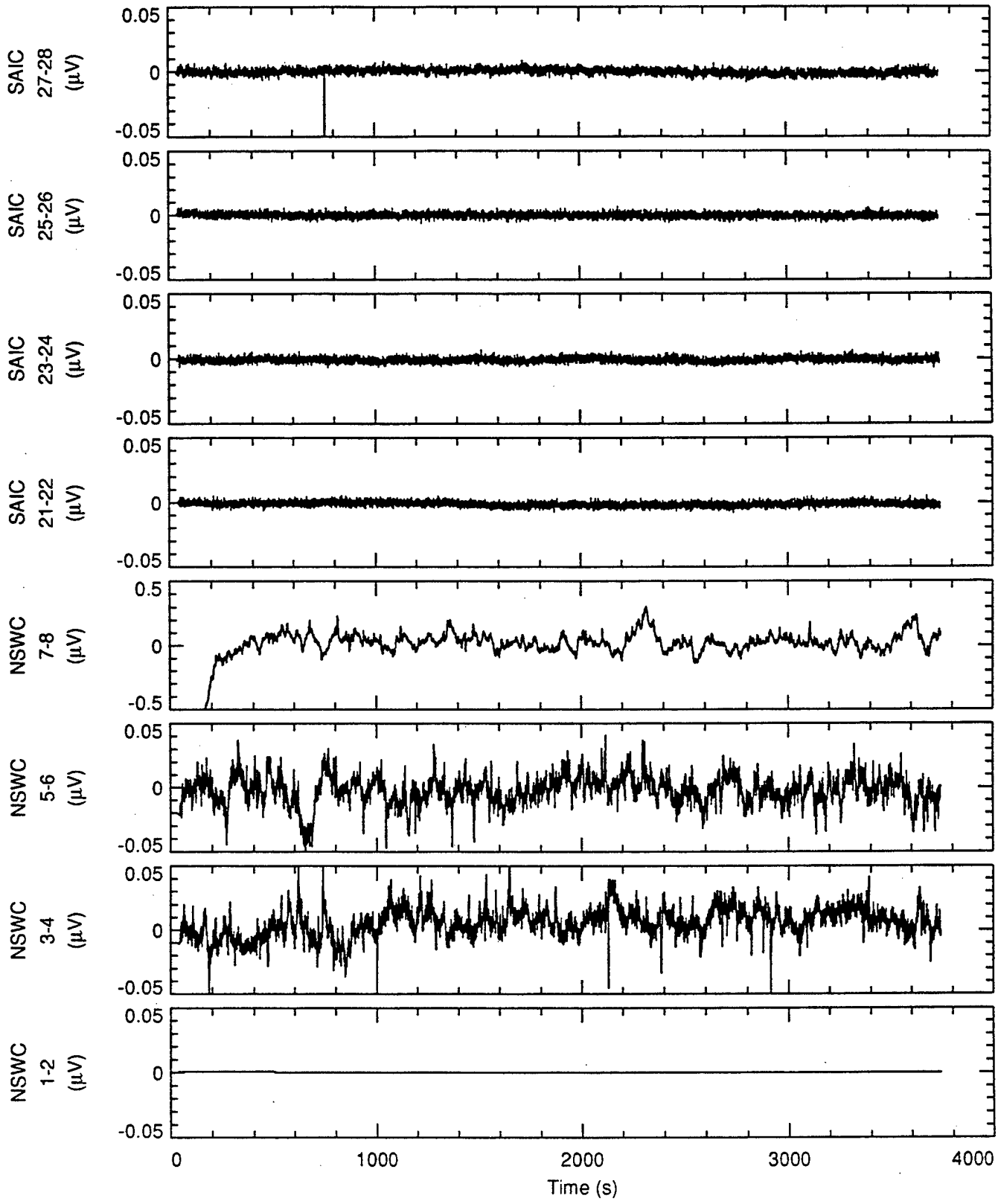
SAIC 27-28 (μV)
SAIC 25-26 (μV)
SAIC 23-24 (μV)
SAIC 21-22 (μV)
NSWC 7-8 (μV)
NSWC 5-6 (μV)
NSWC 3-4 (μV)
NSWC 1-2 (μV)
0.05
0
-0.05
0.5
-0.5
0
1000
2000
3000
4000
Time (s)

Figure A.4a

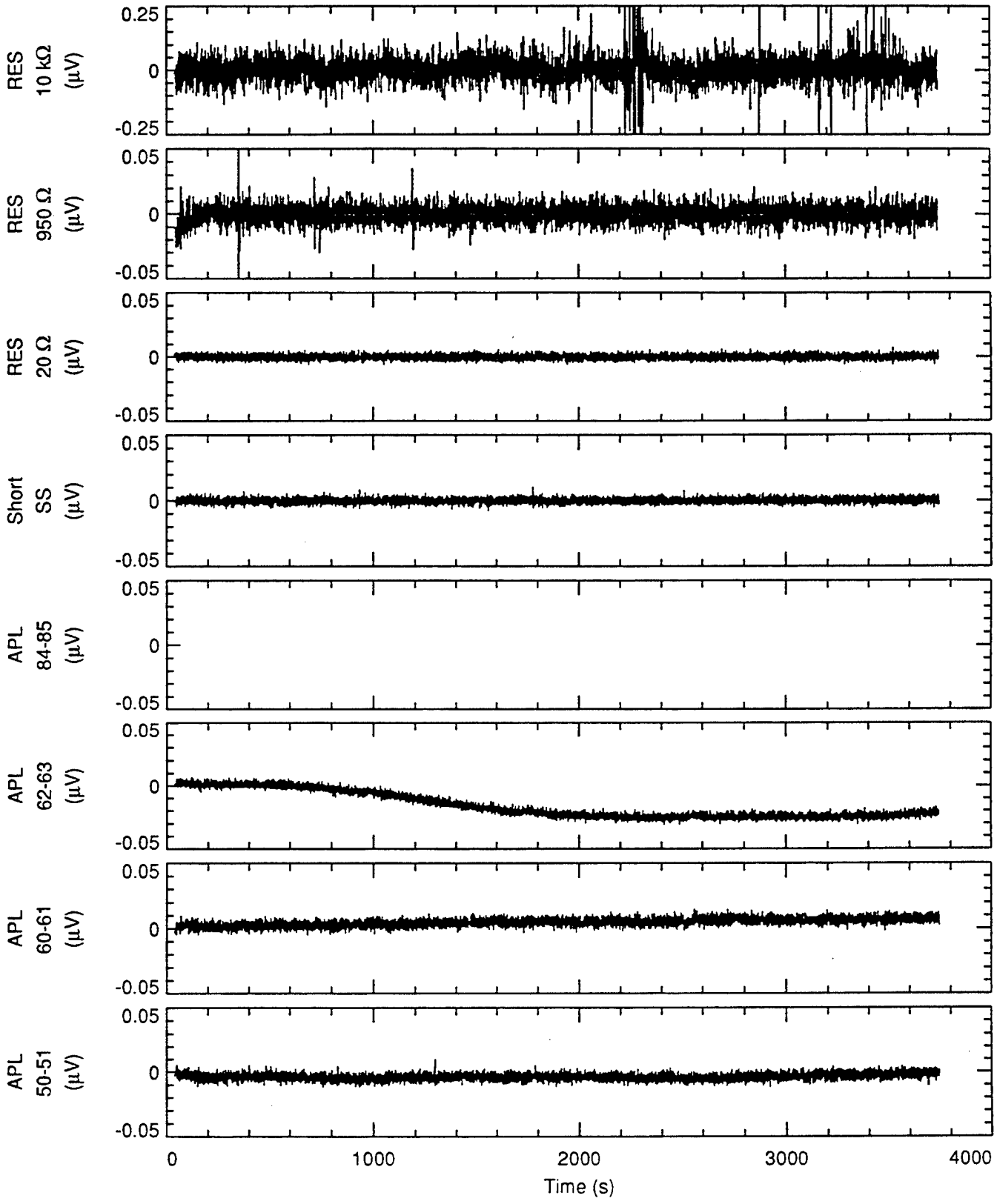
RES 10 kΩ (μV)
RES 950 Ω (μV)
RES 20 Ω (μV)
Short SS (μV)
APL 84-85 (μV)
APL 62-63 (μV)
APL 60-61 (μV)
APL 50-51 (μV)
0.25
0
-0.25
0.05
0
-0.05
0
1000
2000
3000
4000
Time (s)

Figure A.4b

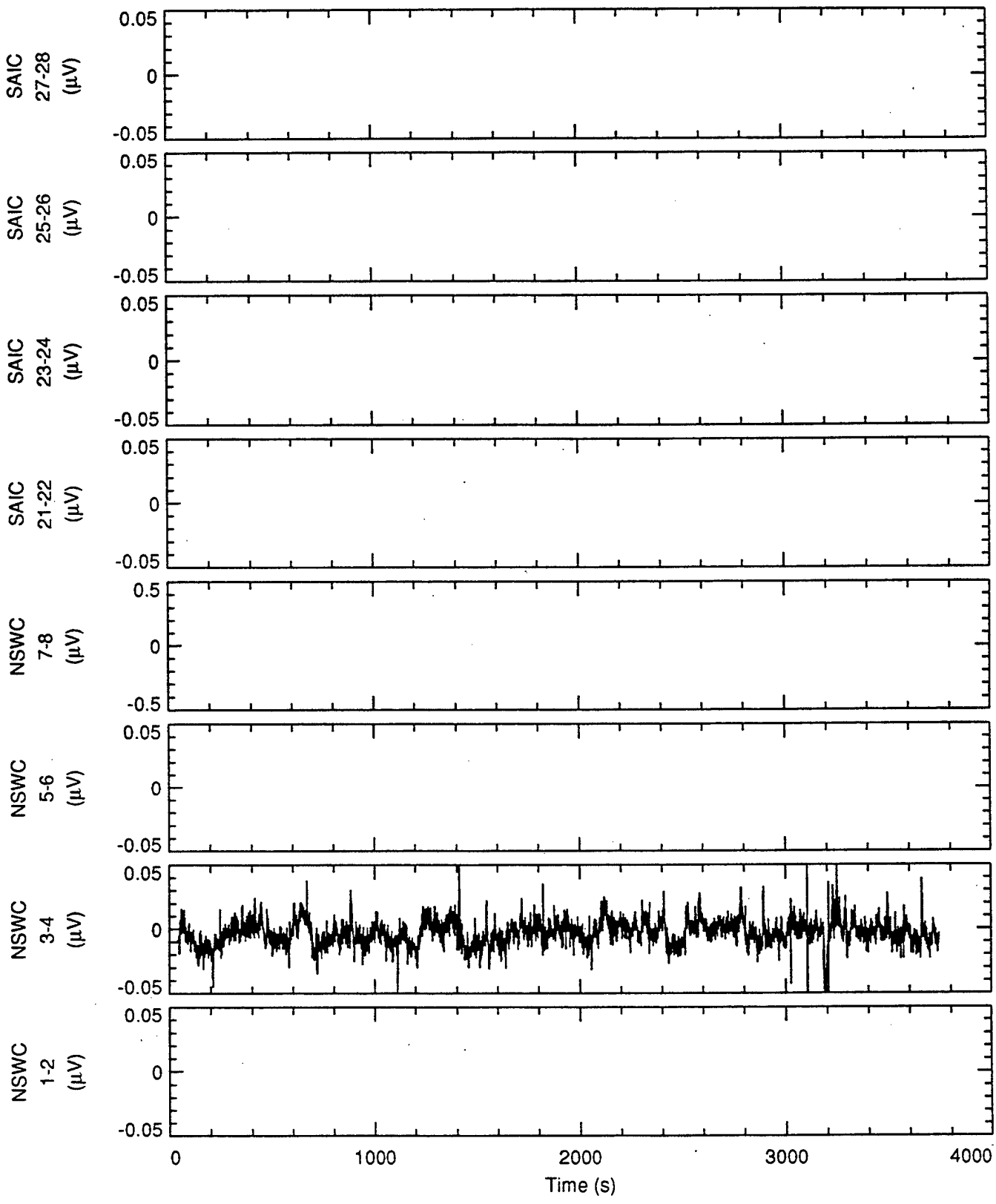
SAIC 27-28 (μV)
SAIC 25-26 (μV)
SAIC 23-24 (μV)
SAIC 21-22 (μV)
NSWC 7-8 (μV)
NSWC 5-6 (μV)
NSWC 3-4 (μV)
NSWC 1-2 (μV)
0.05
0
-0.05
0.5
-0.5
0
1000
2000
3000
4000
Time (s)

Figure A.5a

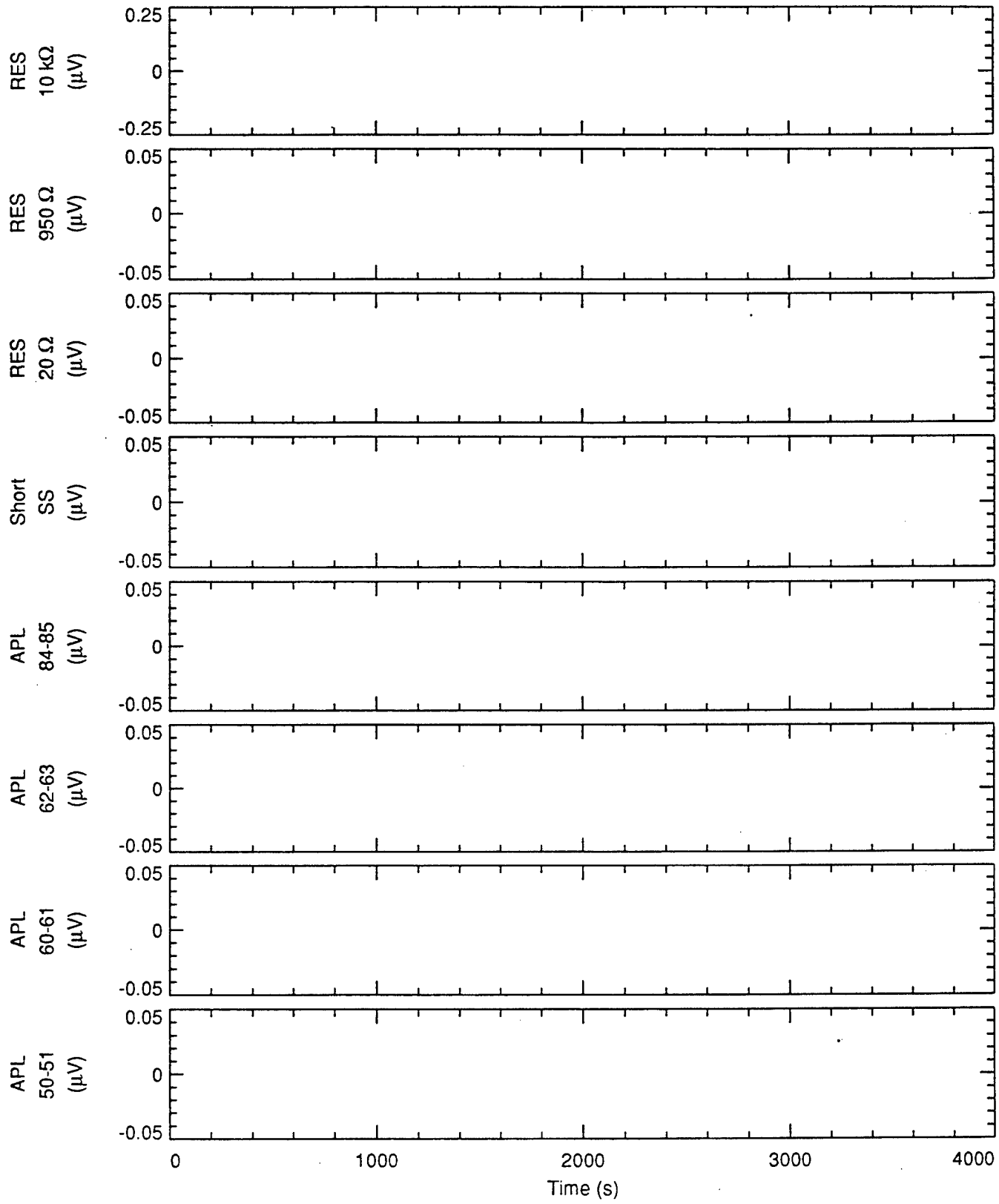
RES 10 kΩ (μV)
RES 950 Ω (μV)
RES 20 Ω (μV)
Short SS (μV)
APL 84-85 (μV)
APL 62-63 (μV)
APL 60-61 (μV)
APL 50-51 (μV)
0.25
0
-0.25
0.05
0
-0.05
0
1000
2000
3000
4000
Time (s)

Figure A.5b

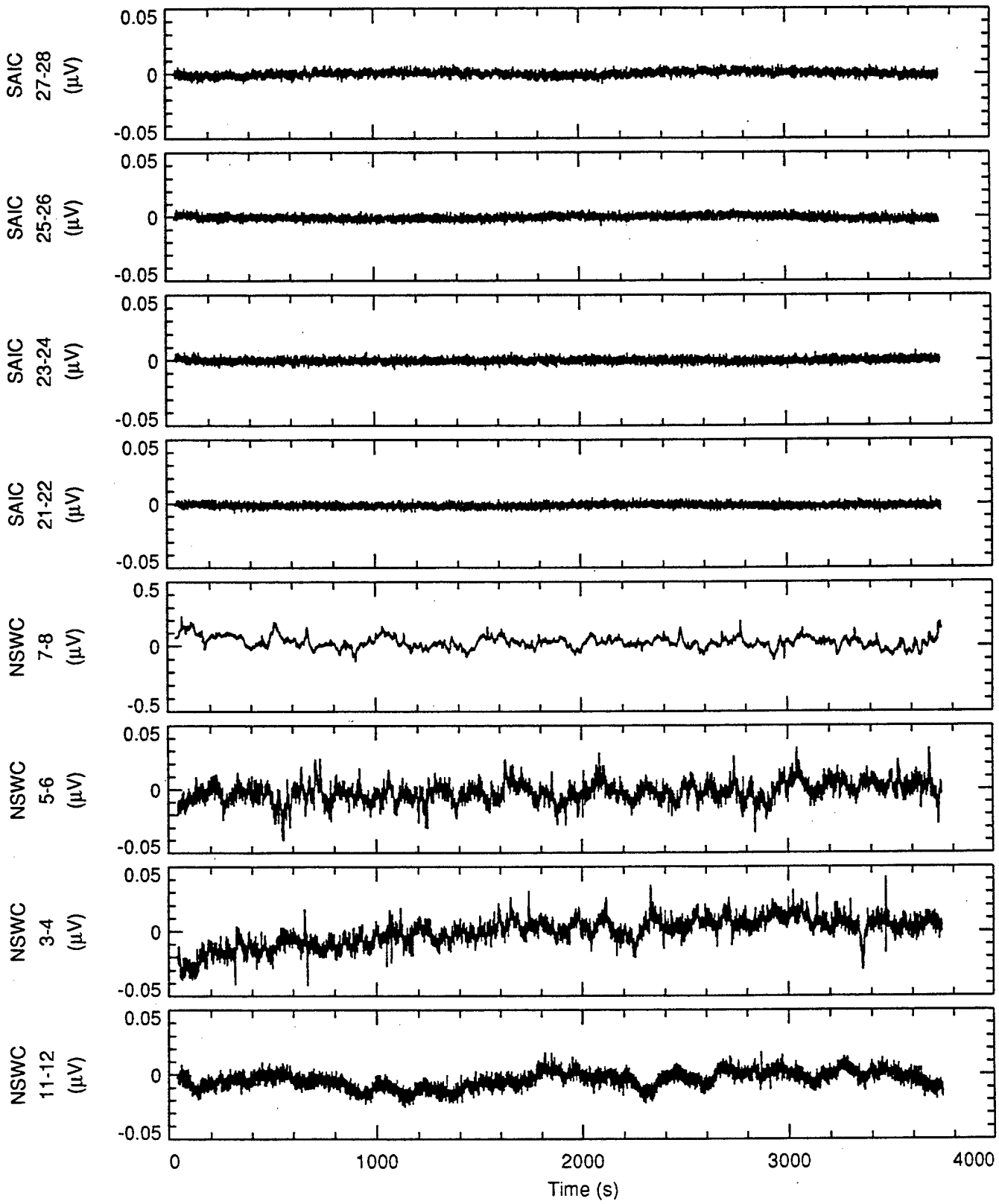
SAIC 27-28 (μV)
SAIC 25-26 (μV)
SAIC 23-24 (μV)
SAIC 21-22 (μV)
NSWC 7-8 (μV)
NSWC 5-6 (μV)
NSWC 3-4 (μV)
NSWC 11-12 (μV)
0.05
0
-0.05
0.5
-0.5
0
1000
2000
3000
4000
Time (s)

Figure A.6a

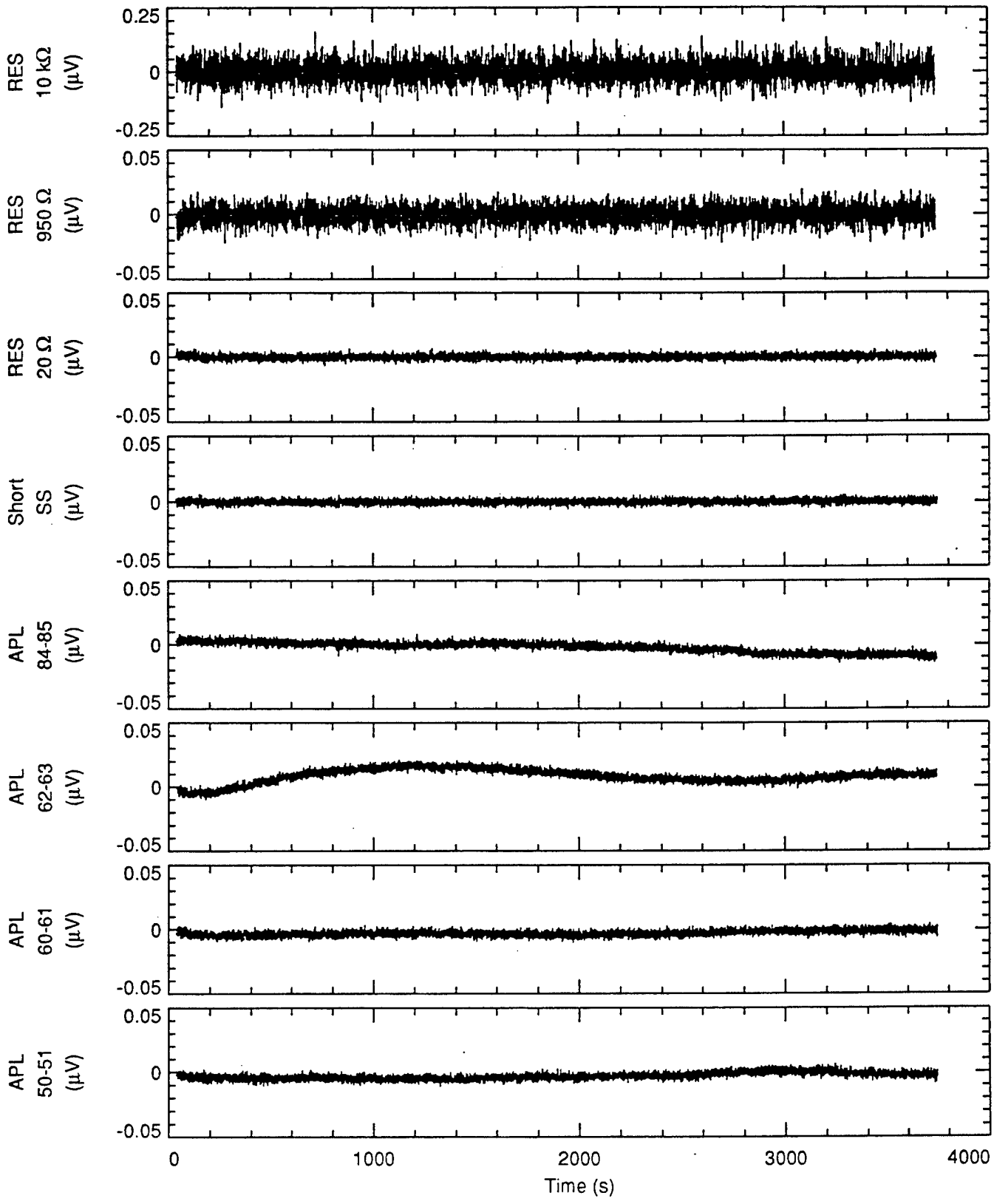
RES 10 kΩ (μV)
RES 950 Ω (μV)
RES 20 Ω (μV)
Short SS (μV)
APL 84-85 (μV)
APL 62-63 (μV)
APL 60-61 (μV)
APL 50-51 (μV)
0.25
0
-0.25
0.05
0
-0.05
0
1000
2000
3000
4000
Time (s)

Figure A.6b

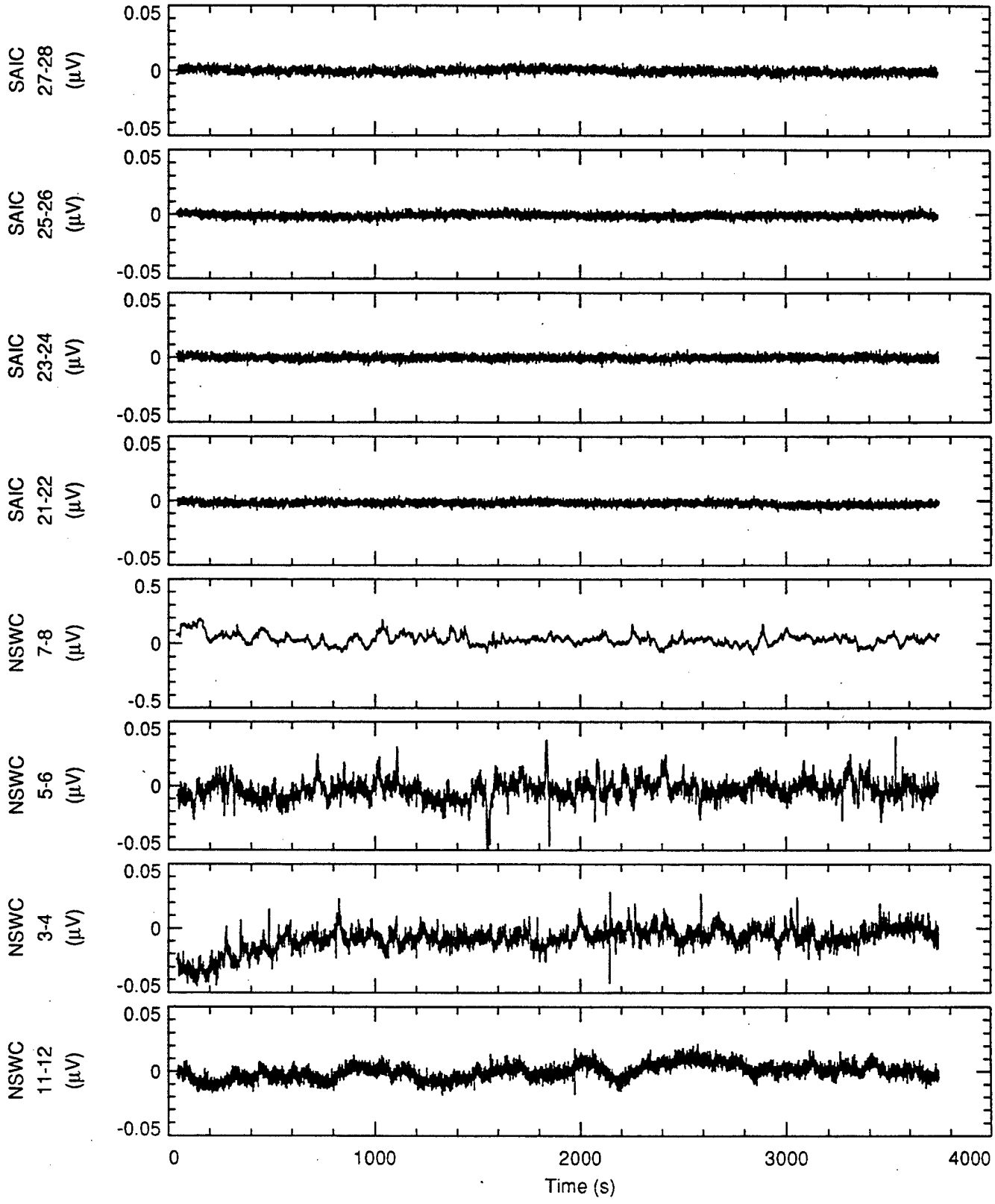
SAIC 27-28 (μV)
SAIC 25-26 (μV)
SAIC 23-24 (μV)
SAIC 21-22 (μV)
NSWC 7-8 (μV)
NSWC 5-6 (μV)
NSWC 3-4 (μV)
NSWC 11-12 (μV)
0.05
0
-0.05
0.5
-0.5
0
1000
2000
3000
4000
Time (s)

Figure A.7a

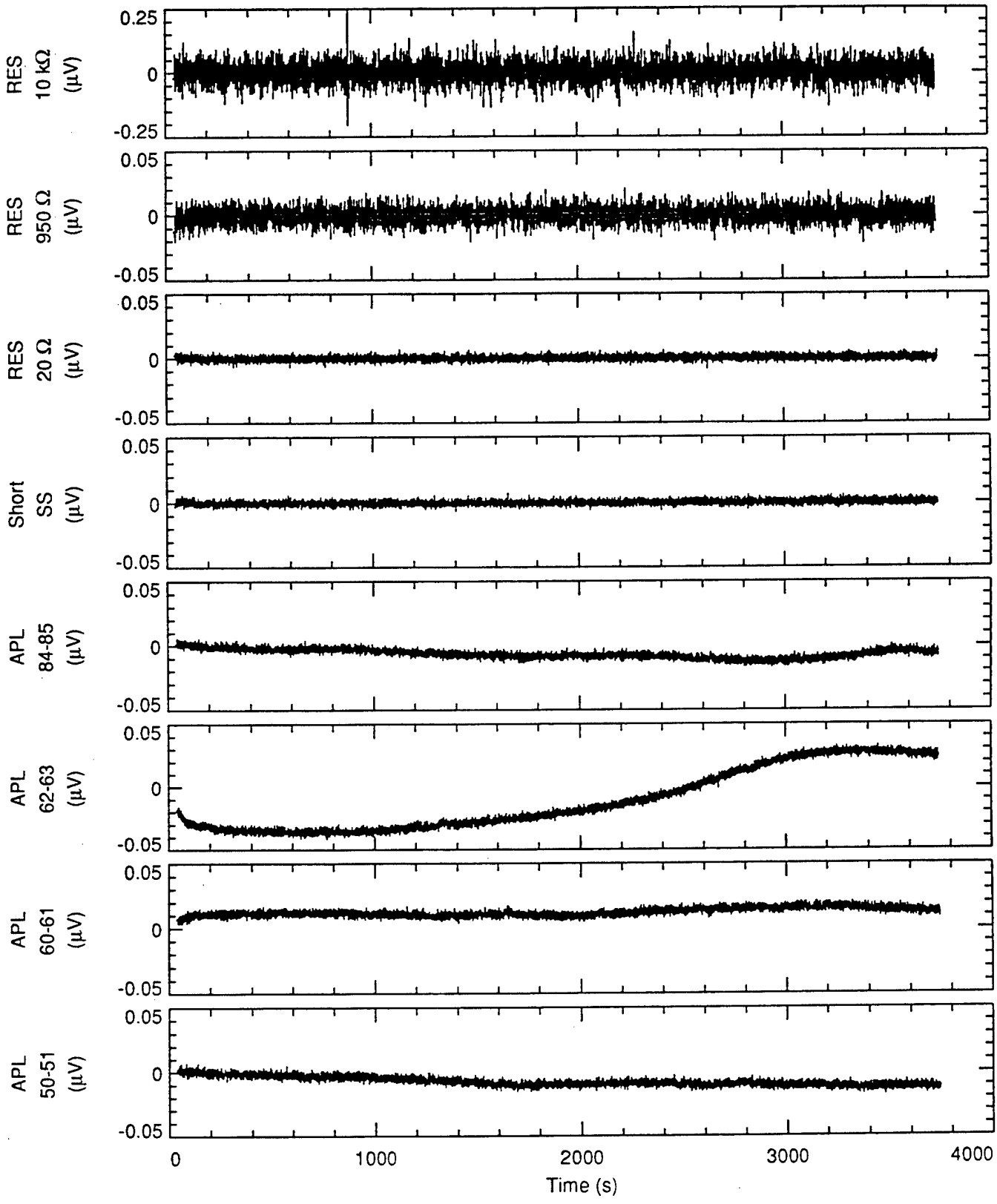
RES 10 kΩ (μV)
RES 950 Ω (μV)
RES 20 Ω (μV)
Short SS (μV)
APL 84-85 (μV)
APL 62-63 (μV)
APL 60-61 (μV)
APL 50-51 (μV)
0.25
0
-0.25
0.05
0
-0.05
0
1000
2000
3000
4000
Time (s)

Figure A.7b

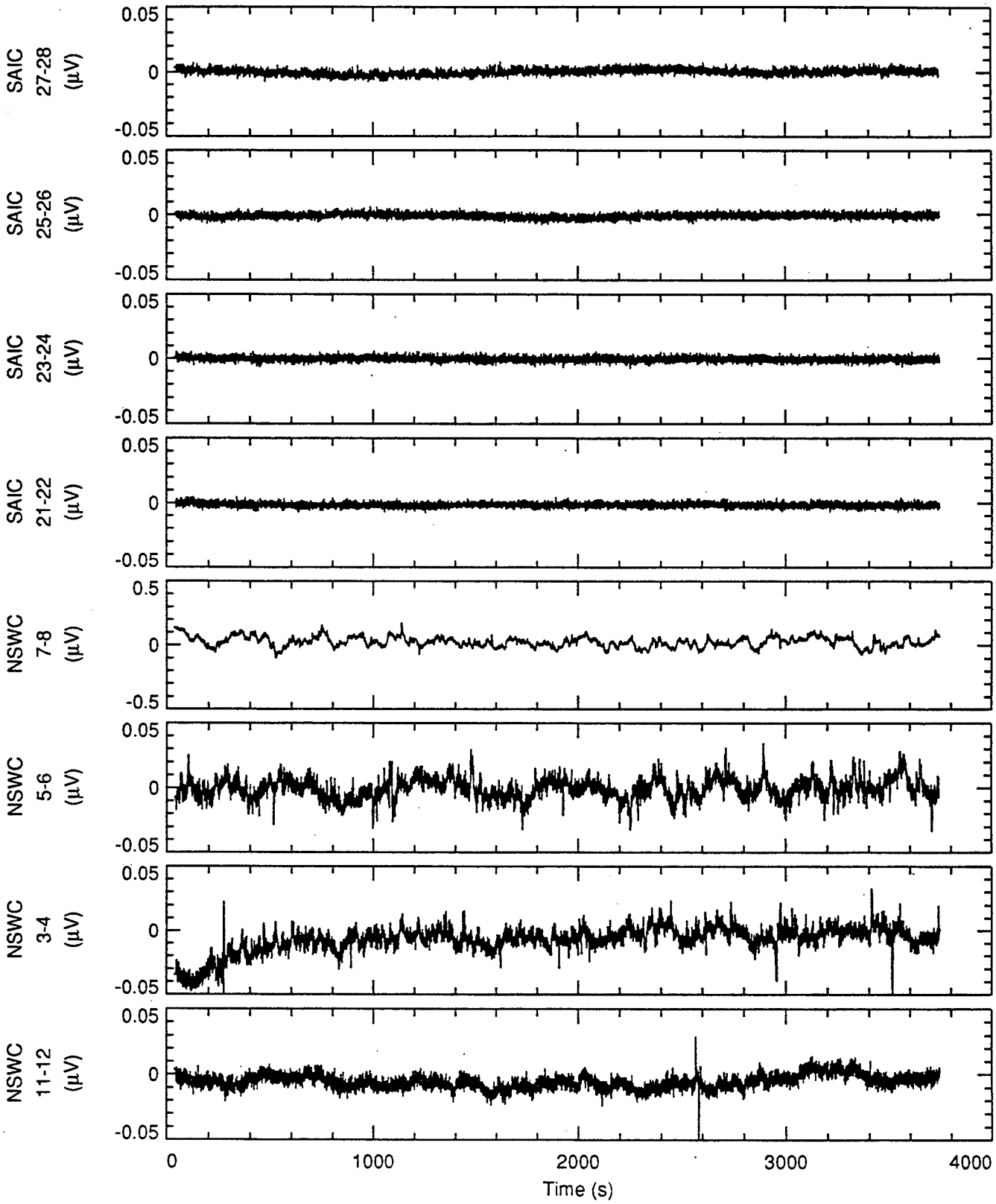
SAIC 27-28 (μV)
SAIC 25-26 (μV)
SAIC 23-24 (μV)
SAIC 21-22 (μV)
NSWC 7-8 (μV)
NSWC 5-6 (μV)
NSWC 3-4 (μV)
NSWC 11-12 (μV)
0.05
0
-0.05
0.5
-0.5
0
1000
2000
3000
4000
Time (s)

Figure A.8a

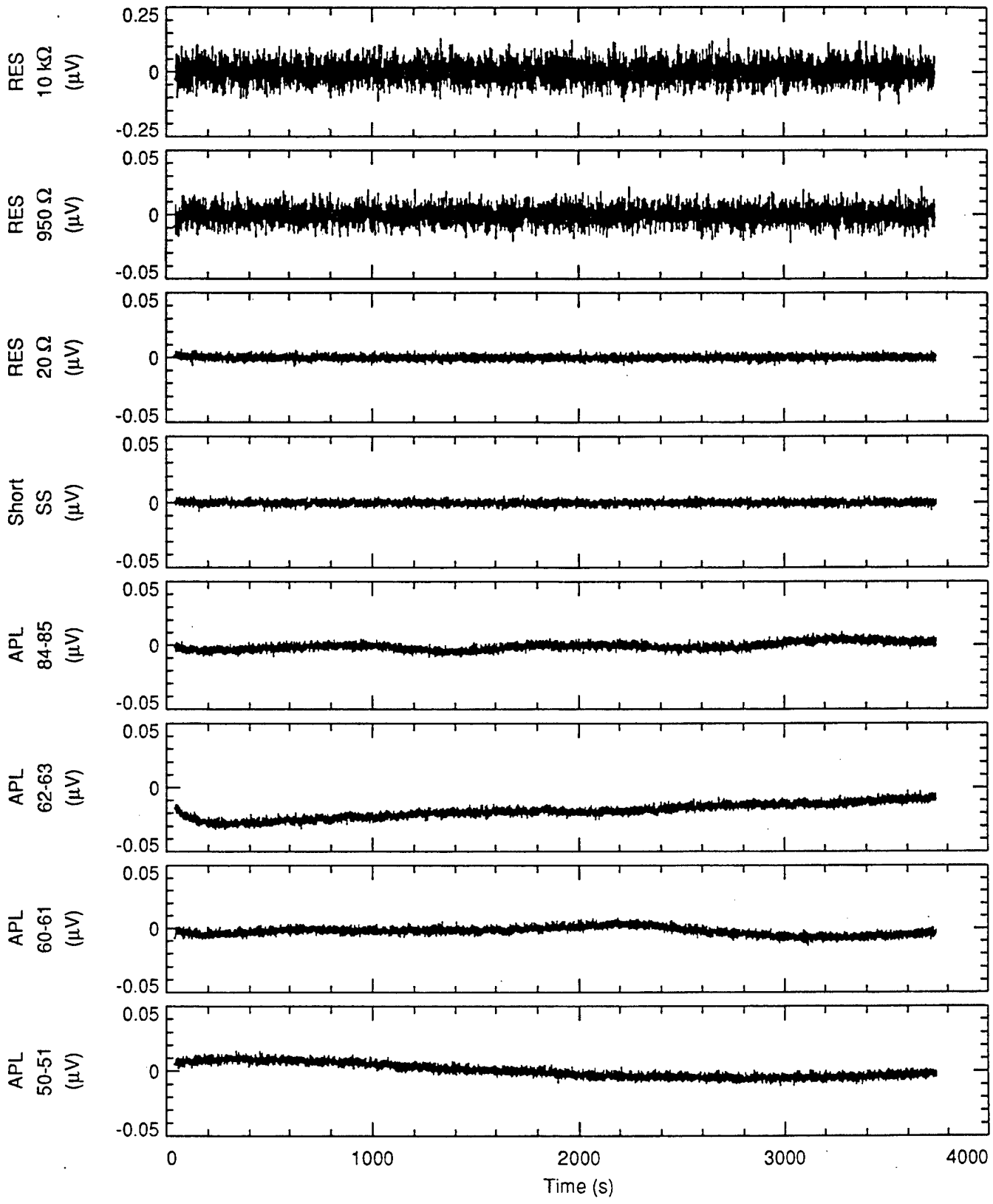
RES 10 kΩ (μV)
RES 950 Ω (μV)
RES 20 Ω (μV)
Short SS (μV)
APL 84-85 (μV)
APL 62-63 (μV)
APL 60-61 (μV)
APL 50-51 (μV)
0.25
0
-0.25
0.05
0
-0.05
0
1000
2000
3000
4000
Time (s)

Figure A.8b

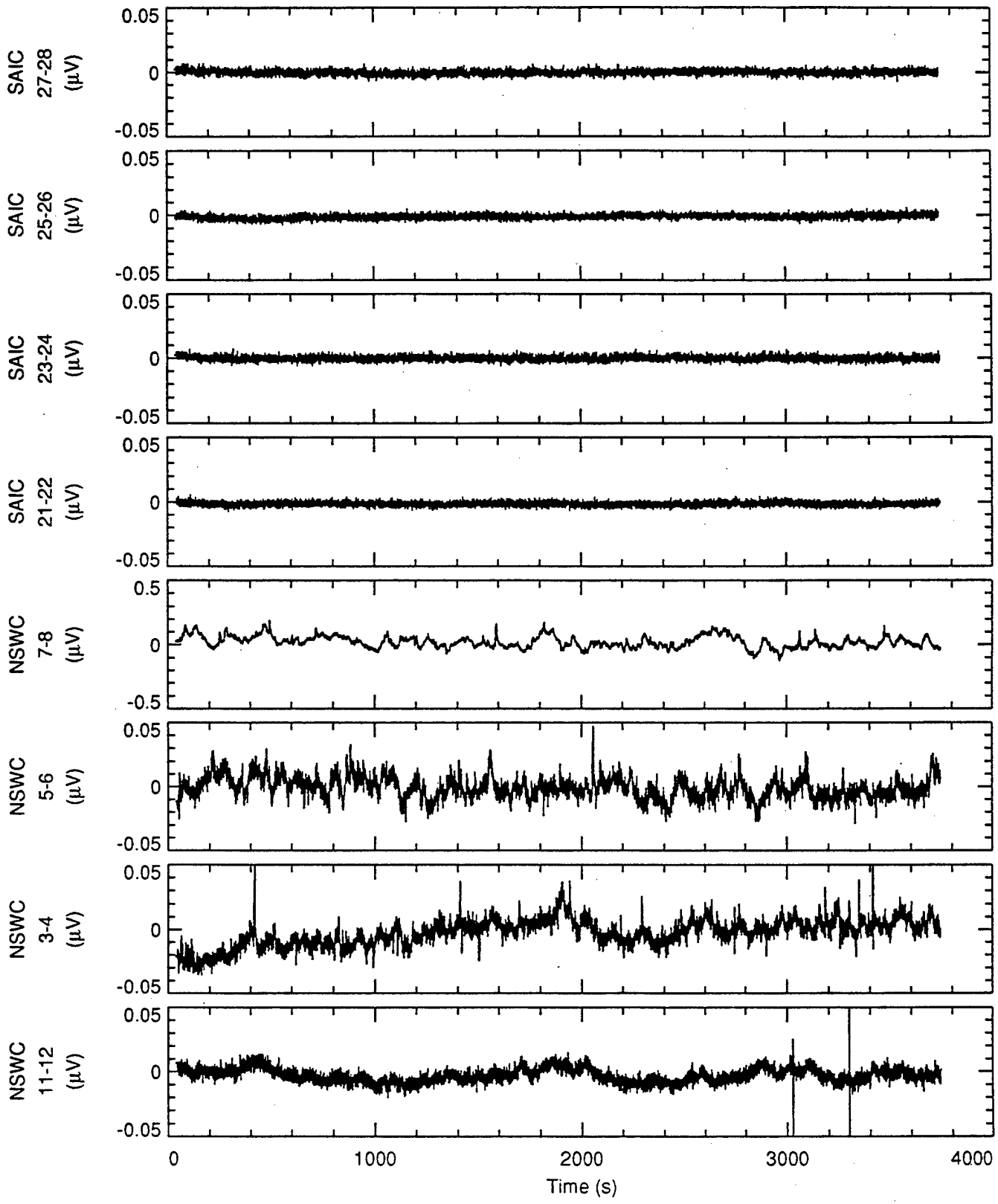
SAIC 27-28 (μV)
SAIC 25-26 (μV)
SAIC 23-24 (μV)
SAIC 21-22 (μV)
NSWC 7-8 (μV)
NSWC 5-6 (μV)
NSWC 3-4 (μV)
NSWC 11-12 (μV)
0.05
0
-0.05
0.5
-0.5
0
1000
2000
3000
4000
Time (s)

Figure A.9a

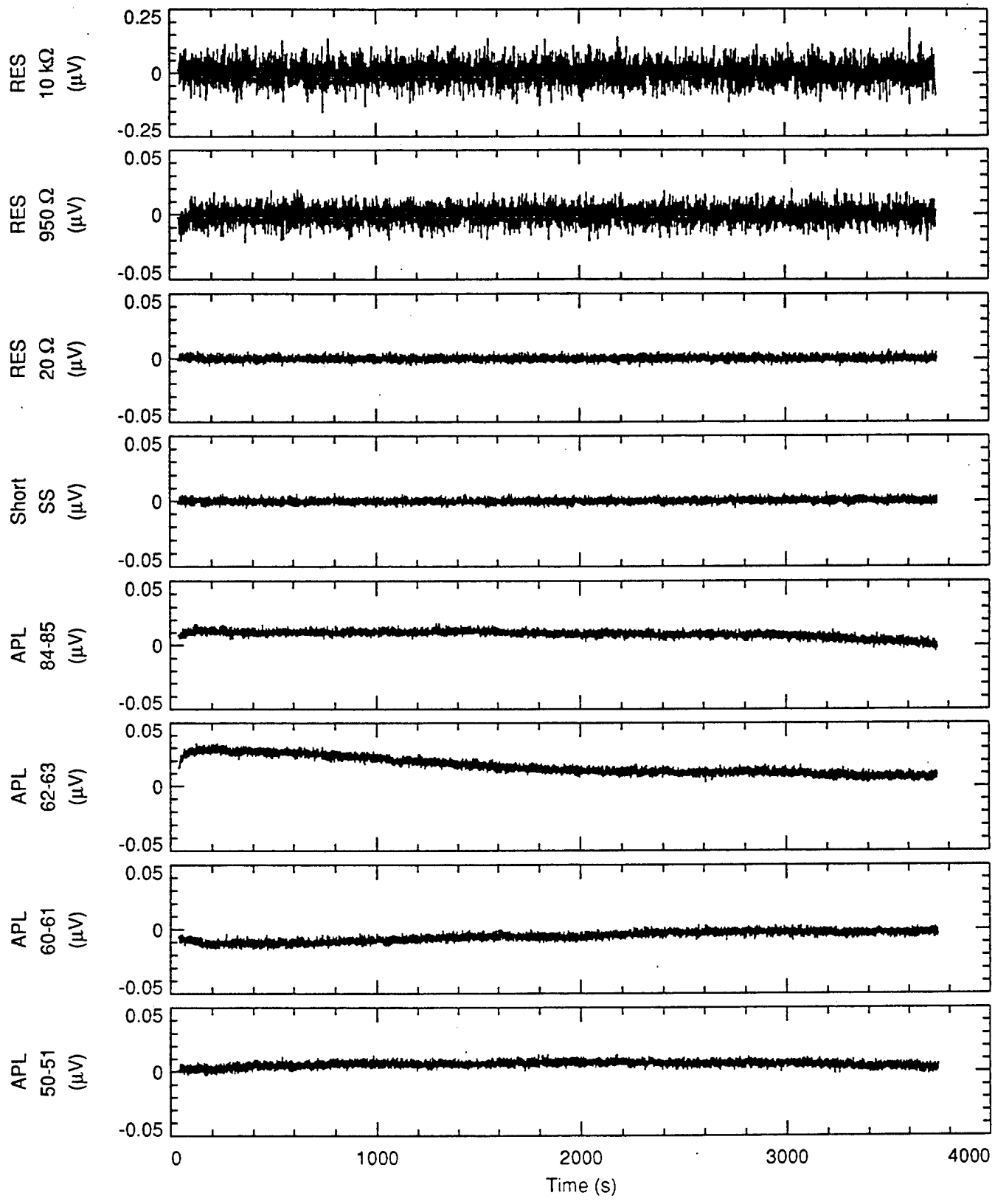
RES 10 kΩ (μV)
RES 950 Ω (μV)
RES 20 Ω (μV)
Short SS (μV)
APL 84-85 (μV)
APL 62-63 (μV)
APL 60-61 (μV)
APL 50-51 (μV)
0.25
0
-0.25
0.05
0
-0.05
0
1000
2000
3000
4000
Time (s)

Figure A.9b

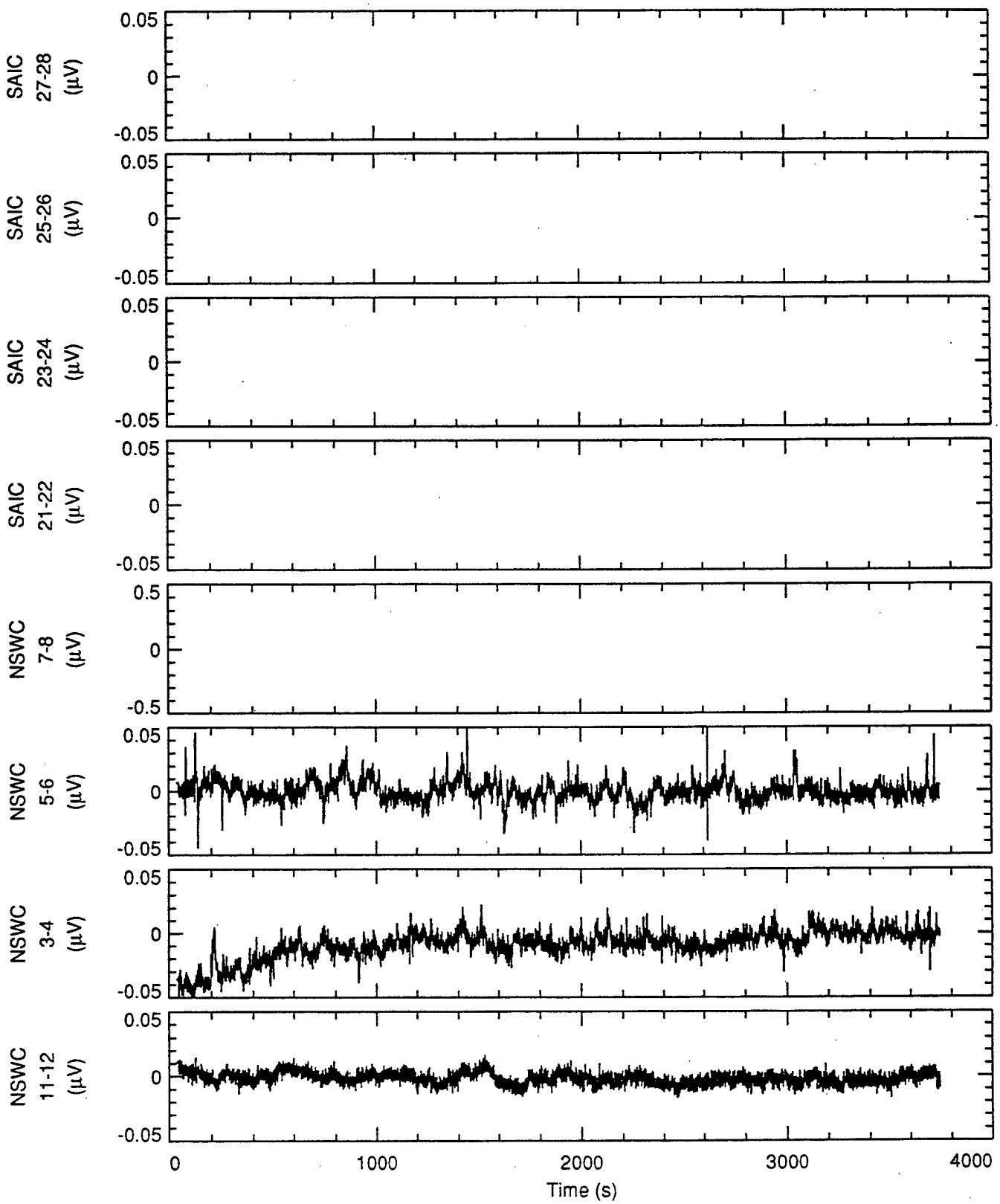
SAIC 27-28 (μV)
SAIC 25-26 (μV)
SAIC 23-24 (μV)
SAIC 21-22 (μV)
NSWC 7-8 (μV)
NSWC 5-6 (μV)
NSWC 3-4 (μV)
NSWC 11-12 (μV)
0.05
0
-0.05
0.5
-0.5
0
1000
2000
3000
4000
Time (s)

Figure A.10a

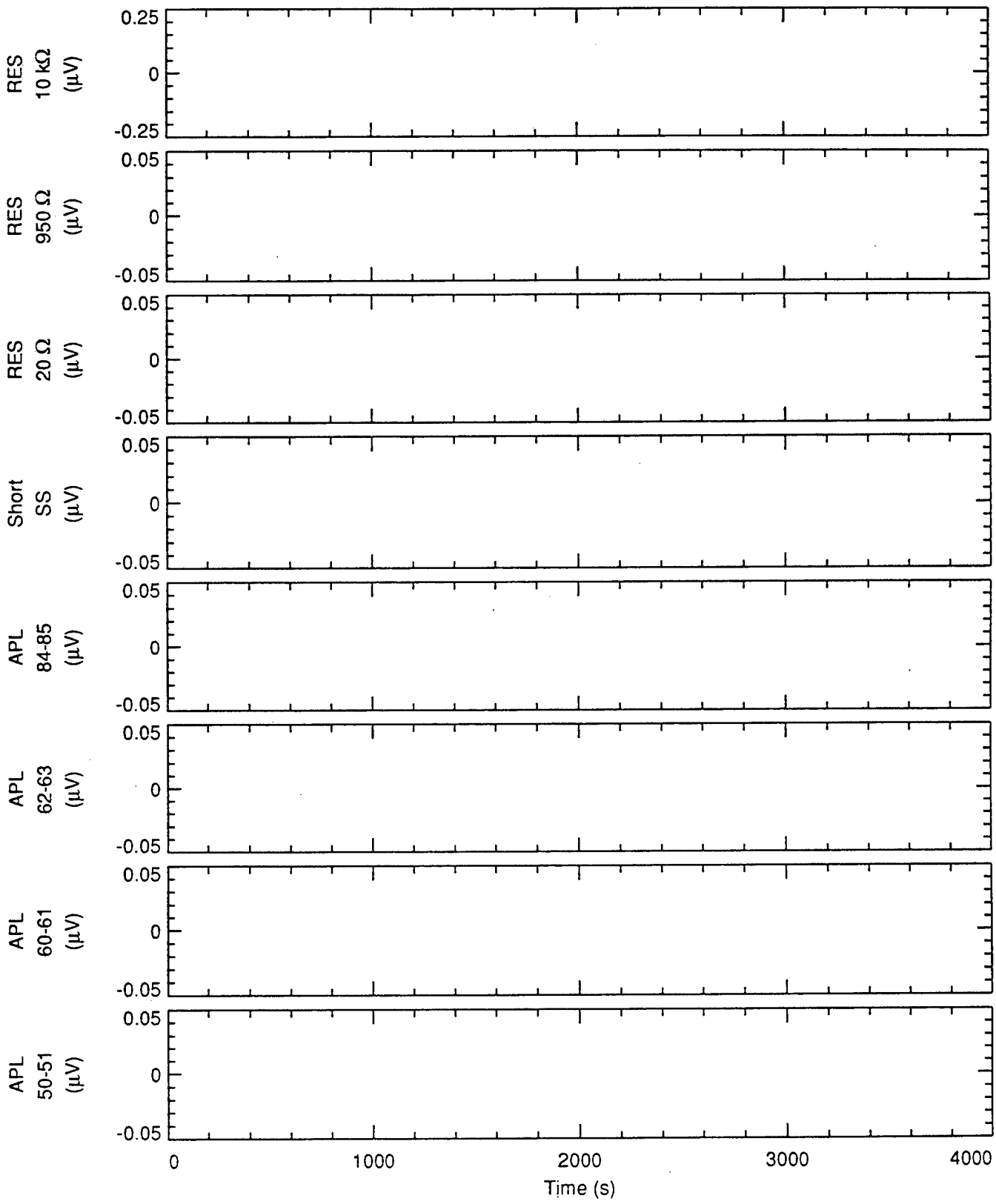
RES 10 kΩ (μV)
RES 950 Ω (μV)
RES 20 Ω (μV)
Short SS (μV)
APL 84-85 (μV)
APL 62-63 (μV)
APL 60-61 (μV)
APL 50-51 (μV)
0.25
0
-0.25
0.05
0
-0.05
0
1000
2000
3000
4000
Time (s)

Figure A.10b

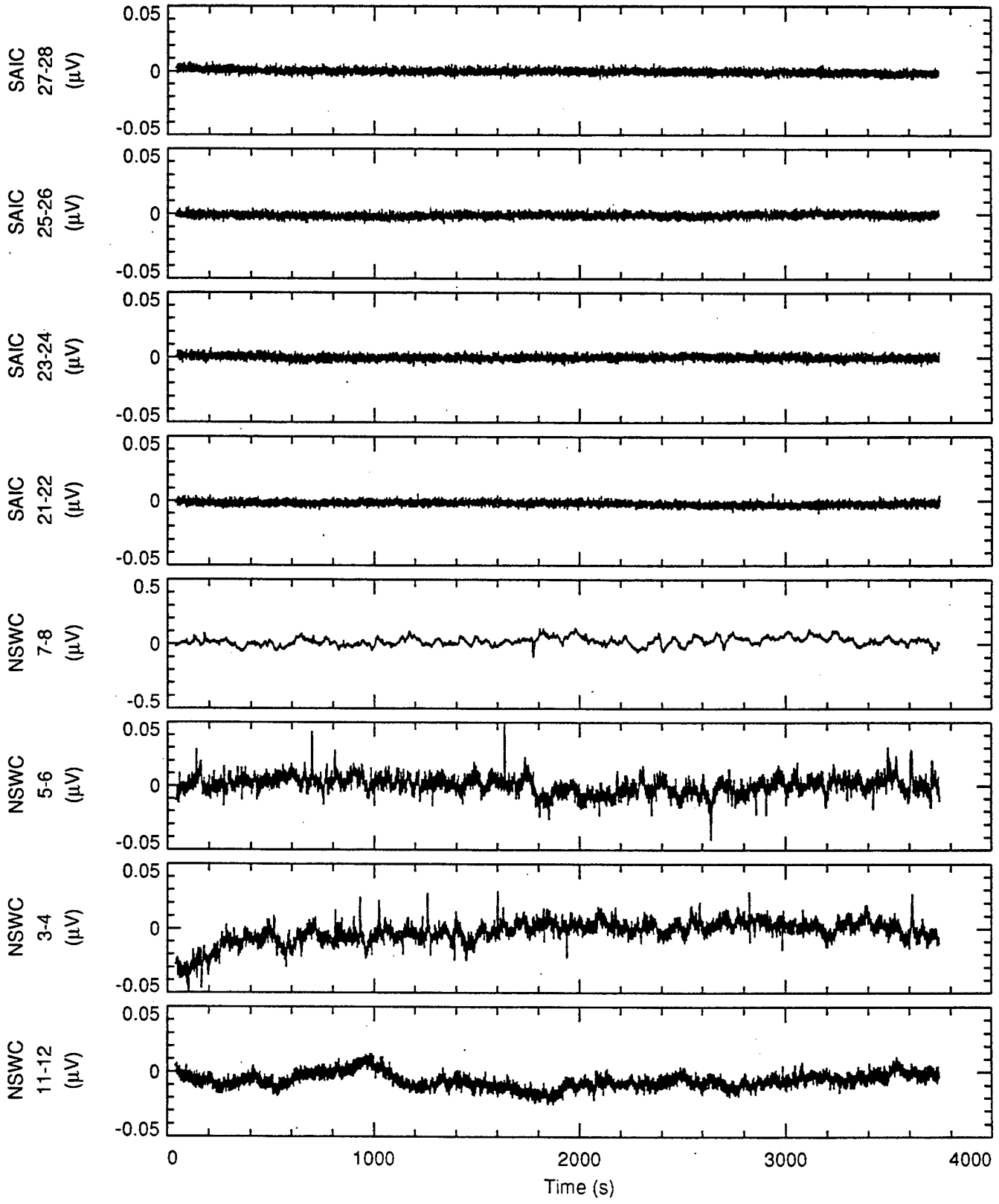
SAIC 27-28 (μV)
SAIC 25-26 (μV)
SAIC 23-24 (μV)
SAIC 21-22 (μV)
NSWC 7-8 (μV)
NSWC 5-6 (μV)
NSWC 3-4 (μV)
NSWC 11-12 (μV)
0.05
0
-0.05
0.5
-0.5
0
1000
2000
3000
4000
Time (s)

Figure A.11a

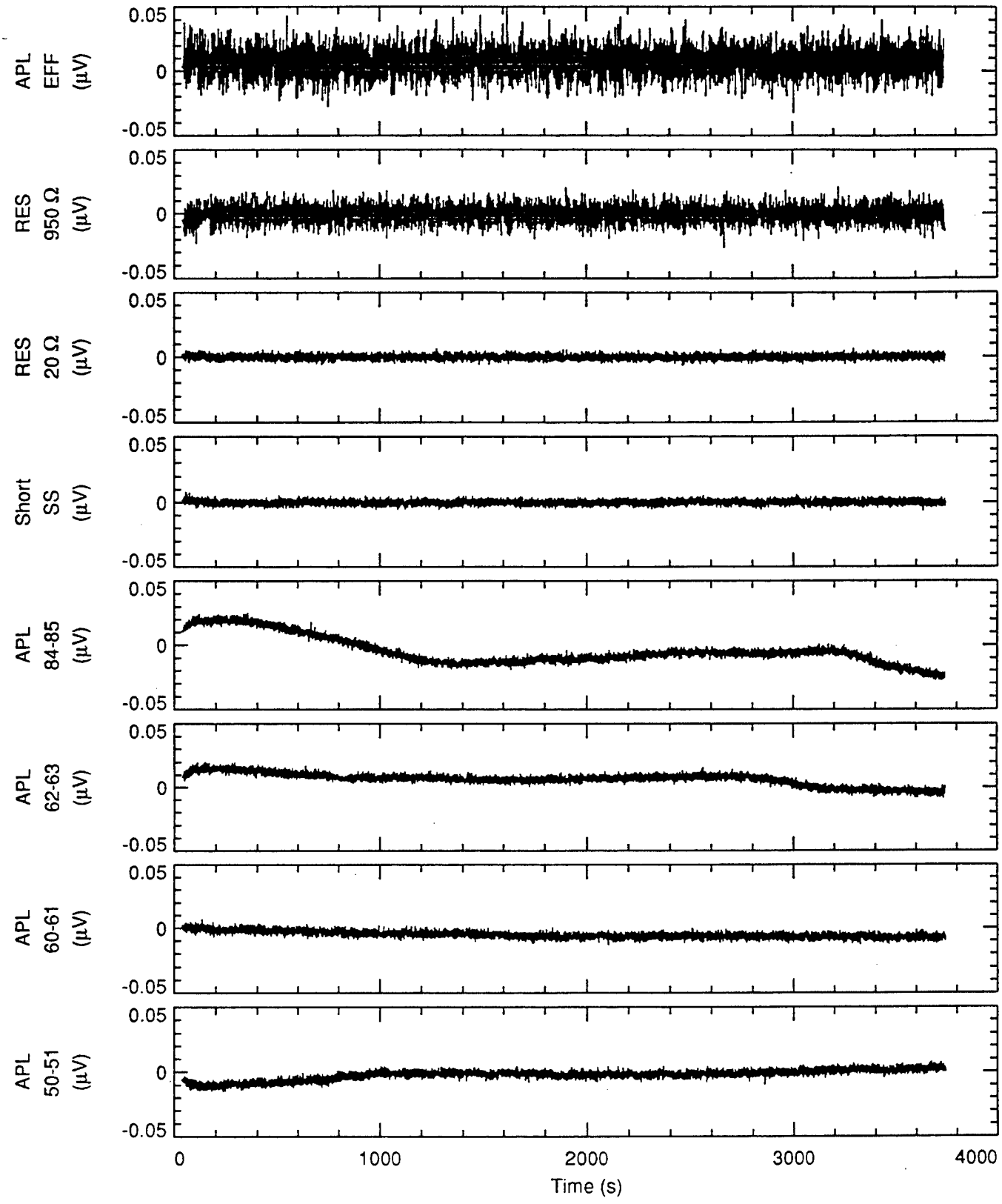
APL EFF (μV)
RES 950 Ω (μV)
RES 20 Ω (μV)
Short SS (μV)
APL 84-85 (μV)
APL 62-63 (μV)
APL 60-61 (μV)
APL 50-51 (μV)
0.05
0
-0.05
0
1000
2000
3000
4000
Time (s)

Figure A.11b

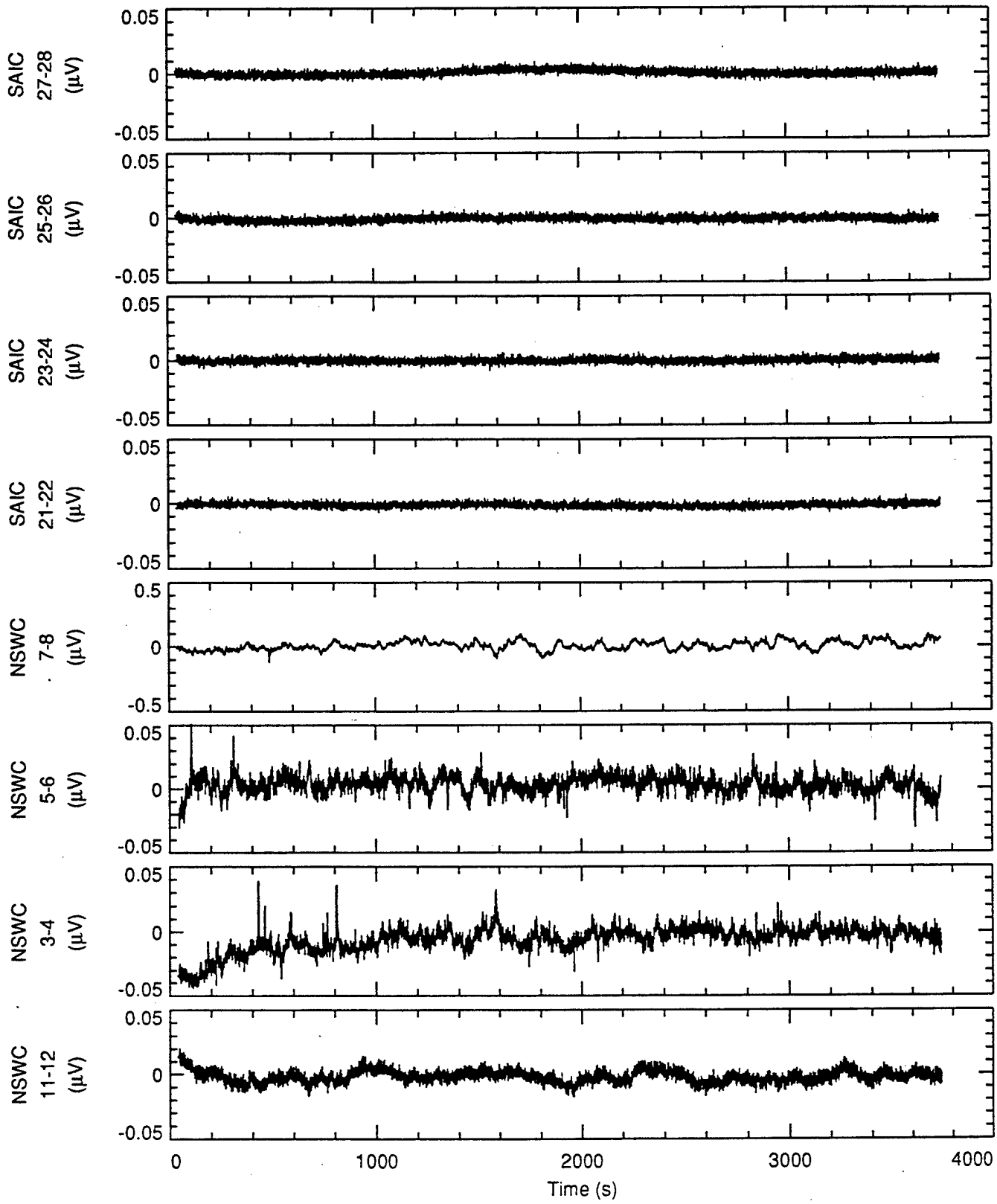
SAIC 27-28 (μV)
SAIC 25-26 (μV)
SAIC 23-24 (μV)
SAIC 21-22 (μV)
NSWC 7-8 (μV)
NSWC 5-6 (μV)
NSWC 3-4 (μV)
NSWC 11-12 (μV)
0.05
0
-0.05
0.5
-0.5
0
1000
2000
3000
4000
Time (s)

Figure A.12a

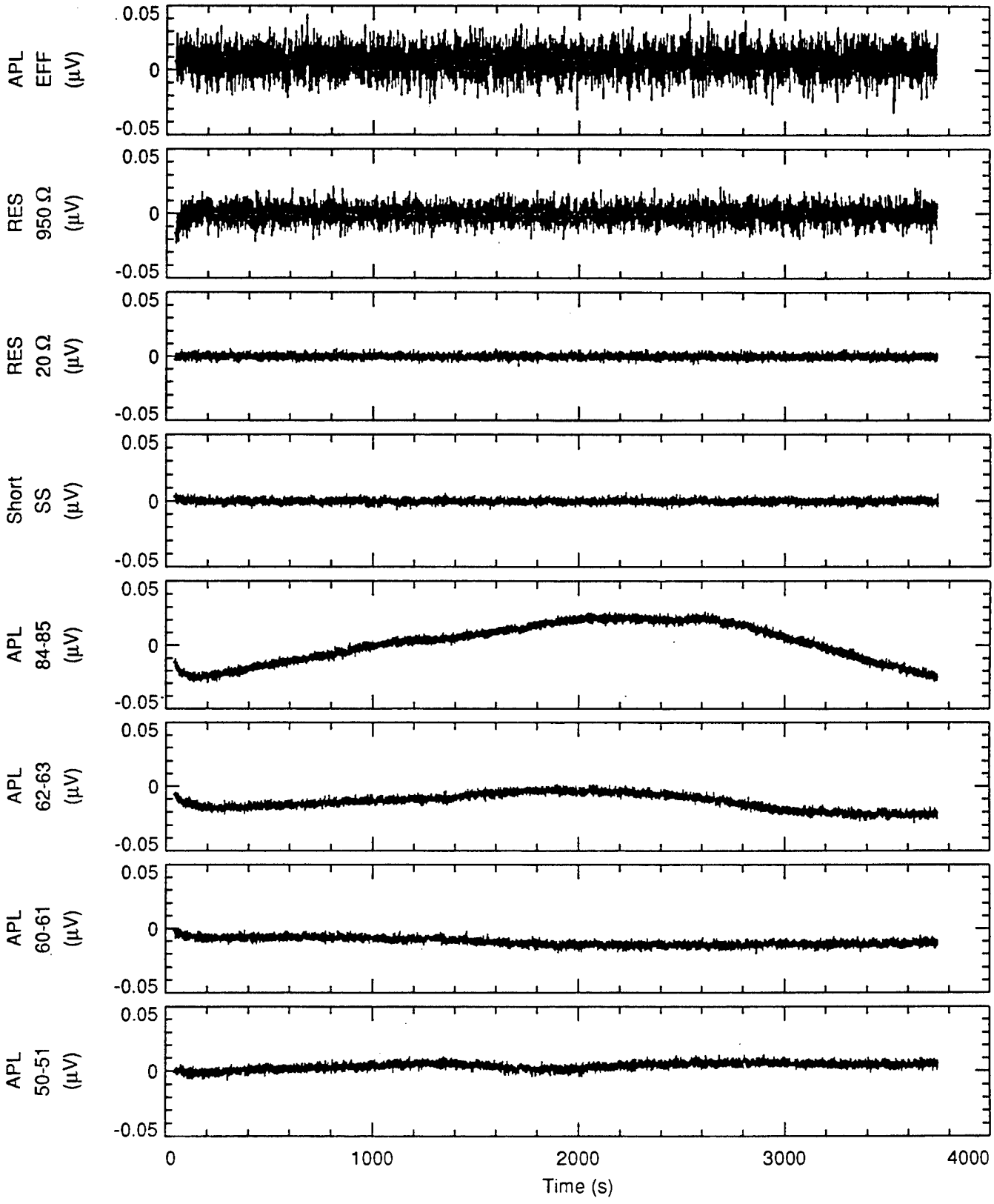
APL EFF (μV)
RES 950 Ω (μV)
RES 20 Ω (μV)
Short SS (μV)
APL 84-85 (μV)
APL 62-63 (μV)
APL 60-61 (μV)
APL 50-51 (μV)
0.05
0
-0.05
0
1000
2000
3000
4000
Time (s)

Figure A.12b

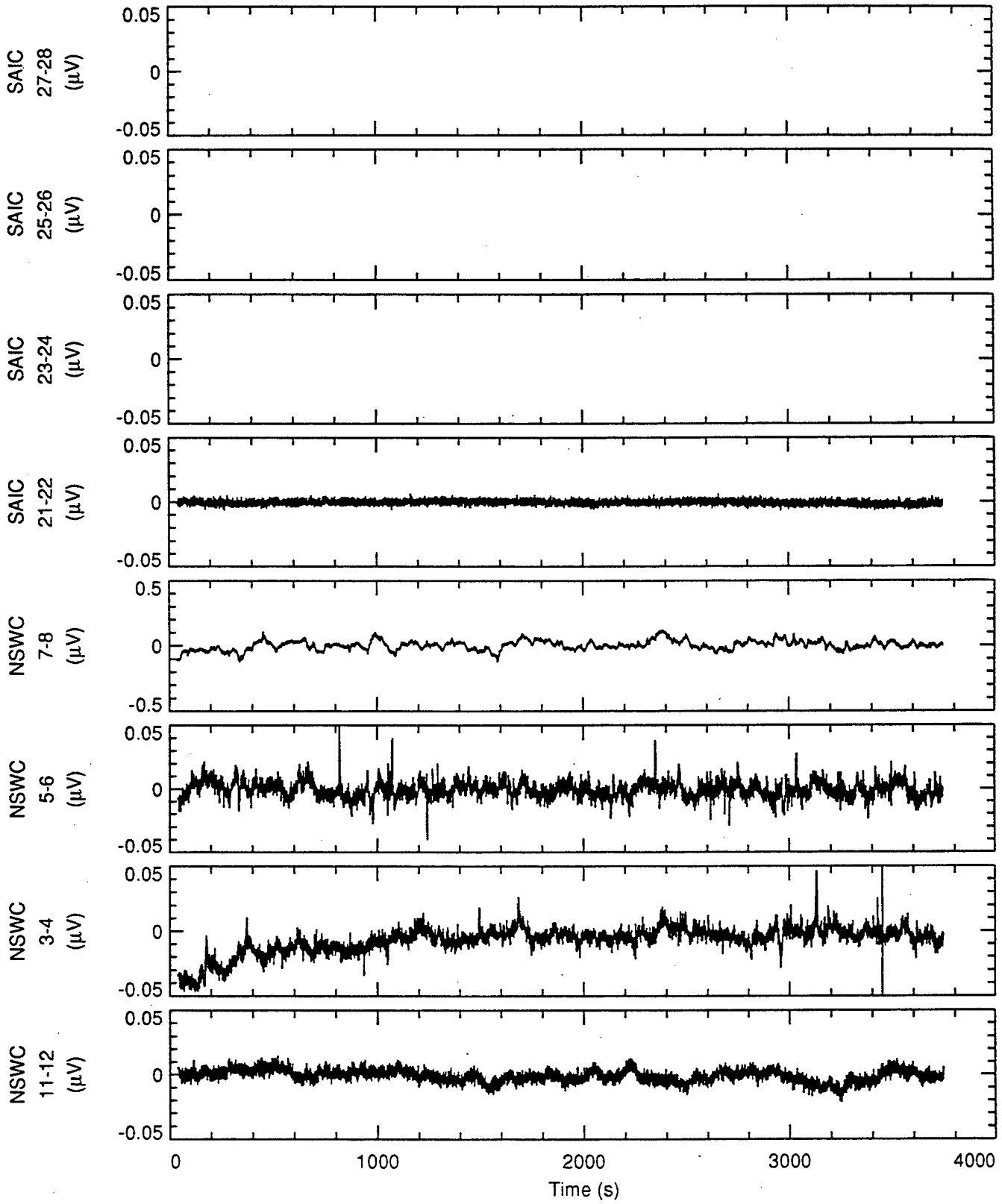
SAIC 27-28 (μV)
SAIC 25-26 (μV)
SAIC 23-24 (μV)
SAIC 21-22 (μV)
NSWC 7-8 (μV)
NSWC 5-6 (μV)
NSWC 3-4 (μV)
NSWC 11-12 (μV)
0.05
0
-0.05
0.5
-0.5
0
1000
2000
3000
4000
Time (s)

Figure A.13a

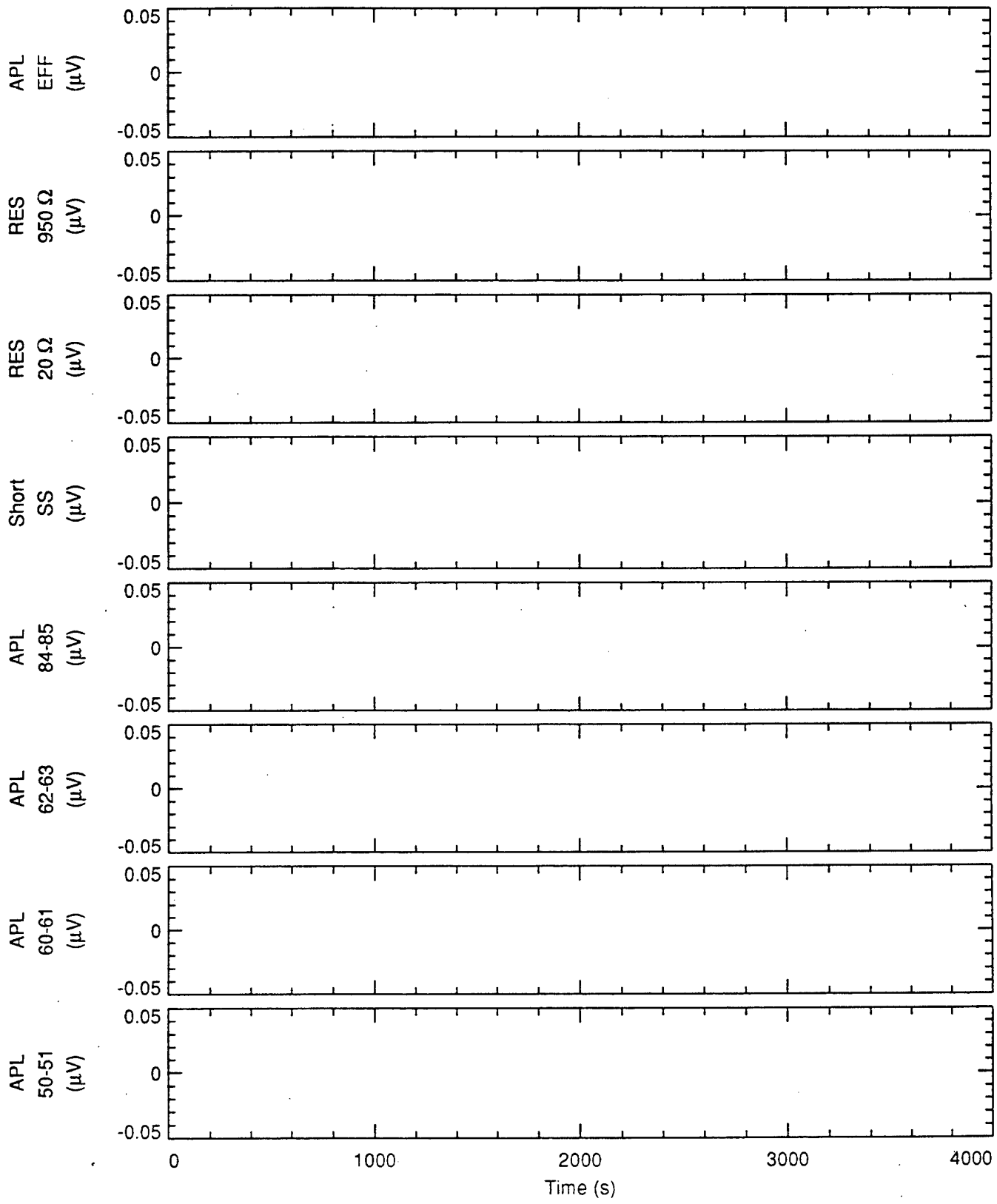
APL EFF (μV)
RES 950 Ω (μV)
RES 20 Ω (μV)
Short SS (μV)
APL 84-85 (μV)
APL 62-63 (μV)
APL 60-61 (μV)
APL 50-51 (μV)
0.05
0
-0.05
0
1000
2000
3000
4000
Time (s)

Figure A.13b

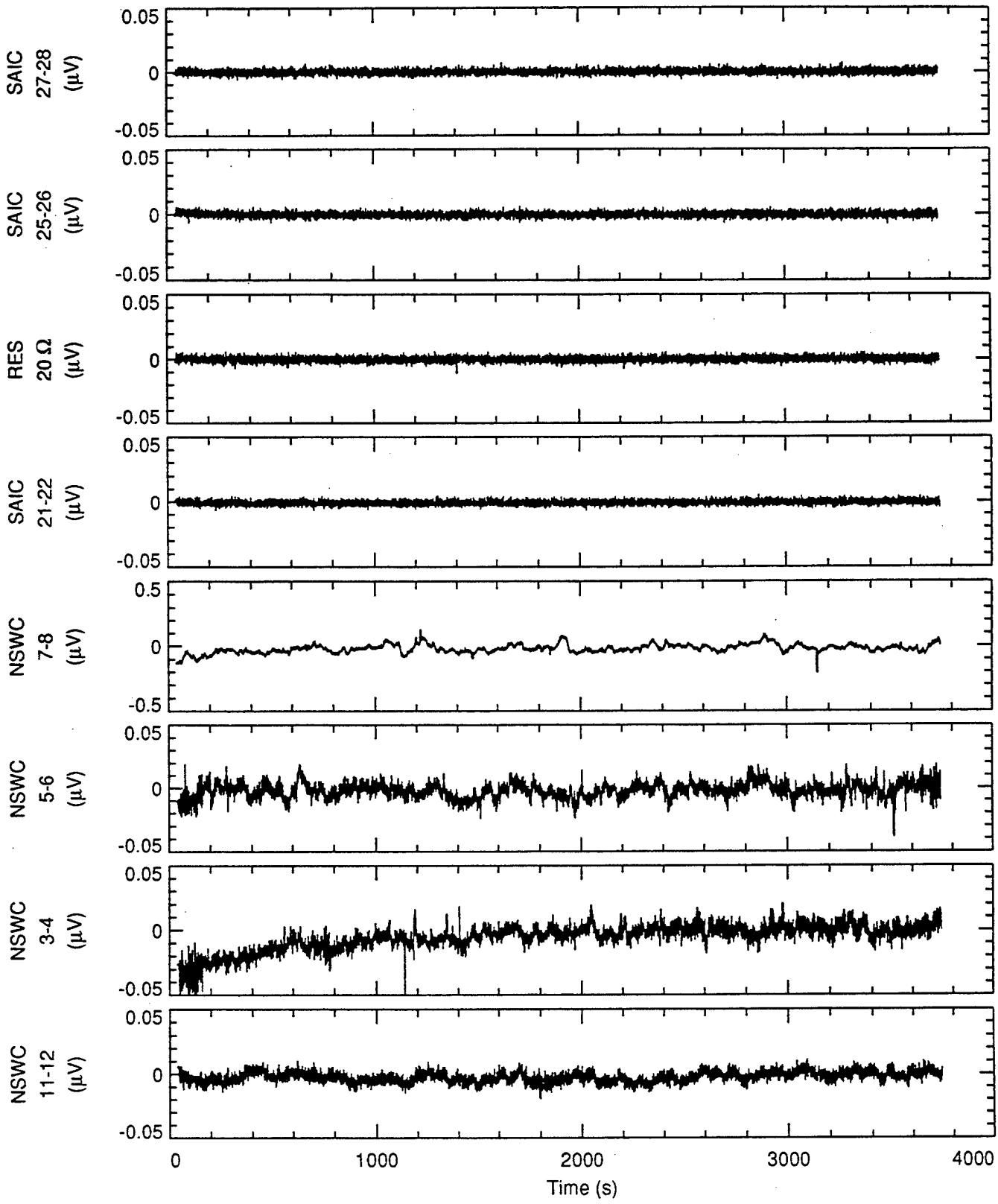
SAIC 27-28 (μV)
SAIC 25-26 (μV)
RES 20 Ω (μV)
SAIC 21-22 (μV)
NSWC 7-8 (μV)
NSWC 5-6 (μV)
NSWC 3-4 (μV)
NSWC 11-12 (μV)
0.05
0
-0.05
0.5
-0.5
0
1000
2000
3000
4000
Time (s)

Figure A.14a

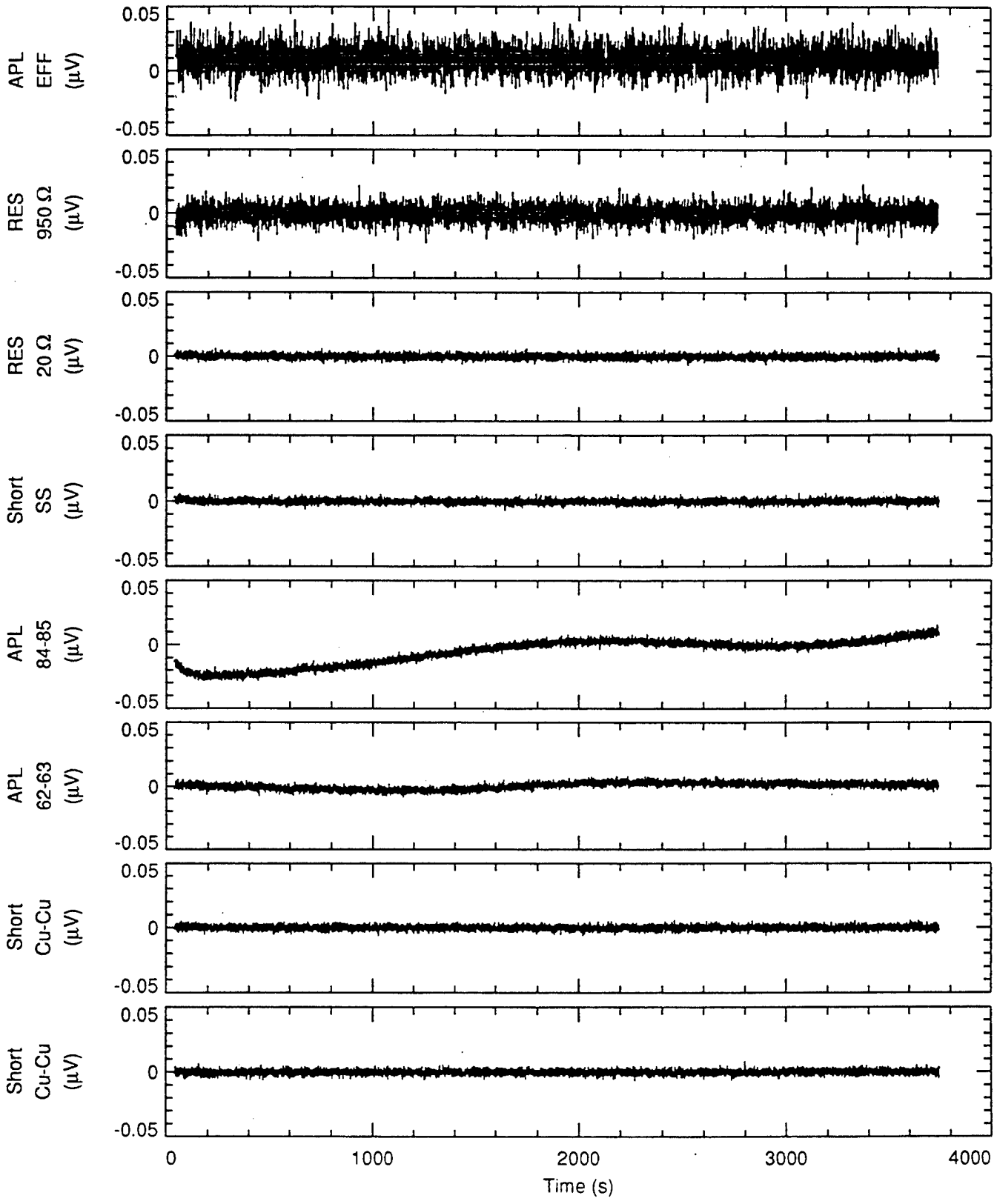
APL EFF (μV)
RES 950 Ω (μV)
RES 20 Ω (μV)
Short SS (μV)
APL 84-85 (μV)
APL 62-63 (μV)
Short Cu-Cu (μV)
Short Cu-Cu (μV)
0.05
0
-0.05
0
1000
2000
3000
4000
Time (s)

Figure A.14b

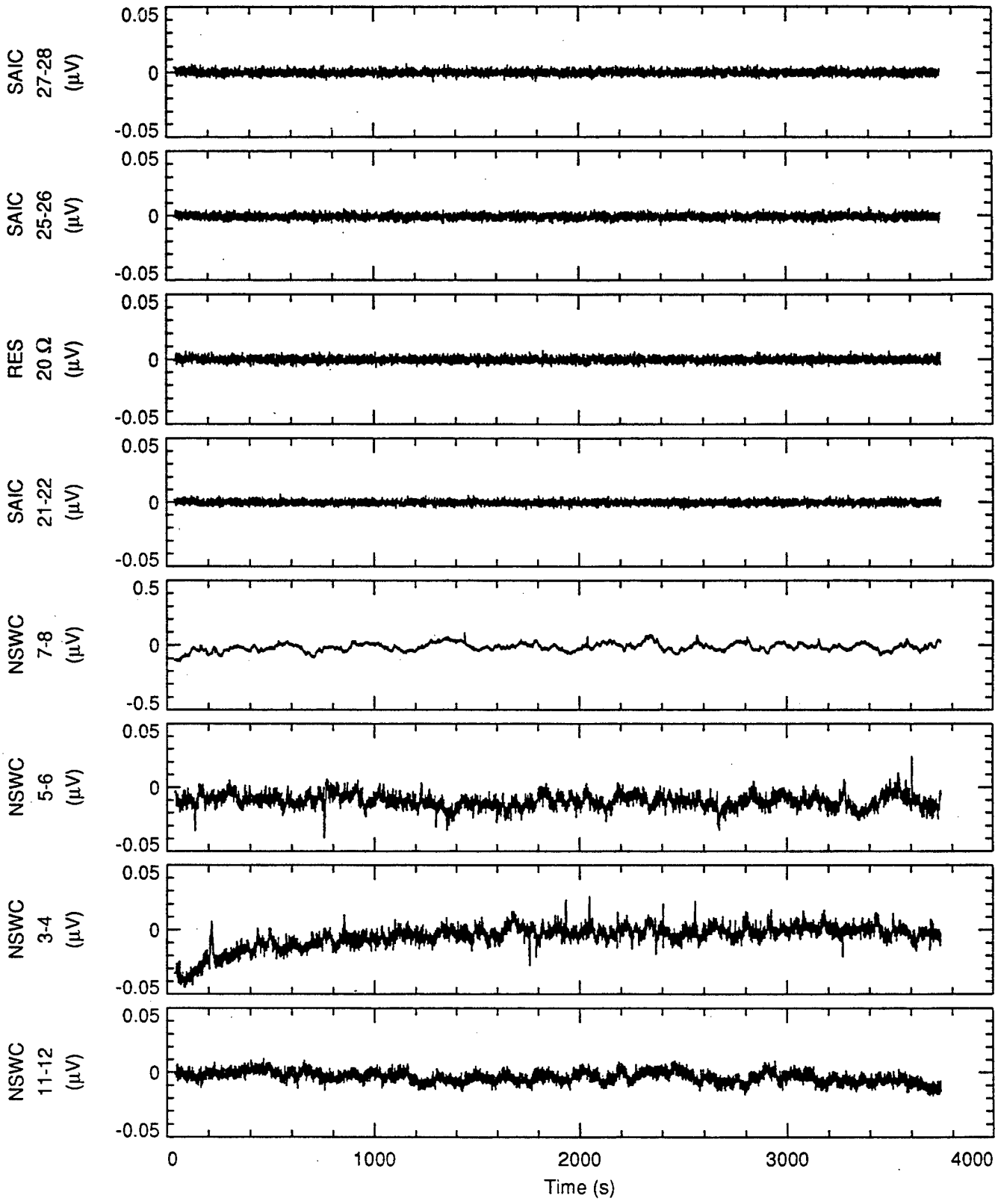
SAIC 27-28 (μV)
SAIC 25-26 (μV)
RES 20 Ω (μV)
SAIC 21-22 (μV)
NSWC 7-8 (μV)
NSWC 5-6 (μV)
NSWC 3-4 (μV)
NSWC 11-12 (μV)
0.05
0
-0.05
0.5
-0.5
0
1000
2000
3000
4000
Time (s)

Figure A.15a

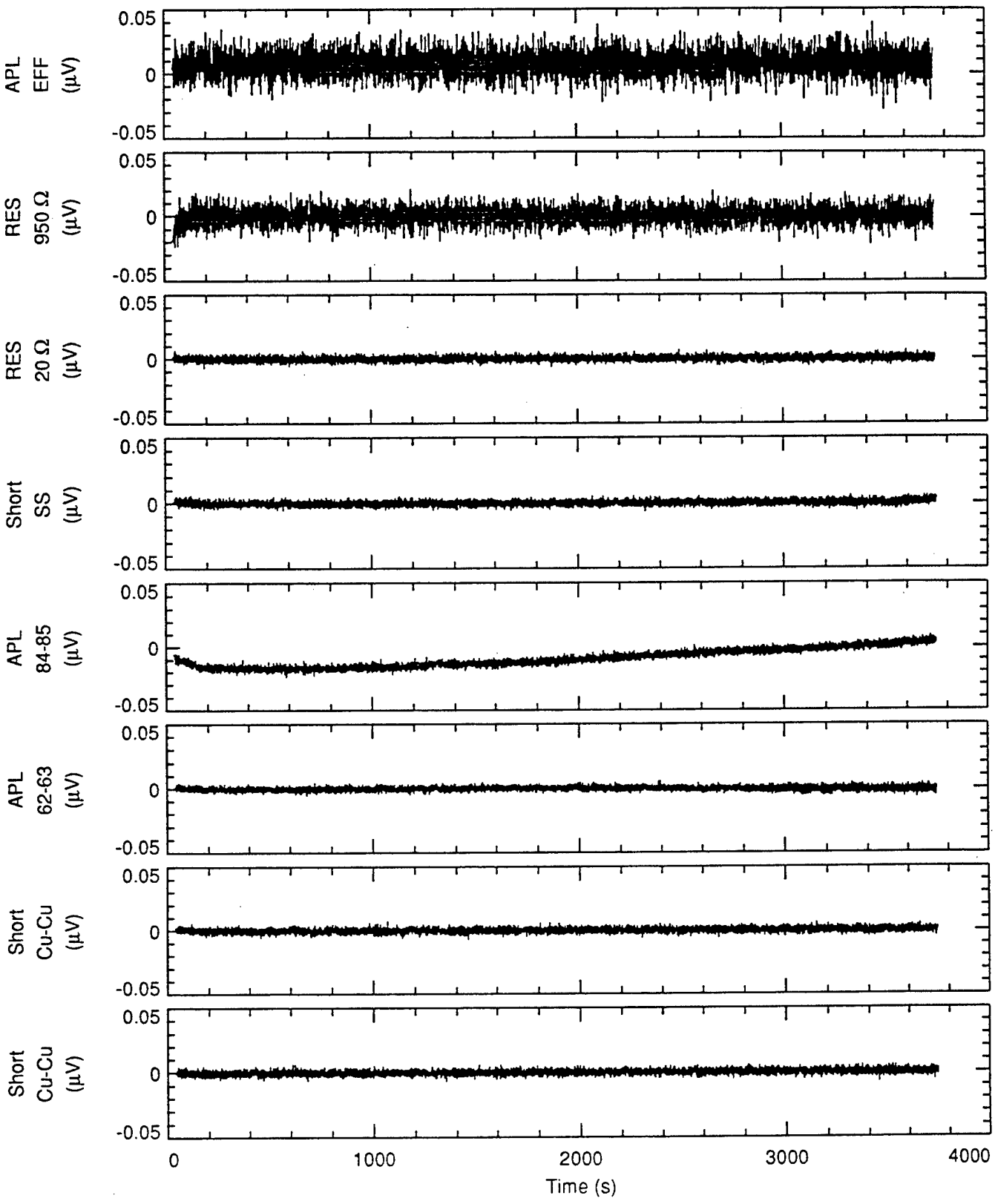
APL EFF (μV)
RES 950 Ω (μV)
RES 20 Ω (μV)
Short SS (μV)
APL 84-85 (μV)
APL 62-63 (μV)
Short Cu-Cu (μV)
Short Cu-Cu (μV)
0.05
0
-0.05
0
1000
2000
3000
4000
Time (s)

Figure A.15b

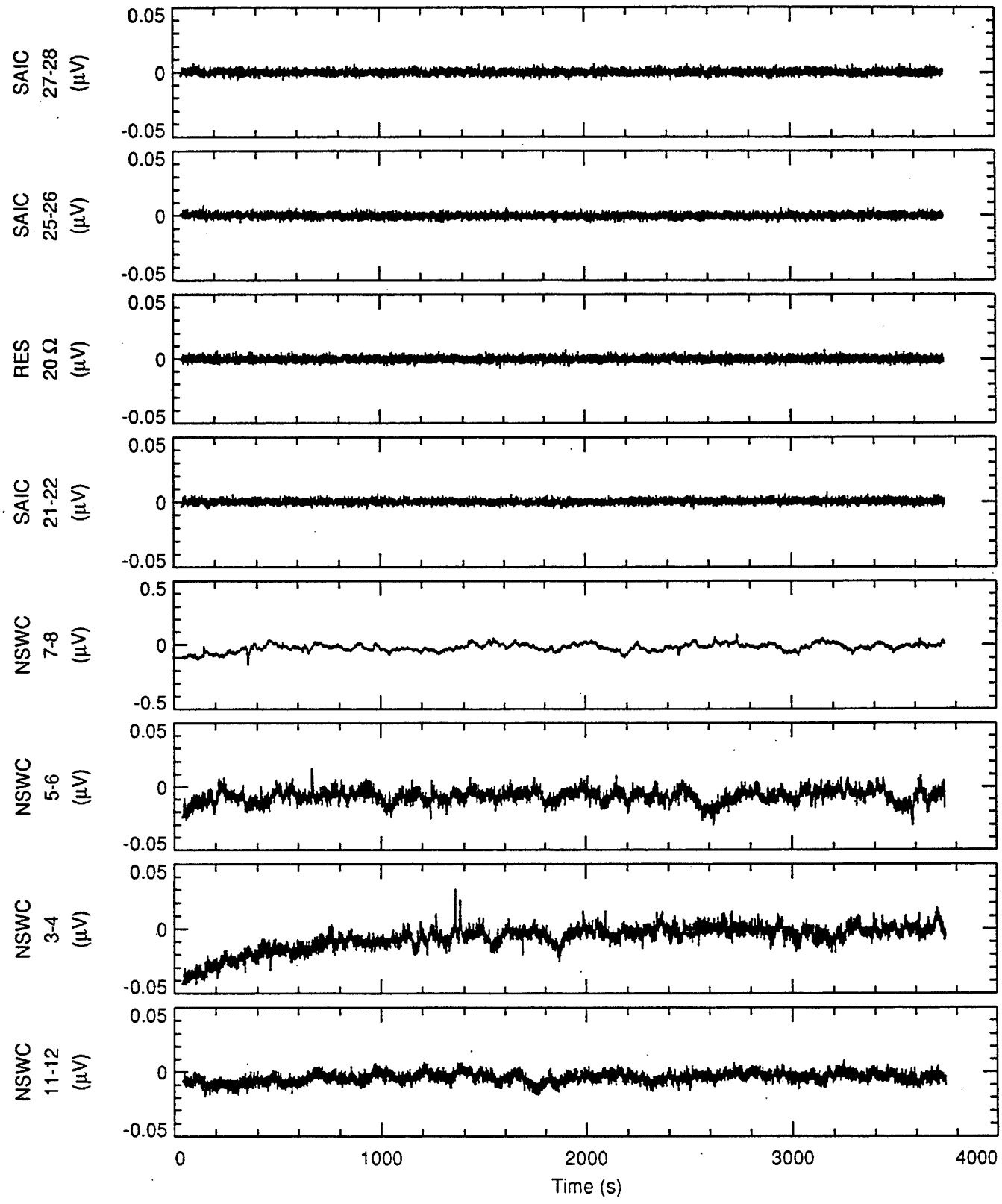
SAIC 27-28 (μV)
SAIC 25-26 (μV)
RES 20 Ω (μV)
SAIC 21-22 (μV)
NSWC 7-8 (μV)
NSWC 5-6 (μV)
NSWC 3-4 (μV)
NSWC 11-12 (μV)
0.05
0
-0.05
0.5
-0.5
0
1000
2000
3000
4000
Time (s)

Figure A.16a

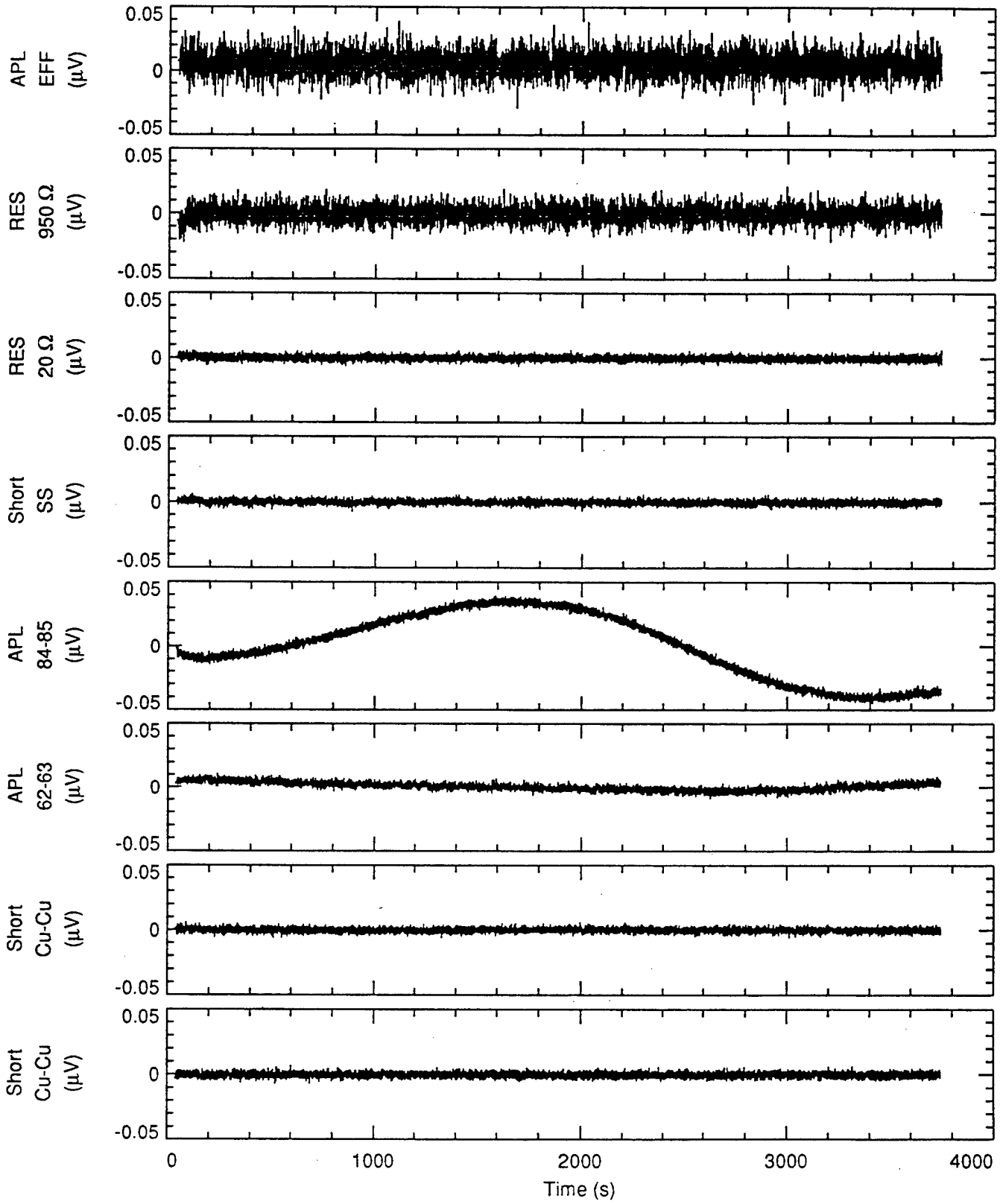
APL EFF (μV)
RES 950 Ω (μV)
RES 20 Ω (μV)
Short SS (μV)
APL 84-85 (μV)
APL 62-63 (μV)
Short Cu-Cu (μV)
Short Cu-Cu (μV)
0.05
0
-0.05
0
1000
2000
3000
4000
Time (s)

Figure A.16b

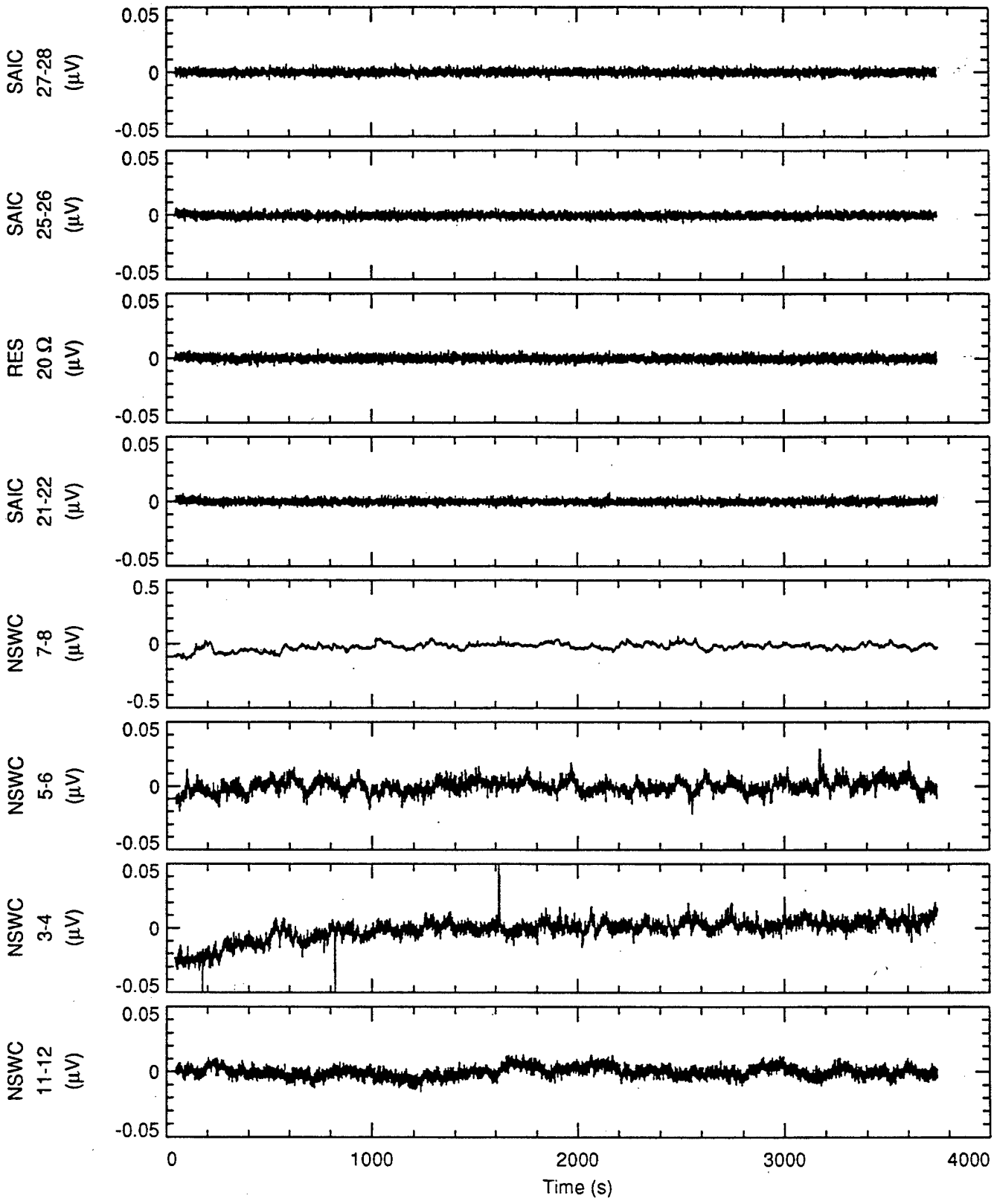
SAIC 27-28 (μV)
SAIC 25-26 (μV)
RES 20 Ω (μV)
SAIC 21-22 (μV)
NSWC 7-8 (μV)
NSWC 5-6 (μV)
NSWC 3-4 (μV)
NSWC 11-12 (μV)
0.05
0
-0.05
0.5
-0.5
0
1000
2000
3000
4000
Time (s)

Figure A.17a

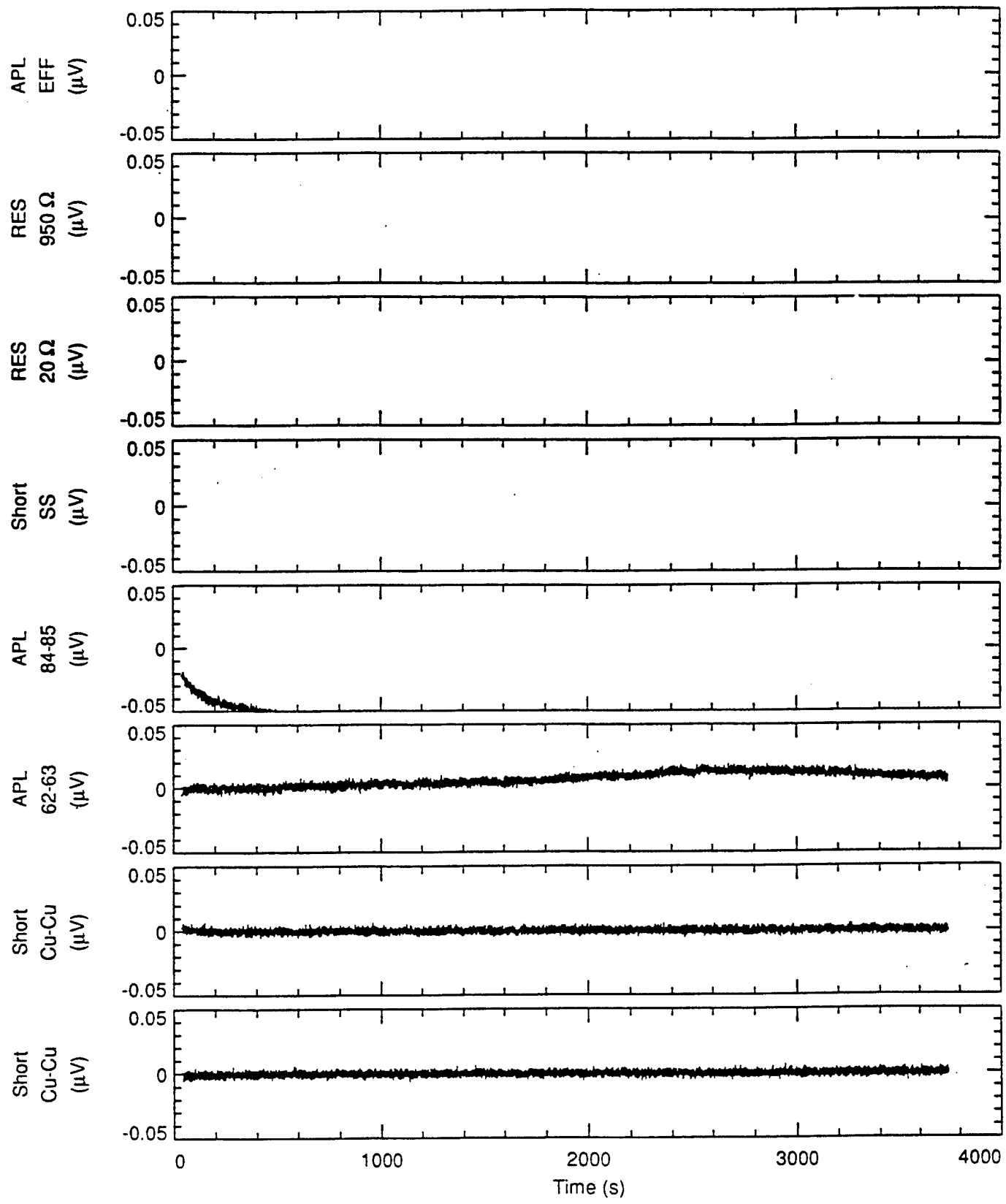
APL EFF (μV)
RES 950 Ω (μV)
RES 20 Ω (μV)
Short SS (μV)
APL 84-85 (μV)
APL 62-63 (μV)
Short Cu-Cu (μV)
Short Cu-Cu (μV)
0.05
0
-0.05
0
1000
2000
3000
4000
Time (s)

Figure A.17b

APPENDIX B: Electrode Spectra

The spectra shown here are from the MF and HF sampling in the isothermal bath. The MF and HF spectra in each figure are computed separately and shown together. There is different spectral processing for the MF and HF spectra. The spectral processing is explained in Section 5. The spurious emissions of the Keithley 1801 preamplifier have been removed in order to show the electrode spectra. We have assumed that the electrodes have no spectral lines.

There are 16 figures. The first four show spectra from the APL electrodes at 4, 10, 15, and 17-19°C. The next four are for the NSWC electrodes at the same temperatures. The third group of four shows the SAIC electrodes. The last four show the resistor noises. The resistor noise is less than any of the electrodes.

The "LF" program was used with all 16 scanner channels sampled as well as temperature. The first 12 channels were electrodes and the last 4 were resistors. Initially the overall sample rate was 50 s, but we were concerned that 5 samples per scanner channel were insufficient and increased the number of samples to 10, resulting in a sample interval of 120 s.

Initially the "LF" program used a Keithley 181 Nanovoltmeter on the 2 mV range. This is because the Keithley 2001 and K-1801 had not yet been delivered. The K-181 was known to be inferior to the K-2001/K-1801 combination, but we felt that we could debug the experimental procedure with the K-181. The K-181 noise level with 0.25 second integration time is 100 nV peak to peak.

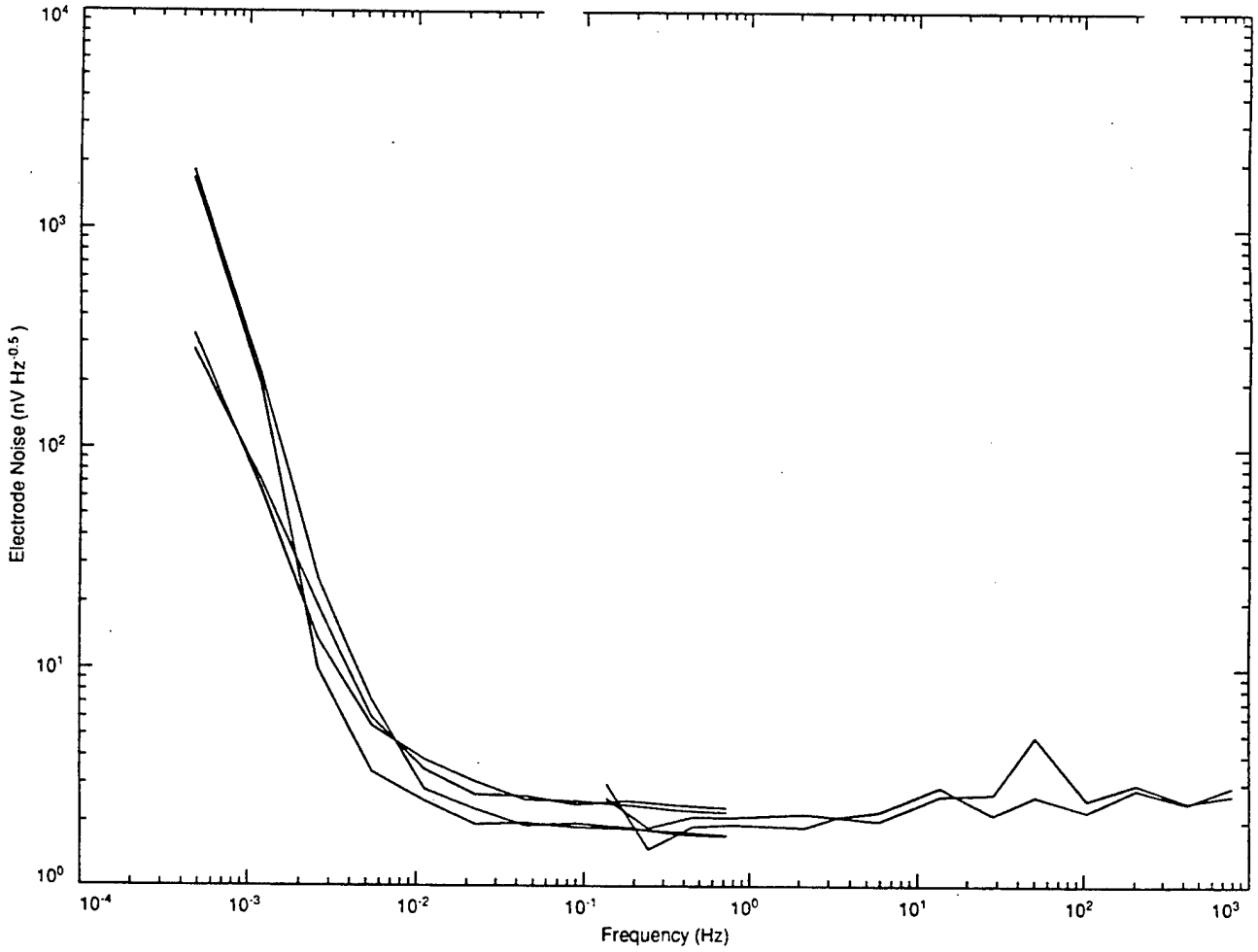

Figure B.1 APL electrode spectra at 4°C. Four electrode pairs were sampled for the the spectra below 1 Hz while two were sampled above 1 Hz. The better pairs have about 100 nV/$\sqrt{\text{Hz}}$ noise at 1 mHz and reach the instrumentation noise floor of 2 to 3 nV/$\sqrt{\text{Hz}}$ at about 30 mHz.

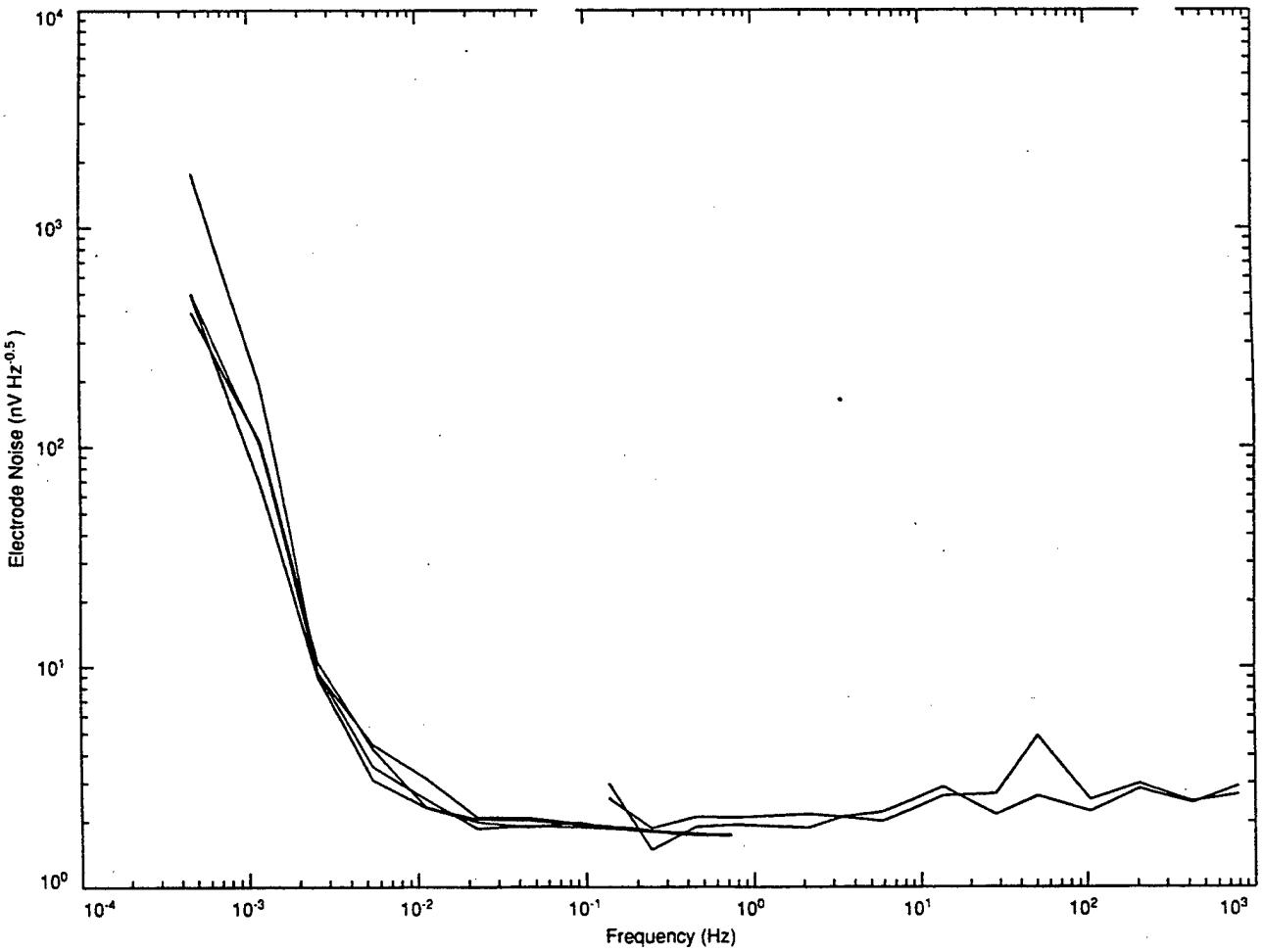

Figure B.2 APL electrode spectra at 10°C. Almost the same results as Figure B.1 except the noise floor is reached at a slightly lower frequency and all pairs are quieter at 100 mHz.

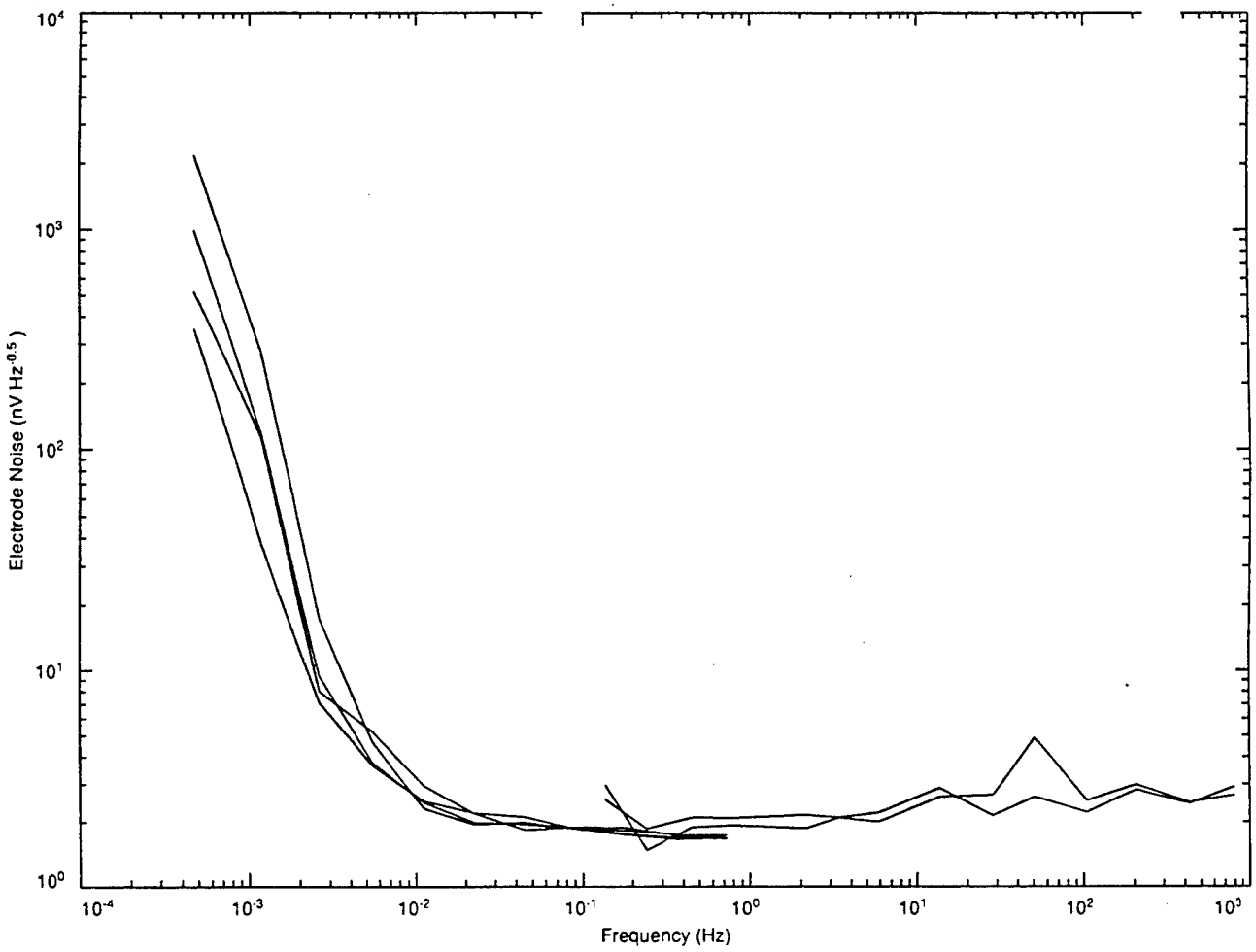

Figure B.3 APL electrode spectra at 15°C. No real difference from Figure B.2.

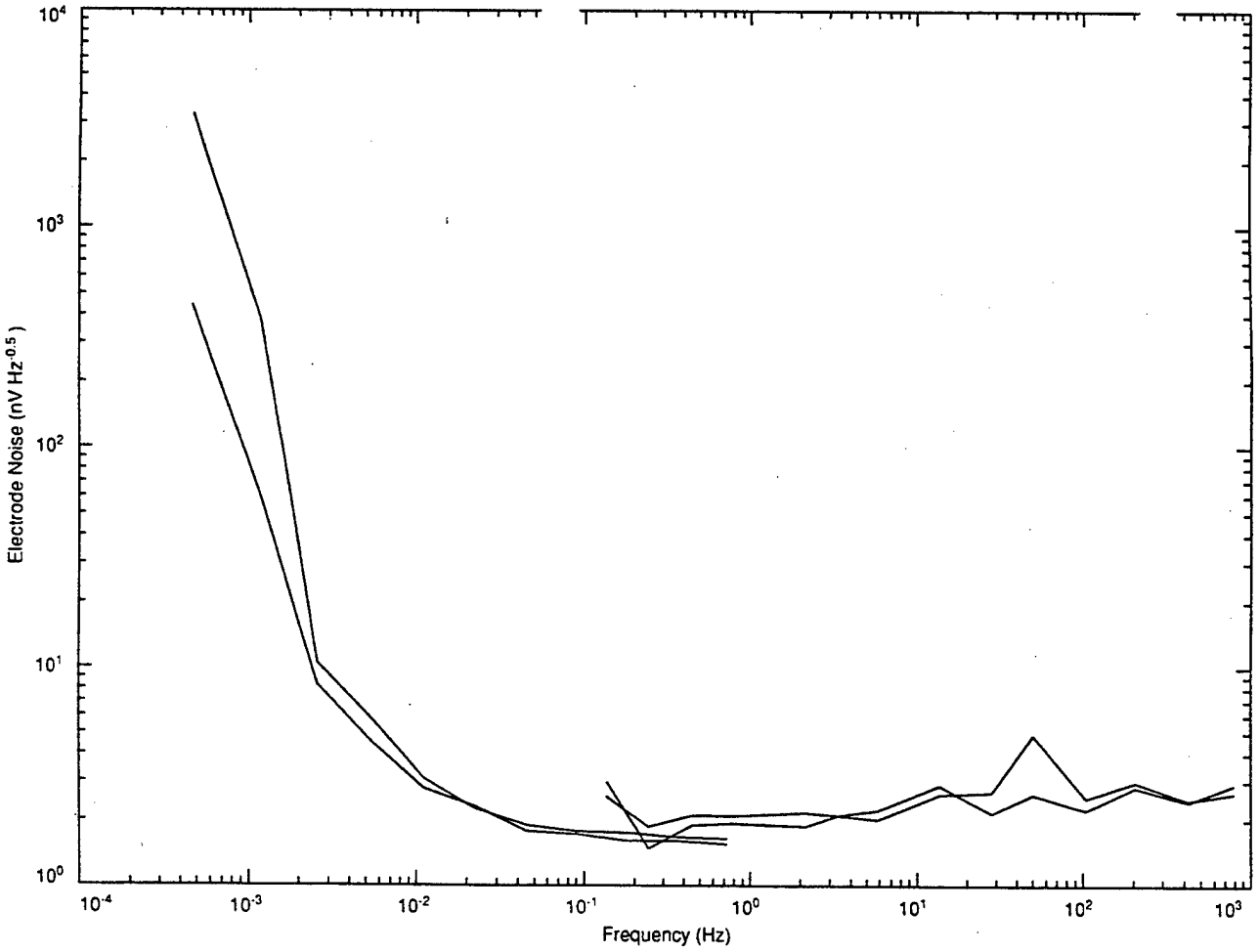

Figure B.4 APL electrode spectra at 17 to 19°C with the bath controller off. The two best pairs of Figures B.1–B3 were removed from the bath to be installed in sensors. The best remaining pair has half the noise it did in the 15°C test; at 1 mHz, it had about 150 nV/$\sqrt{\text{Hz}}$ while here it has 70 nV/$\sqrt{\text{Hz}}$.

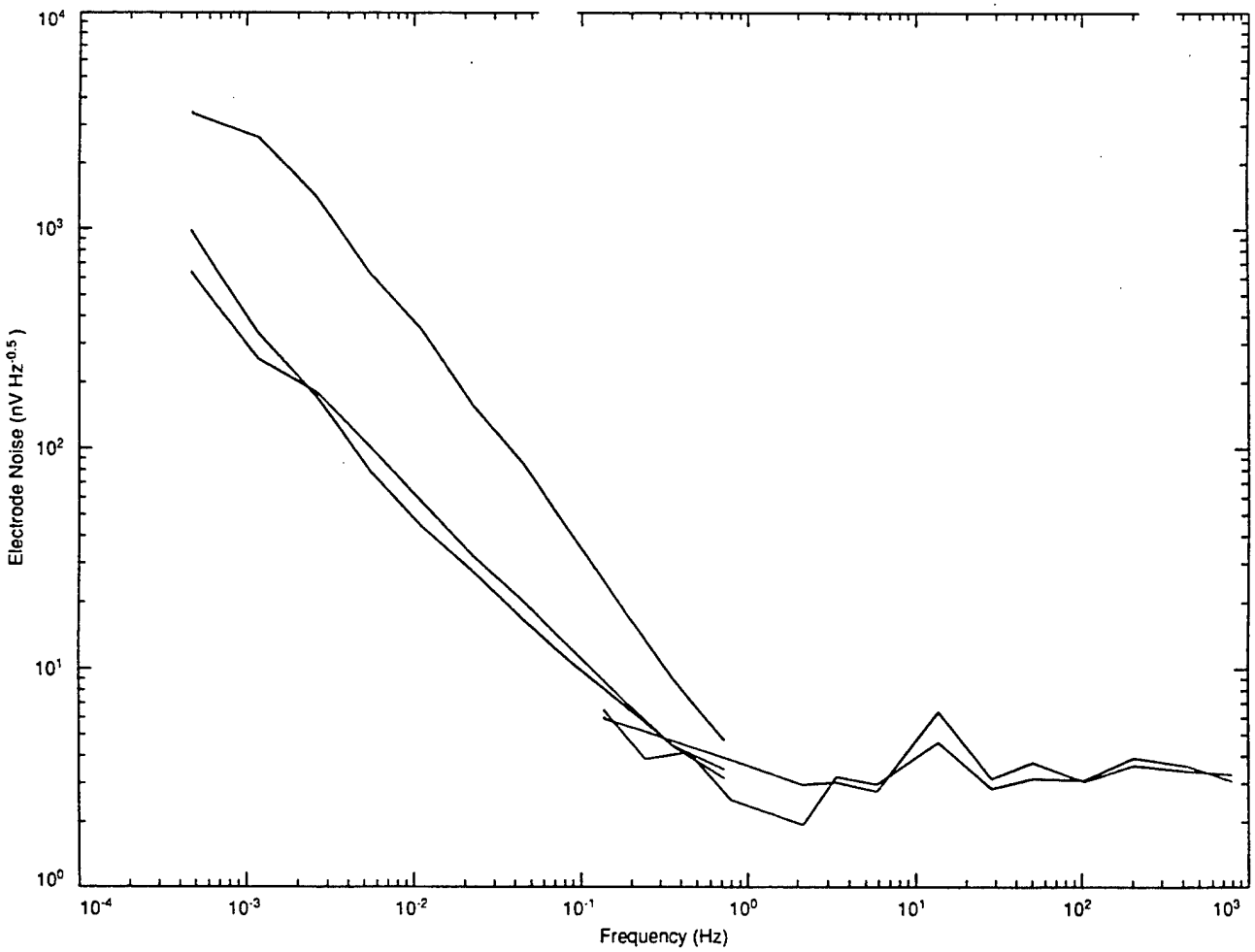

Figure B.5 NSWC electrode spectra at 4°C. Three electrode pairs are shown. The one not shown exceeded the full-scale range of the Keithley 1801 preamplifier. One is obviously noisier than the rest. The slope of the spectrum is much less than the APL and SAIC electrodes. All three pairs reach the instrument noise floor at about 1 Hz. At 1 mHz, the noise of the best electrodes is about 30 to 40 nV/$\sqrt{\text{Hz}}$. The noise floor for the NSWC electrodes, 3–4 nV/$\sqrt{\text{Hz}}$, is somewhat higher than for the APL and SAIC electrodes. This is probably because of higher electrode resistance.

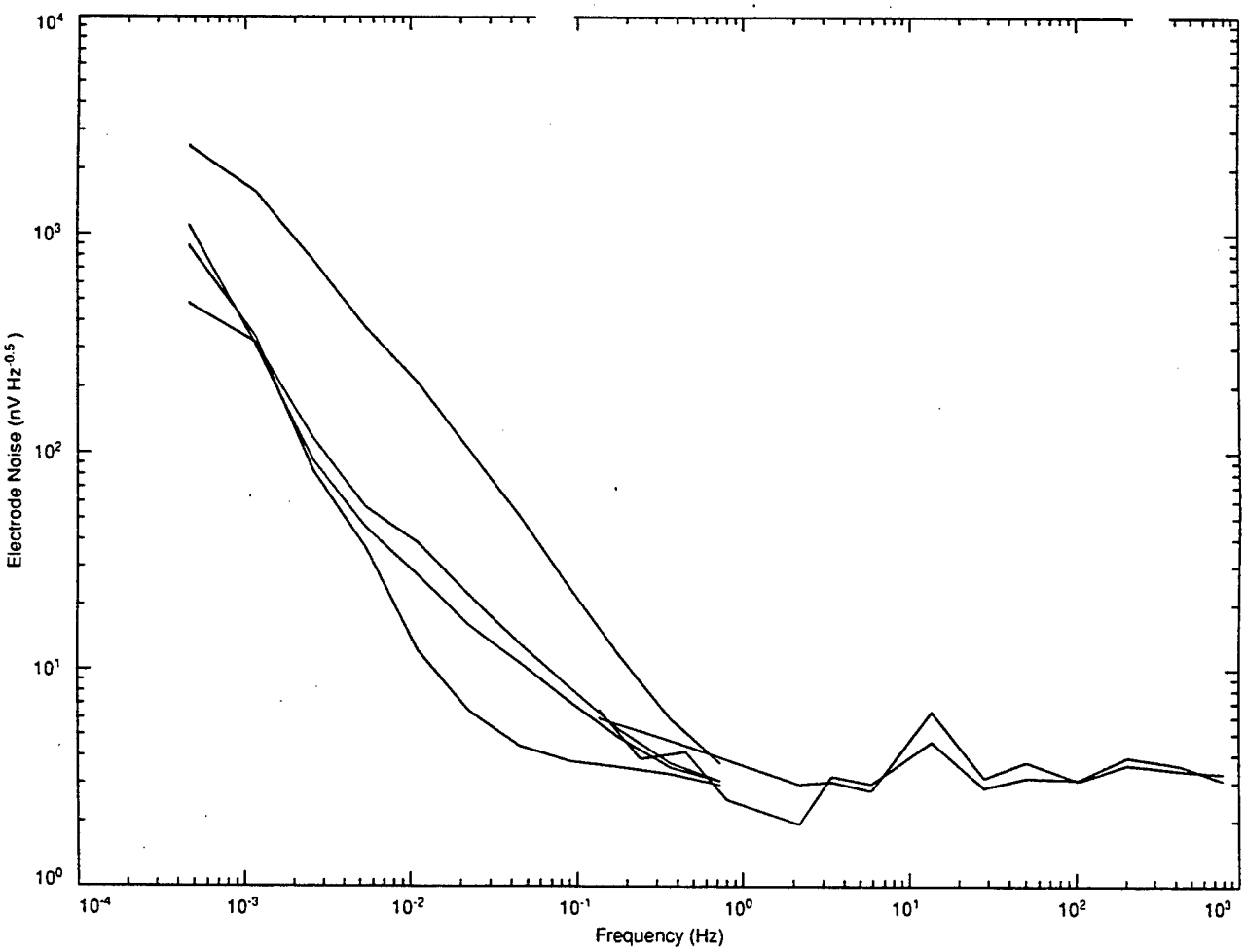

Figure B.6 NSWC electrode spectra at 10°C. Four electrode pairs are shown. The pair that was not shown in Figure B.5 is replaced with a new pair which is much better. The new electrodes reach the noise floor at about 50 mHz, about a decade and a half lower than the other three pair. Even though the new pair is much quieter at 50 mHz, it has the same noise at 1 mHz as the others and Figure B.5.

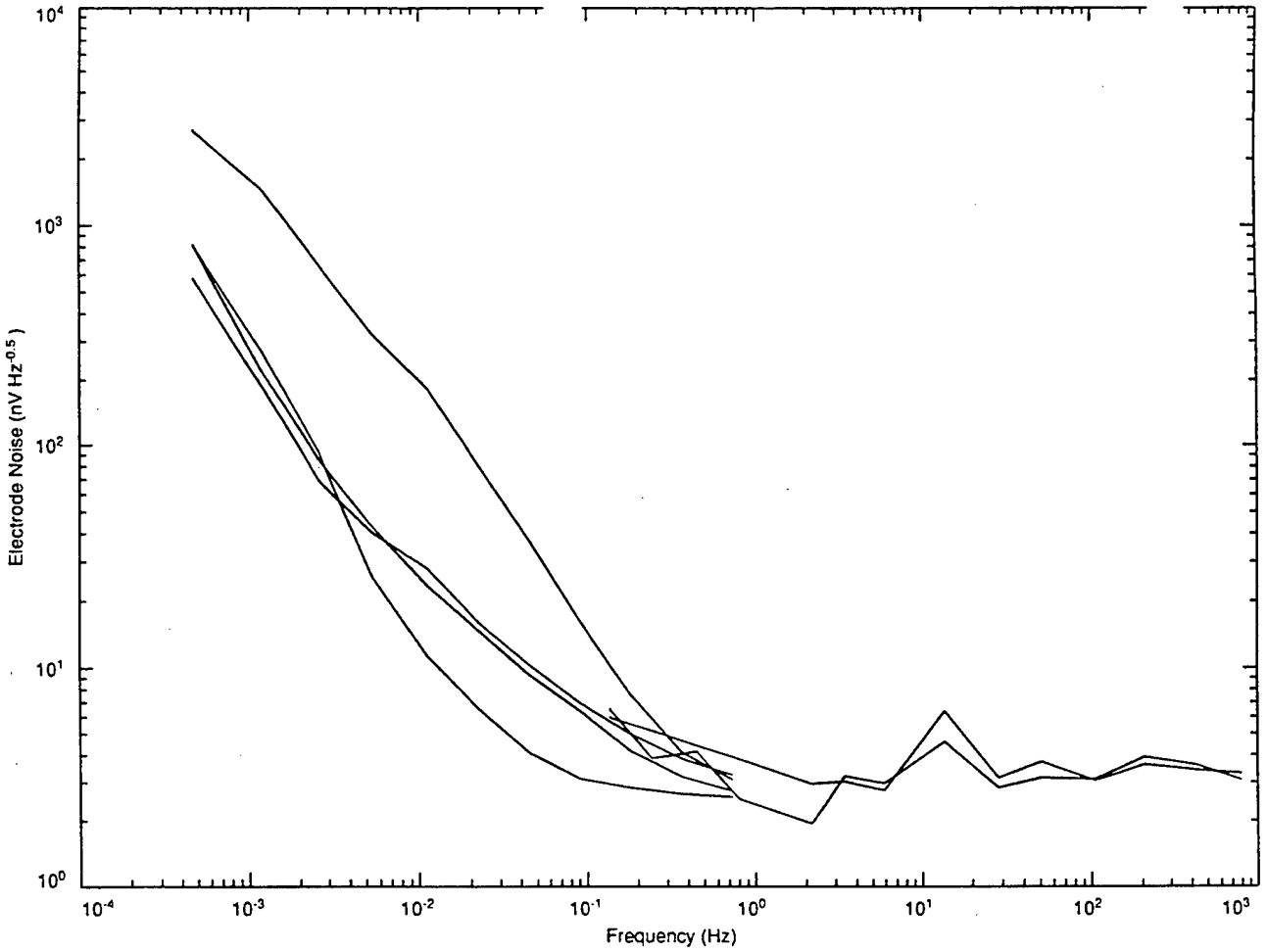

Figure B.7 NSWC electrode spectra at 15°C. The spectral levels are nearly the same as Figure B.6.

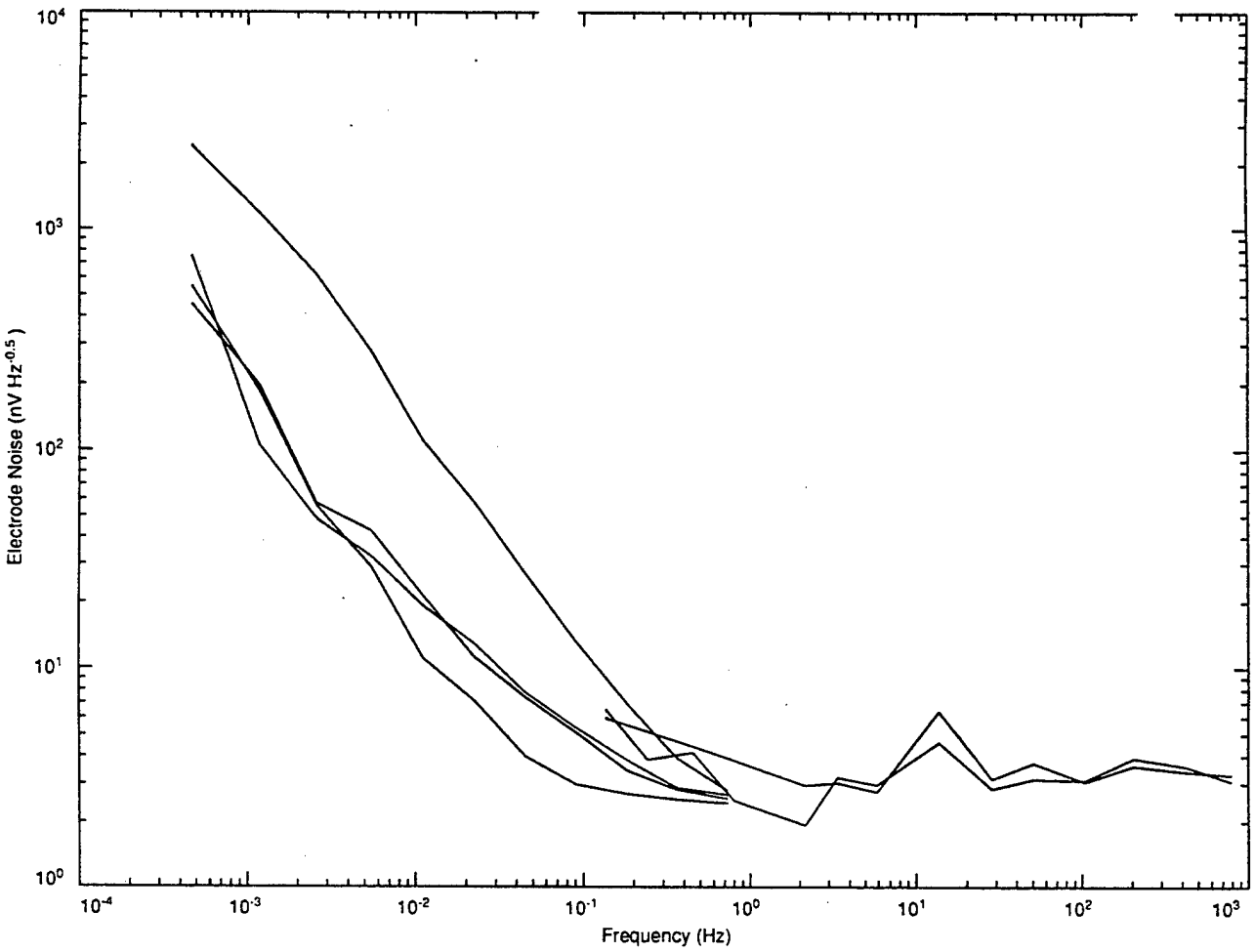

Figure B.8 NSWC electrode spectra at 17–19°C while the bath controller is turned off. The spectral levels are nearly the same as Figure B.6.

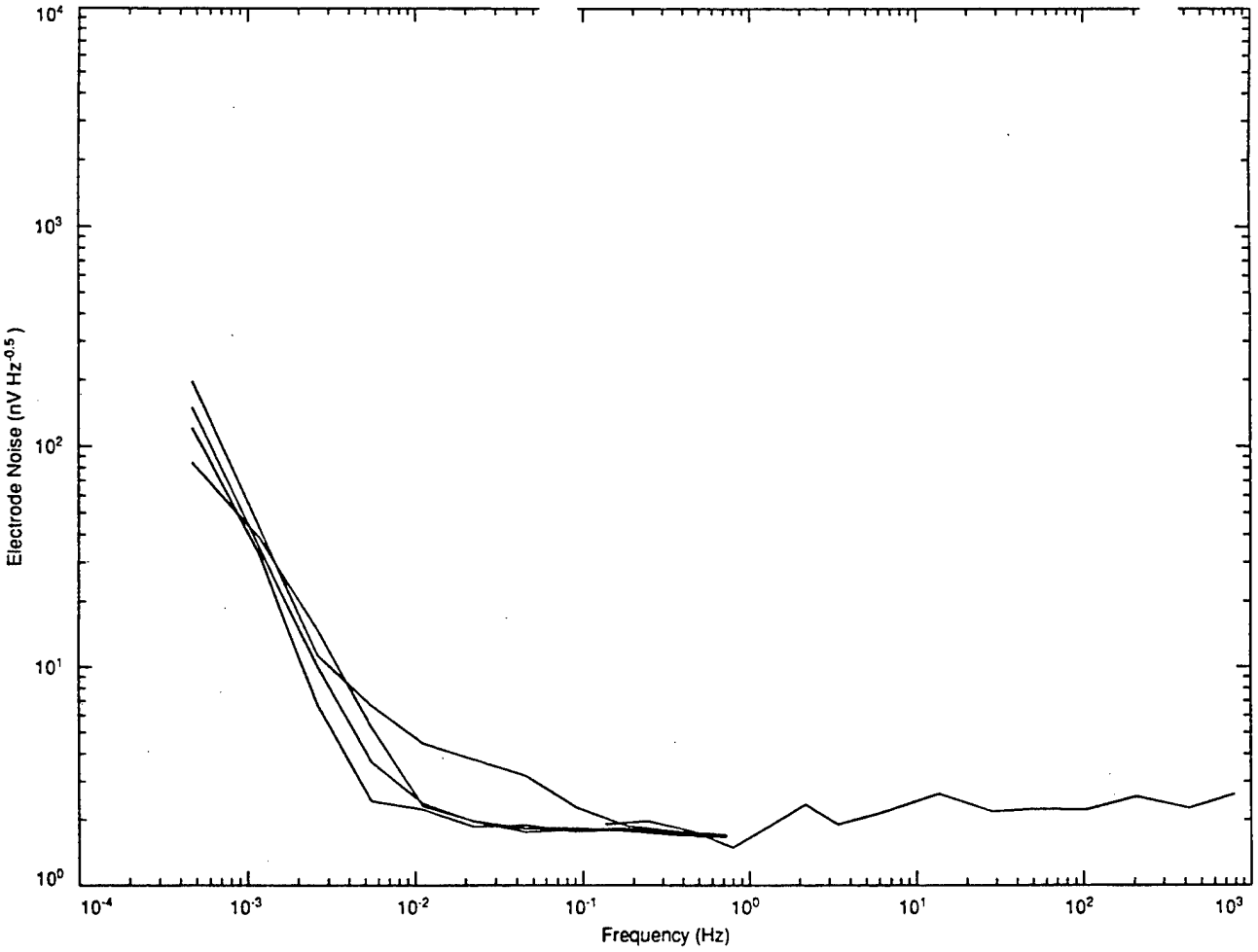

Figure B.9 SAIC electrode spectra at 4°C. These are the quietest with the exception of one pair with elevated noise from 5 mHz to 0.2 Hz. Note that this pair has mended its ways and falls in with the rest in the 15 and 17–19°C runs, Figures B.11 and B.12. The quietest have noise of 40 nV/$\sqrt{\text{Hz}}$ at 1 mHz and reach the instrumentation noise floor at 10 mHz. The noise of the SAIC electrodes at 1 mHz is significantly less than the APL electrodes, but both reach the same noise floor at the same frequency.

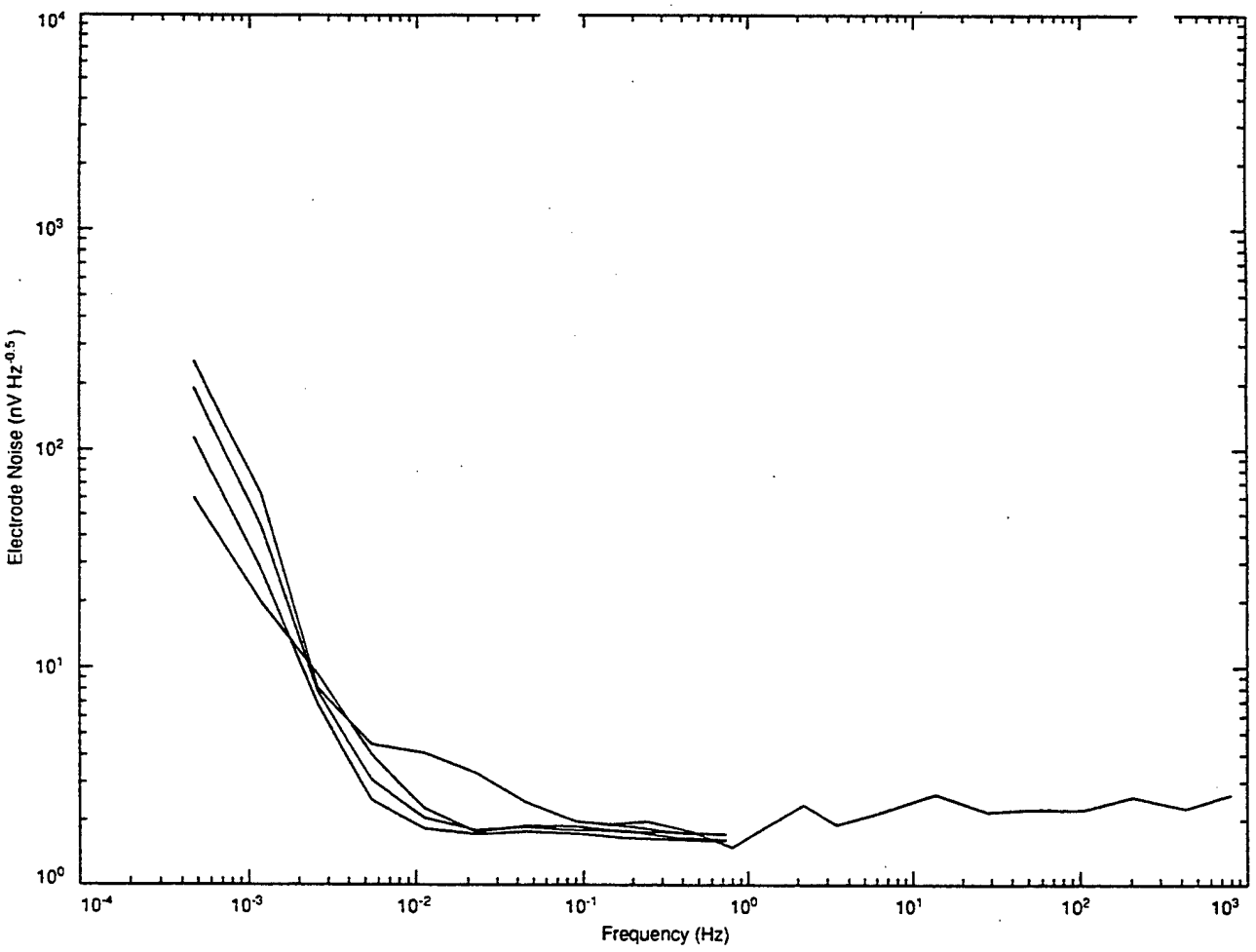

Figure B.10 SAIC electrode spectra at 10°C. The best have somewhat lower noise, 25 nV/$\sqrt{\text{Hz}}$ at 1 mHz than at 4°C.

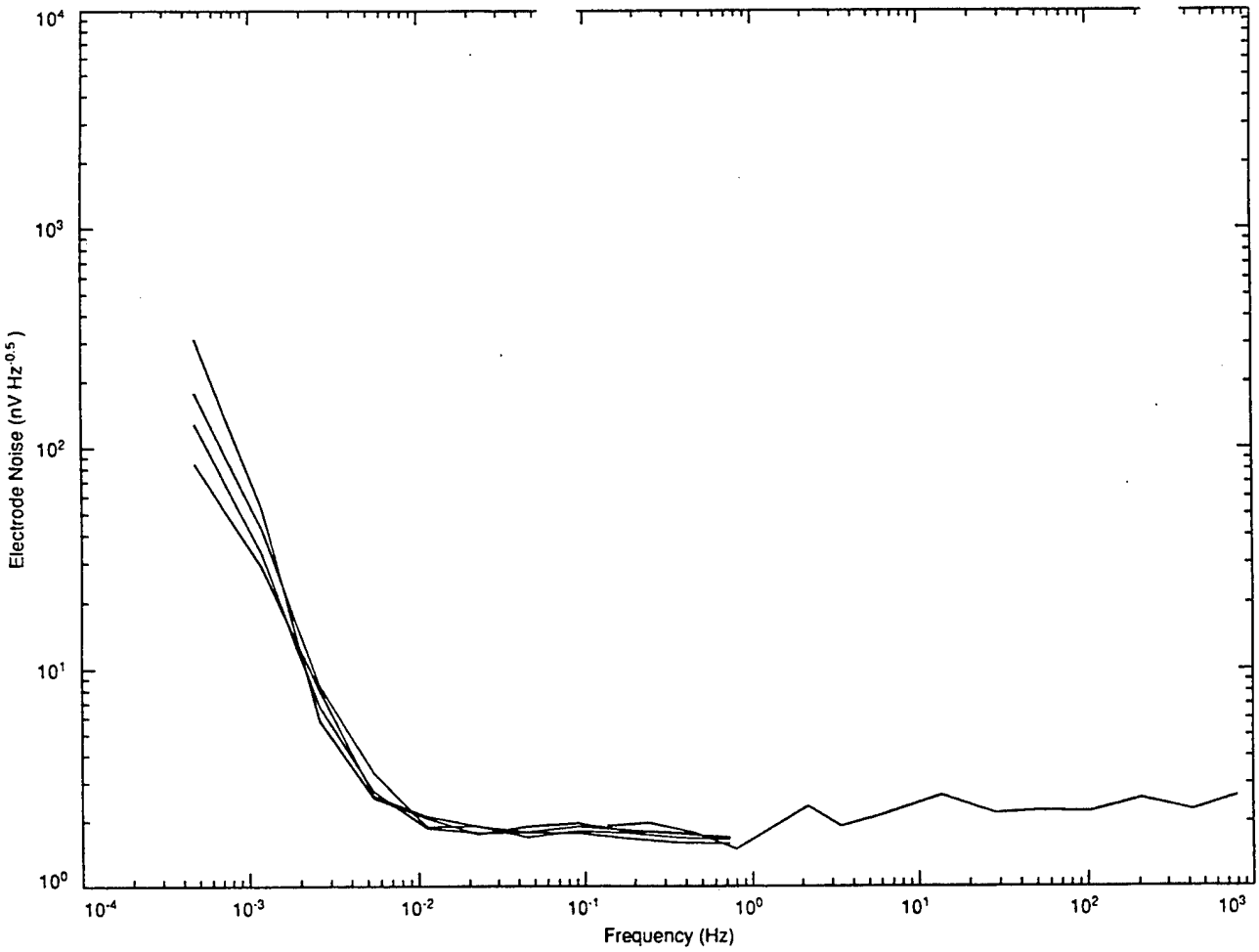

Figure B.11 SAIC electrode spectra at 15°C. The best have 30 nV/$\sqrt{\text{Hz}}$ noise at 1 mHz. The noise floor is reached at a slightly lower frequency than Figures B.9 and B.10.

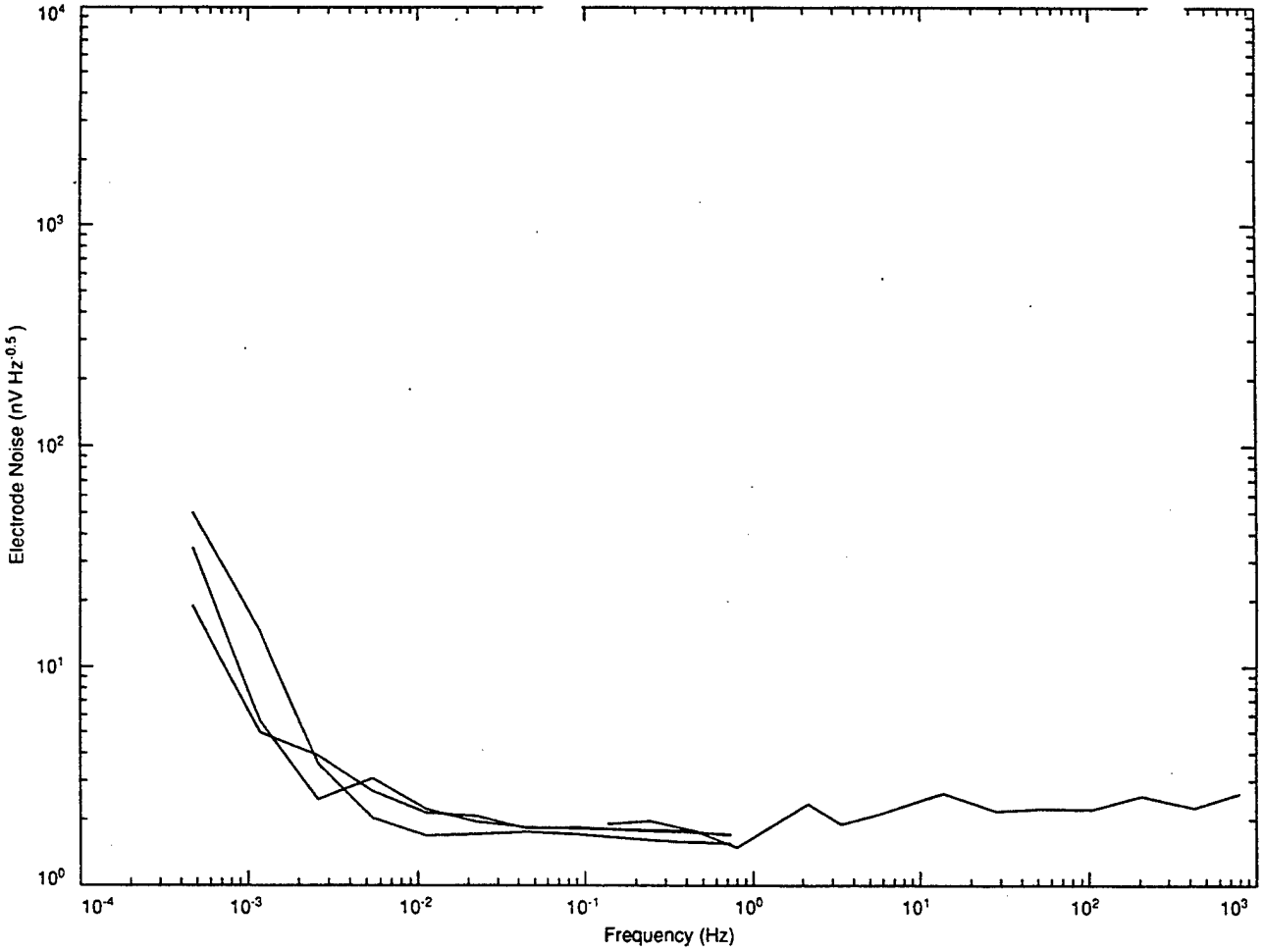

Figure B.12 SAIC electrode spectra at 17-19°C with the bath controller off. Compared to the three SAIC "constant temperature" figures, B.9–B.11, this shows a very dramatic decrease in noise at 1 mHz. The average noise at 1 mHz is 7 nV/$\sqrt{\text{Hz}}$; the best is 5 nV/$\sqrt{\text{Hz}}$. The electrode noise is only slightly above the resistor noises shown in the following four figures.

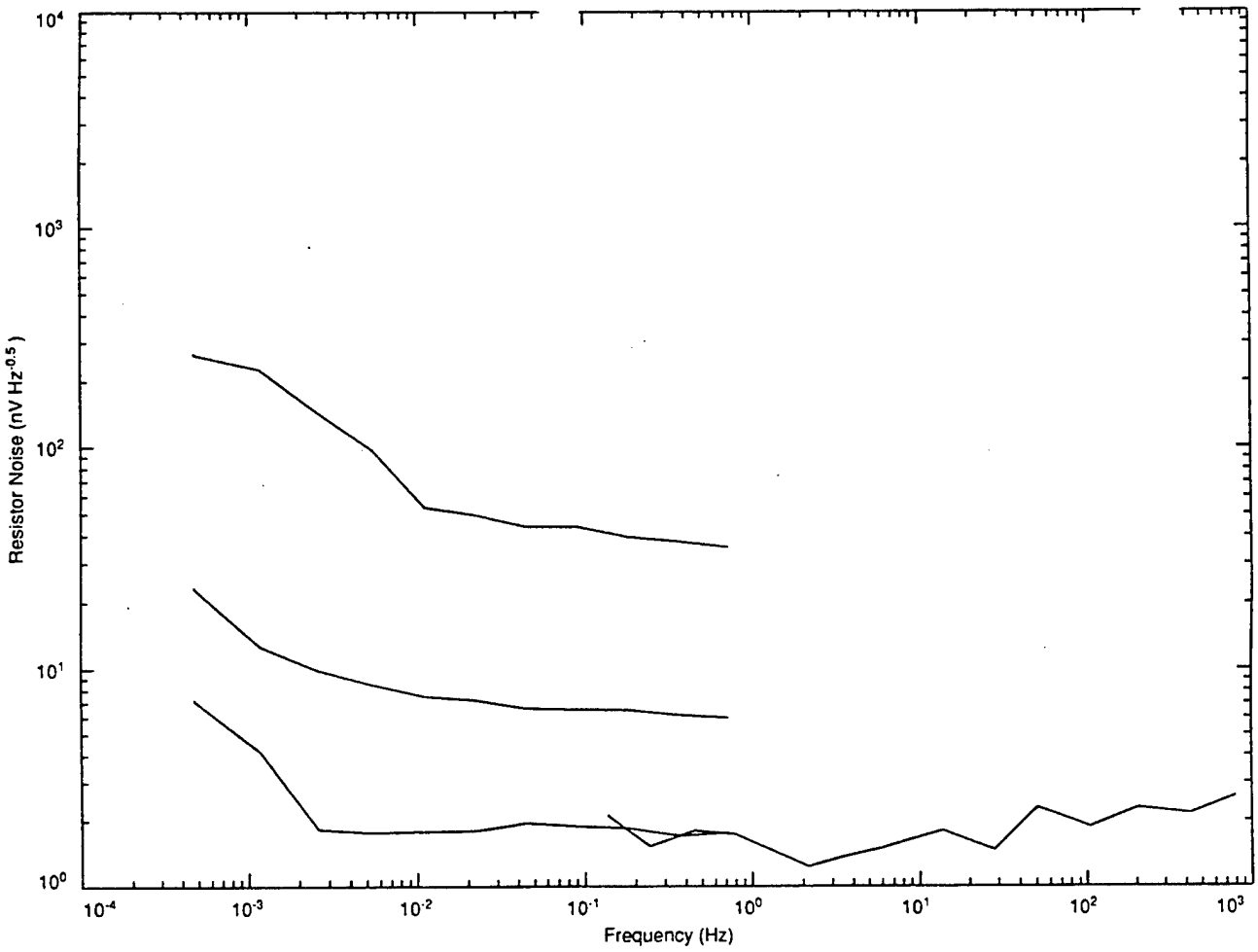

Figure B.13 Resistor spectra at 4°C. The three groups of measured spectra less than 1 Hz correspond to three values of resistance, 10 kΩ, 950 kΩ, and 20 Ω. The single high frequency spectrum is measured with a 20 Ω resistor. These measured spectra have the same noise at all frequencies above 10 mHz and the noise decreases as resistance decreases. We feel that the rise in noise below 10 mHz is due to the thermal noise of the scanner.

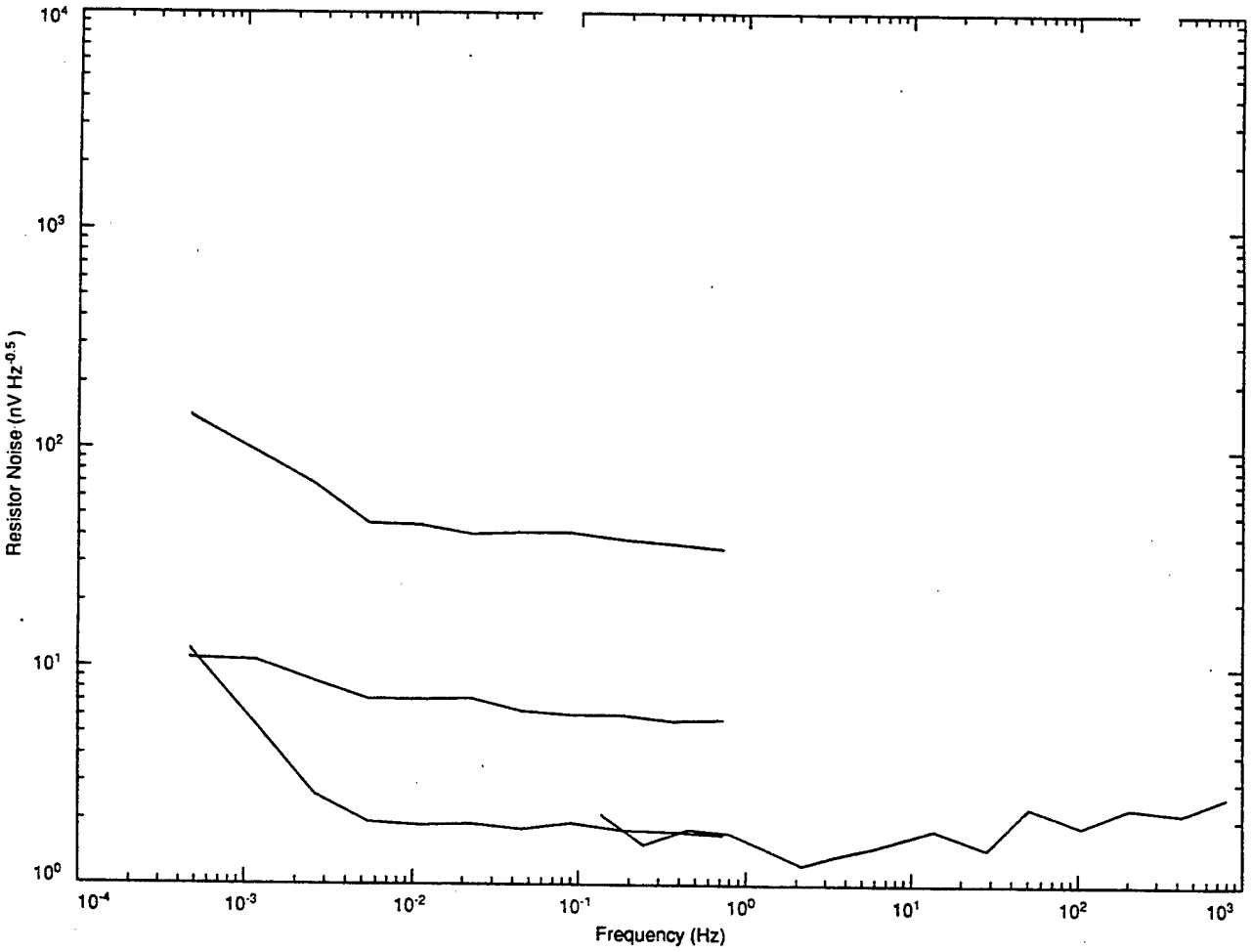

Figure B.14 Resistor spectra at 10°C. See Figure B.13 for discussion.

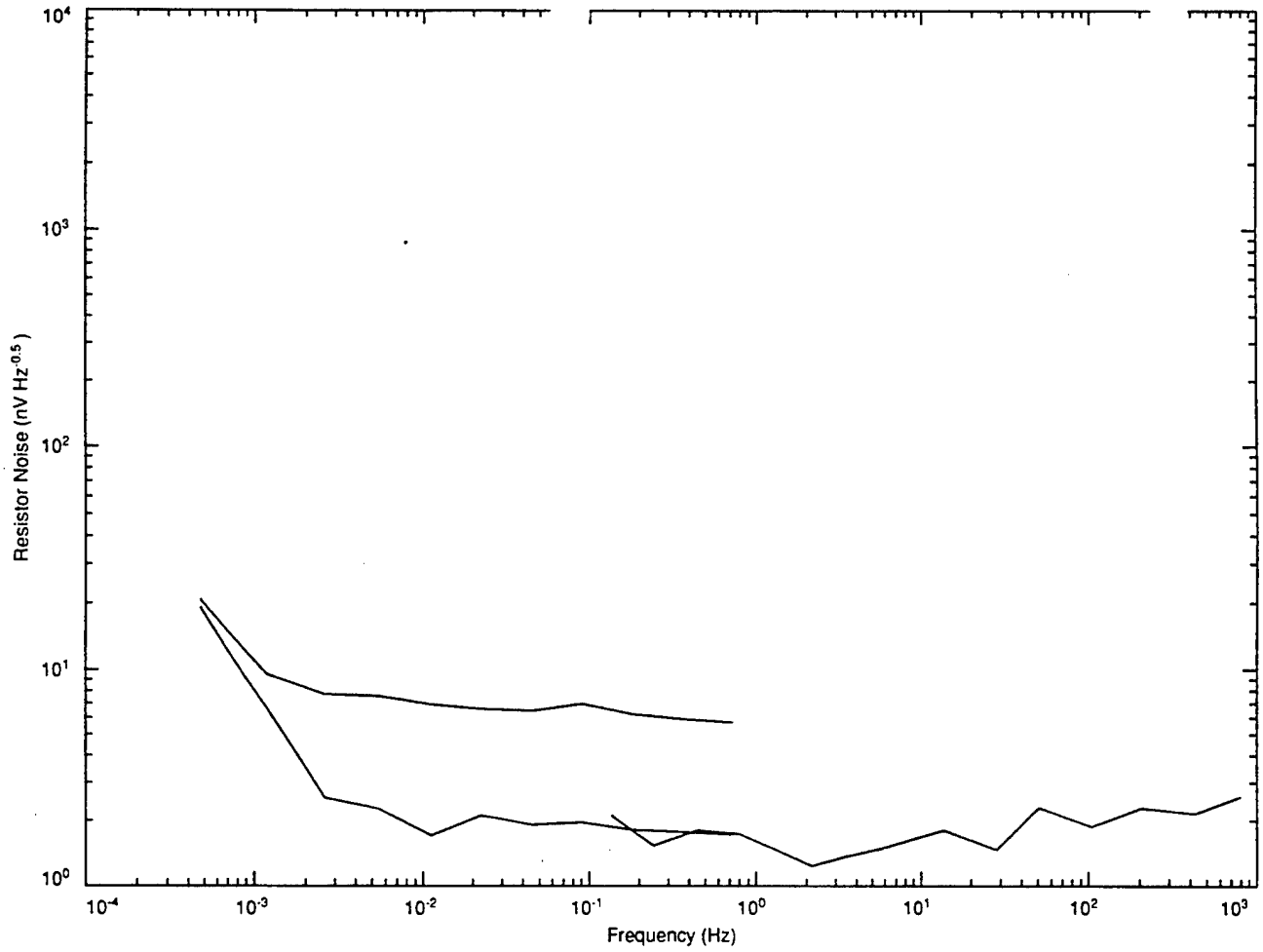

Figure B.15 Resistor spectra of 950 kΩ and 20 Ω resistors at 15°C. See Figure B.13 for discussion.

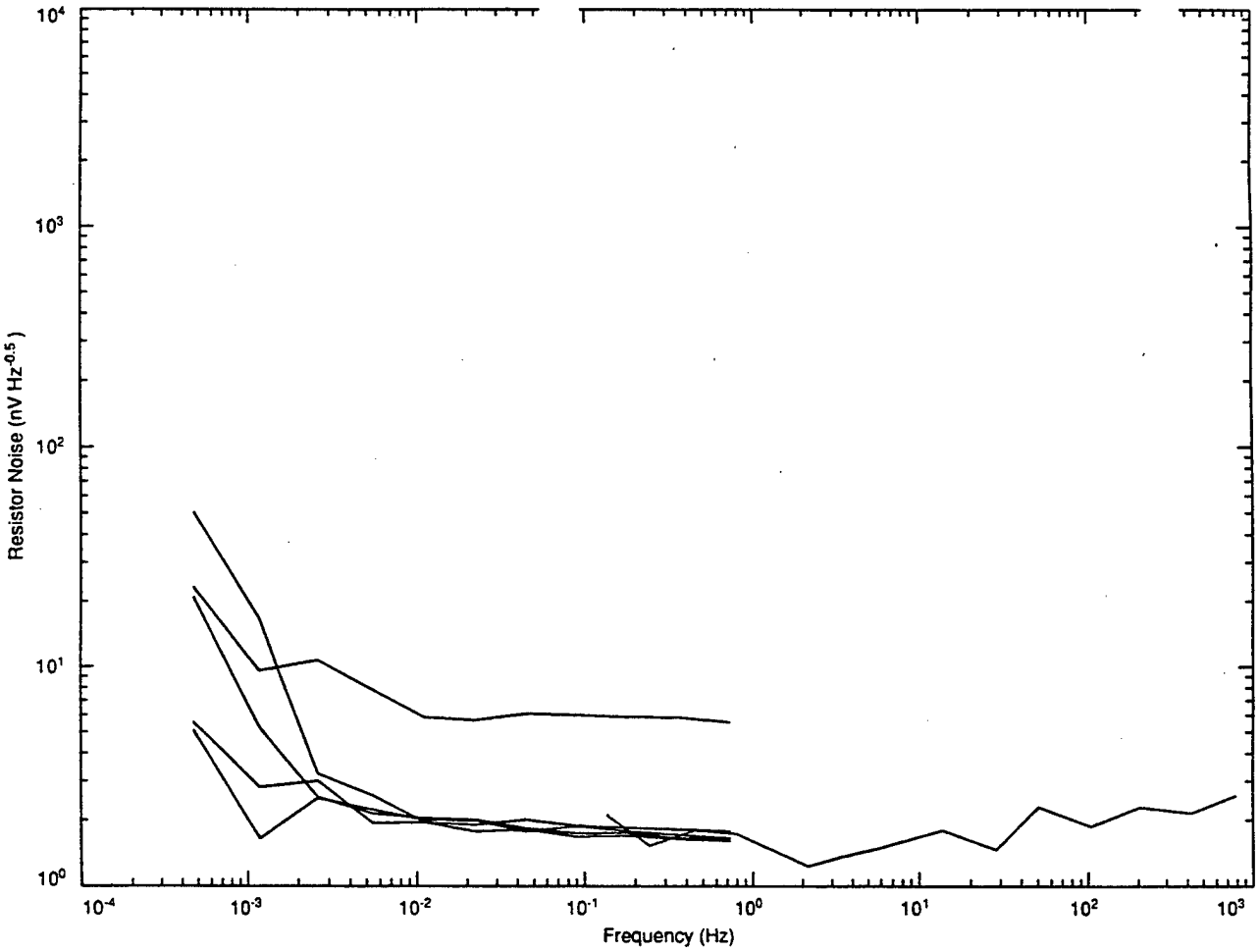

Figure B.16 Resistor spectra of 950 kΩ and 20 Ω resistors while the isothermal bath warmed slowly from 17 to 19°C. See Figure B.13 for discussion.

APPENDIX C: E-Field Sensor Time Series

Notes for Installation of All Systems

Both the APL and NSWC systems had 5 to 10 foot cable runs from the electrodes to their amplifiers and so were quite susceptible to external influences.

Faraday shields were placed in an attempt to minimize noise. Faraday shields are conductors placed between two other conductors and connected to circuit common in order to reduce the electrostatic influence between two signal carrying wires. The theory is that each signal wire will have a capacitance only to the Faraday shield and not to each other. The Faraday shield will carry each conductor's capacitive current separately to ground instead of allowing the capacitive current to flow to the other signal wire. This effectively capacitively isolates the signal wires from each other.

We put Faraday shields around the Keithley 1801 Preamp, the APL electrode cables and the cabling from the NSWC electrodes to their amplifier. A Faraday shield was put around the cabling from the SAIC data receiver to its associated Keithley 181 Nano-voltmeter.

Mu-metal shields were tried to reduce magnetically induced pickup in the signal cables as well as in the magnetic amplifier in the Keithley 1801 Preamp. The theory here is that the magnetic fields will be attracted to the mu-metal and reduce the magnetic field in nearby locations. We installed mu-metal plates above and below cables that had been coiled up as well around the K-1801 and the NSWC amplifier.

All the systems were sensitive to RFI (radio frequency interference). This was determined by using a portable cellular telephone in the same room as well as with an ARGOS oceanographic data transmitter. A standard marine band buoy relocation beacon also caused substantial interference. The cellular phone output is about 1 watt in the 800 MHz band. The ARGOS transmitter is about 1 watt at 401.65 MHz. Both transmitters caused very large effects in all the systems. We ignored portions of records where RFI was present.

Measurement Instrumentation

In the salt water tank, the equipment used in the isothermal tests was applied again along with additional equipment. The isothermal test equipment was used with the APL sensors. The additional equipment was required for the higher level signals from the SAIC and NSWC systems. The computer and peripherals for the system tests in the salt water tank were placed on a cart located within 1 foot of the west end of the tank. The close proximity was to keep the cabling short as well as allow other uses to the room by not blocking the aisle. In hindsight, it might have been better to have the computer a bit farther away: the 67 Hz magnetic field from computer monitor vertical sweep induced potentials in the tank.

Figure 5.2 shows a schematic plan view of electrodes and equipment in tank.

The cabling to the upper scanner card was redone to include several APL sensors and some resistors. The output of the upper scanner card was connected to the K-1801 preamp. The output of the lower scanner card was disconnected from the upper scanner card output and connected to the high level input of a Keithley 181 (hereafter denoted as the K-181). The K-181 was used to measure the high level outputs of the SAIC and NSWC systems. The low frequency band SAIC output and the NSWC output were each connected to two input channels of the lower scanner card. The lower scanner card became unused later as we switched to using two K-181s, one for the SAIC system and one for the NSWC system. The K-181s were connected directly to the high level outputs of the two systems. This was done to eliminate the settling time requirements in the K-181s.

The APL sensors utilized the Keithley 705 Scanner with two Keithley 6178 Nanovolt Scanner cards, the Keithley 1801 Preamp, the Keithley 2001 Multimeter, and the Macintosh IIfx computer. These are used as for the isothermal electrode tests. The APL sensors had no integral amplifier and so required a preamp. Several APL sensors were installed in the salt water tank and were all cabled through the scanner to the preamp in the same fashion as during the isothermal tests.

Table C.1 lists the scanner channels for the salt water tank tests.

Table C.1

Scanner	Description	Notes
ch11	EFF block	3 kΩ salt bridge shunt
ch12	As	EFF style, thin tubes
ch13	Ab	big tubes, leaked
ch14	A3	new style, solid agarose
ch15	A2	new style, agarose plugs
ch16	N/C	not used
ch17	A1	new style, agarose plugs
ch18	20 Ω	Resistor

The SAIC system and NSWC systems had significant gain and so produced potentials that exceeded the full scale range of the K-1801 preamp. A separate dedicated Keithley 181 Nanovoltmeter was used to measure each system for the low frequency sampling.

Thus, three voltmeters were used in the salt water tank setup, the K-2001 with the K-1801 for the APL sensors and a K-181 each for the NSWC and SAIC systems. The main reason for using three separate voltmeters was to be able to obtain data from three systems, APL, NSWC and SAIC, more rapidly than if a scanner were used. Each time the scanner changes channels a step change occurs at the preamp input. The preamp output takes at least 2 seconds to settle and make a stable measurement. With three channels (APL, NSWC and SAIC) operating, the overall sample interval would be at least 6 s. With three voltmeters, a sample interval almost ten times shorter, about 0.7 s, was

obtained. More rapid sampling allows a lower noise density estimate to be made. This is the mode used for most of the low frequency sampling in the salt water tank.

Another reason for using three voltmeters was that the K-2001 was difficult to use in the combination mode of preamp and high level inputs. There was no way to use the K-2001 front panel connection when the preamp was in use because there was no automatic way to change between operating the K-2001 with and without the preamp. A large mechanical button had to be pressed to alternate between the two modes. One solution would have been to attenuate the high level signals to be less than the 2 mV full scale range of the K-1801 preamp. If we had done this, the attenuated signals could have been passed through the scanner to the preamp. However, we wanted to avoid low level signals if possible since they allow for increased noise pickup.

The passive filter on the K-1801 preamp input was put into three different configurations during the 30-day salt water tank tests. These changes were different attempts to balance noise and frequency response. Initially, the RC low pass filter was the same as for the isothermal tests, a 100 Ω resistor and a 5 μF capacitor. The second set of values, 20 Ω and 5 μF, was installed on January 18 at 10:30 AM. The third configuration with no filter was installed at about 4 PM on February 2. The last filter, 20 Ω and 0.5 μF, was installed at 6 PM on February 2. The frequency responses of these filters requires knowledge of the internal resistance of the sensors, which we estimate at about 100 Ω mainly due to the salt-bridge pipe connecting the electrodes to the tank water (Figure 5.1). The salt bridge is 0.5 m long and 0.041 m diameter. At 18 °C and 35 ppt the salt bridge resistance is about 85 Ω. The electrodes themselves are about 10 to 20 Ω. When the sensor resistance is added to the filter resistance the three corner frequencies are, 160 Hz, 265 Hz, and 2650 Hz, respectively.

However, the second corner frequency did not have any effect: there was an error in the "burst_cin_jan19" HF program that prevented the correct preamp filter from being used. The order of requests was incorrect. It appears that data from January 19 to February 2 at 6 PM used the K-1801 medium filter which has a corner frequency of 32 Hz. Only spectra between January 18 and February 2 at 6 PM are believed to be tainted.

The filter was not changed between the low frequency sampling and the high frequency sampling. This is because of the significant time required to unbolt, clean and reconnect the low noise connections at the preamp front end. Another reason for not changing connections is that the preamp specification states that it must be in its thermally insulating foam box for an hour before it meets its specifications.

The low frequency output of the SAIC system was cabled directly to the high level input of one K-181. The single output of the NSWC system was cabled to a Kron-Hite Corporation KH-3322R filter. The filter output was cabled to the high level input of another K-181.

Both sections of the KH-3322R filter were set to 0-dB gain and low pass filtering with a corner frequency of 22 Hz. Initially the filter was not included, but analysis of the data showed that it was noisier than expected in the 0.1 to 1 Hz range. See the "hook" in the spectra in Figure D.4. The filter corner frequency of 22 Hz was chosen to be above the 17 Hz corner frequency of the NSWC amplifier and less than 60 Hz. The intention

was to reduce the 60 Hz without changing the way the NSWC amplifier processed the data.

It seemed that the K-181 was not properly averaging the very large 60 Hz signal present. This could be because the 60 Hz signal had wide skirts. See Figure D.4. The KH filter reduced the 60 Hz component and so allowed the 181 to obtain proper measurements. Later, the large 60 Hz signal was discovered to be a result of an inadvertently large loop area in the cabling to the NSWC electrodes. After this was corrected by rearranging the cabling, the 60 Hz was much reduced. See Figure D.5.

The high frequency sampling of the APL system was performed with exactly the same techniques as was done with the electrodes in the isothermal tests. This involved changing the setup for both the K-2001 and K-1801. The internal preamp filter was changed to 700 Hz, its highest bandwidth setting. The K-2001 was operated for 29500 samples in its burst mode which samples at 2000 Hz.

To obtain high frequency data from the NSWC system the NSWC amplifier output was disconnected from the KH filter and hooked directly to the K-2001 front panel. After the mechanical switch was pressed changing the K-2001 input from the rear panel preamp connection to the front panel, the burst mode sampling program was run. The program set the voltmeter full scale range to 2 V.

The SAIC system has a separate output for the high frequency data. This output was connected in turn to the K-2001 front panel and the burst program used again. The voltmeter full scale range was set to 20 V for the SAIC HF output since the usual signal level was about 5 V peak-to-peak.

A single power cord from an AC power outlet protected with a ground fault circuit interrupter (GFCI) supplied AC power to a power conditioner and then to the computer and all the measurement equipment. The power conditioner was installed to remove spikes and short interruptions from the power supplied to the computer in order to have fewer data interruptions. The computer stopped once because of the power interruption from a lightening stroke. All the equipment chassis were connected to power common through their power cords.

The salt water tank is designed to be set at arbitrary potentials above ground. We chose to operate it at ground potential because that is the case in the field.

Time Series of MF Runs in Salt Water tank

Figures C.1 through C.8 show the MF (medium frequency) time series acquired in the salt water tank. As in the isothermal bath data shown in Appendix A, each segment is about 1 hour and the sample rate is about 0.5 second. All data have been high-pass filtered in software with a one-pole Butterworth filter with a corner frequency of 1 mHz. Most scales are ± 0.05 μV, but a few are wider range to allow for noisier data. The figures are labeled with their file name followed by the segment number. Each segment took about 16 hours to complete, during which time each of the 16 scanner channels was sampled continuously for about 1 hour. Although the data are depicted concurrently for convenience, they are not concurrent. In order to organize the graphs, the order of display is not exactly the order of sampling. These data are those used in the spectra shown from 0.5 mHz to 1 Hz in Appendix D.

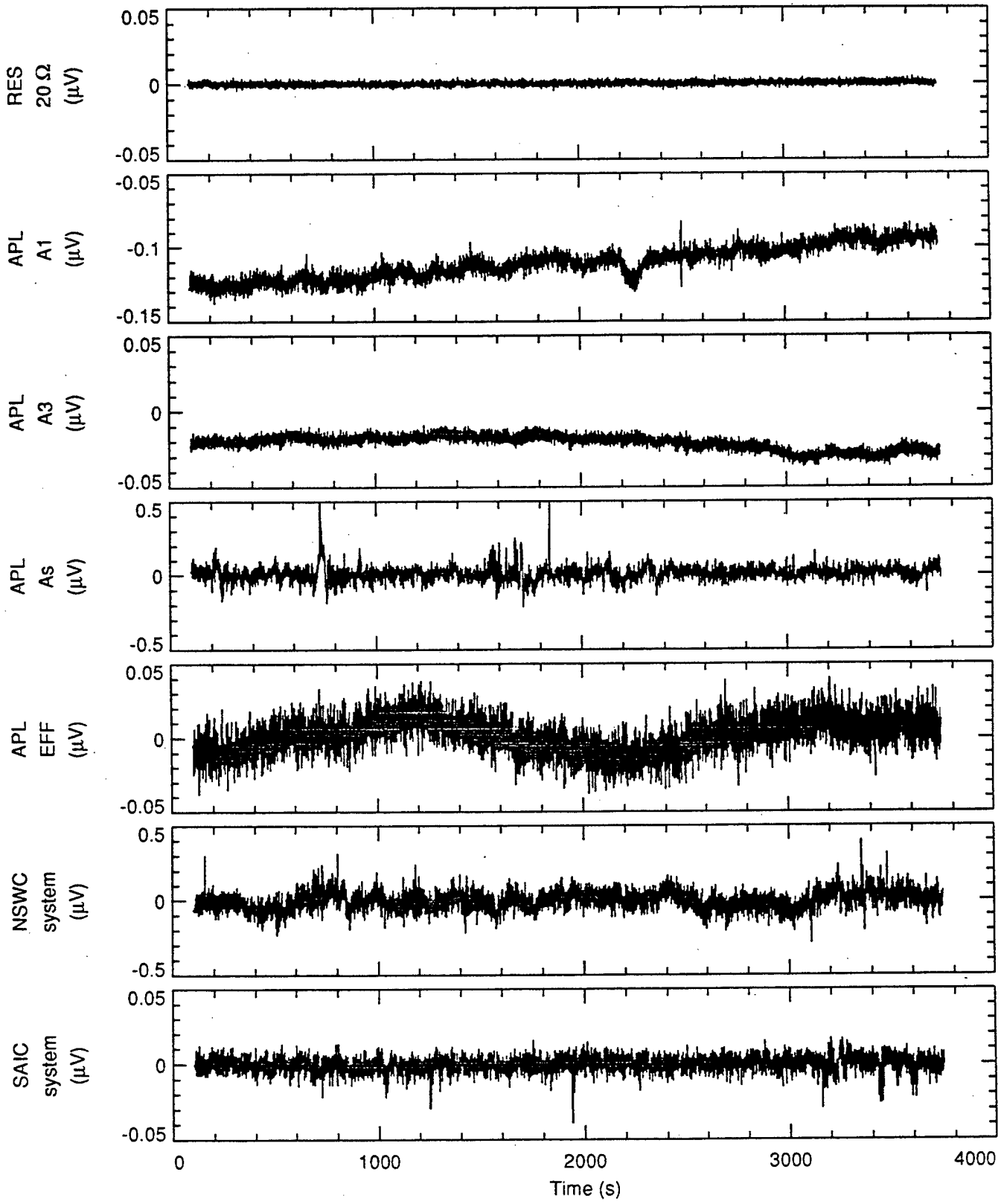

Figure C.1

jan20mf_a.01

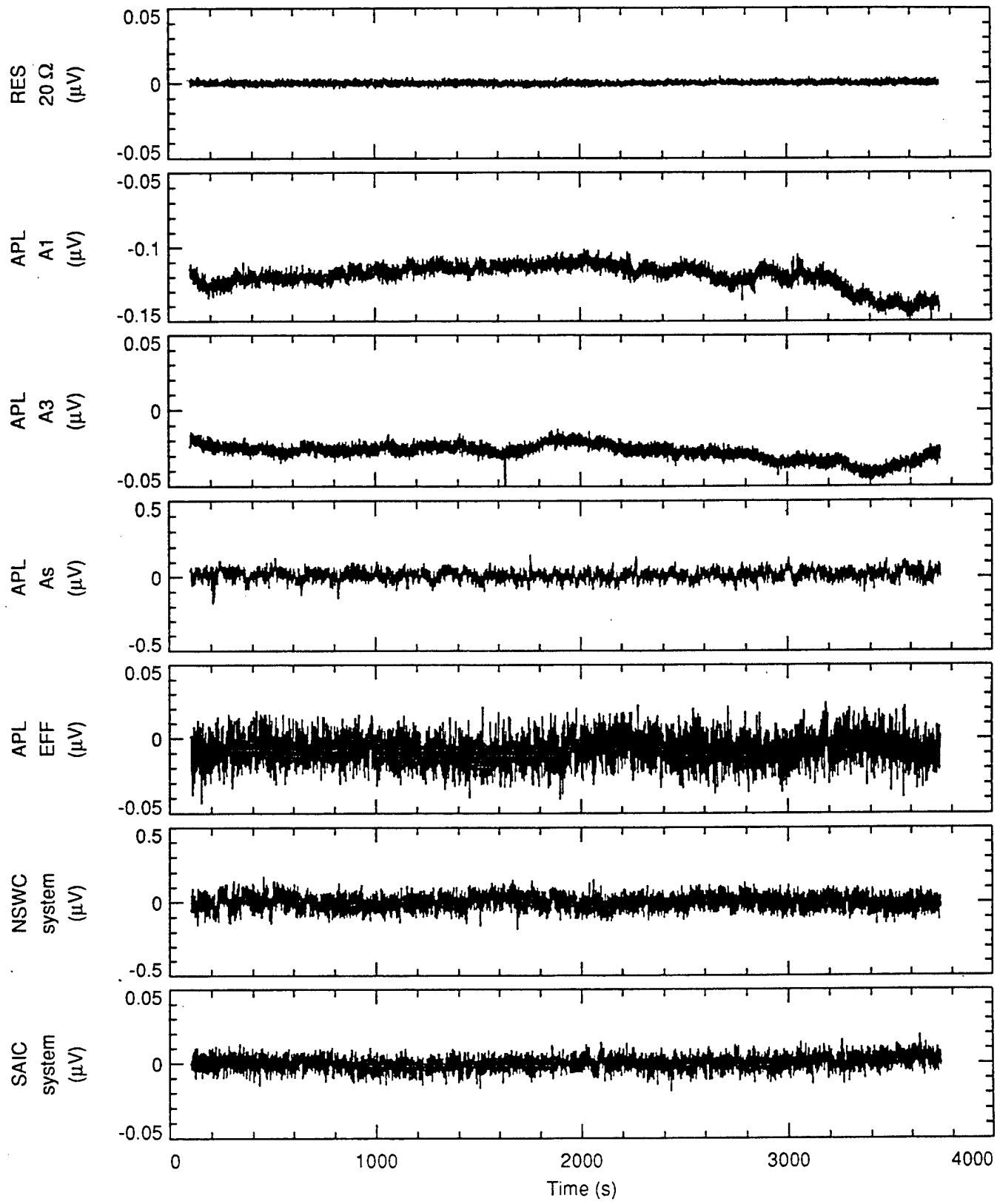

Figure C.2

jan20mf_a.02

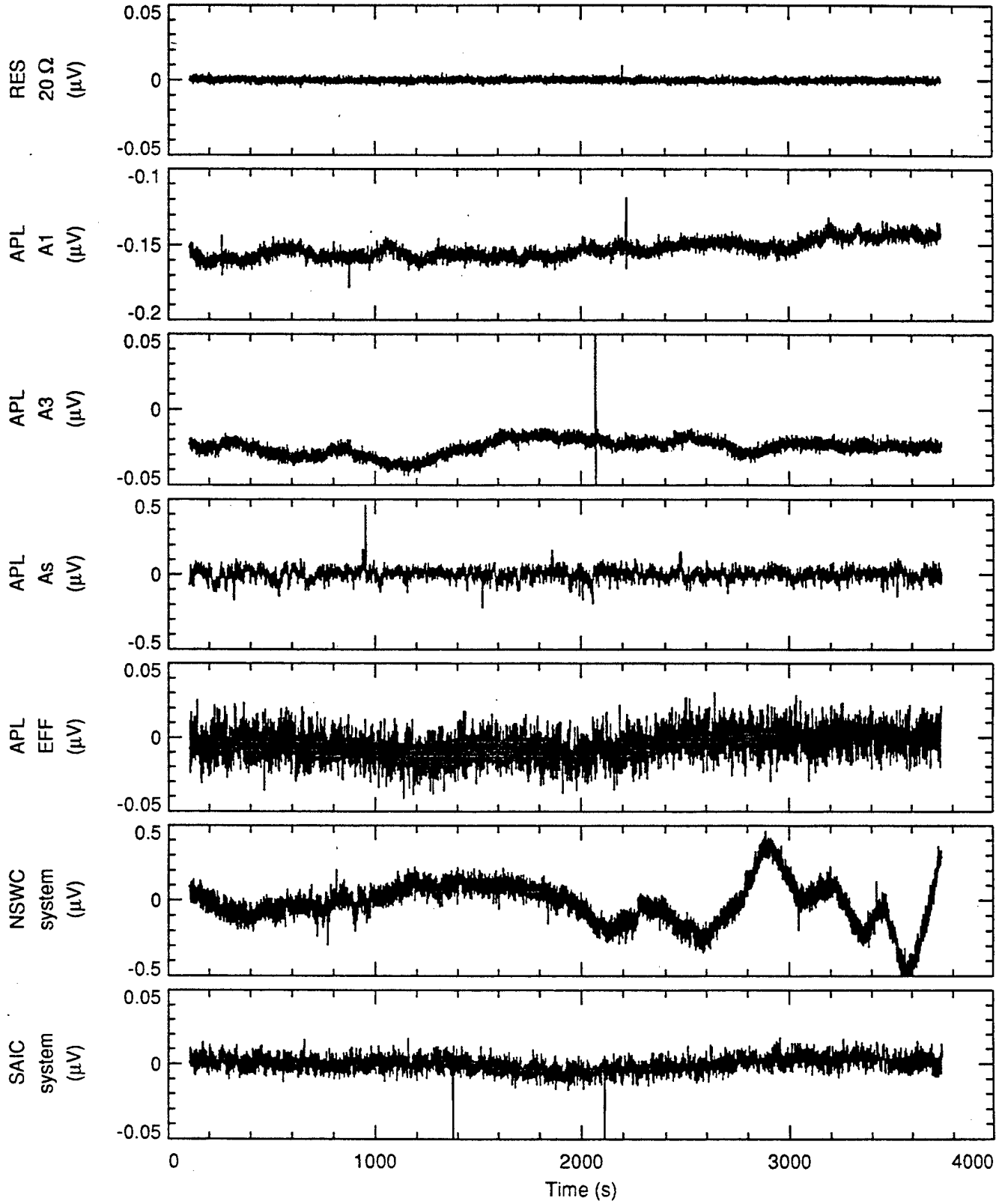

Figure C.3
jan20mf_a.03

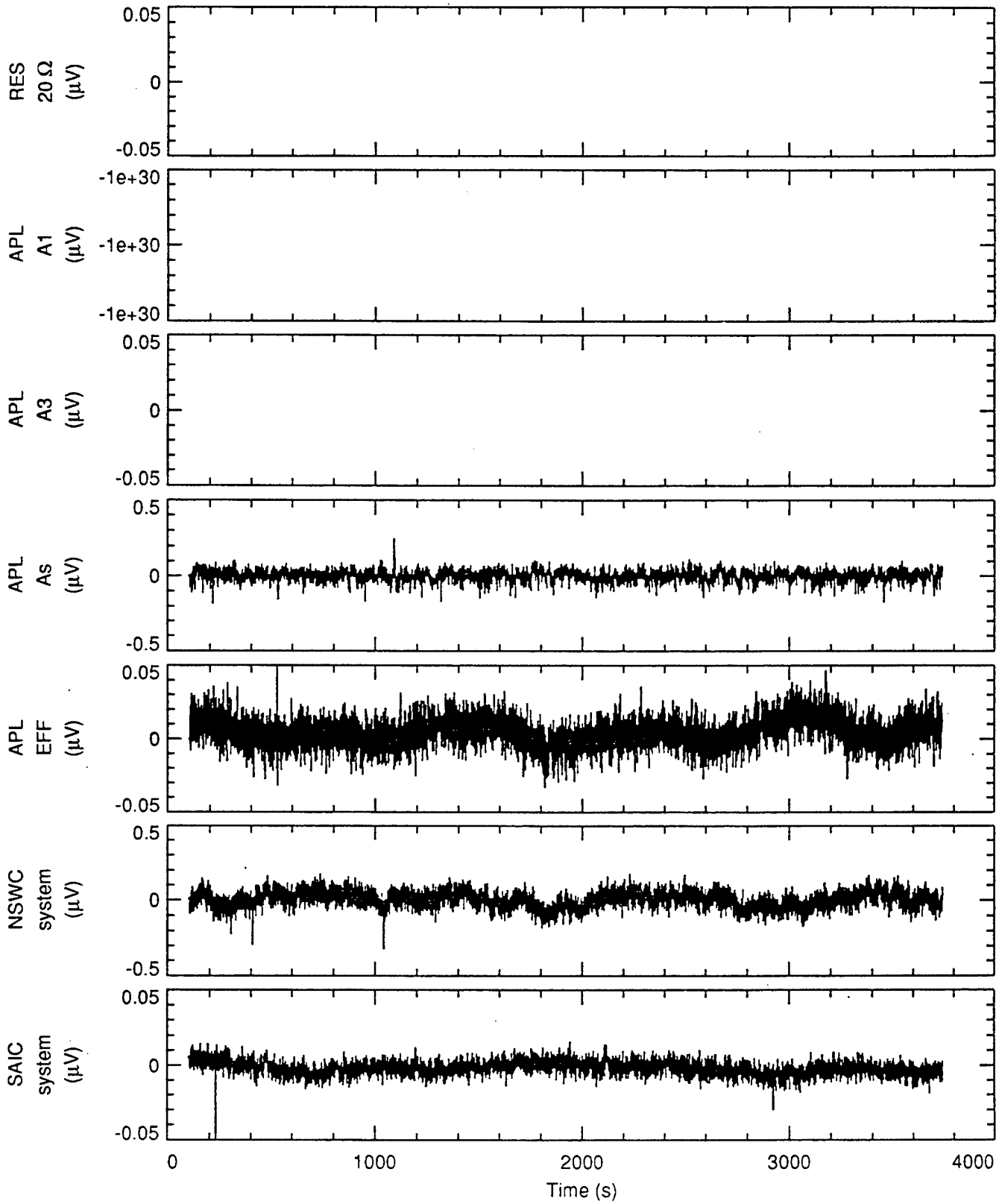

Figure C.4

jan20mf_a.04

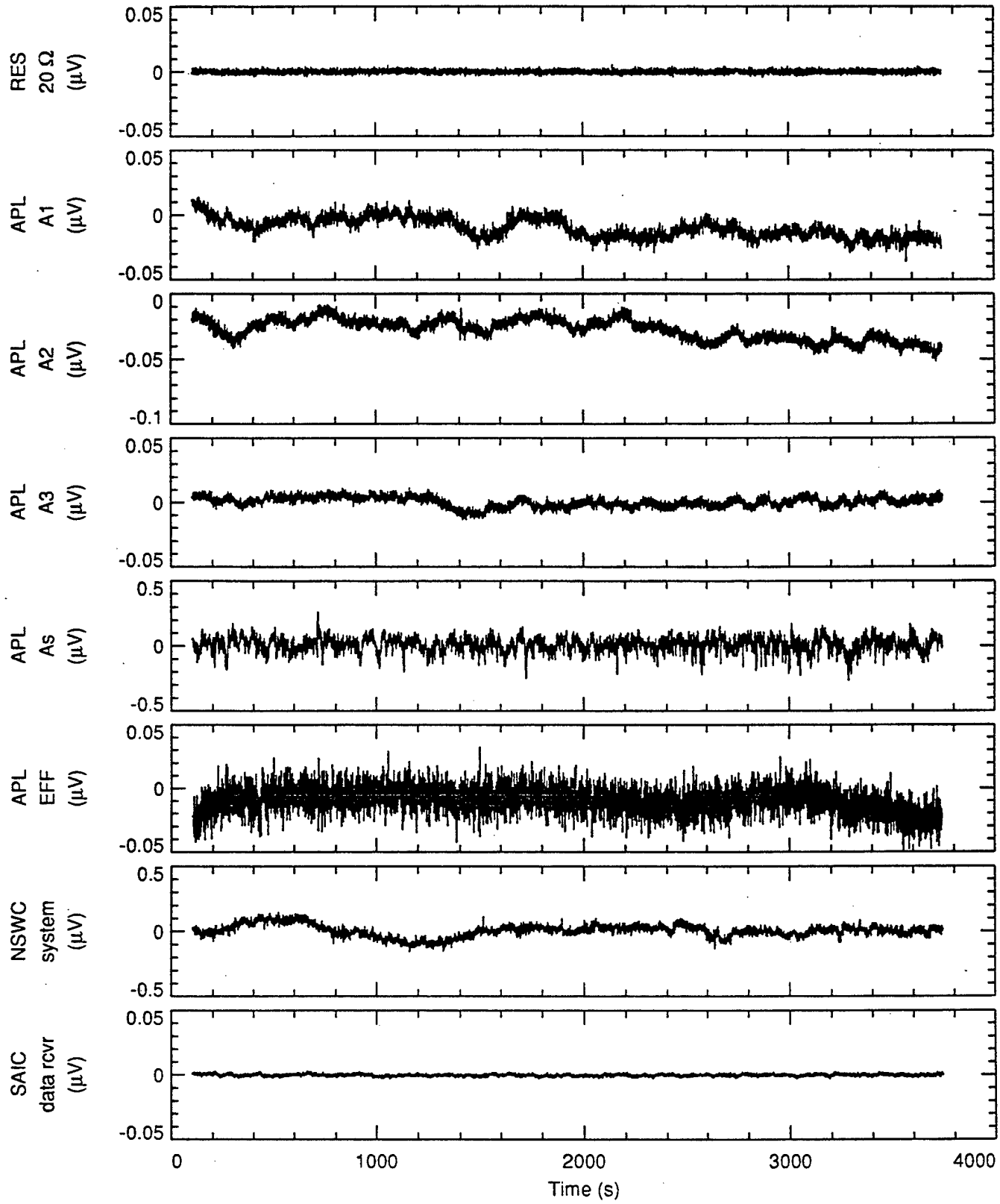

Figure C.5
feb16mf_b.01

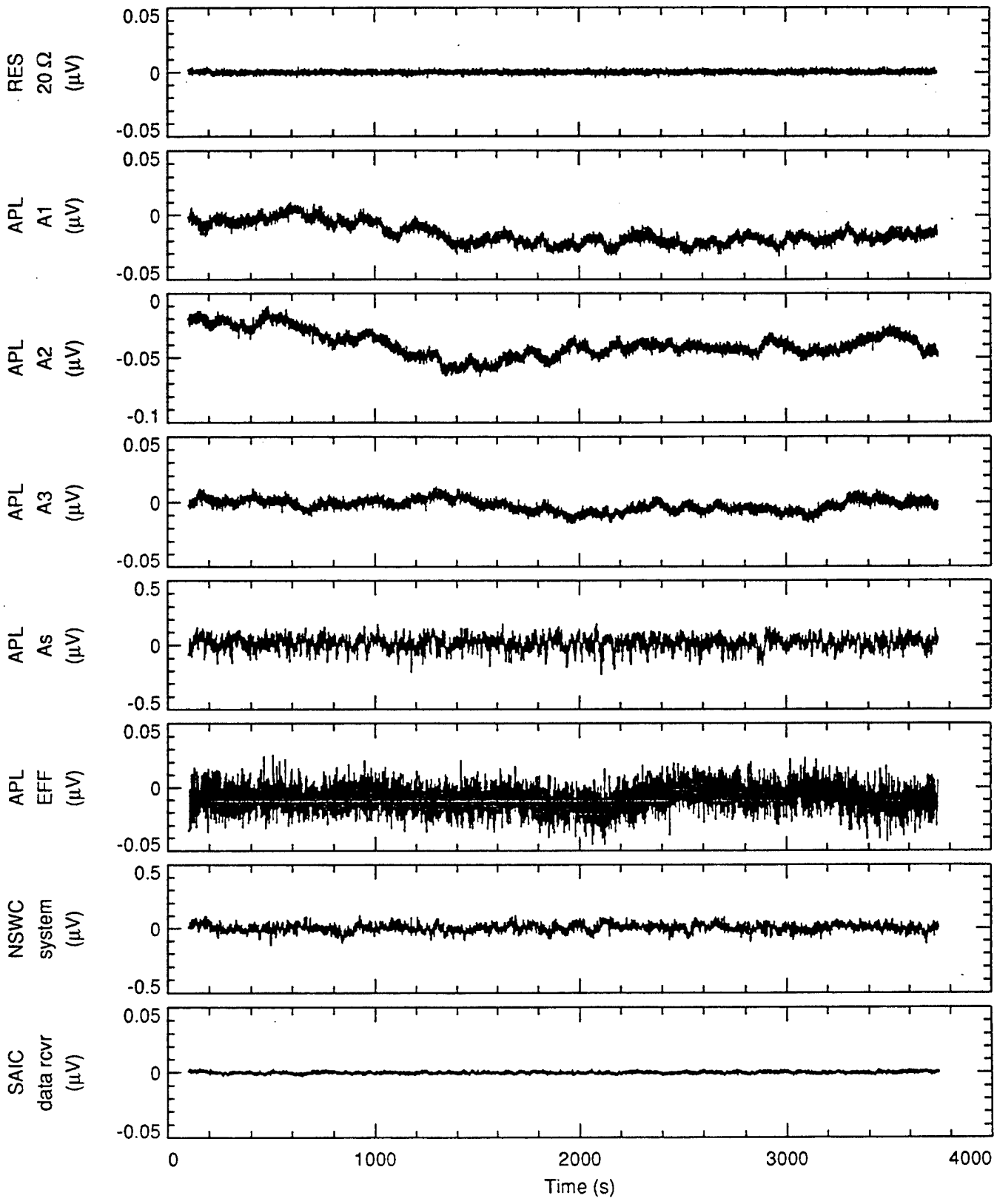

Figure C.6
feb16mf_b.02

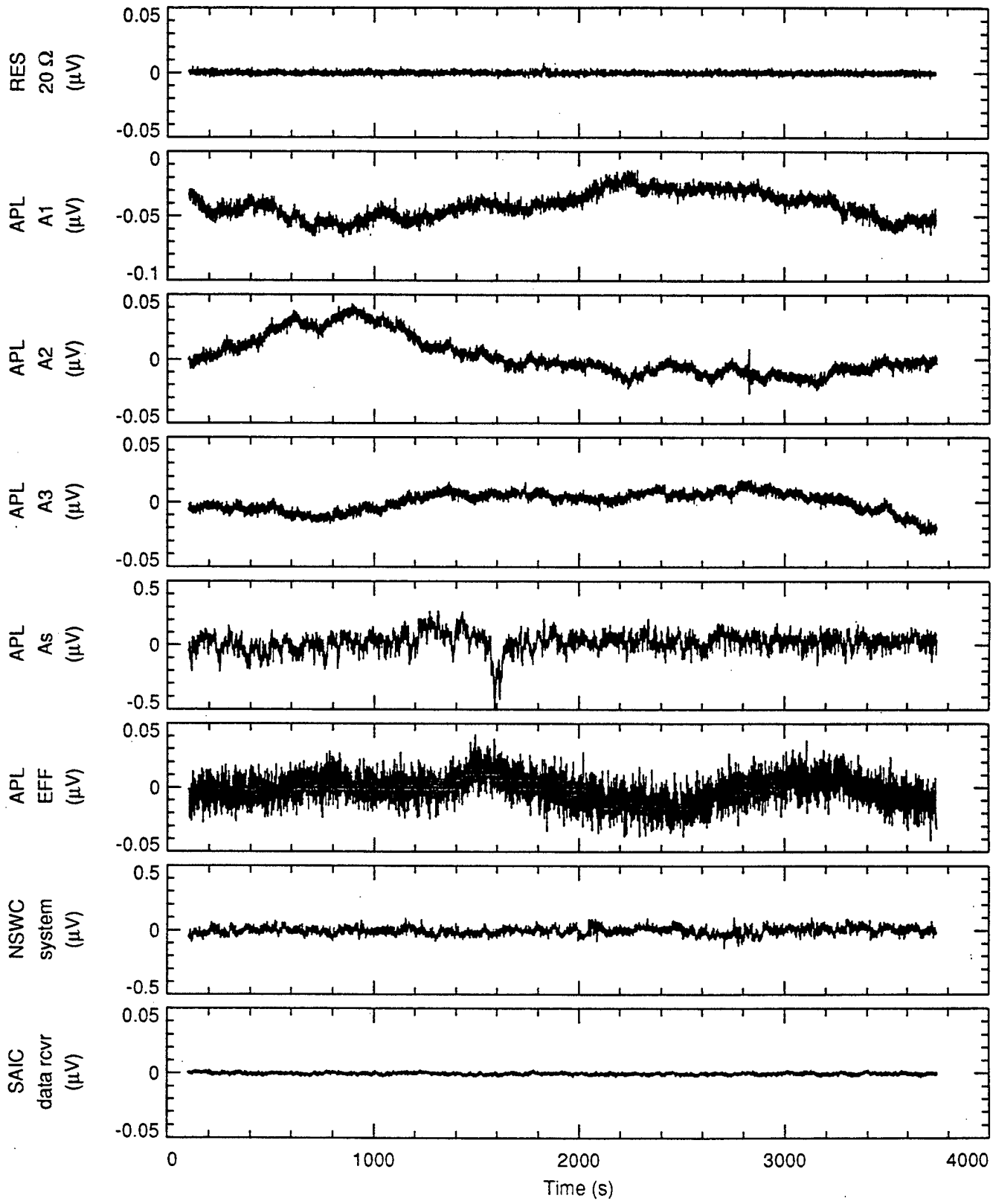

Figure C.7
feb16mf_b.03

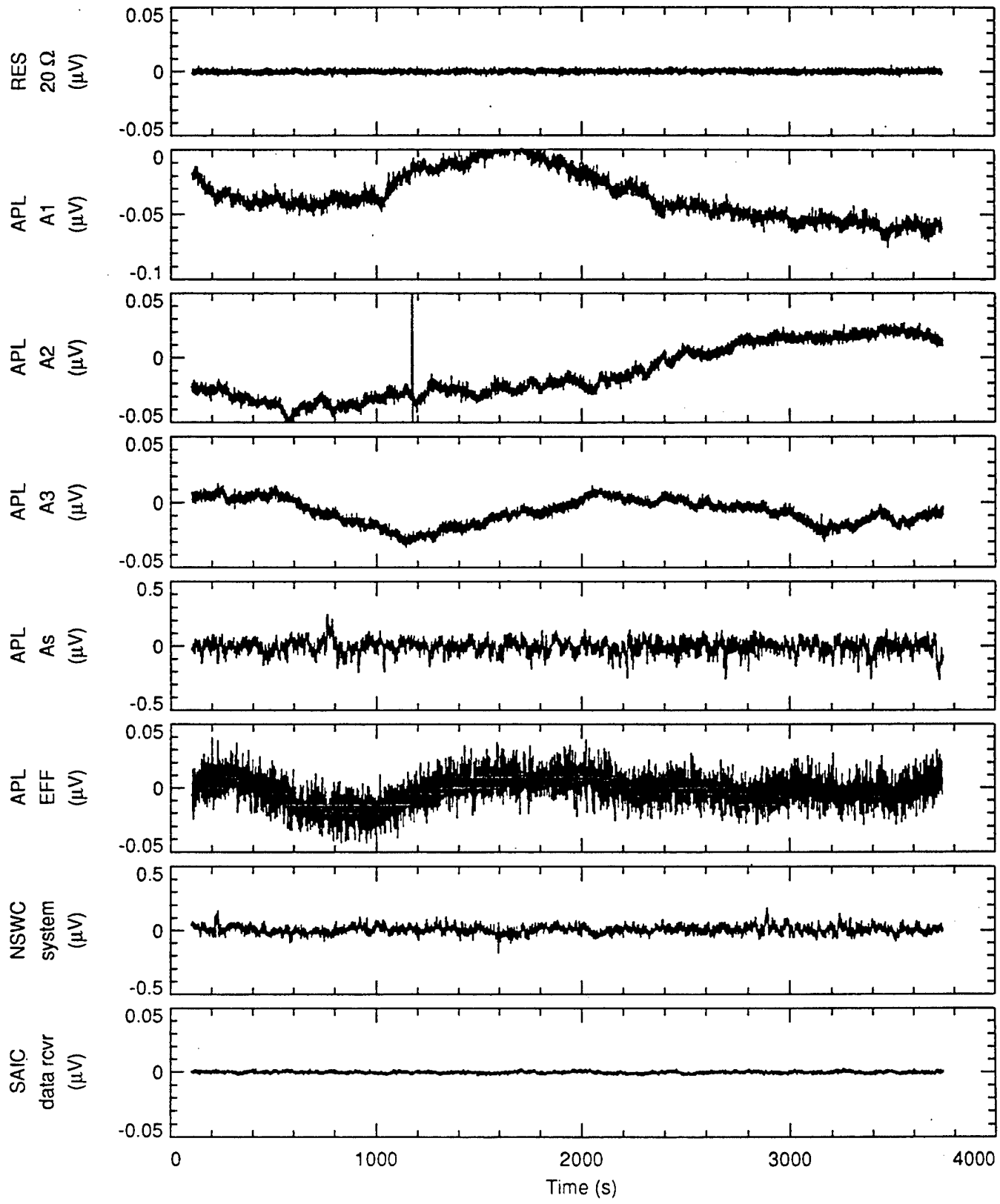

Figure C.8

feb16mf_b.04

42 Days of Tank Data

Figures C.9 through C.52 show data from 42 days of salt water tank testing. These data are the same as shown in Figure 6.1, just expanded in time. The data are from the NS runs, one day per page, same scales all three systems.

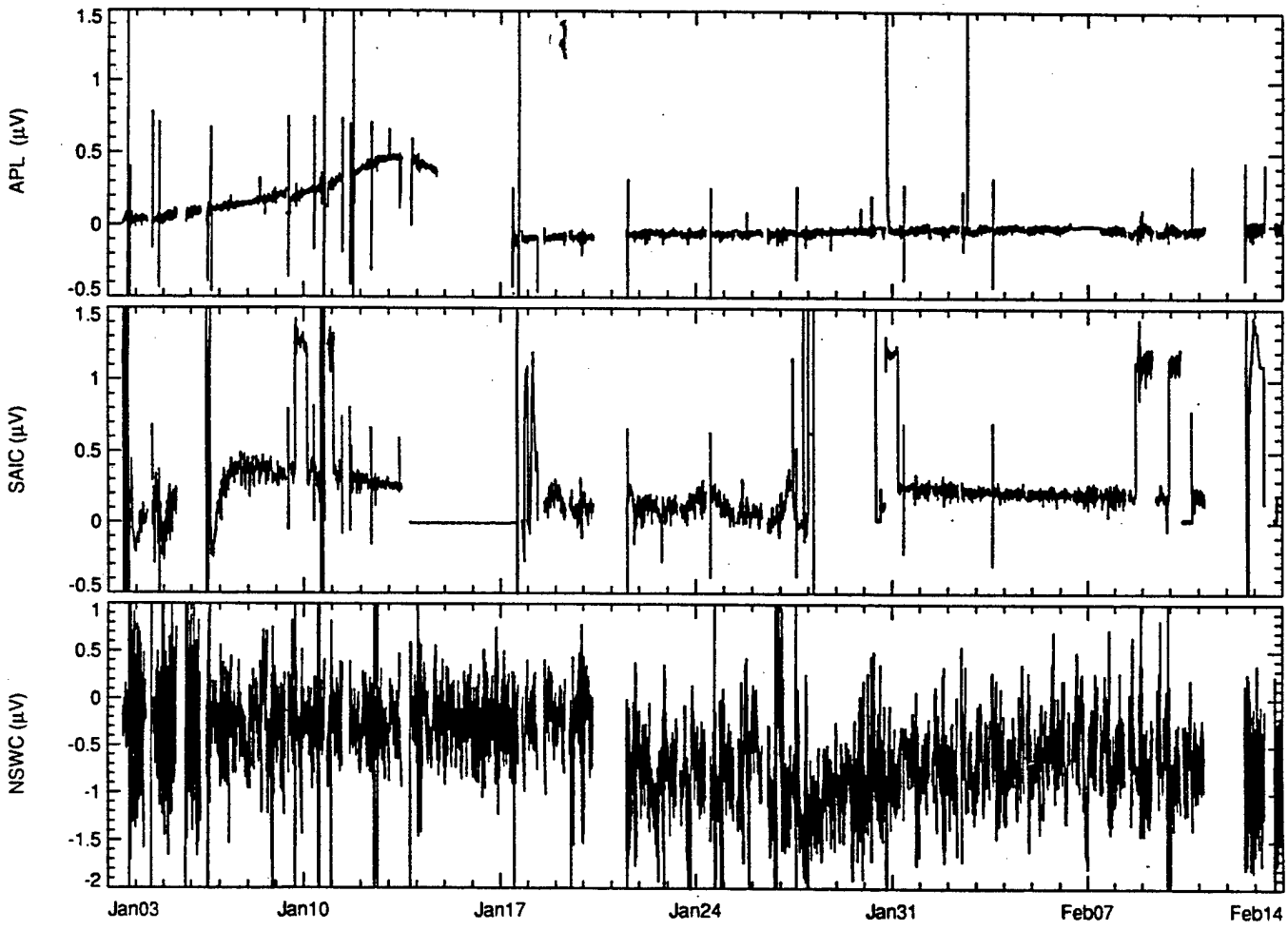

Figure C.9

Salt Water Tank Test Overview. Subsampled to about 70 s.

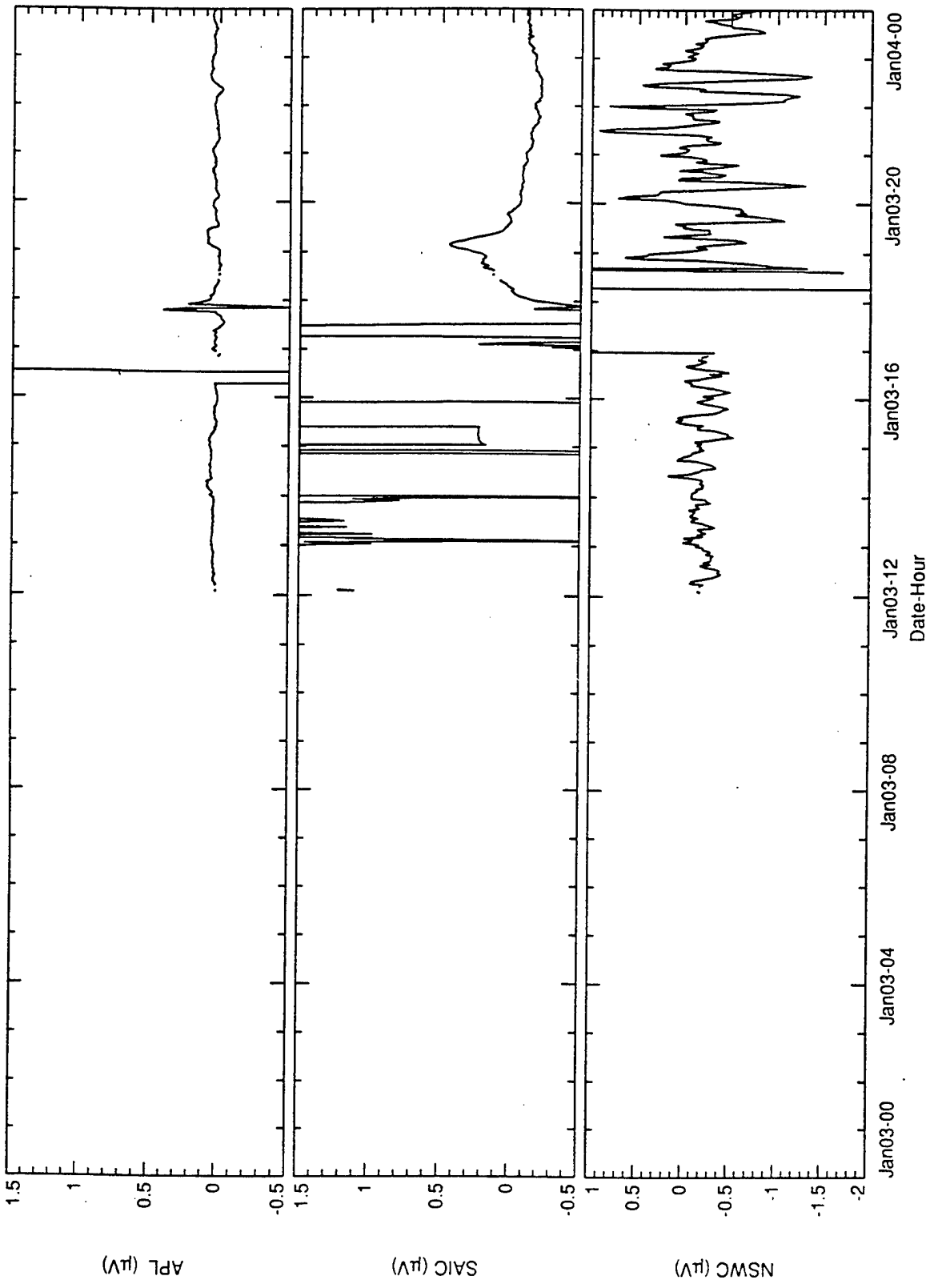

Figure C.10

Salt Water Tank Test Daily. Subsampled to about 70 s.

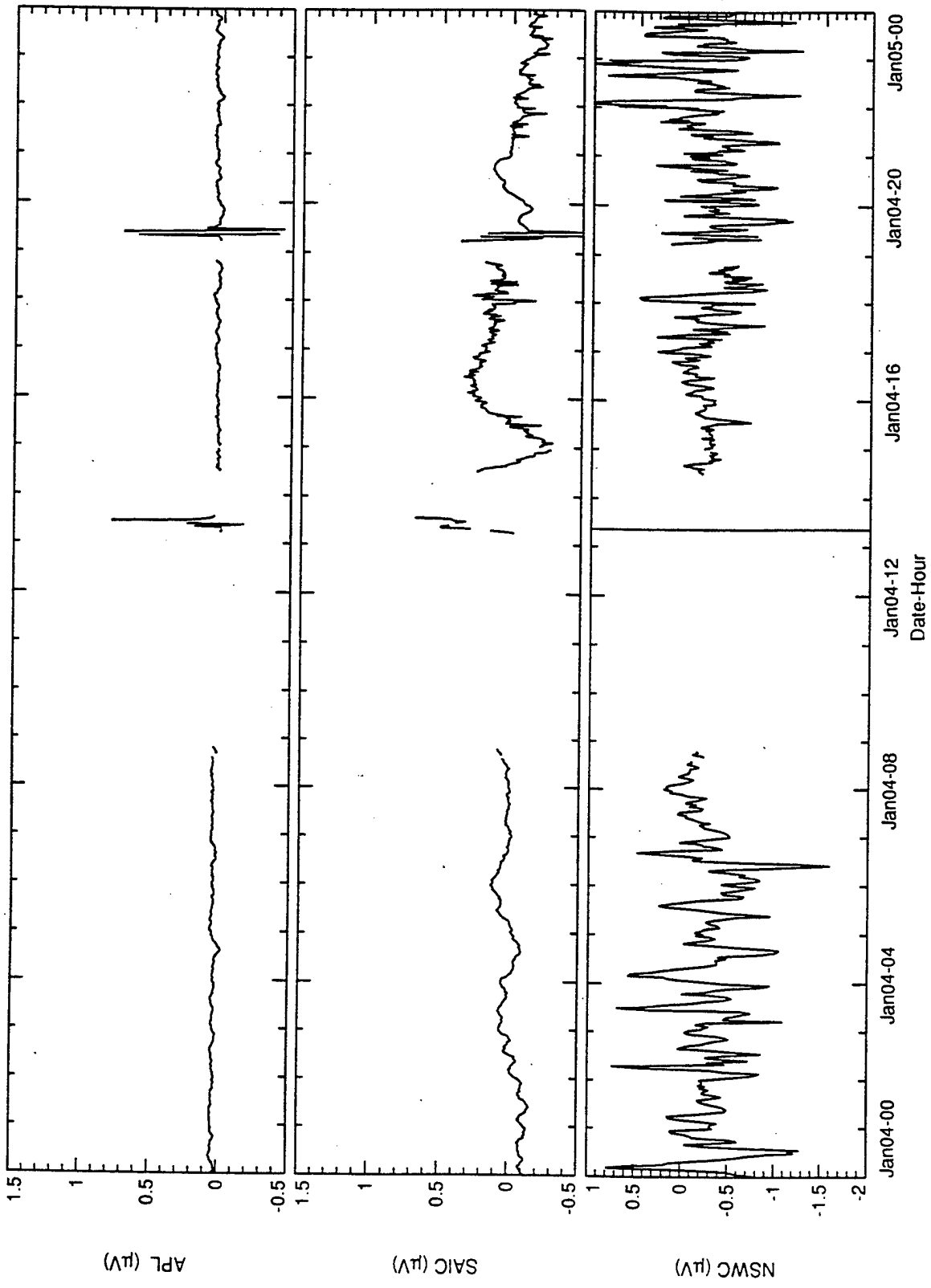

Figure C.11

Salt Water Tank Test Daily. Subsampled to about 70 s.

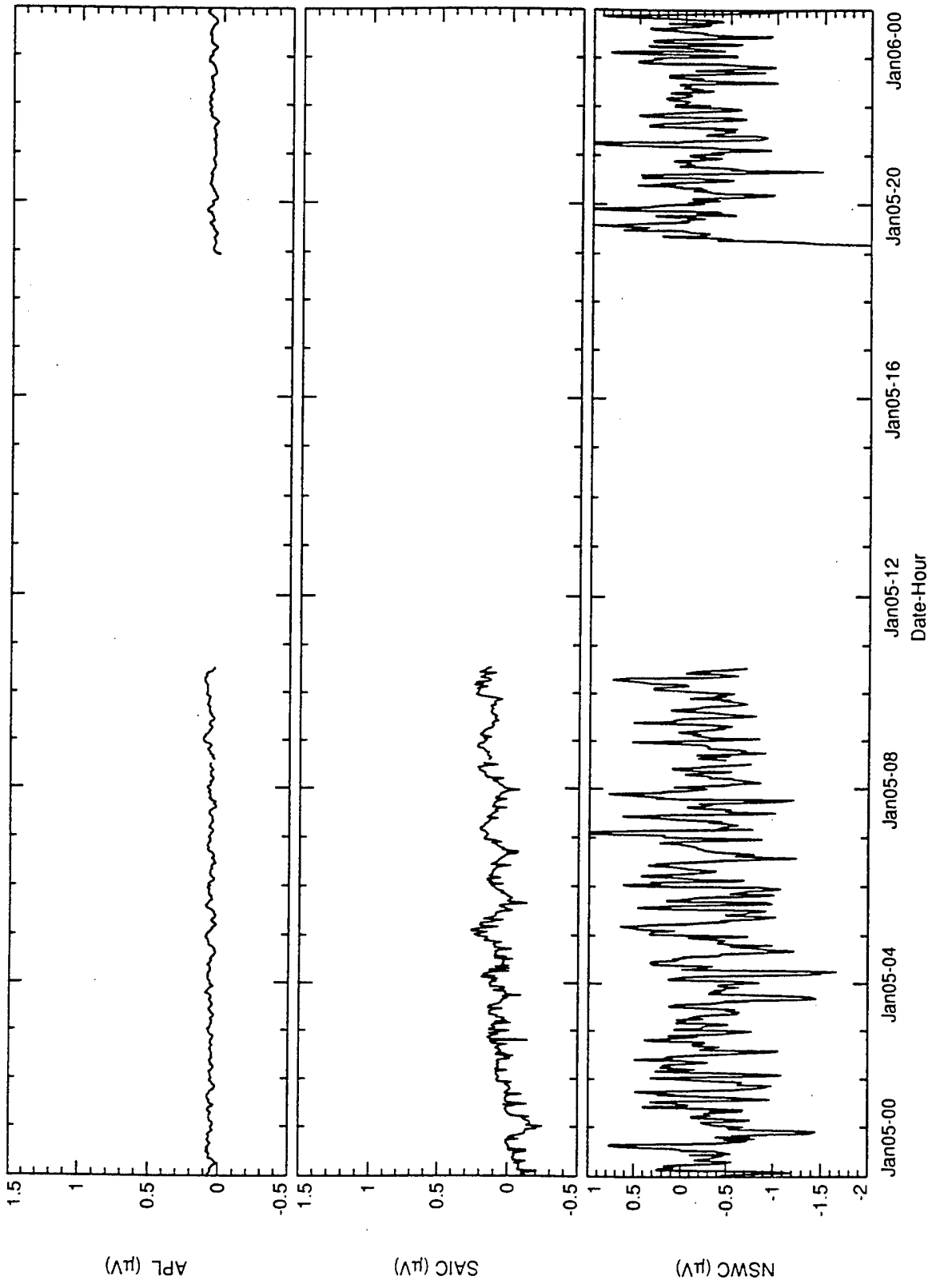

Figure C.12

Salt Water Tank Test Daily. Subsampled to about 70 s.

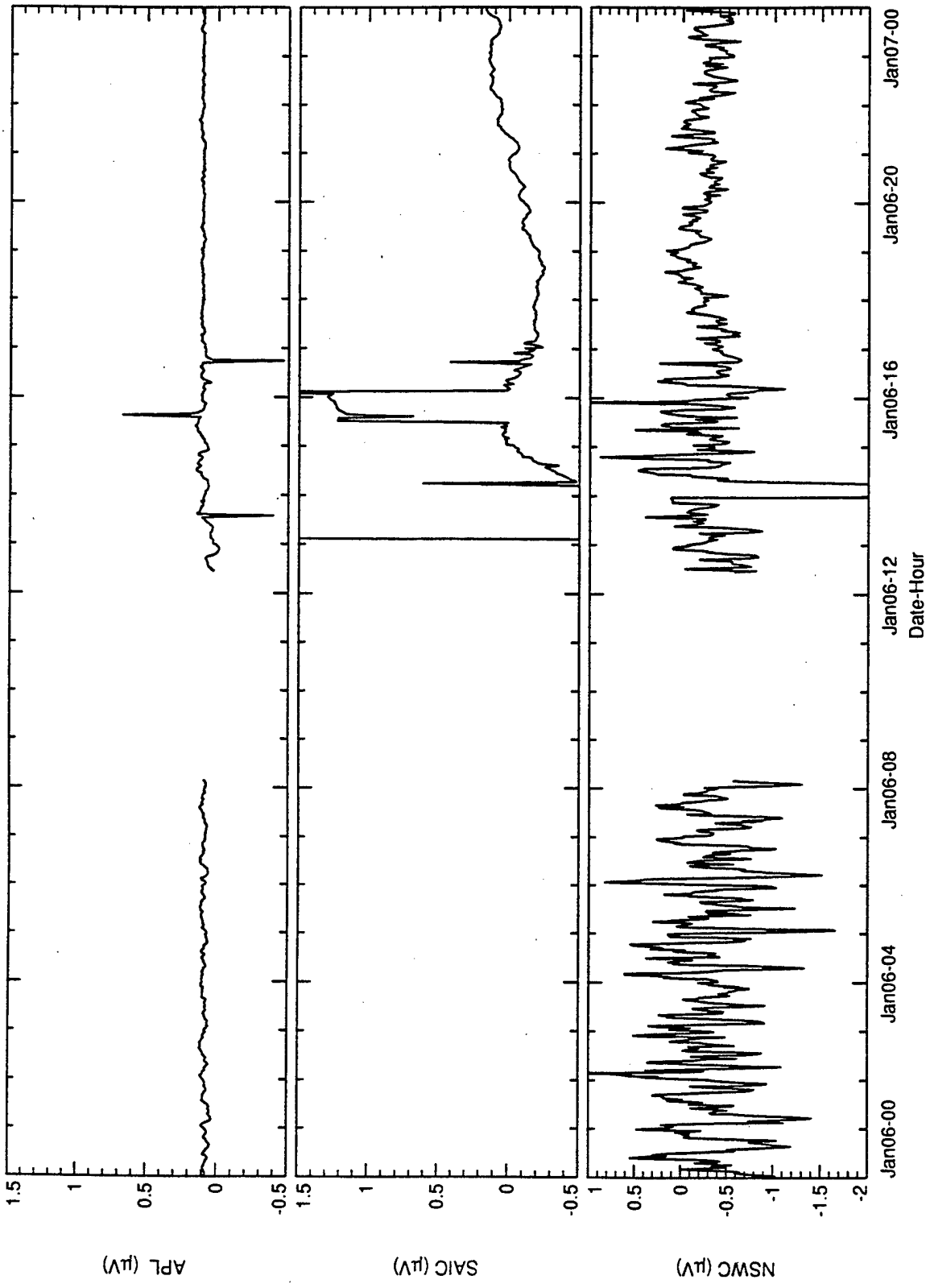

Figure C.13

Salt Water Tank Test Daily. Subsampled to about 70 s.

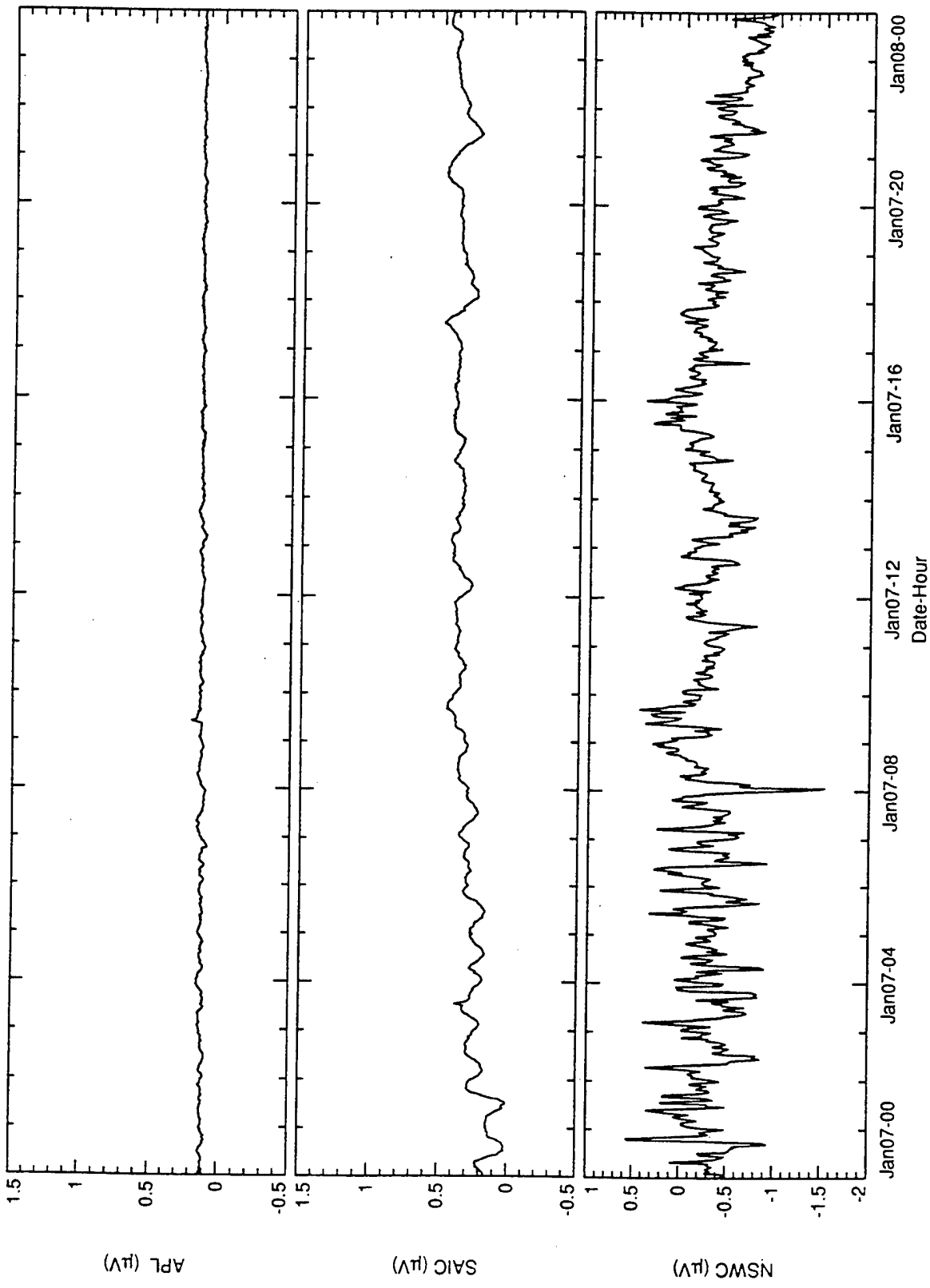

Figure C.14

Salt Water Tank Test Daily. Subsampled to about 70 s.

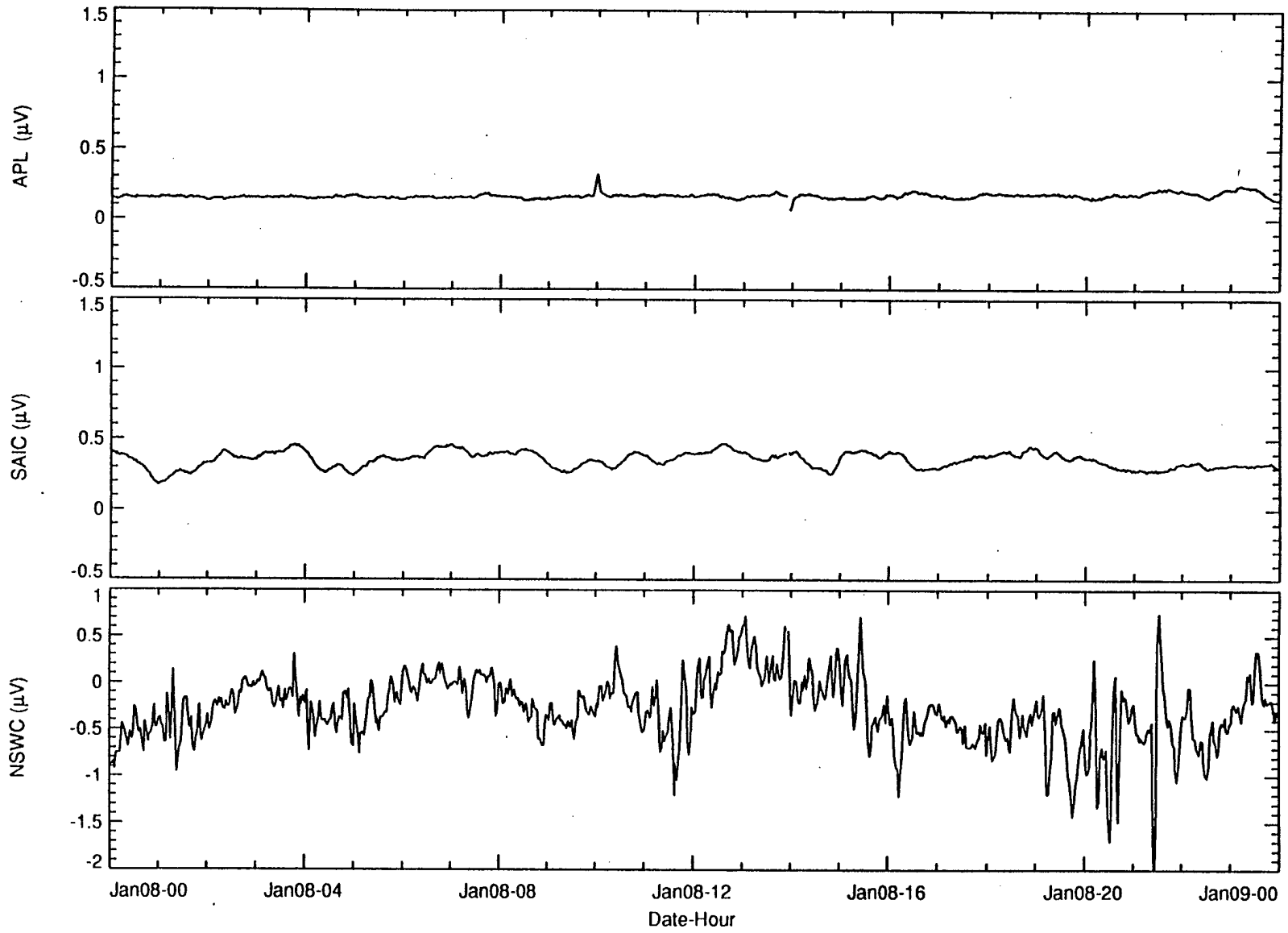

Figure C.15

Salt Water Tank Test Daily. Subsampled to about 70 s.

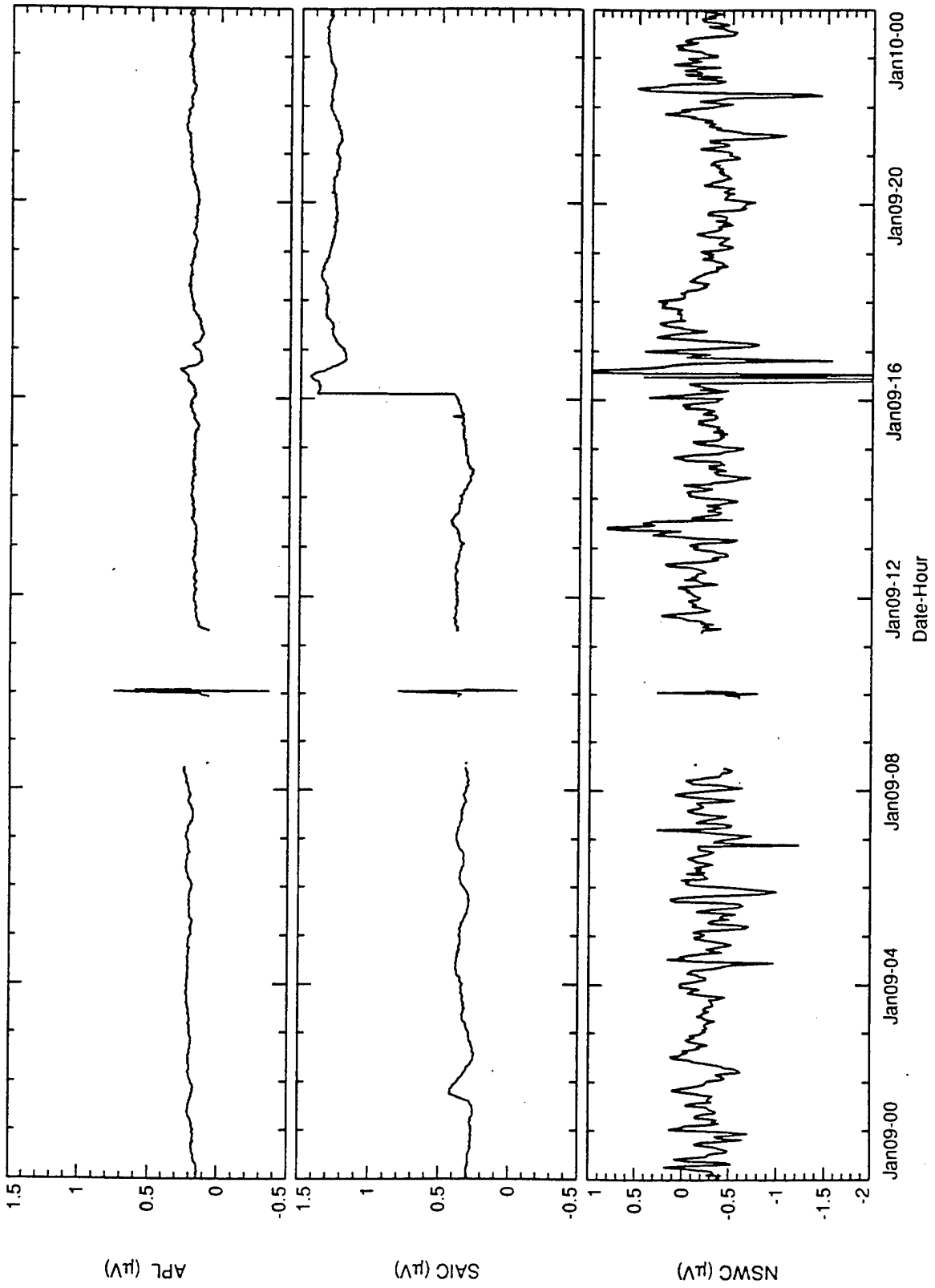

Figure C.16
Salt Water Tank Test Daily. Subsampled to about 70 s.

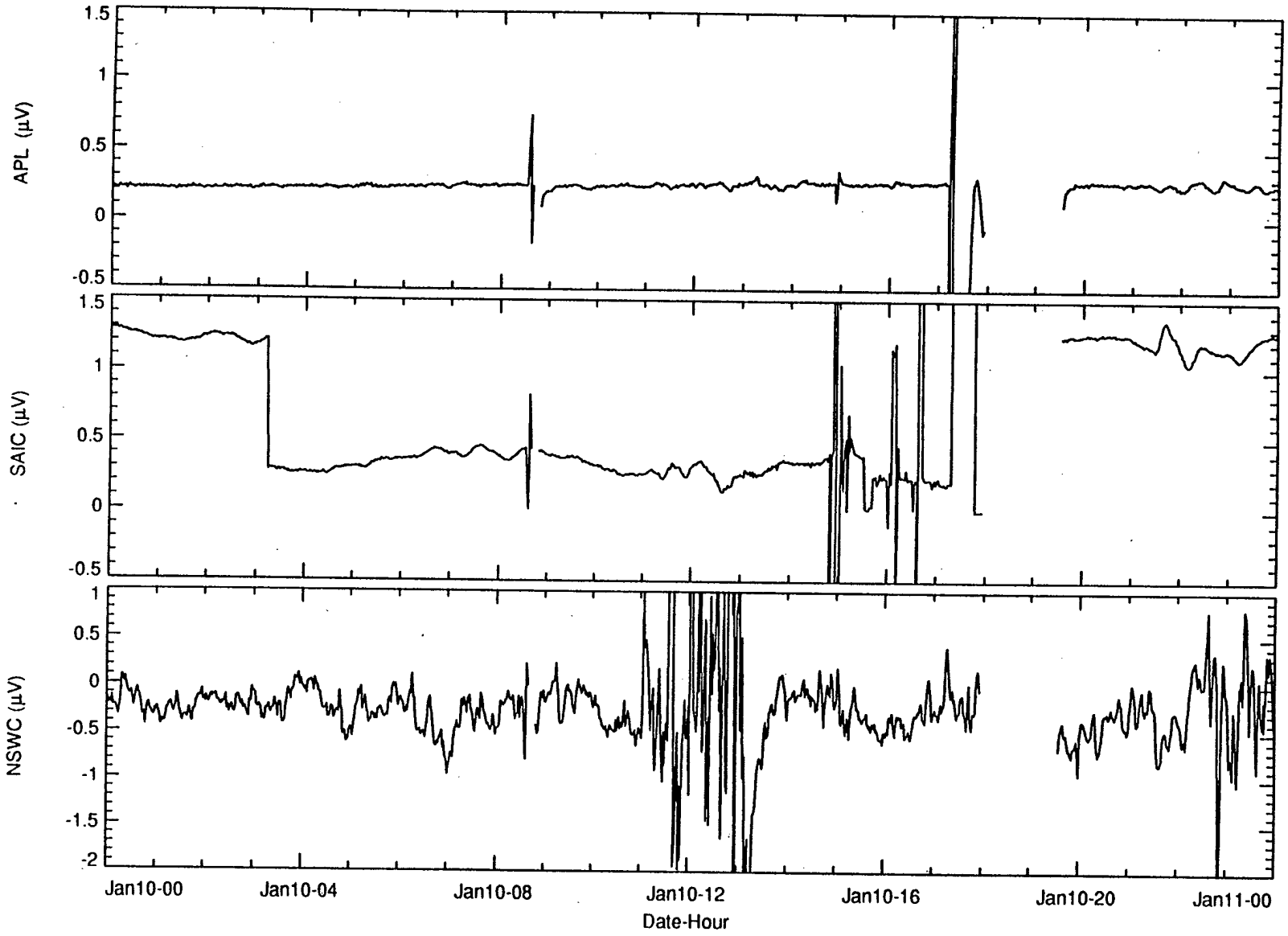

Figure C.17

Salt Water Tank Test Daily. Subsampled to about 70 s.

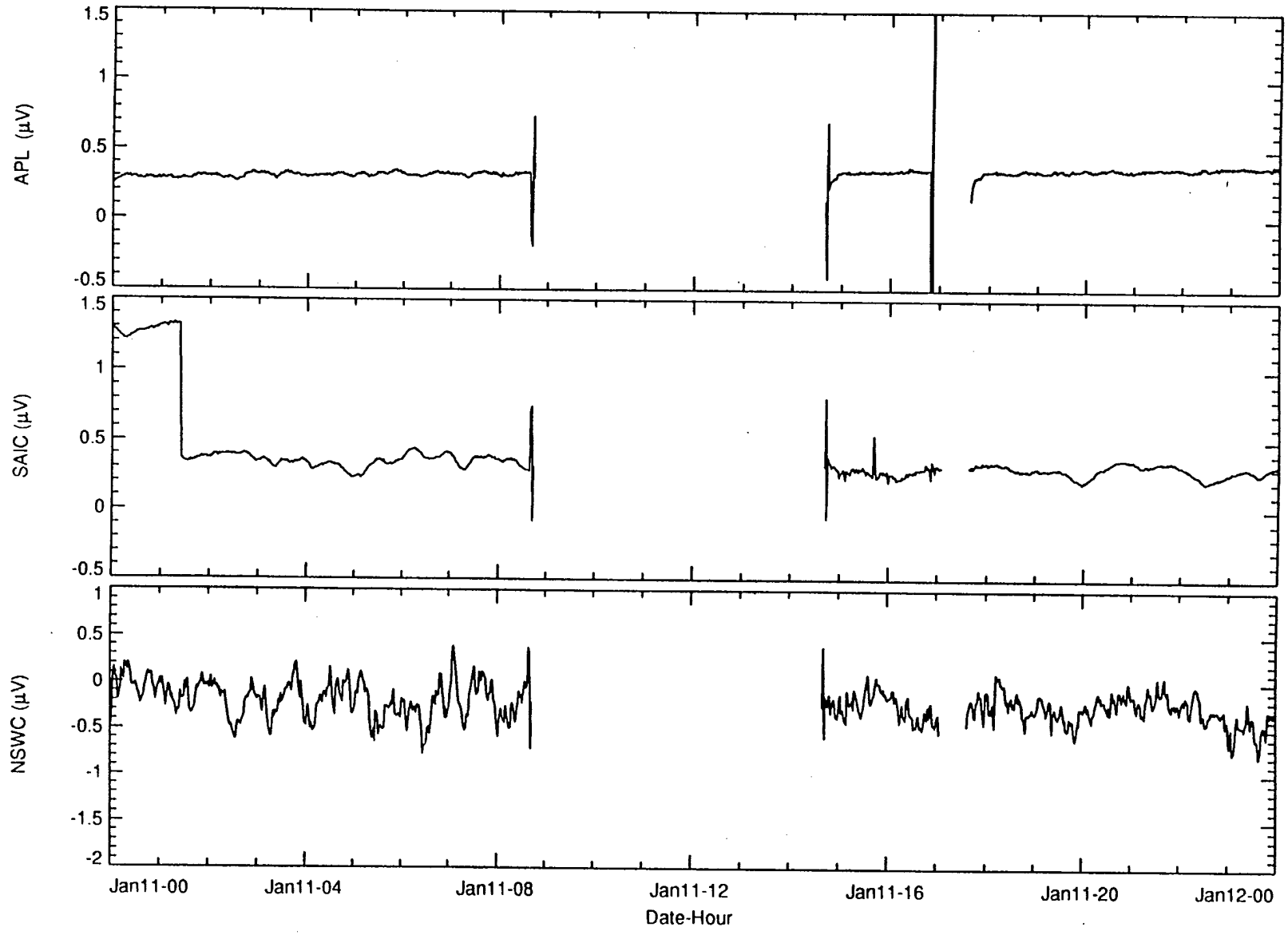

Figure C.18

Salt Water Tank Test Daily. Subsampled to about 70 s.

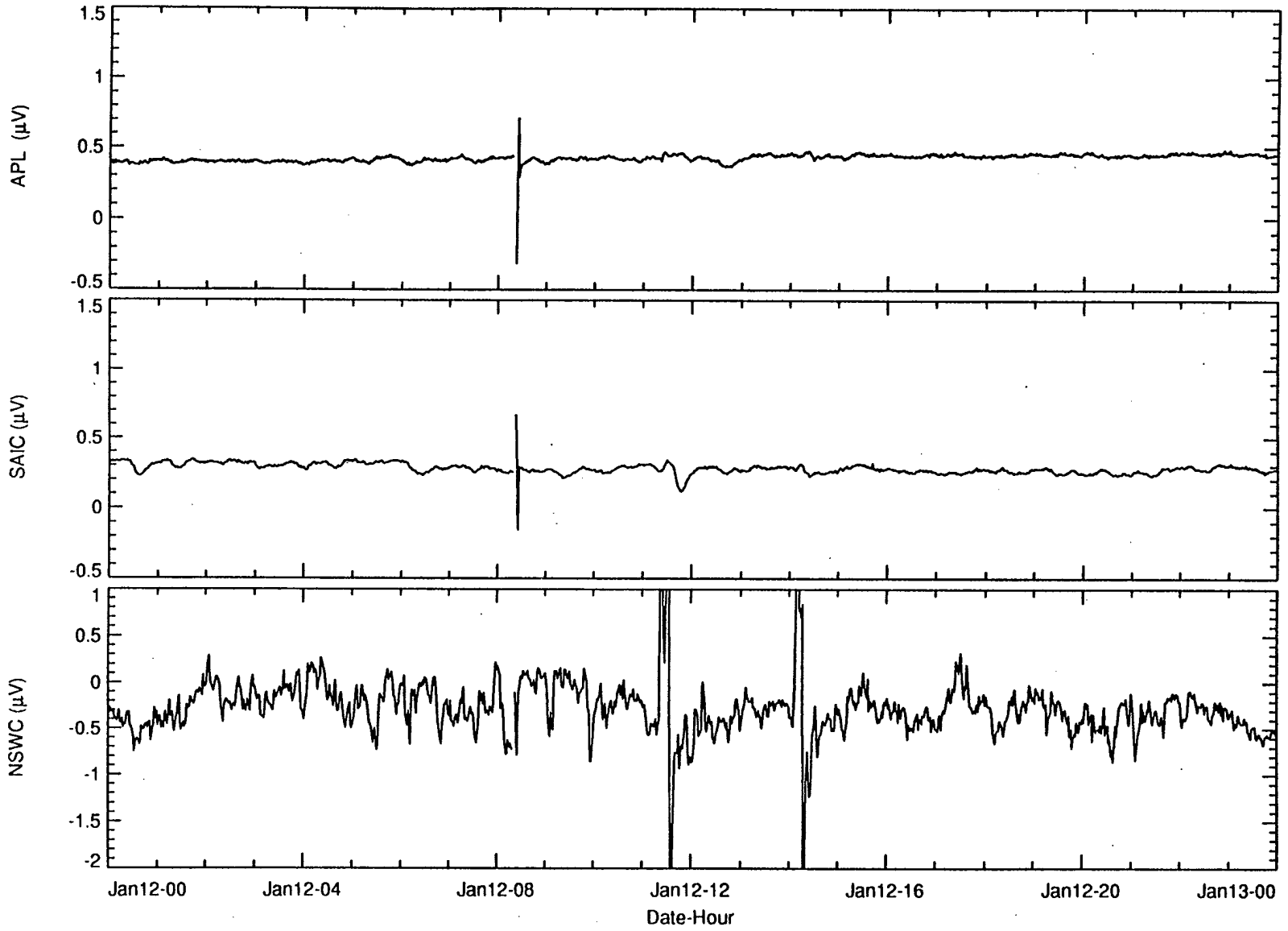

Figure C.19

Salt Water Tank Test Daily. Subsampled to about 70 s.

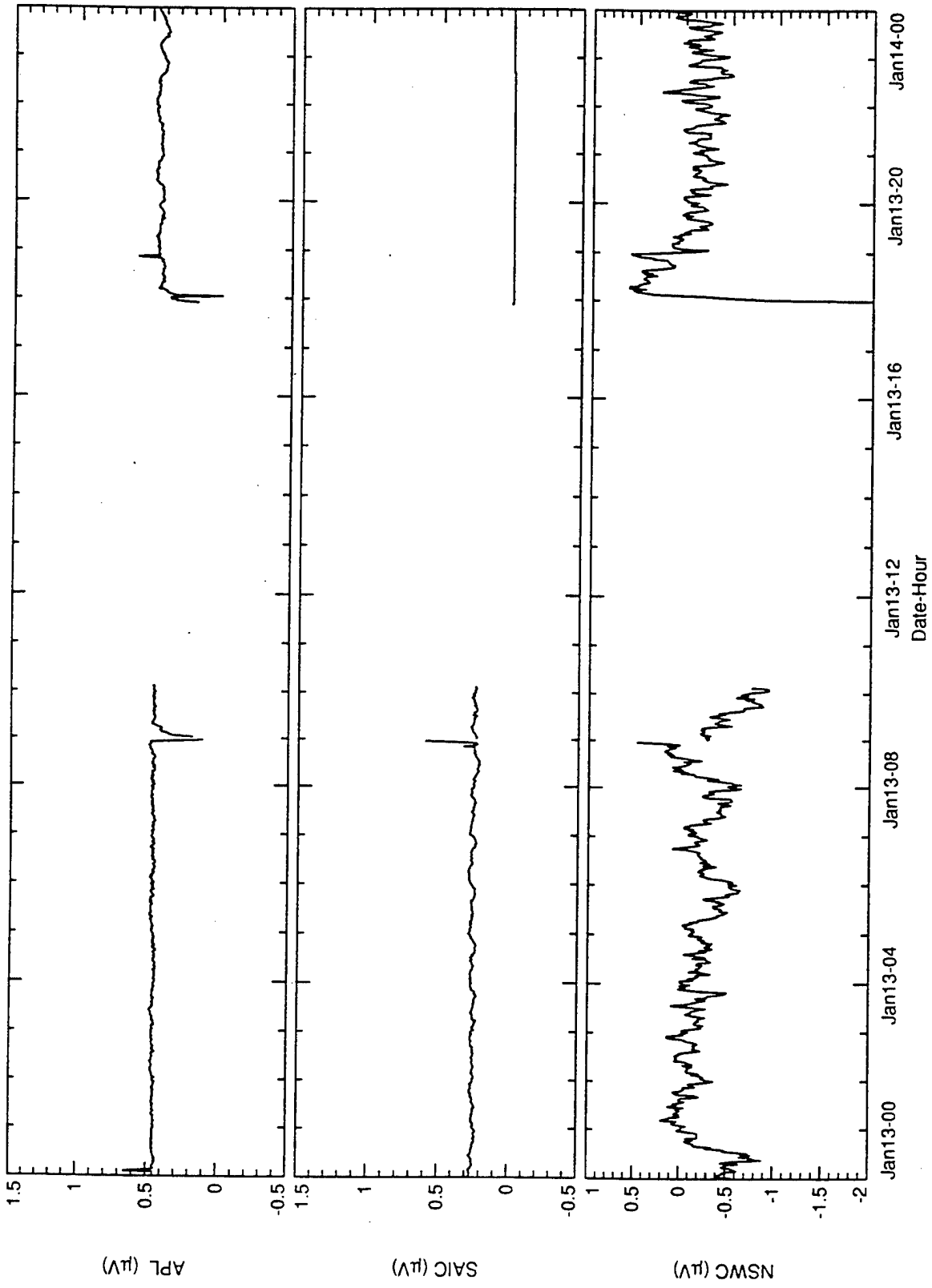

Figure C.20
Salt Water Tank Test Daily. Subsampled to about 70 s.

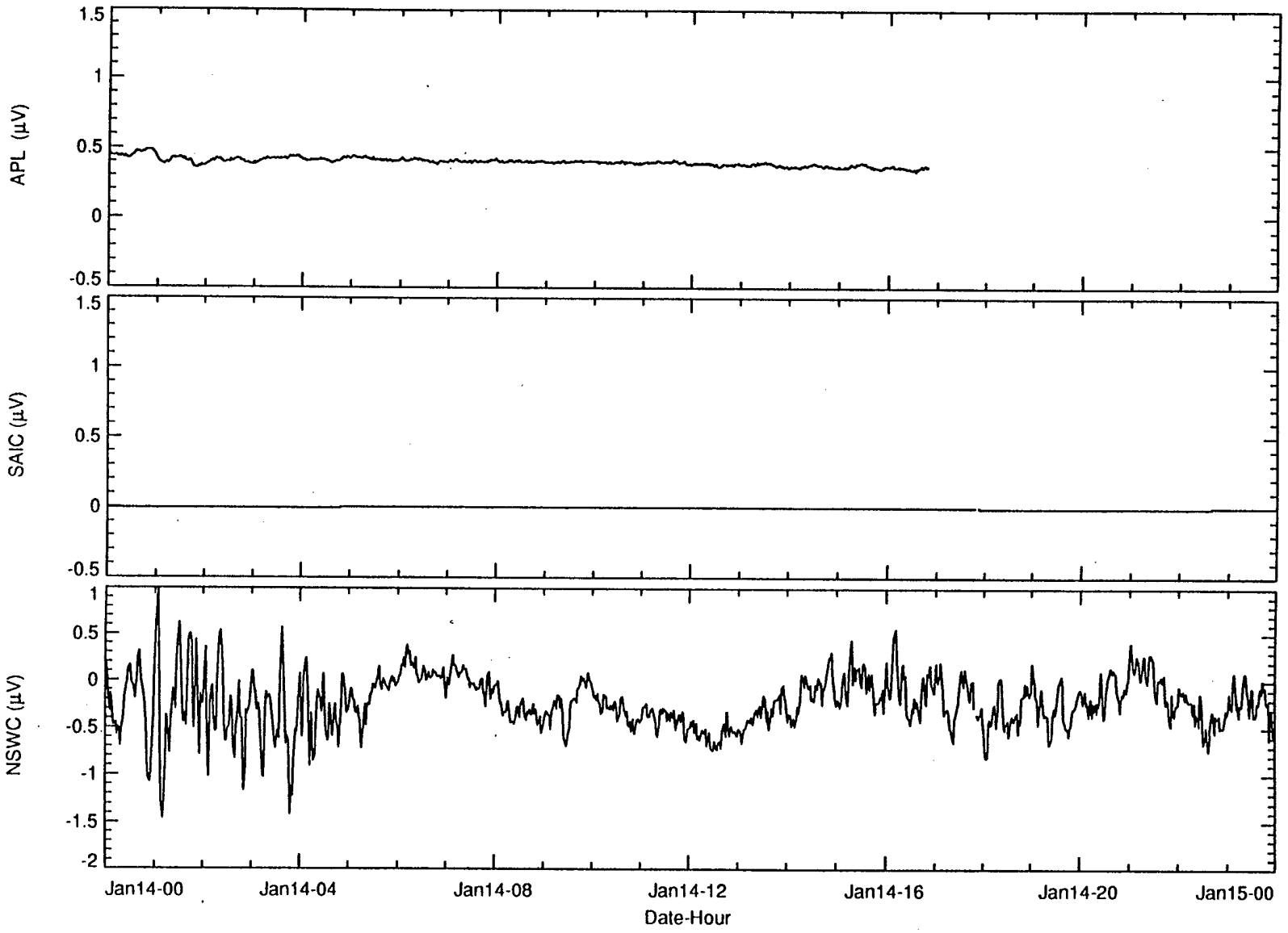

Figure C.21

Salt Water Tank Test Daily. Subsampled to about 70 s.

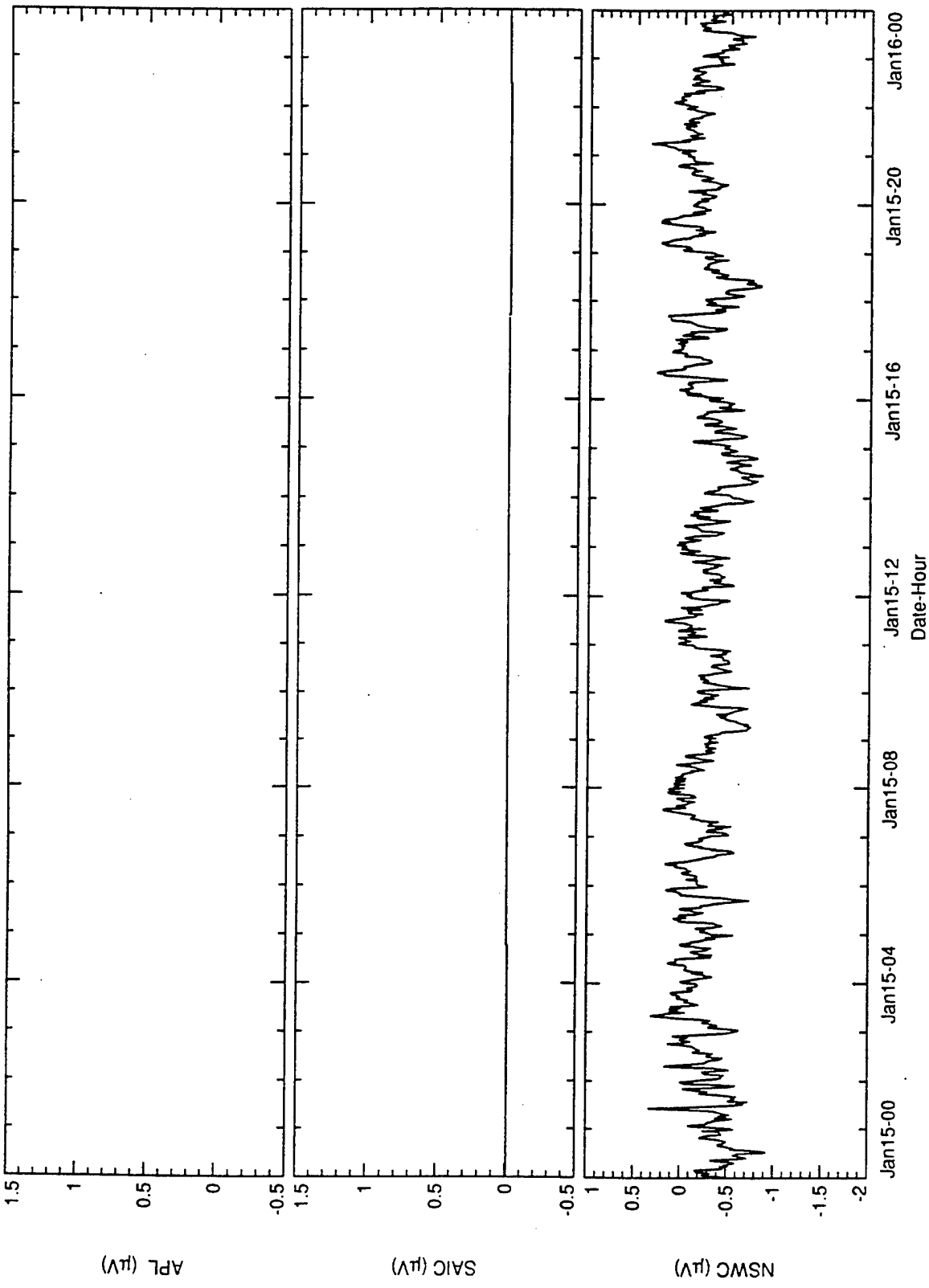

Figure C.22

Salt Water Tank Test Daily. Subsampled to about 70 s.

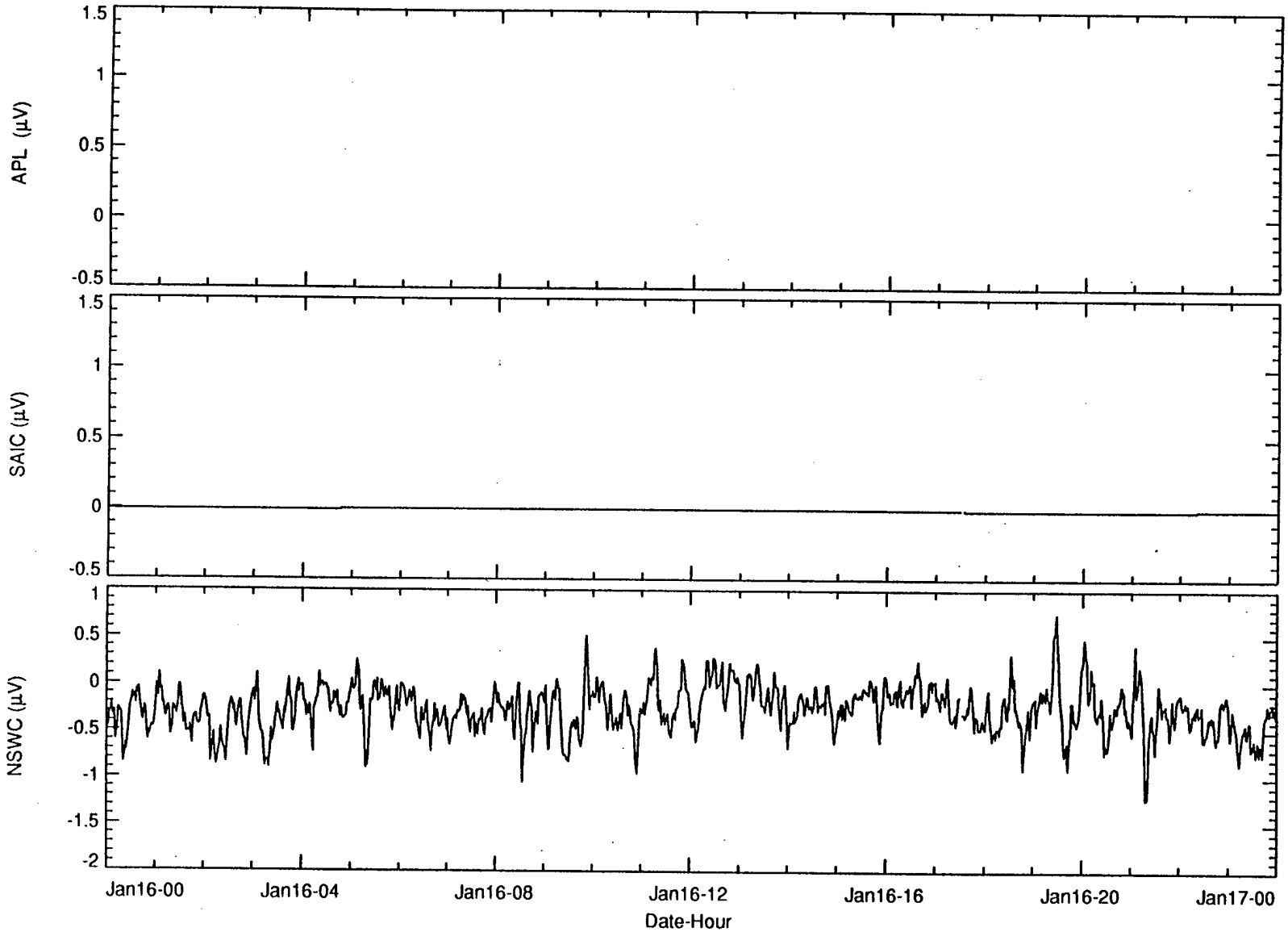

Figure C.23

Salt Water Tank Test Daily. Subsampled to about 70 s.

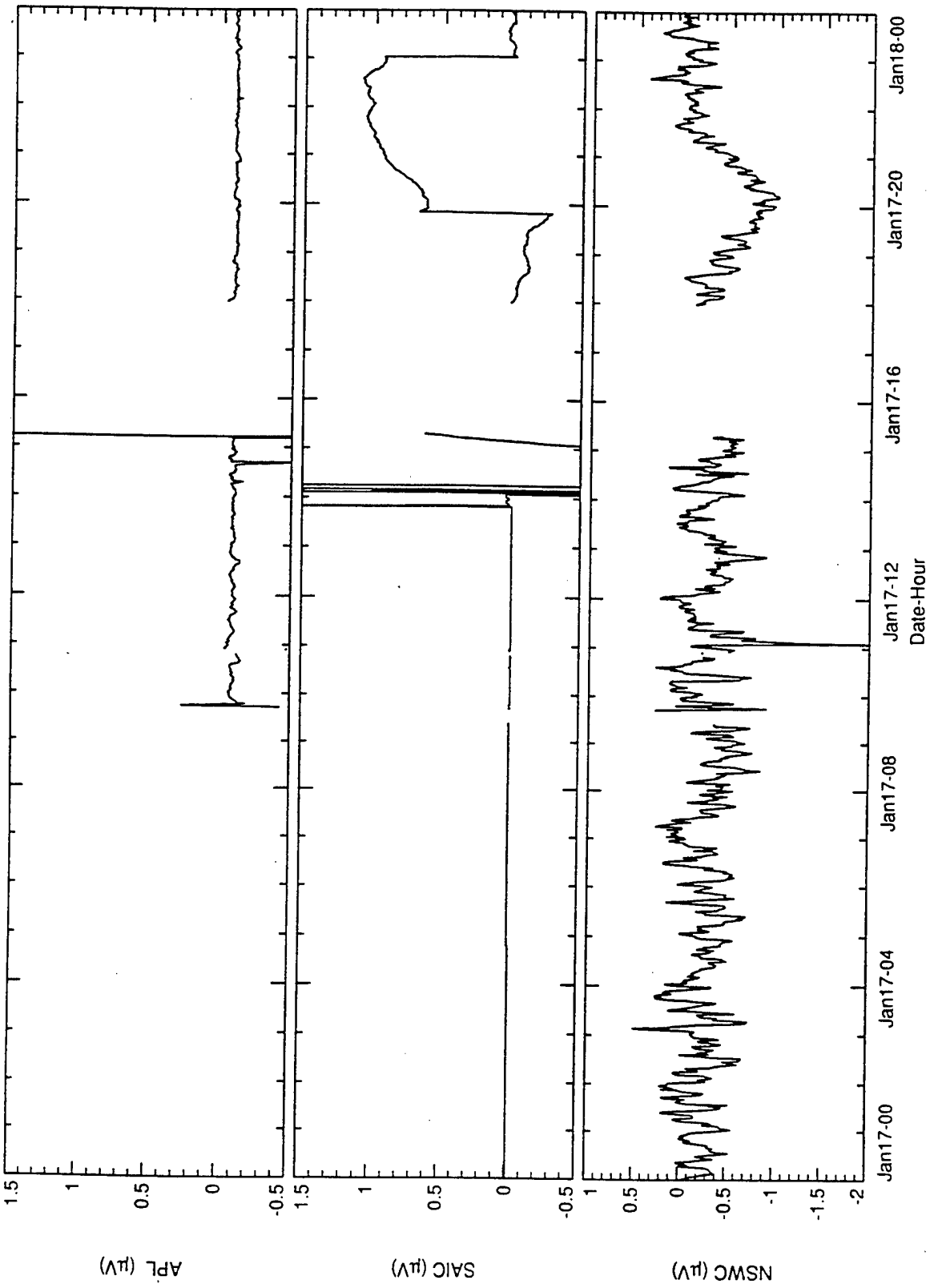

Figure C.24

Salt Water Tank Test Daily. Subsampled to about 70 s.

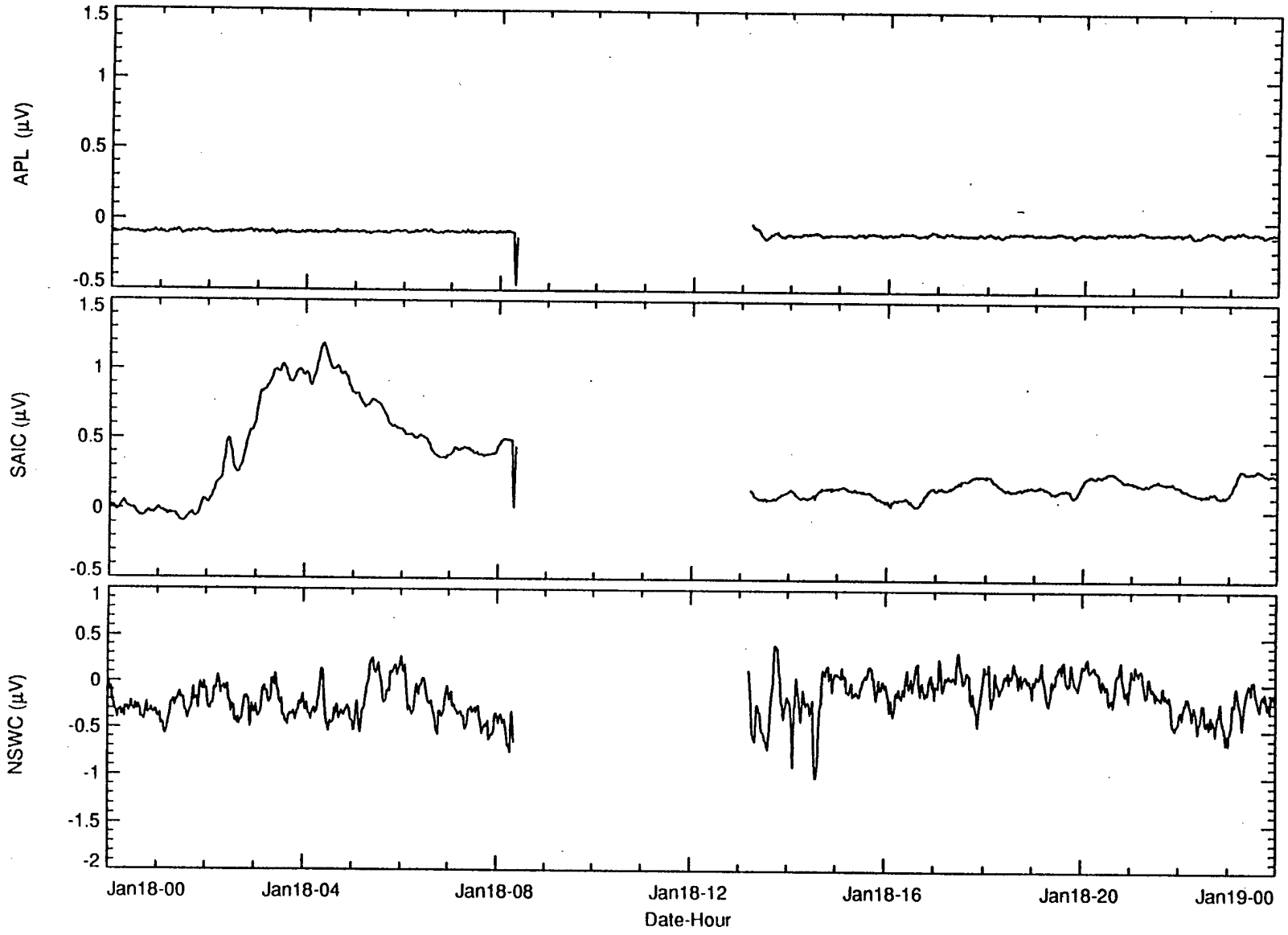

Figure C.25

Salt Water Tank Test Daily. Subsampled to about 70 s.

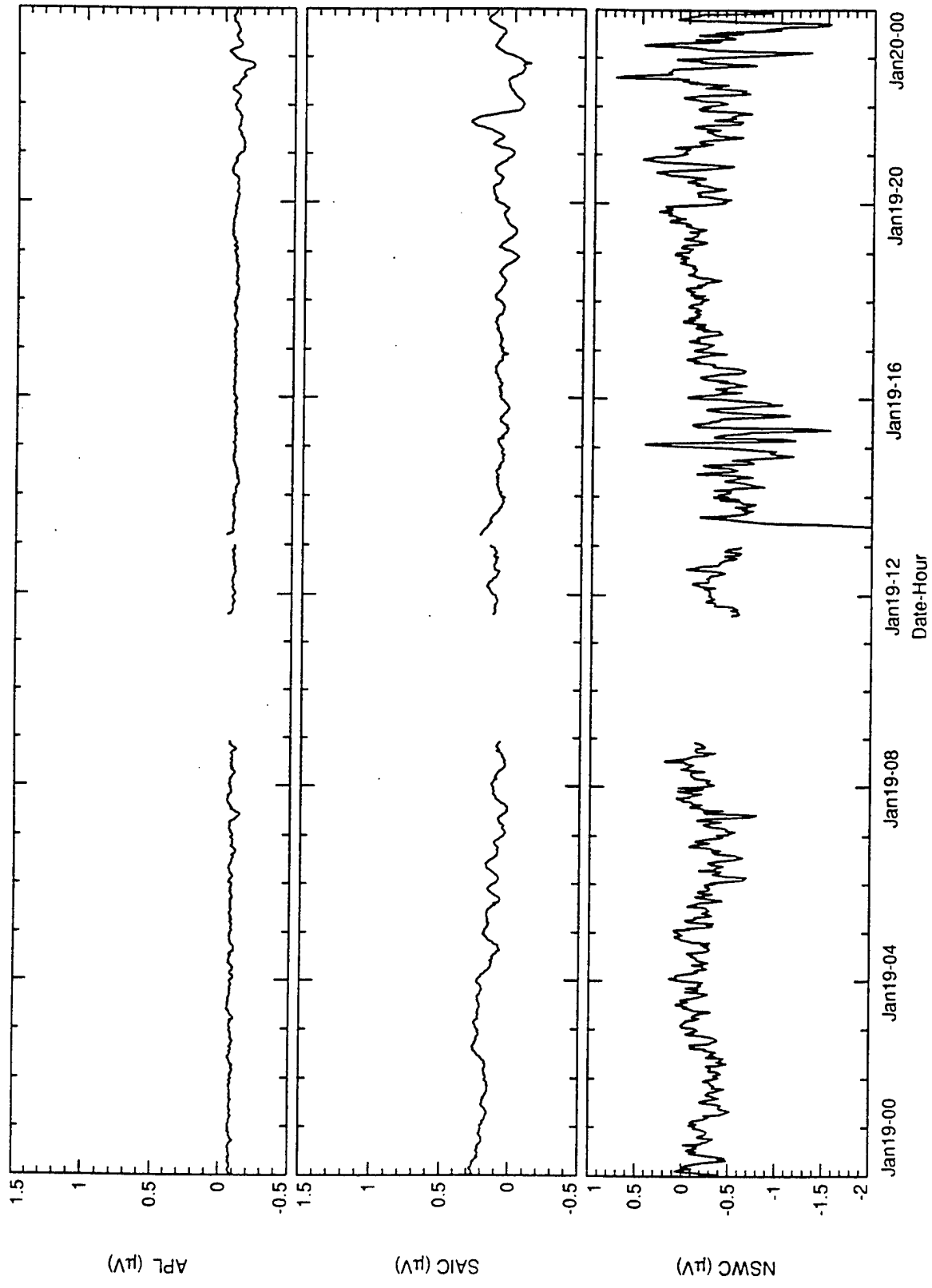

Figure C.26
Salt Water Tank Test Daily. Subsampled to about 70 s.

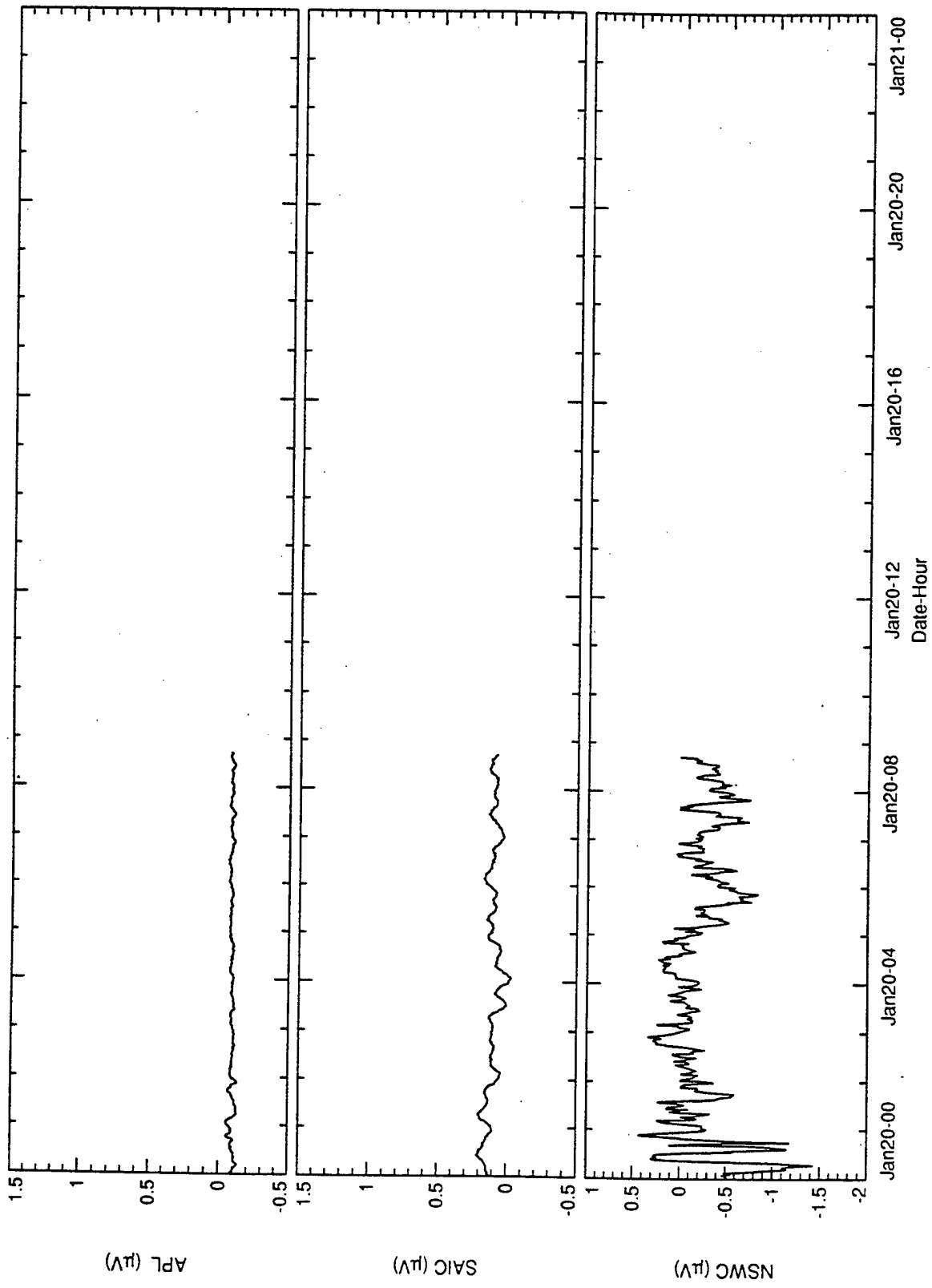

Figure C.27

Salt Water Tank Test Daily. Subsampled to about 70 s.

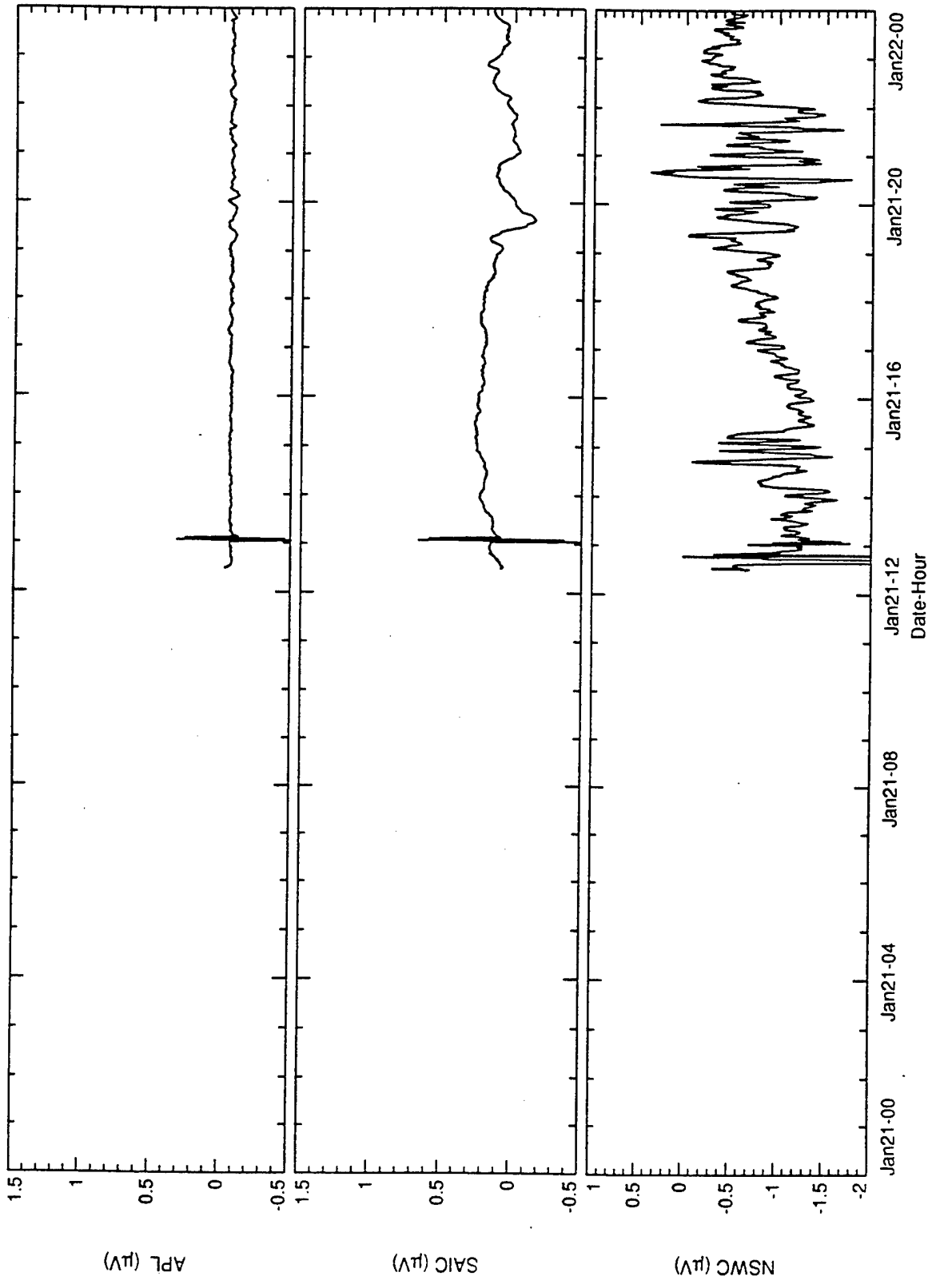

Figure C.28
Salt Water Tank Test Daily. Subsampled to about 70 s.

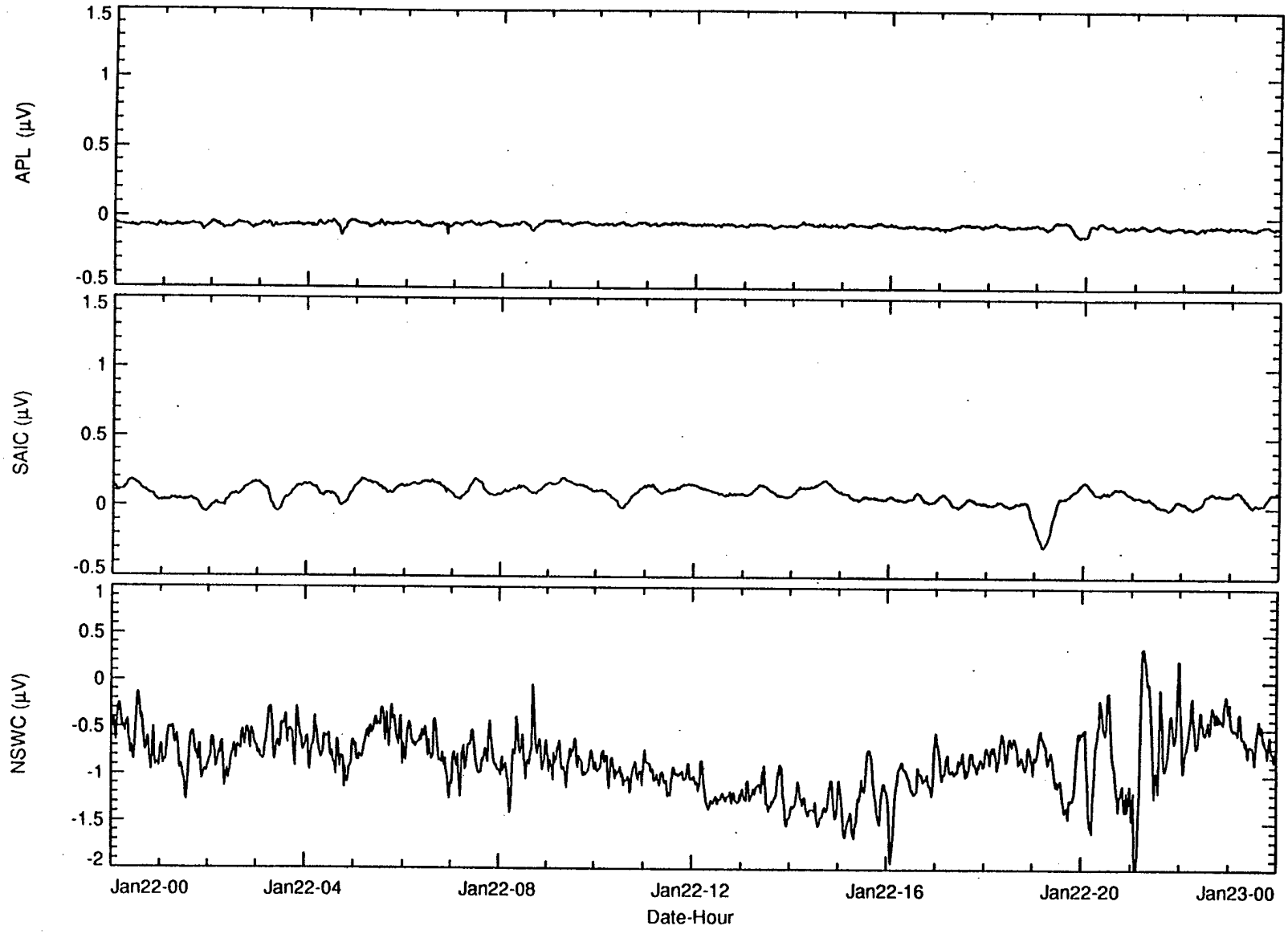

Figure C.29

Salt Water Tank Test Daily. Subsampled to about 70 s.

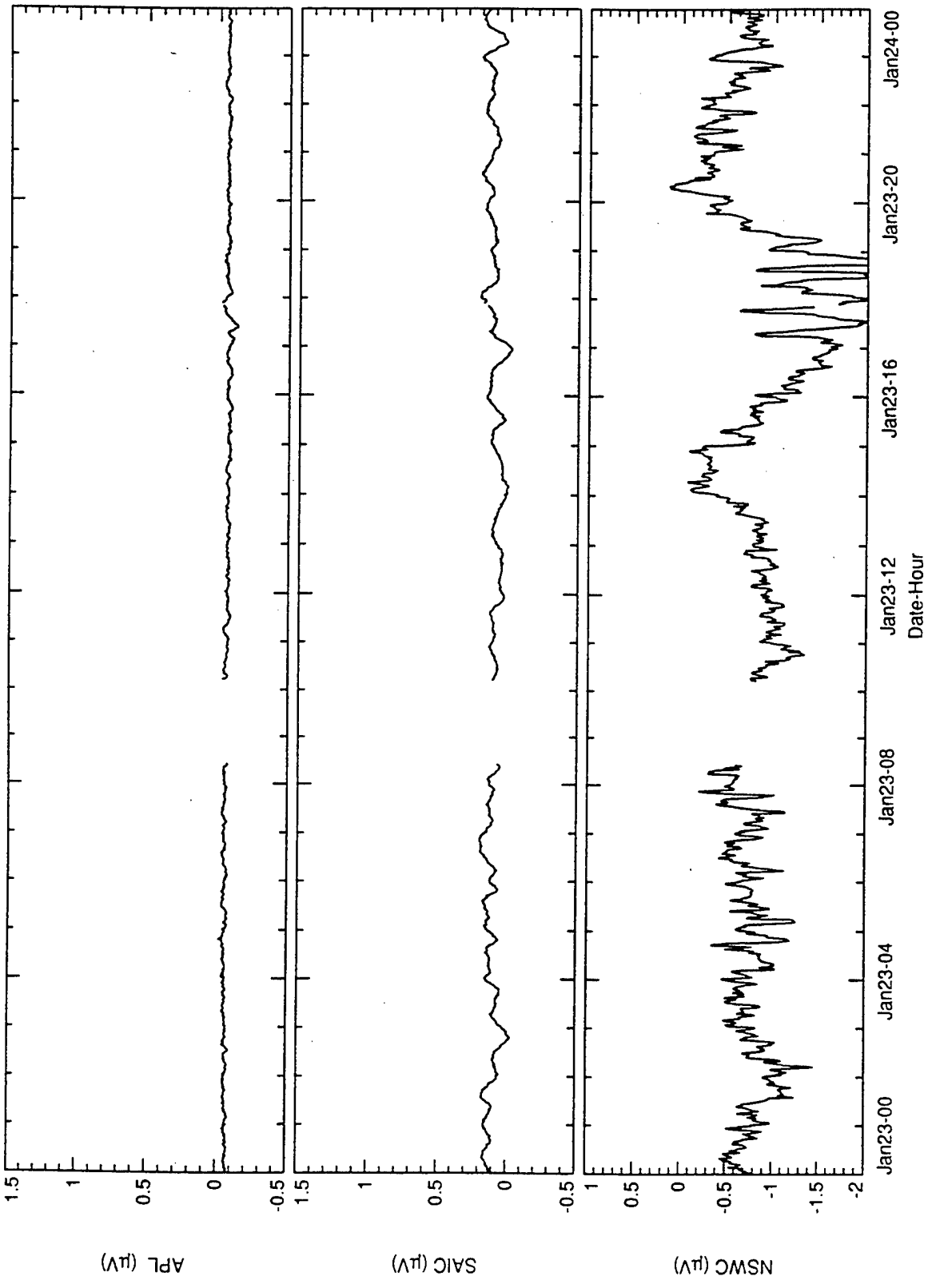

Figure C.30

Salt Water Tank Test Daily. Subsampled to about 70 s.

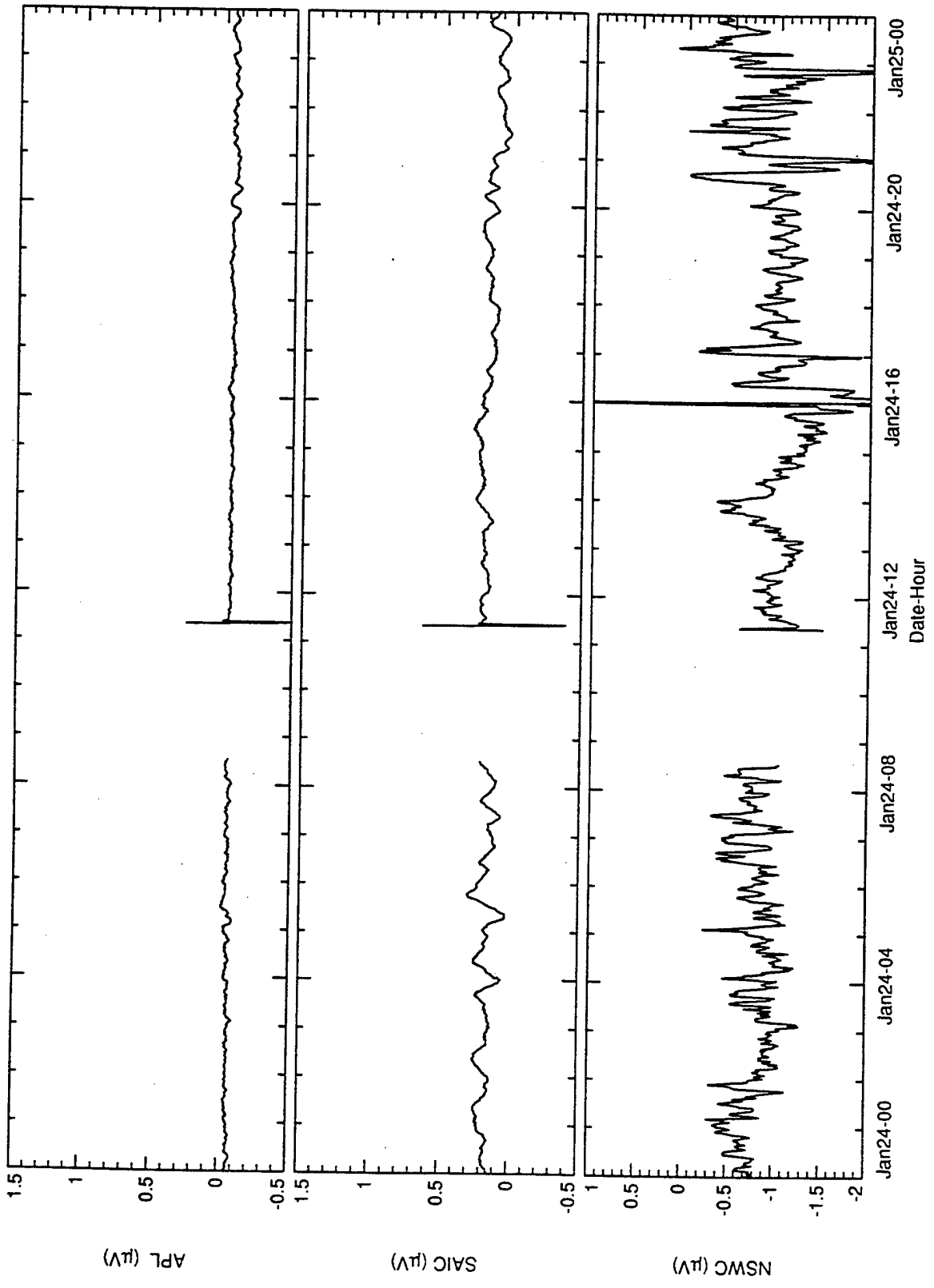

Figure C.31

Salt Water Tank Test Daily. Subsampled to about 70 s.

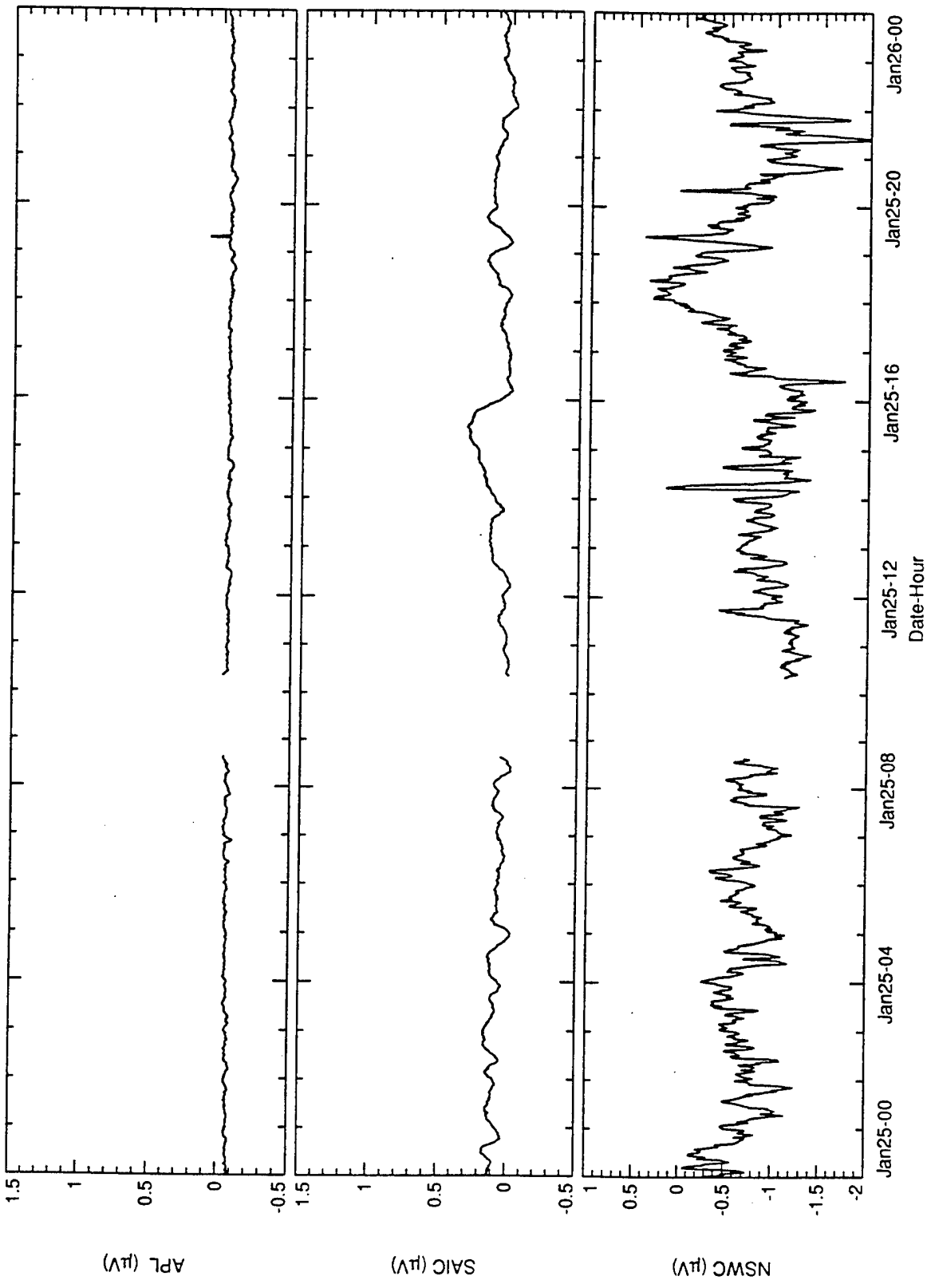

Figure C.32

Salt Water Tank Test Daily. Subsampled to about 70 s.

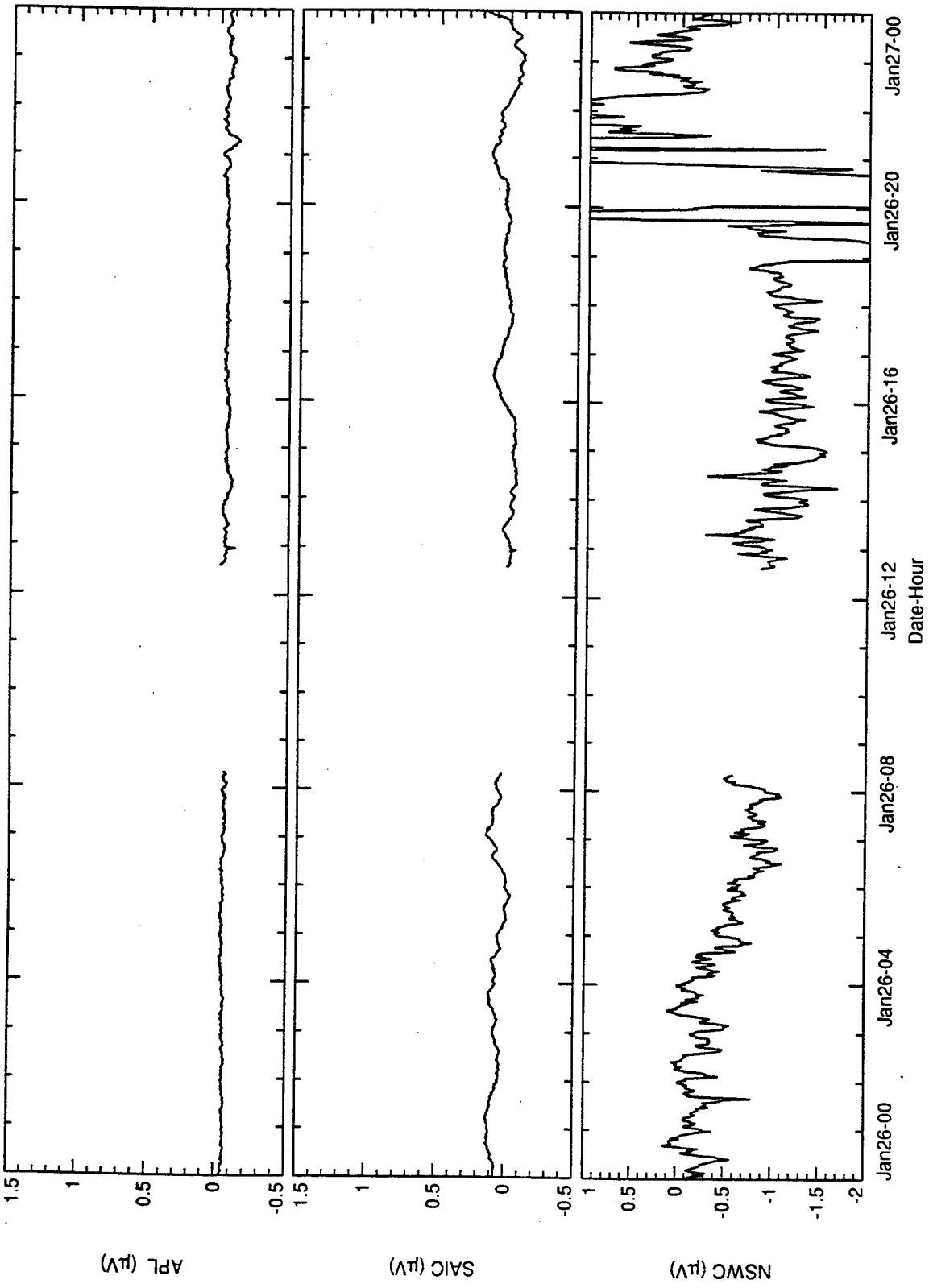

Figure C.33

Salt Water Tank Test Daily. Subsampled to about 70 s.

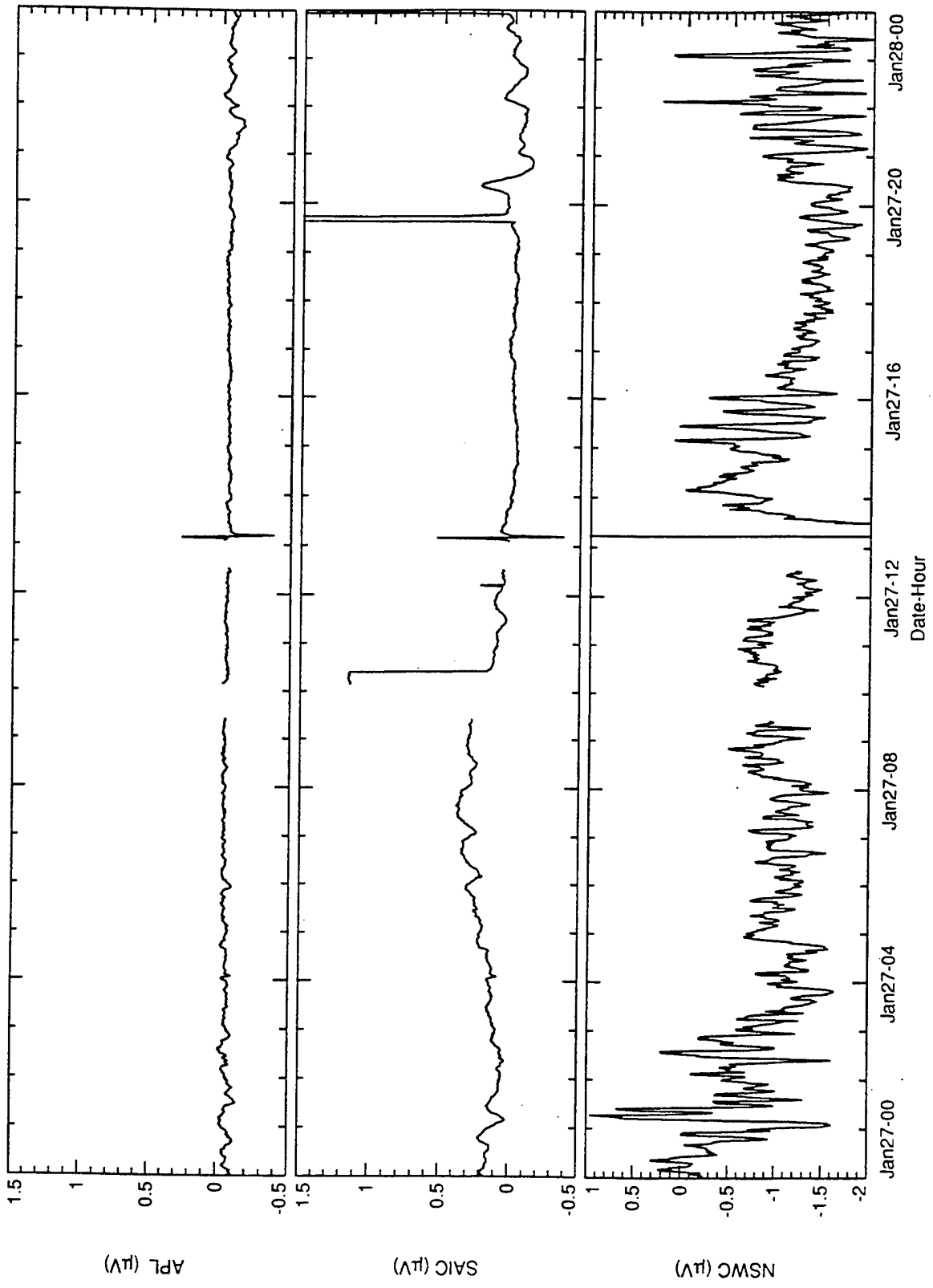

Figure C.34

Salt Water Tank Test Daily. Subsampled to about 70 s.

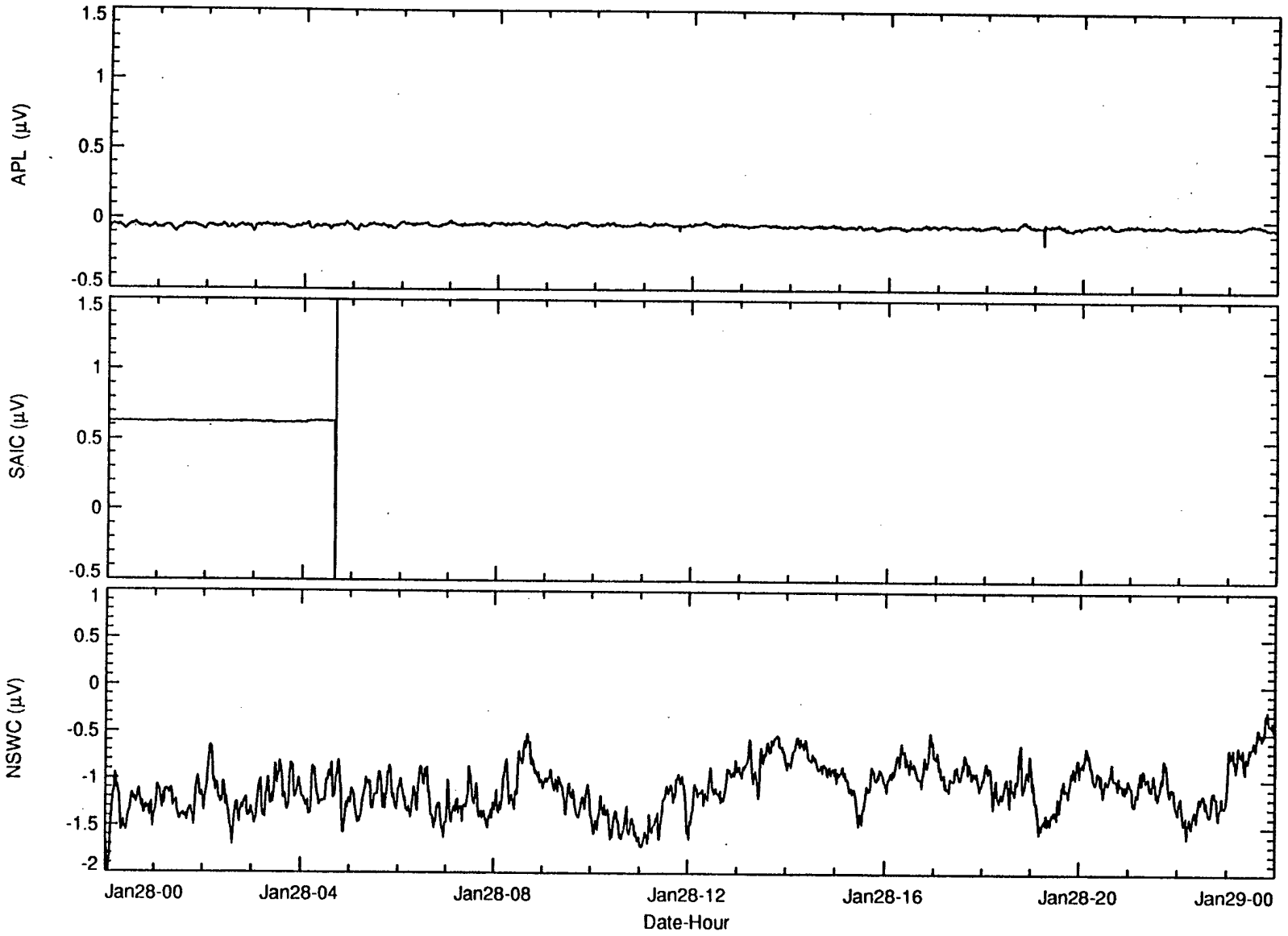

Figure C.35

Salt Water Tank Test Daily. Subsampled to about 70 s.

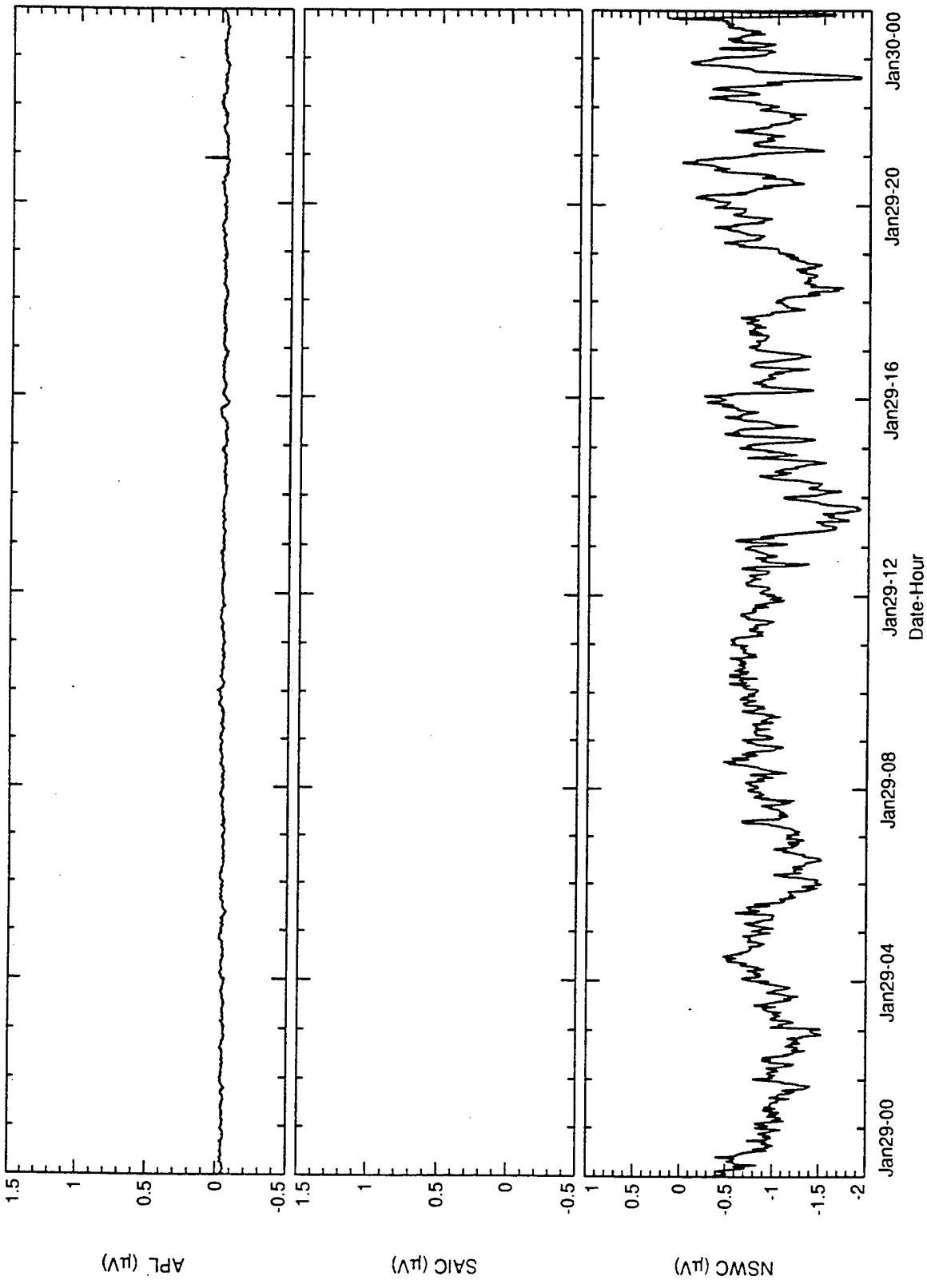

Figure C.36

Salt Water Tank Test Daily. Subsampled to about 70 s.

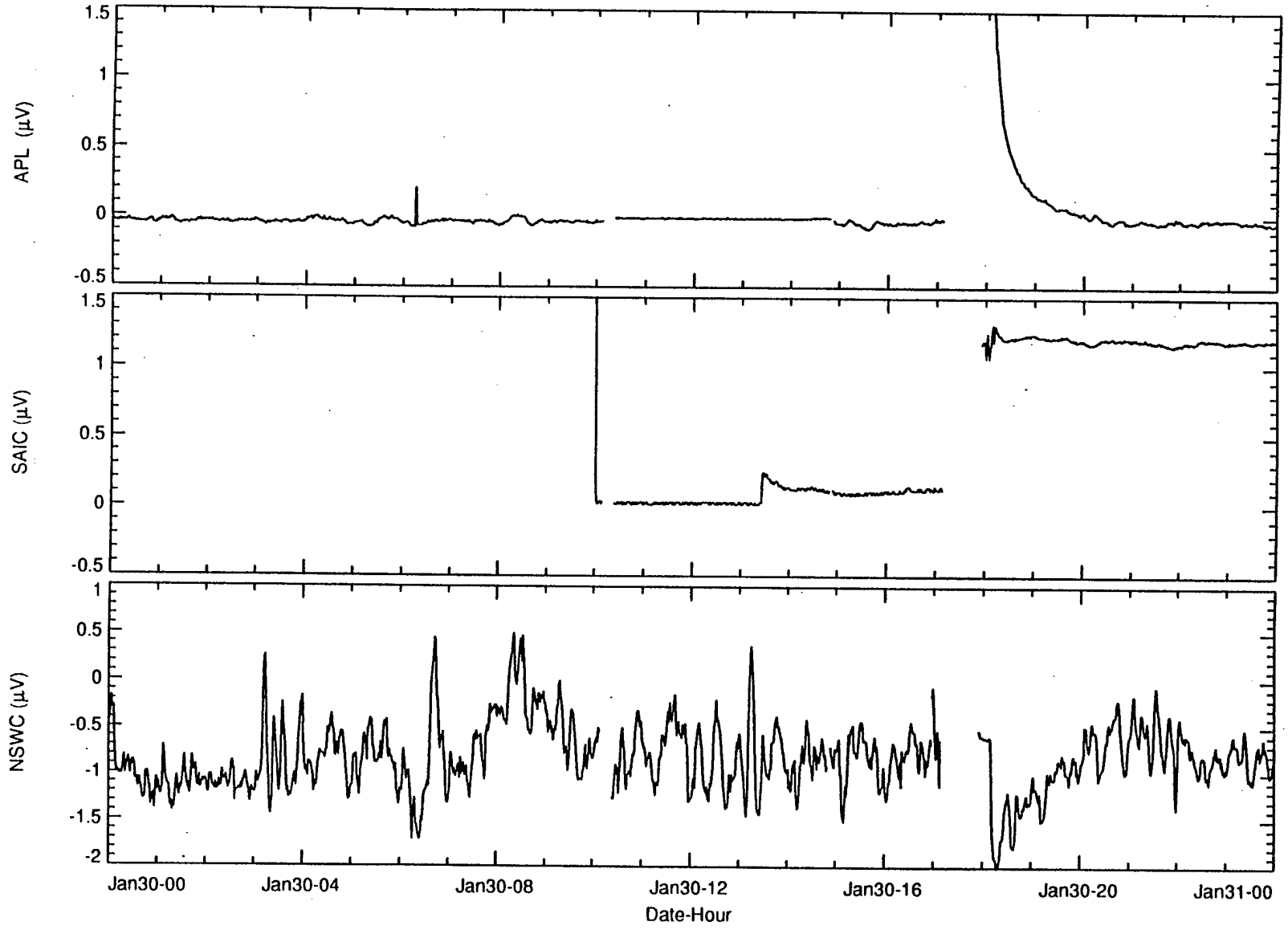

Figure C.37

Salt Water Tank Test Daily. Subsampled to about 70 s.

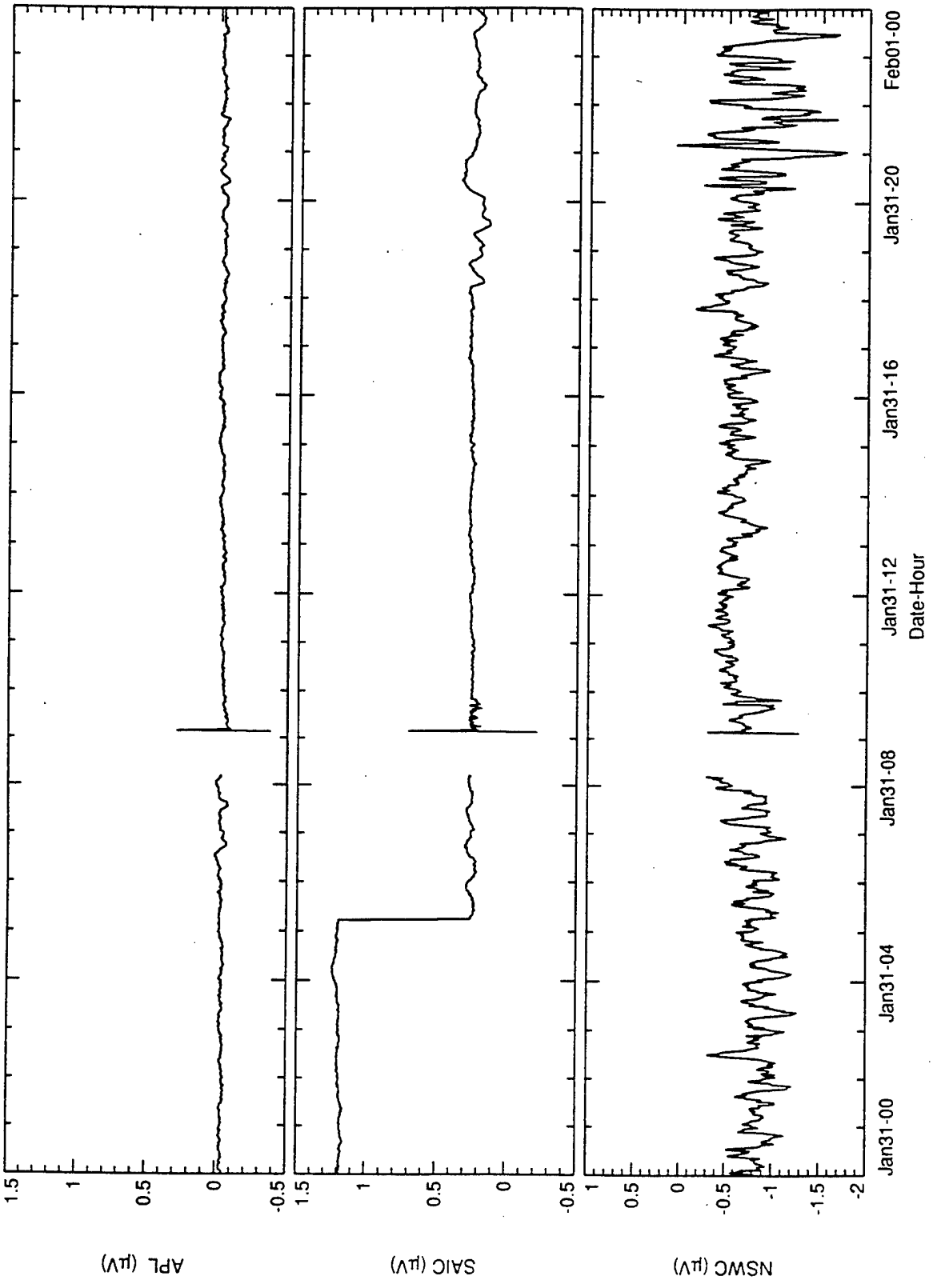

Figure C.38
Salt Water Tank Test Daily. Subsampled to about 70 s.

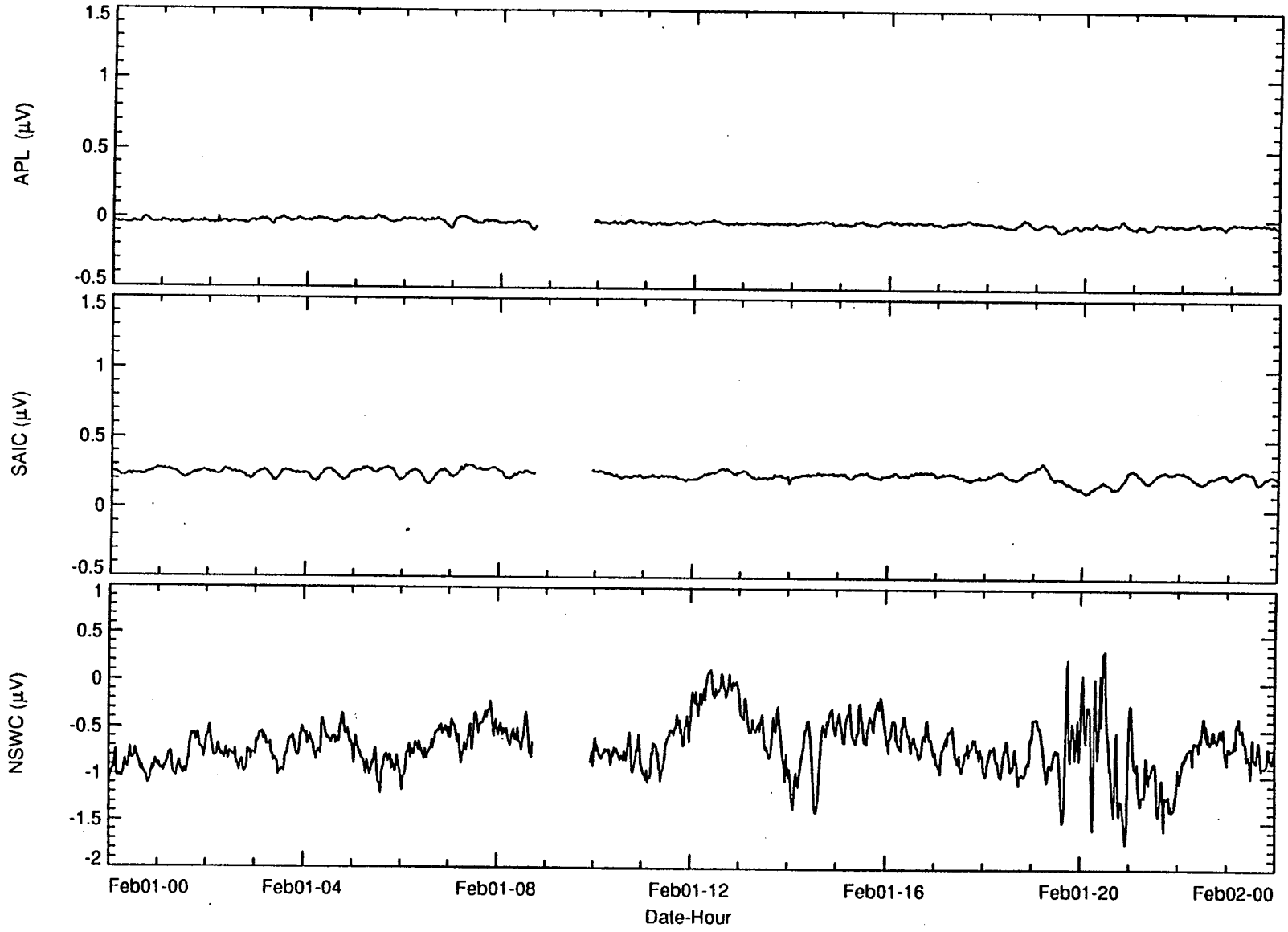

Figure C.39

Salt Water Tank Test Daily. Subsampled to about 70 s.

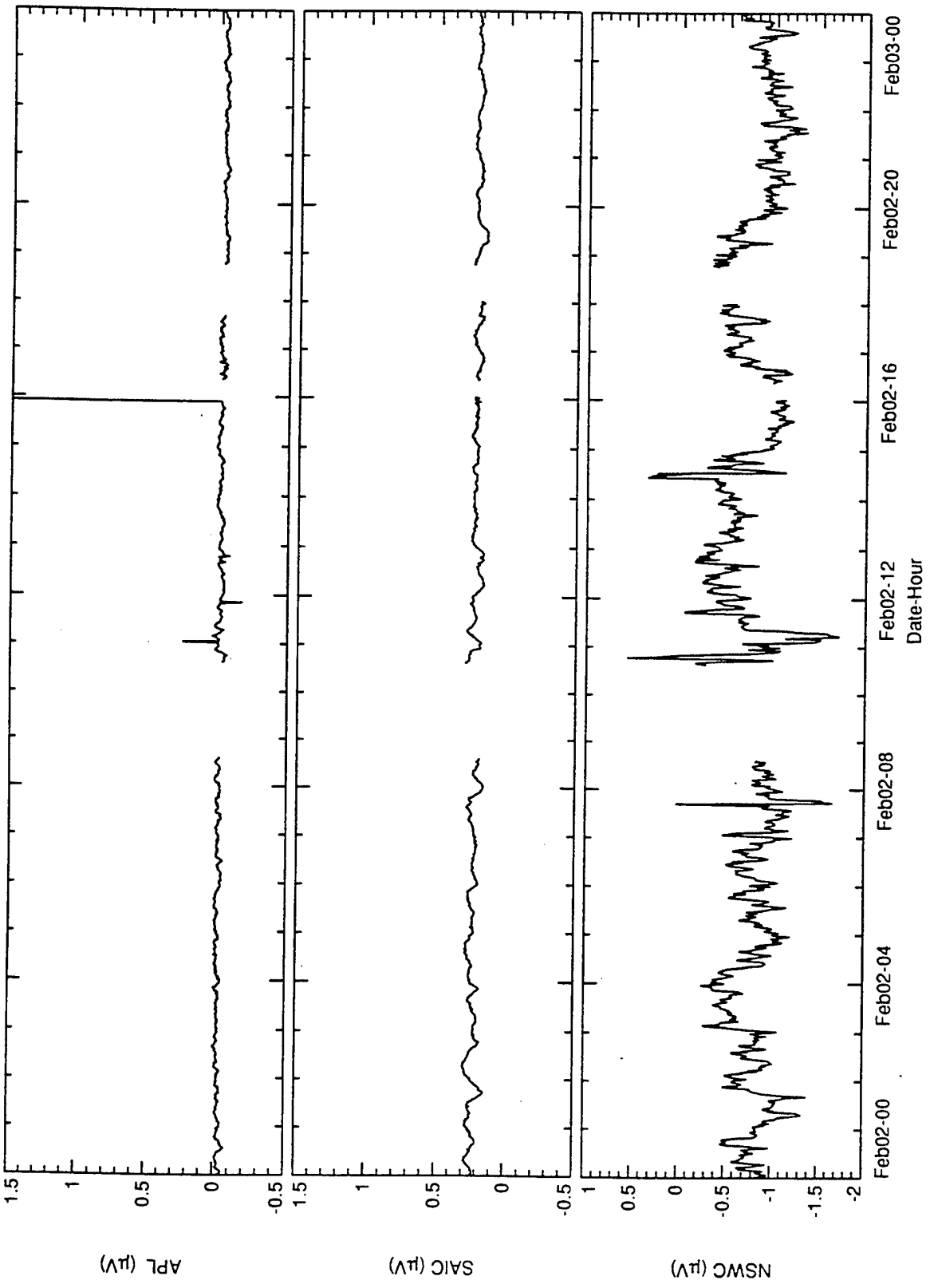

Figure C.40

Salt Water Tank Test Daily. Subsampled to about 70 s.

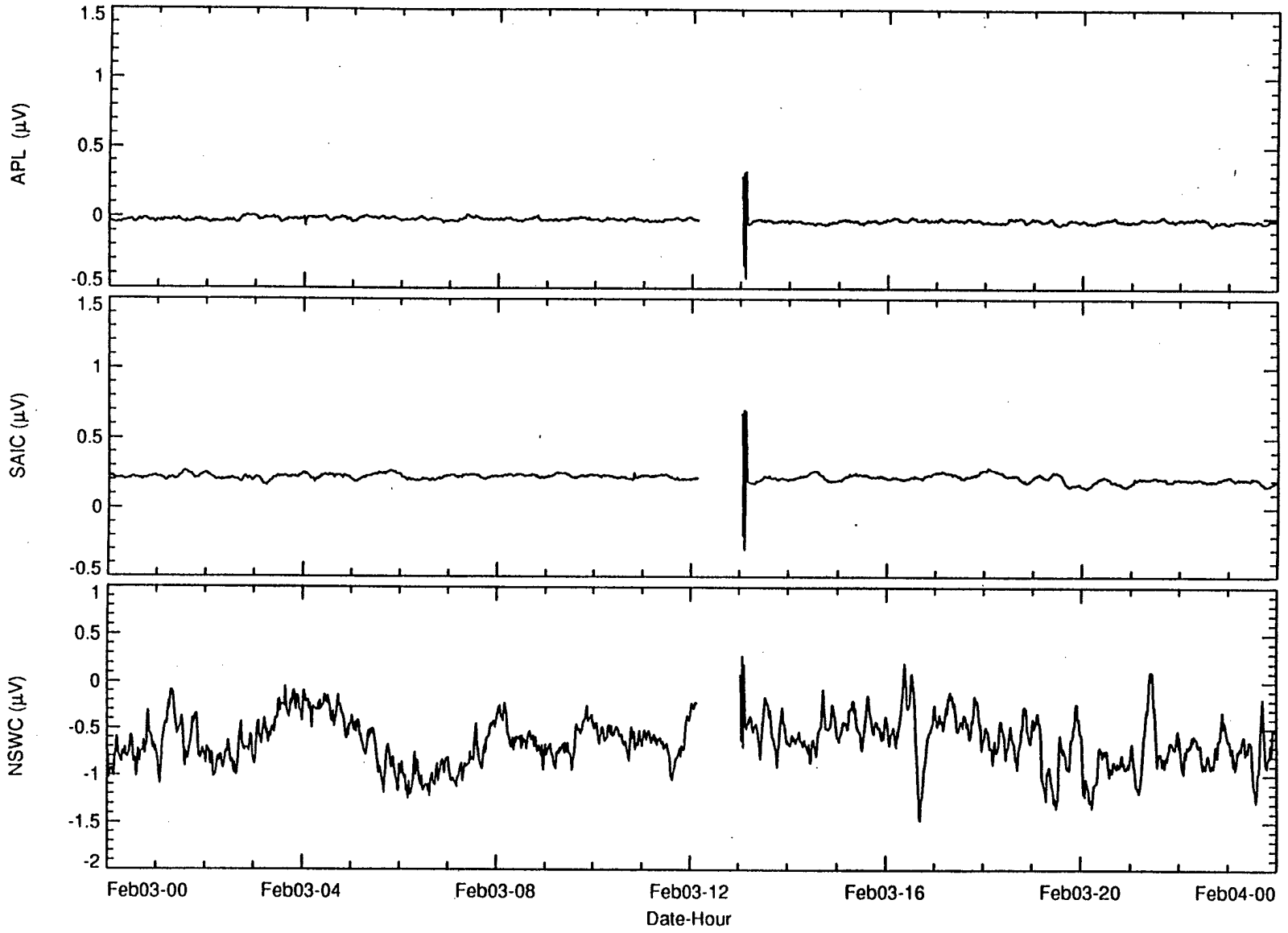

Figure C.41

Salt Water Tank Test Daily. Subsampled to about 70 s.

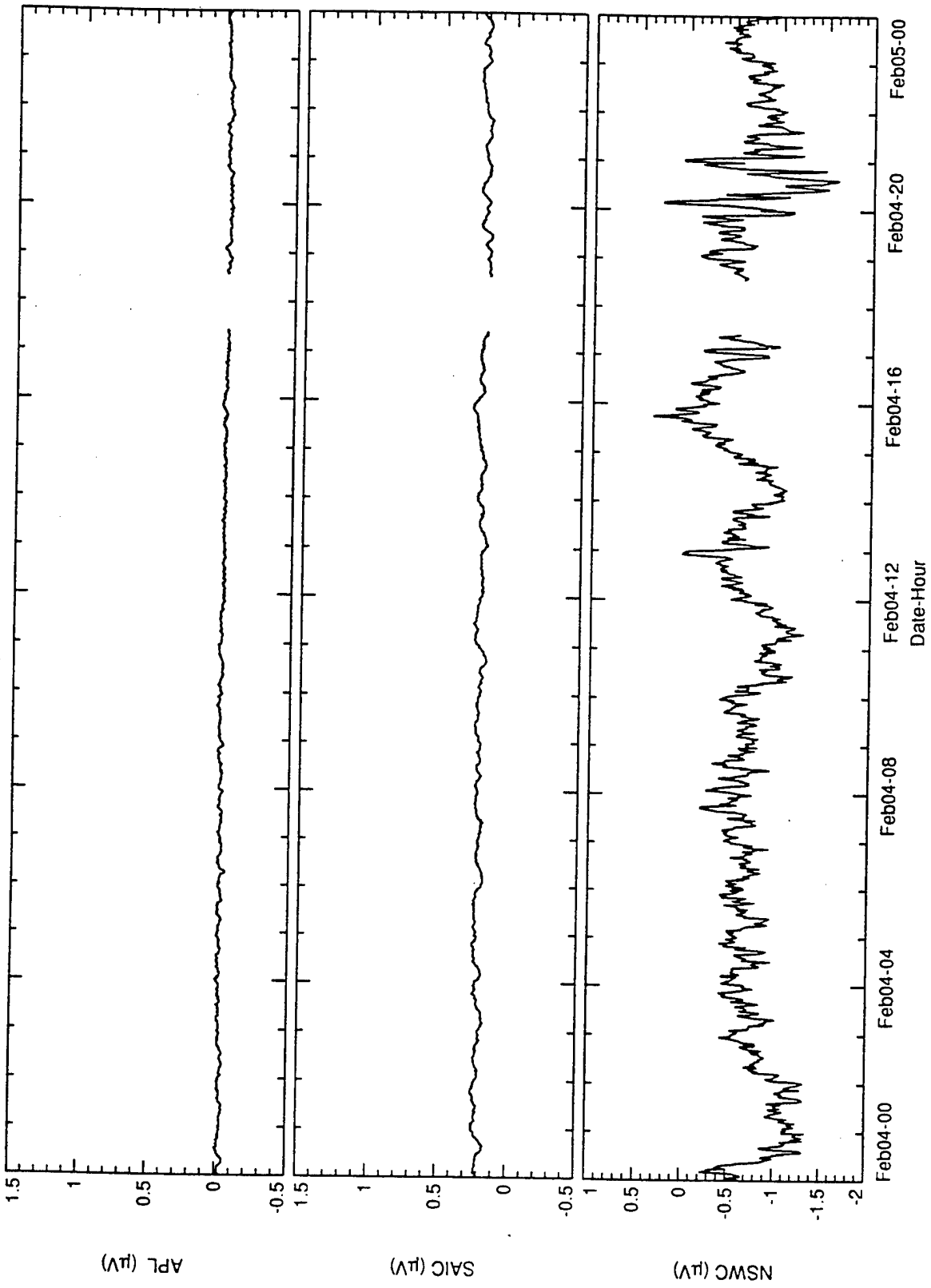

Figure C.42

Salt Water Tank Test Daily. Subsampled to about 70 s.

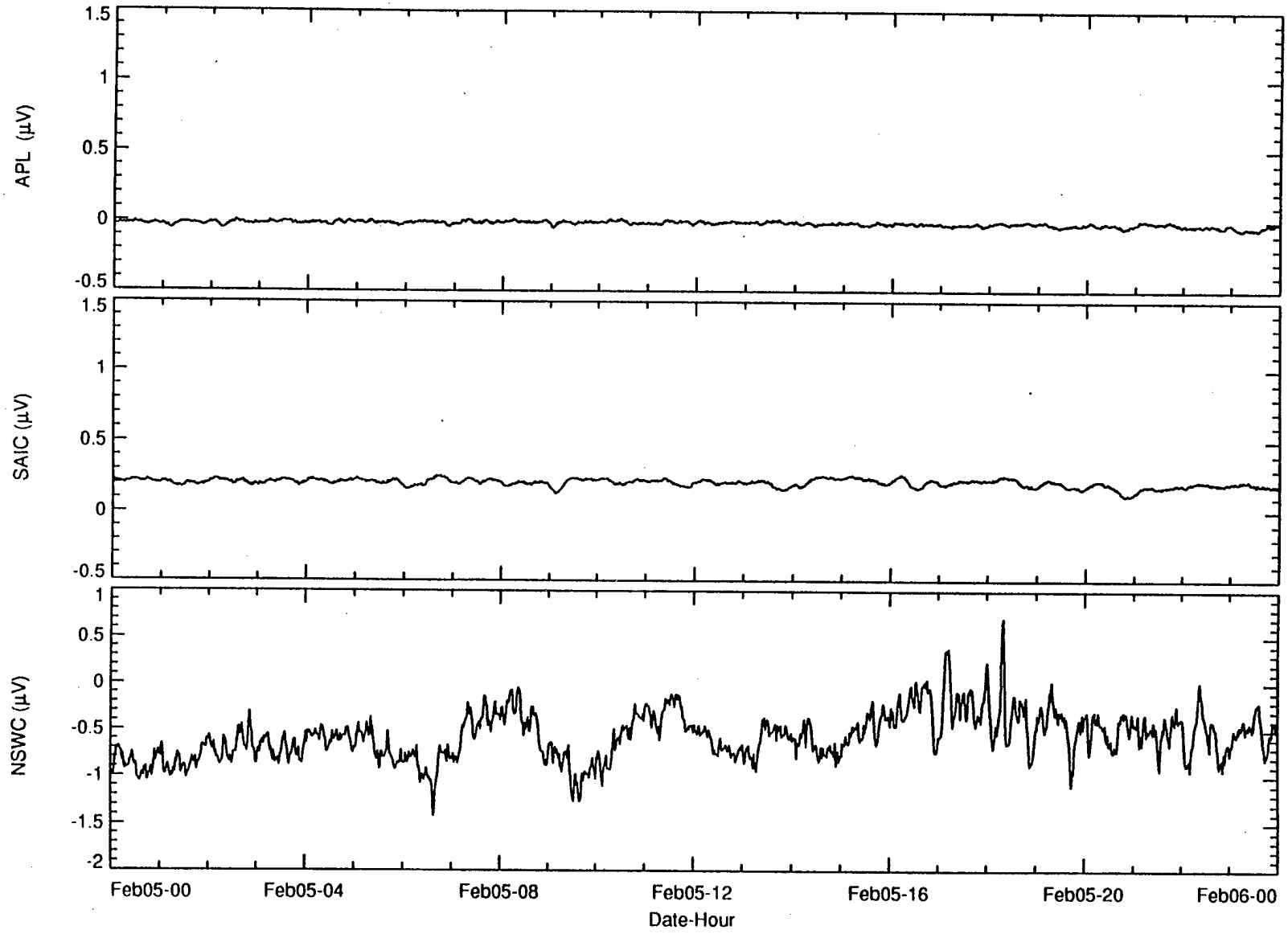

Figure C.43

Salt Water Tank Test Daily. Subsampled to about 70 s.

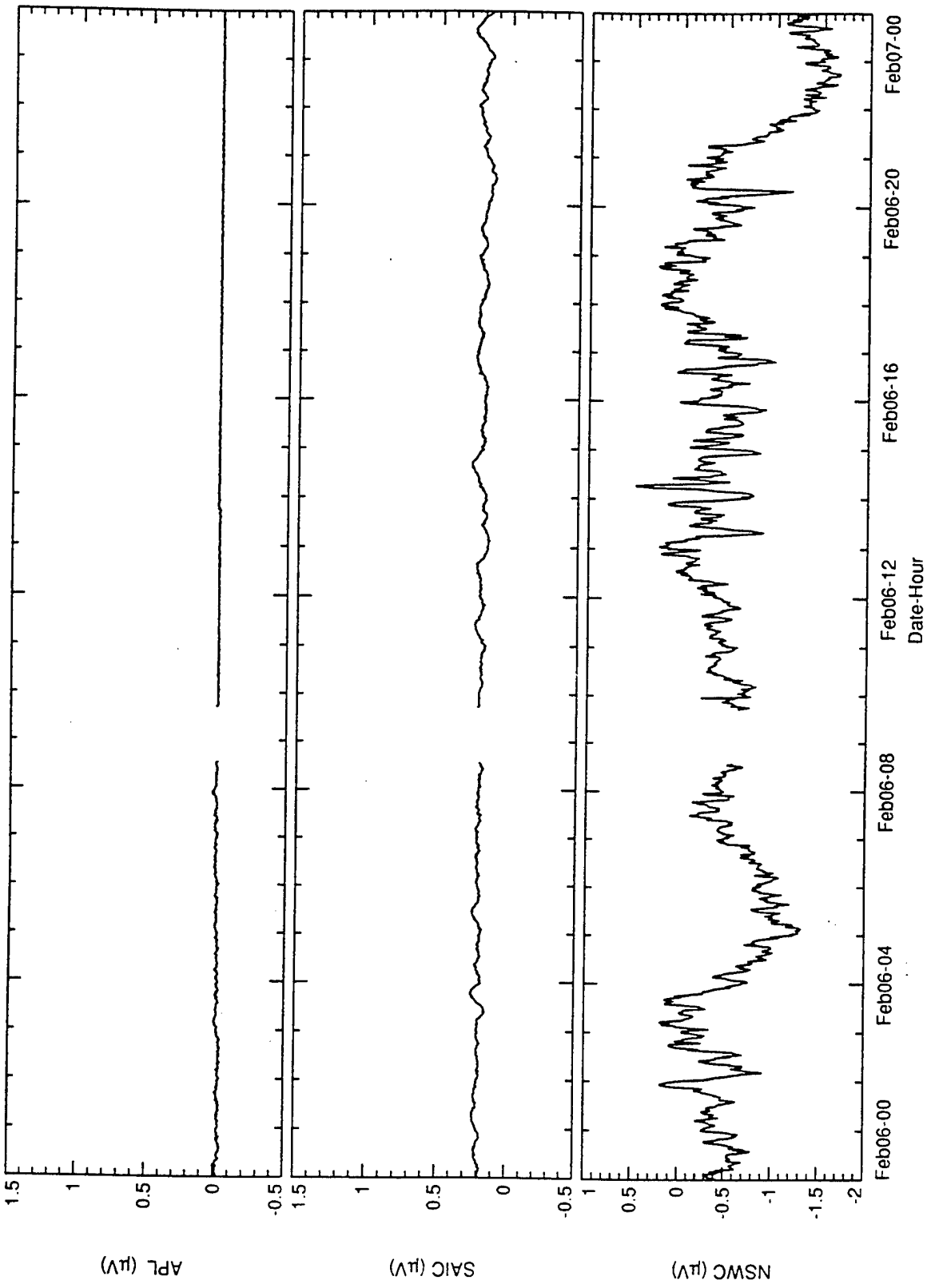

Figure C.44

Salt Water Tank Test Daily. Subsampled to about 70 s.

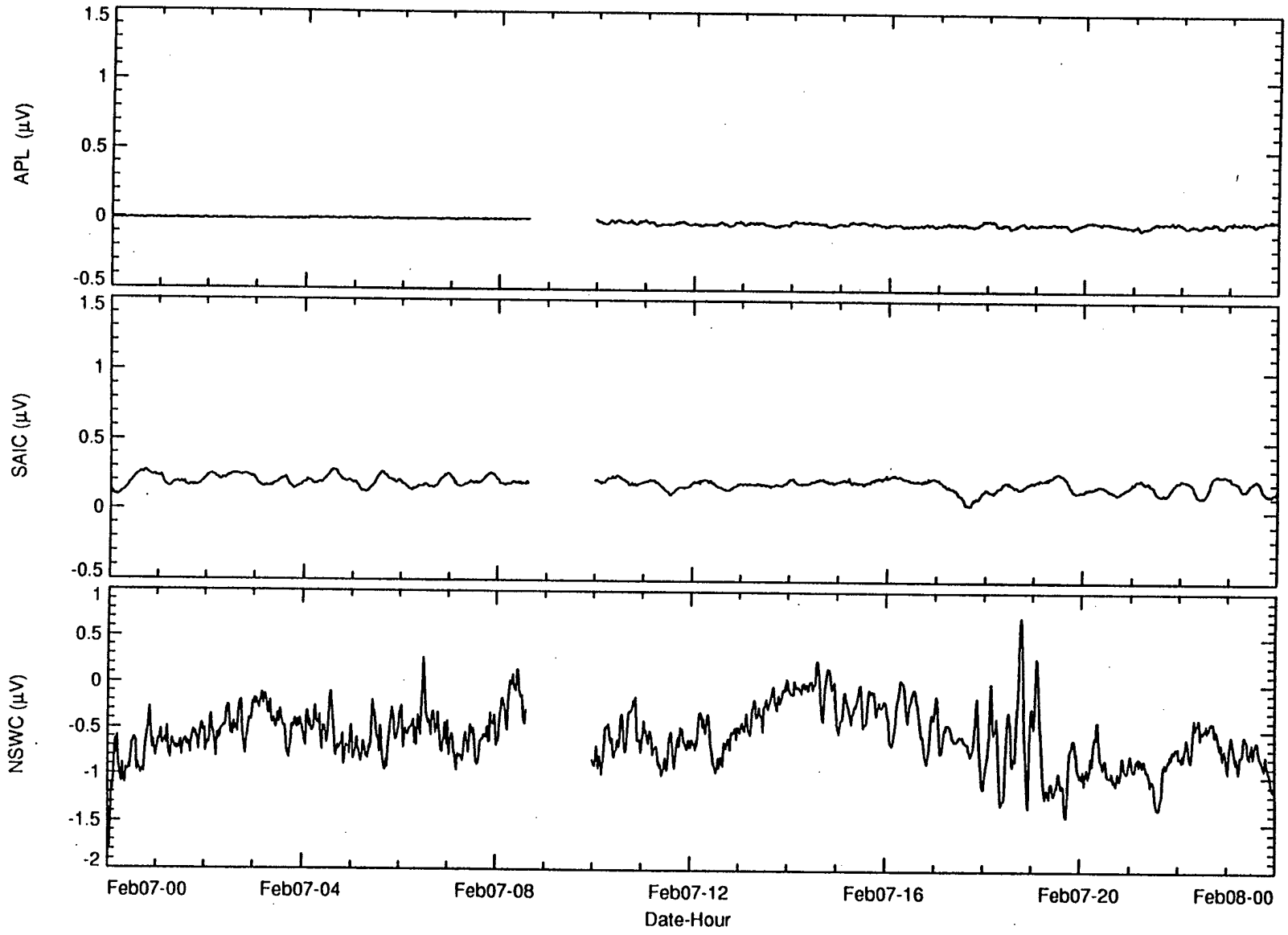

Figure C.45

Salt Water Tank Test Daily. Subsampled to about 70 s.

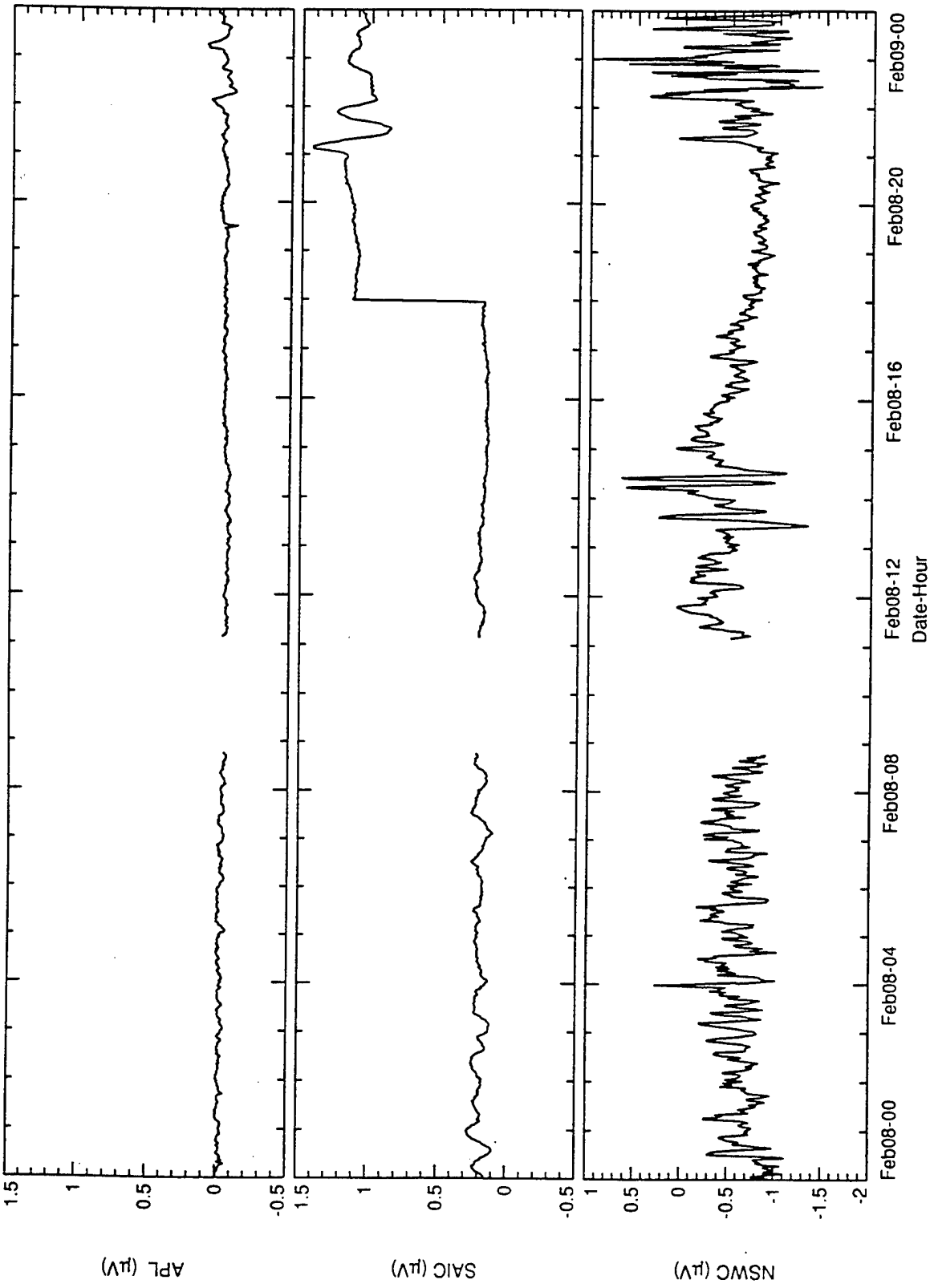

Figure C.46

Salt Water Tank Test Daily. Subsampled to about 70 s.

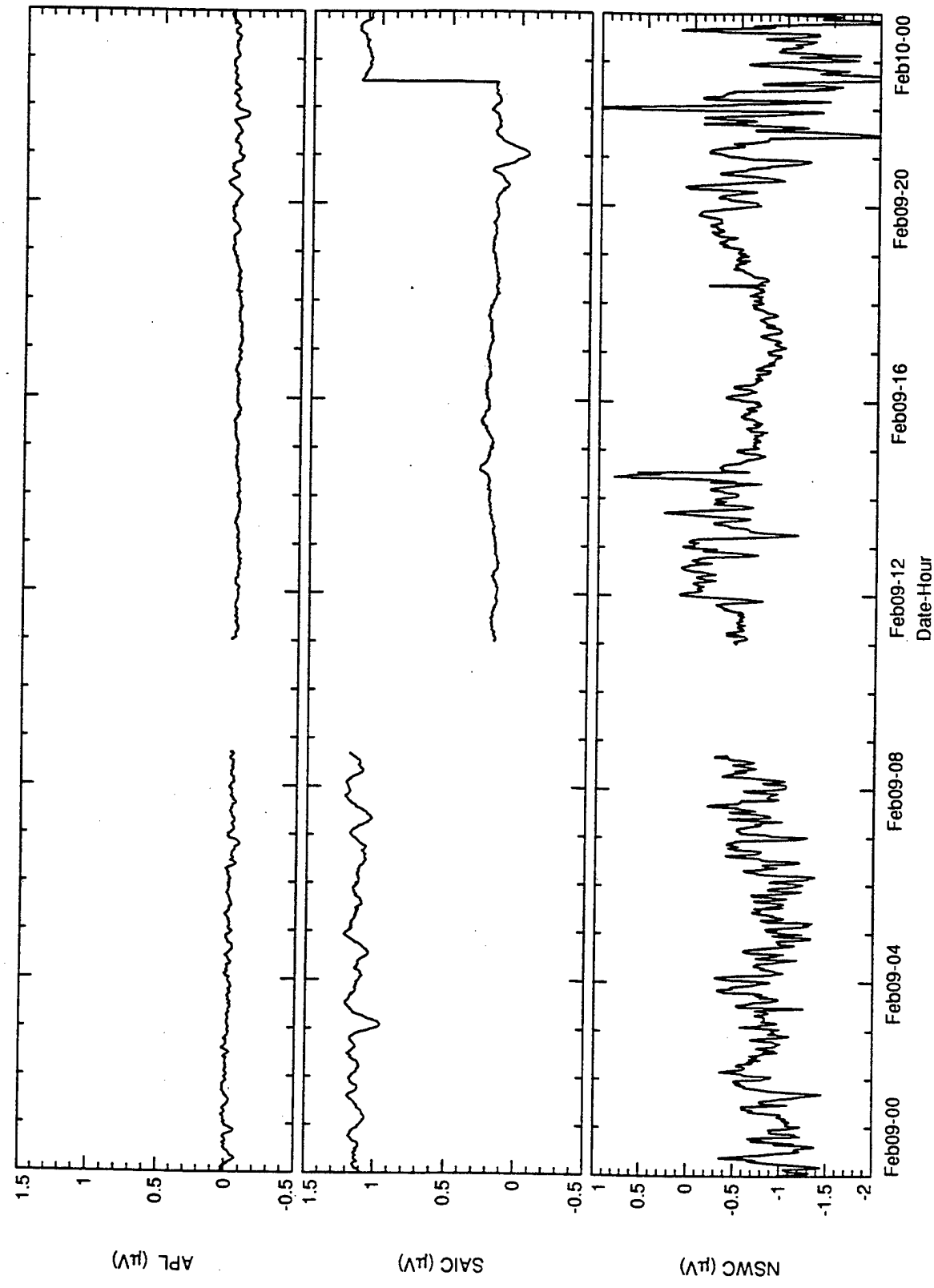

Figure C.47

Salt Water Tank Test Daily. Subsampled to about 70 s.

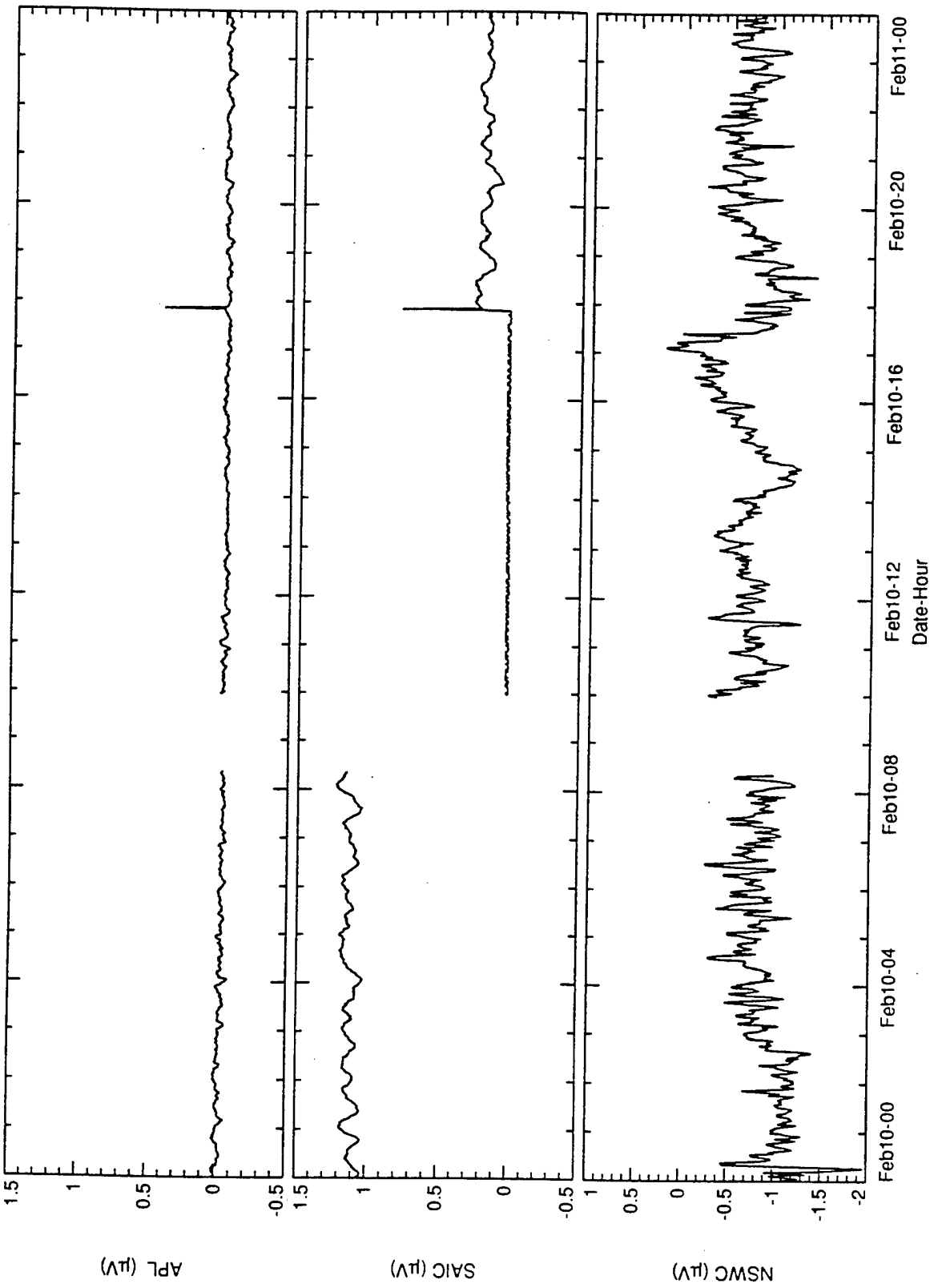

Figure C.48

Salt Water Tank Test Daily. Subsampled to about 70 s.

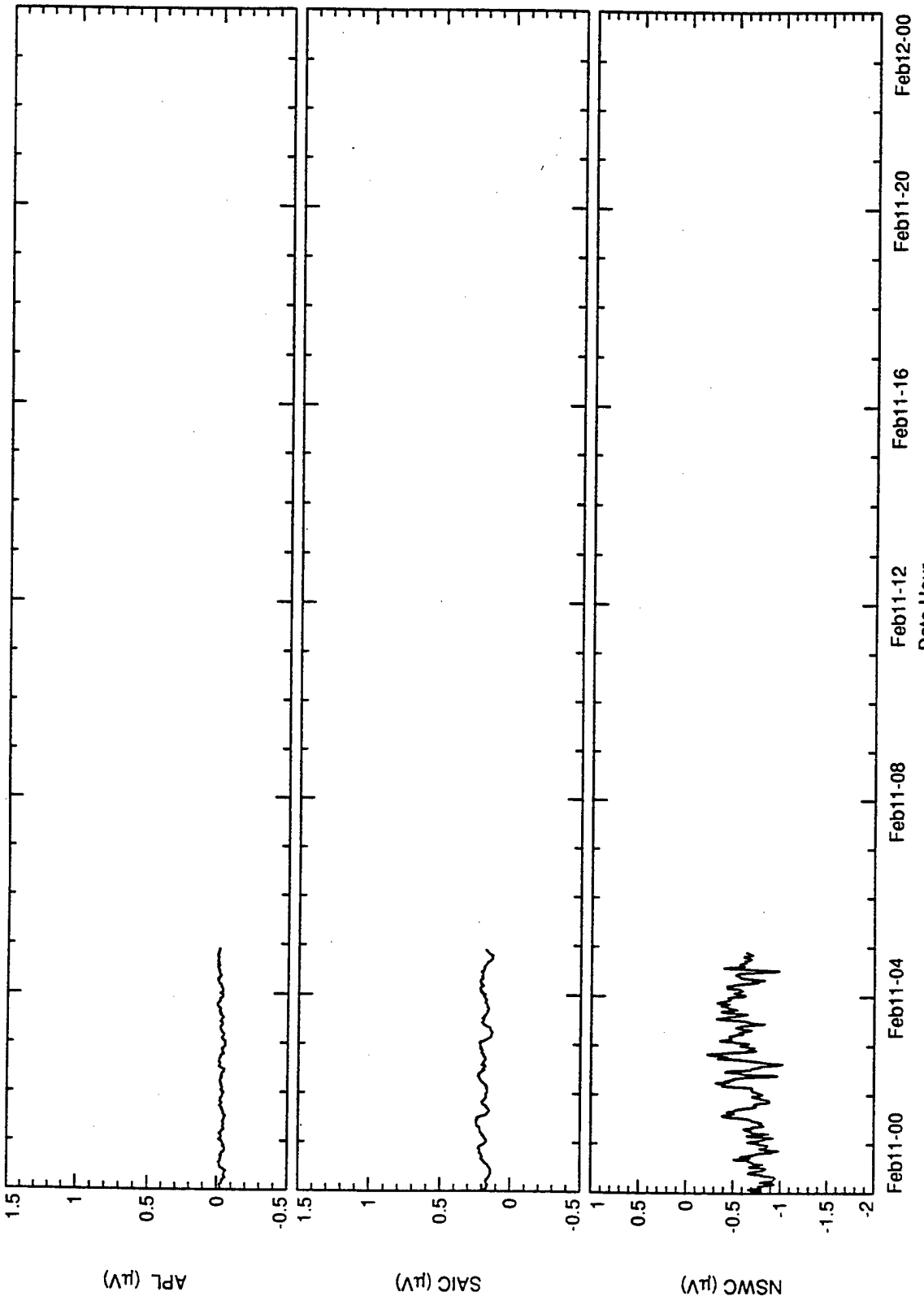

Figure C.49

Salt Water Tank Test Daily. Subsampled to about 70 s.

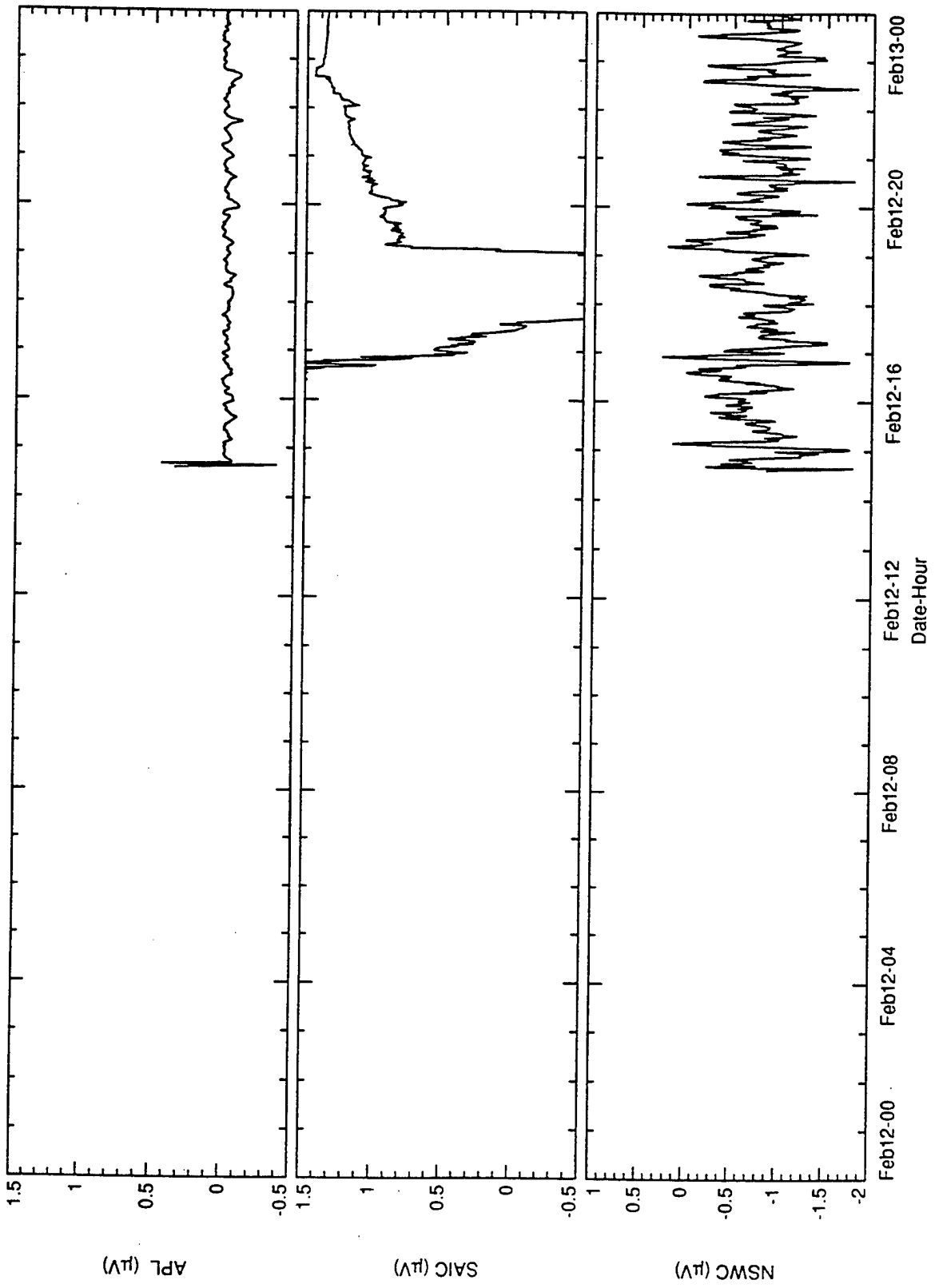

Figure C.50
Salt Water Tank Test Daily. Subsampled to about 70 s.

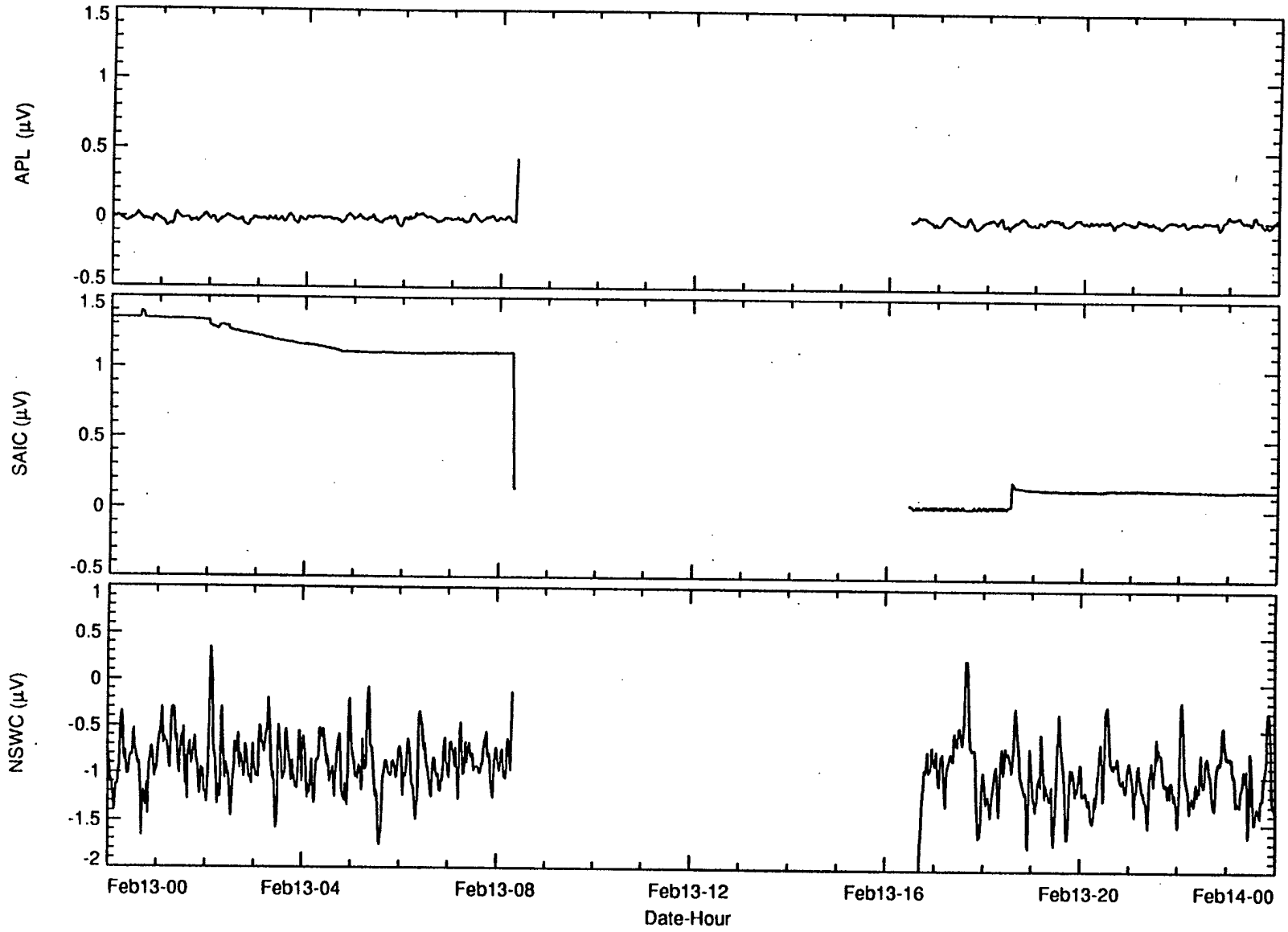

Figure C.51

Salt Water Tank Test Daily. Subsampled to about 70 s.

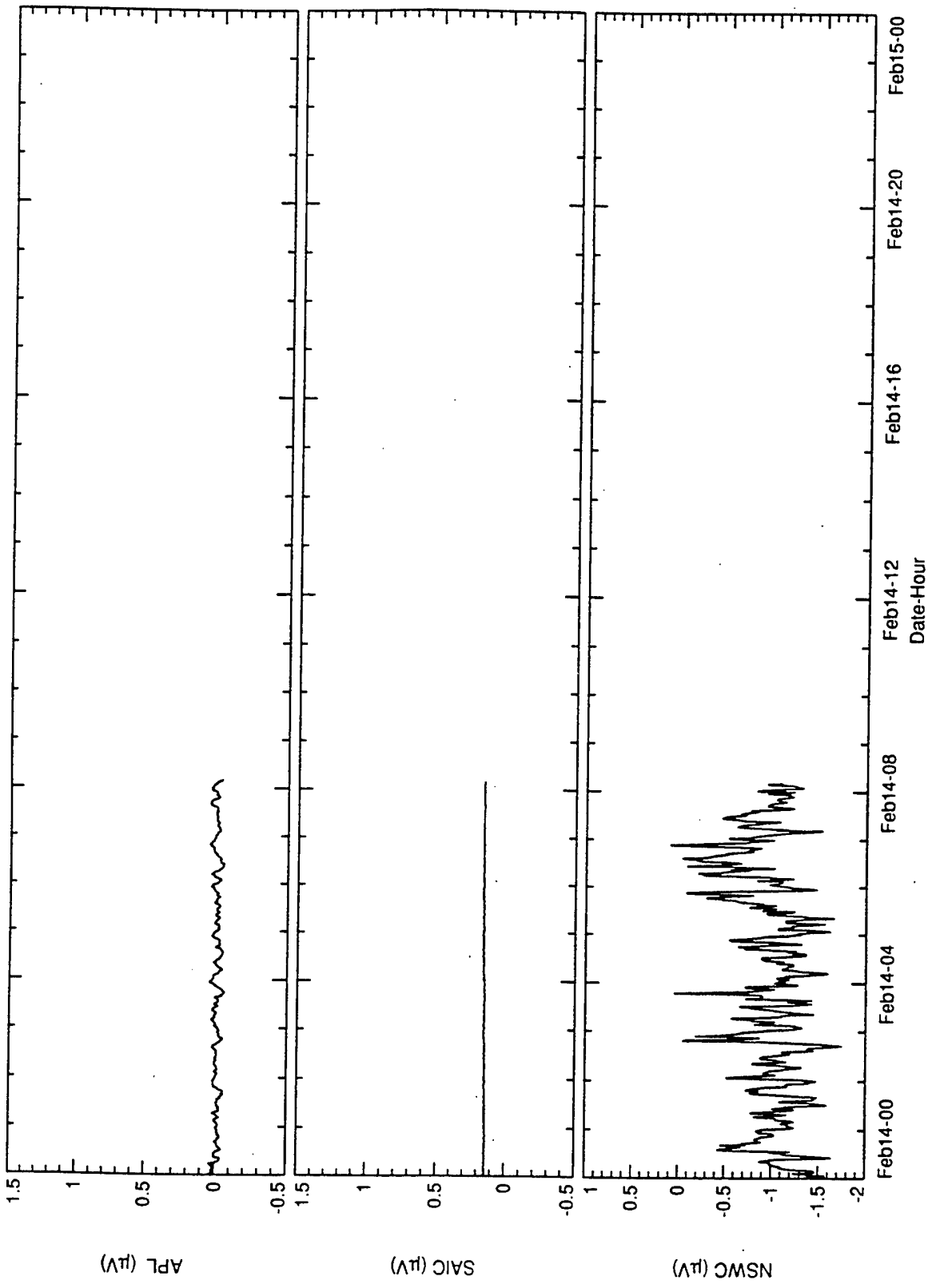

Figure C.52
Salt Water Tank Test Daily. Subsampled to about 70 s.

APPENDIX D: E-Field Sensor Spectra

Combined Spectra of the MF and HF runs for tank

Figures D.1 through D.7 show APL, NSWC, and SAIC system noise. In all figures, the 60-Hz harmonics and aliases are removed. The remaining spikes in the high-frequency spectra are from the preamplifiers used in each system. The APL system uses a chopper-stabilized preamplifier, the Keithley 1801. The chopping produces many spurious peaks in the spectra. The same is probably true of the SAIC preamplifier although the frequencies are different. The NSWC system has very few spurious responses. They may be caused the system's DC-to-DC converter which supplies isolated power to the input stages.

Spectra of all the HF tank runs overplotted on one graph per system

Figures D.8 through D.13 show the average of each day's high frequency spectra during the system tests. There are three separate graphs for the APL sensor because the APL filter was changed twice. Within each of these three groups, the spectra are similar.

The NSWC system was configured in two ways as well, and so there are two figures.

The most striking thing is that the frequencies of the spurious responses of the APL and SAIC systems are not constant.

Spectra of HF tank sampling with applied signal

The tank was driven with a current source square wave with amplitude $\pm 10\ \mu A$ and period 68 ms. The fundamental frequency is 14.71 Hz. The electric field in the tank is about $\pm 1\ \mu V\ m^{-1}$. Only odd harmonics are expected. As expected, the amplitude (square root of the variance density) of the harmonics is proportional to the reciprocal of frequency.

Figures D.14 through D.16 show the response of the APL, NSWC, and SAIC systems to the square wave excitation. These demonstrate that the frequency response of the APL and SAIC systems is nearly flat to 1 kHz. The NSWC system is shown to perform correctly past 200 Hz after adjusting the spectrum for the 17 Hz corner frequency in the NSWC amplifier.

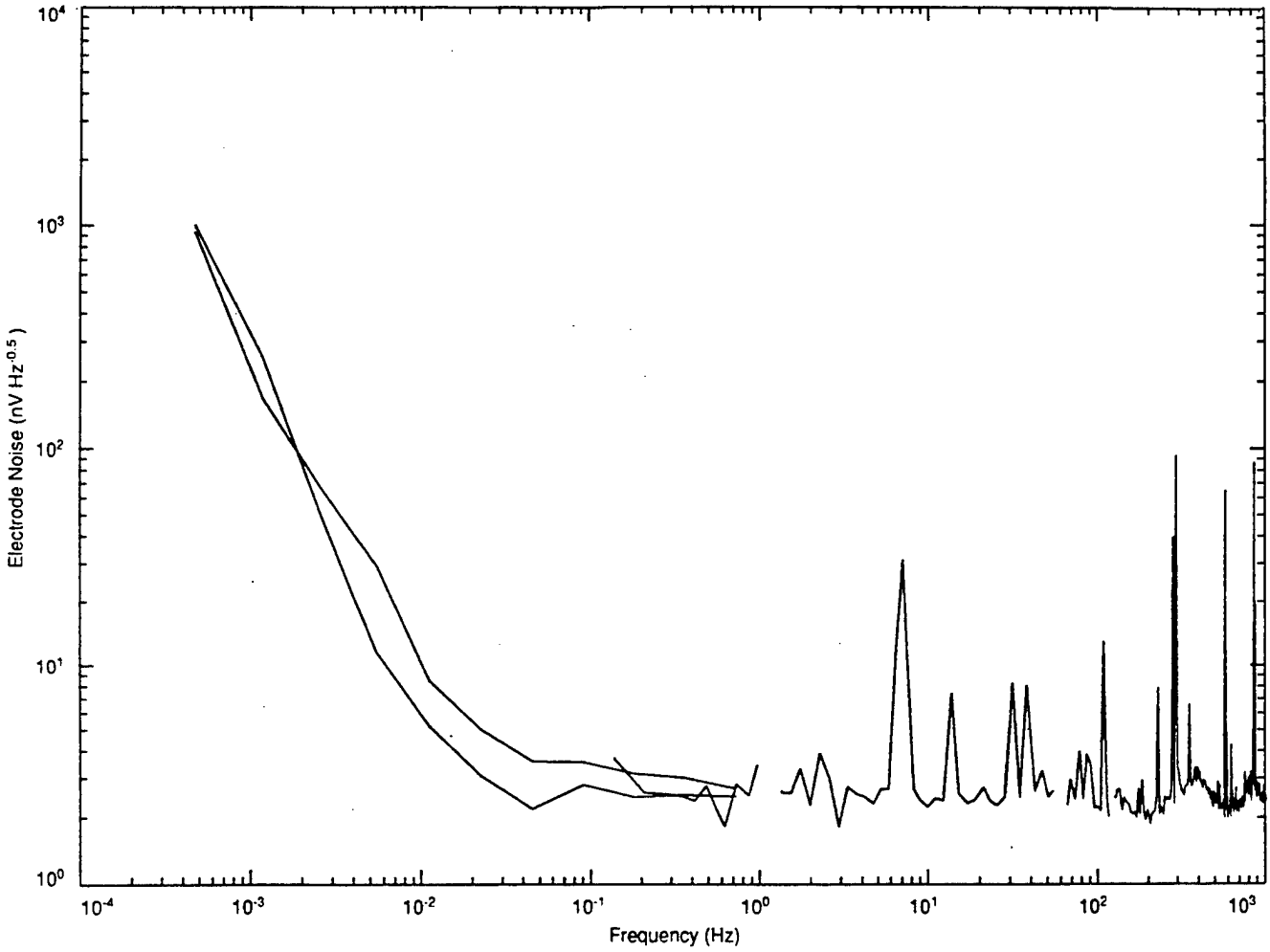

Figure D.1 Measured spectra from 0.5 mHz to 1 Hz are from APL sensors A1 and A3 while the spectrum from 0.1 Hz to 1 kHz is from sensor A3. The 60 Hz harmonics and aliases have been removed before plotting. The remaining spikes in the HF spectrum are from the Keithley 1801 preamplifier. The measurement system noise is about 2.5 nV/$\sqrt{\text{Hz}}$.

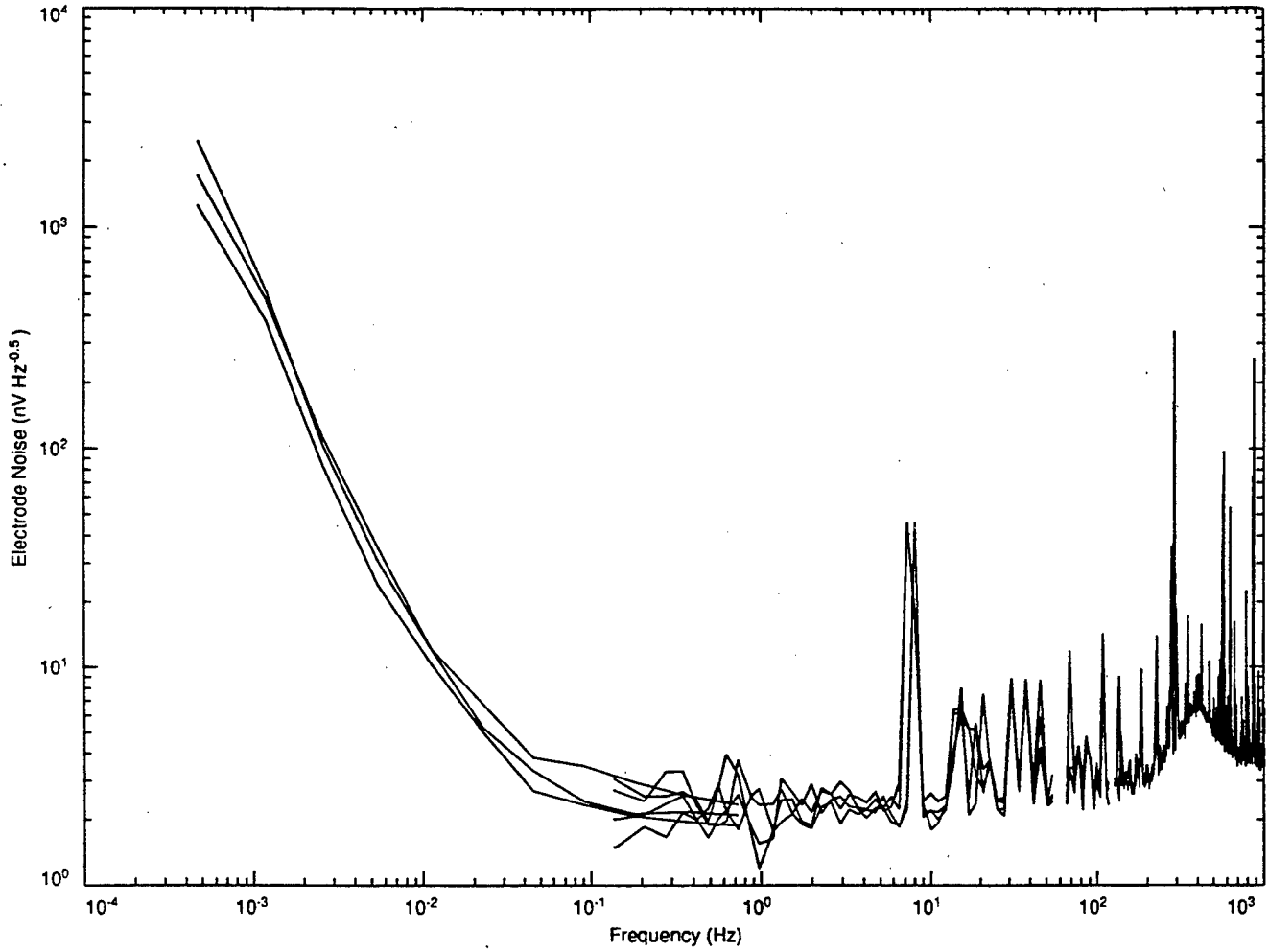

Figure D.2 Very similar to Figure D.1 but at a later date. Three APL sensors, A1, A2 and A3, are shown in the LF band. The HF spectra are from three different days using the A3 sensor. Note that the spurious responses shift in frequency between days. The bump in the HF spectra between 300 and 500 Hz is because the input filter on the 1801 preamplifier was changed to have a higher corner frequency, 1.5 kHz.

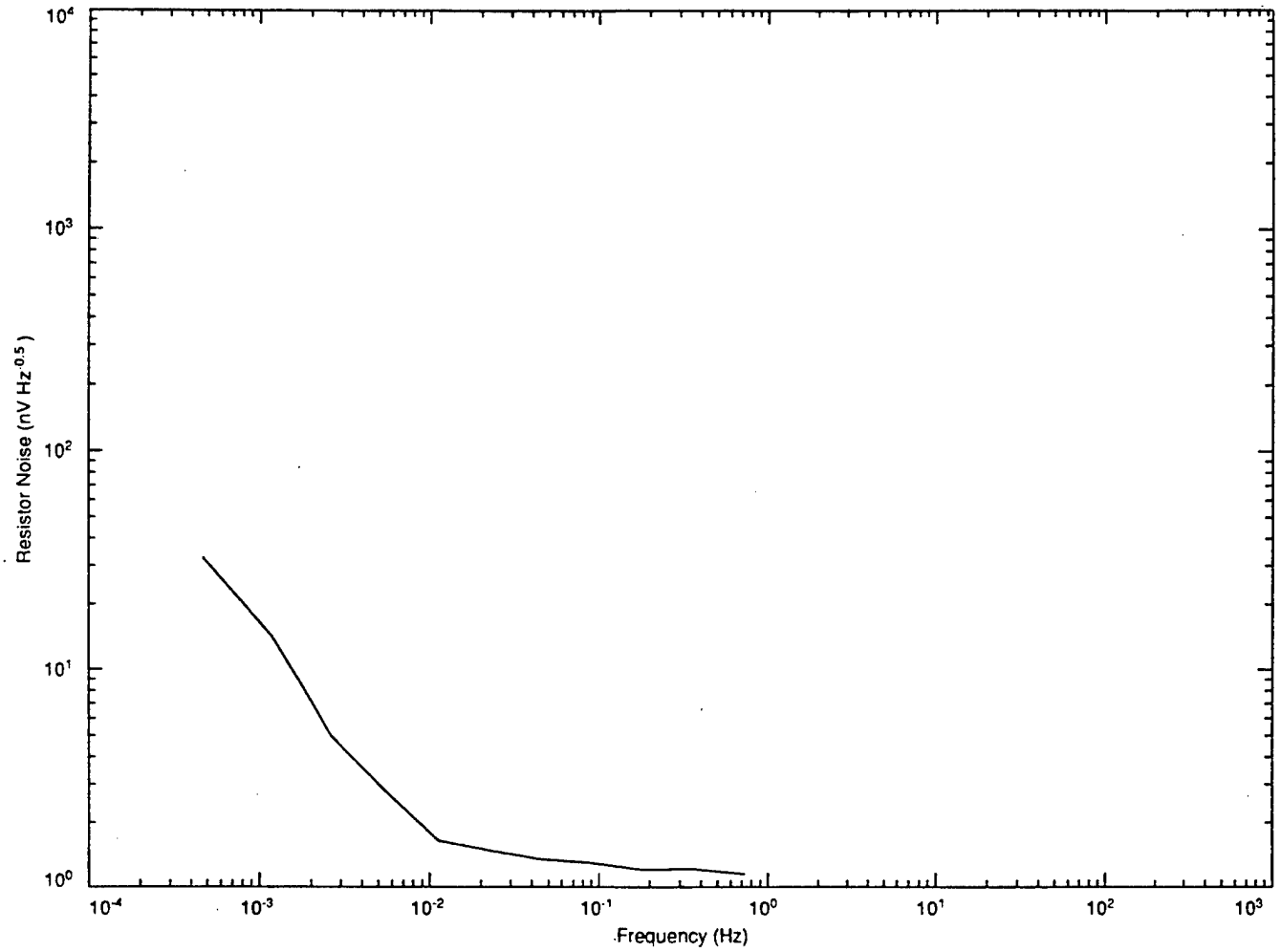

Figure D.3 The spectrum of a 20 Ω resistor is shown for reference. This demonstrates the measurement noise exclusive of electrodes. The white noise here is lower than the APL sensor white noise because the resistances were different. The APL sensors have about 100 Ω resistance in the salt bridge arms while during this measurement the 1801 preamplifier input filter used a 10 Ω resistor and a 5 μF capacitor.

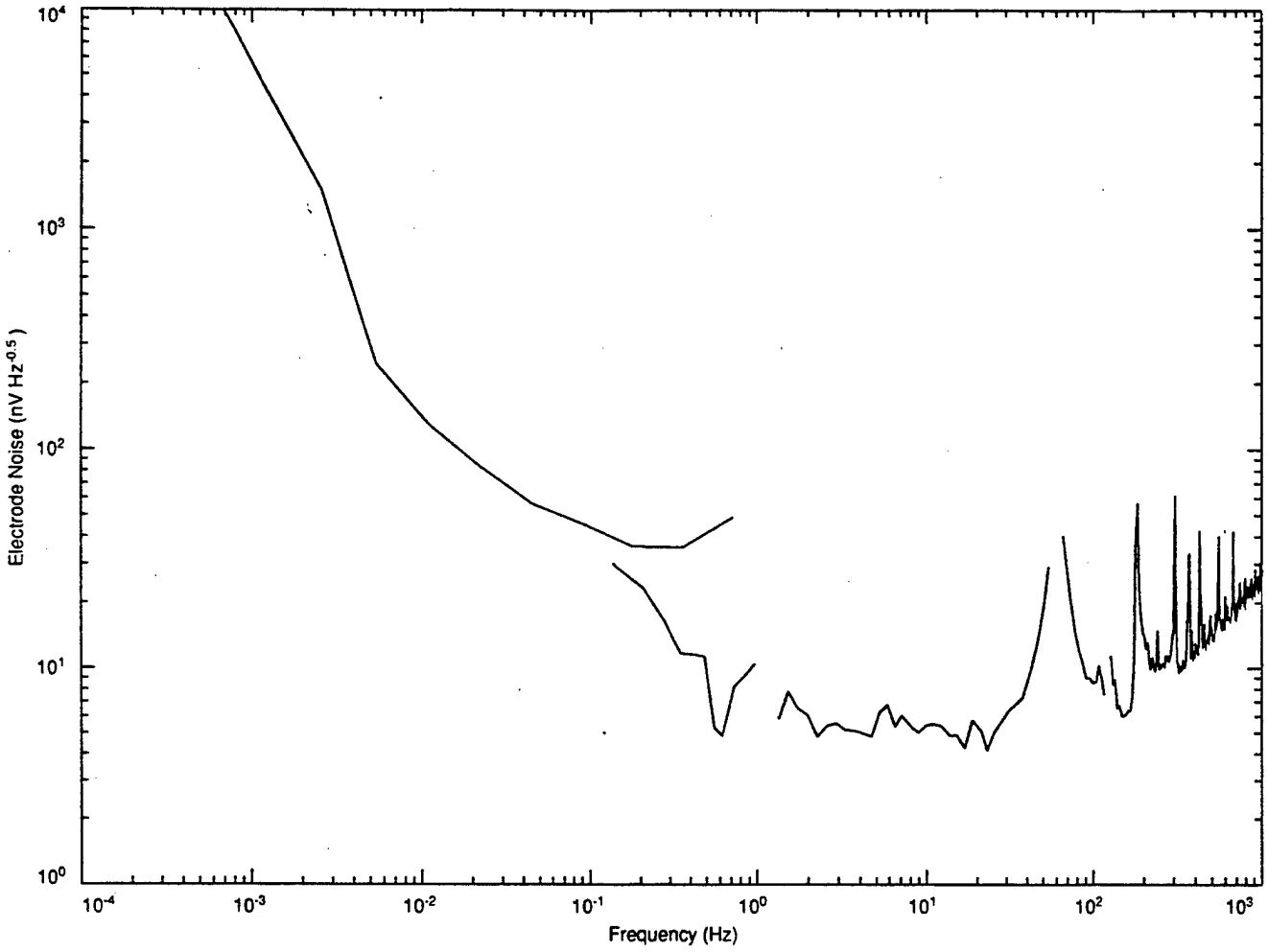

Figure D.4 A spectrum of the NSWC system. The hook in the LF spectrum from 0.03 Hz to 0.7 Hz is because of excessive 60 Hz pickup in a large loop formed in the electrode wiring. The spectral broadening at 60 Hz is also a result of the excessive 60 Hz signal. See the next figure for data with this effect cured. The rise in noise level above 100 Hz is because the HF spectrum has been adjusted to counteract the effect of the 17 Hz corner frequency of the low pass filter in the NSWC amplifier.

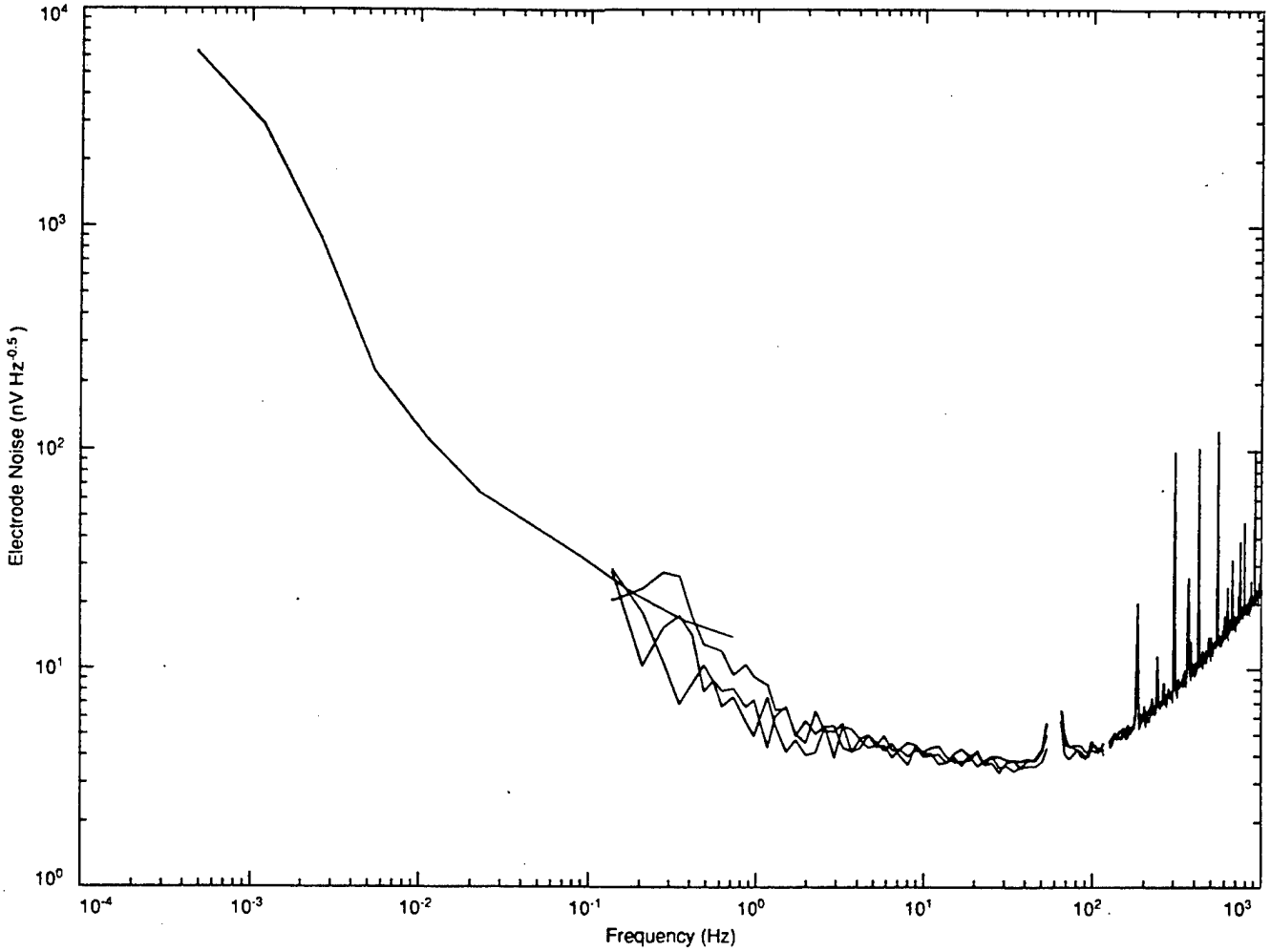

Figure D.5 A later spectrum of the NSWC system. The hook and broadening in Figure D.4 is much decreased. This was accomplished by making the loop five times smaller as well as using a 22 Hz low pass filter in the 0.5 mHz to 0.7 Hz sampling. The rise in noise level above 100 Hz is because the HF spectrum has been adjusted to counteract the effect of the 17 Hz corner frequency of the low pass filter in the NSWC amplifier.

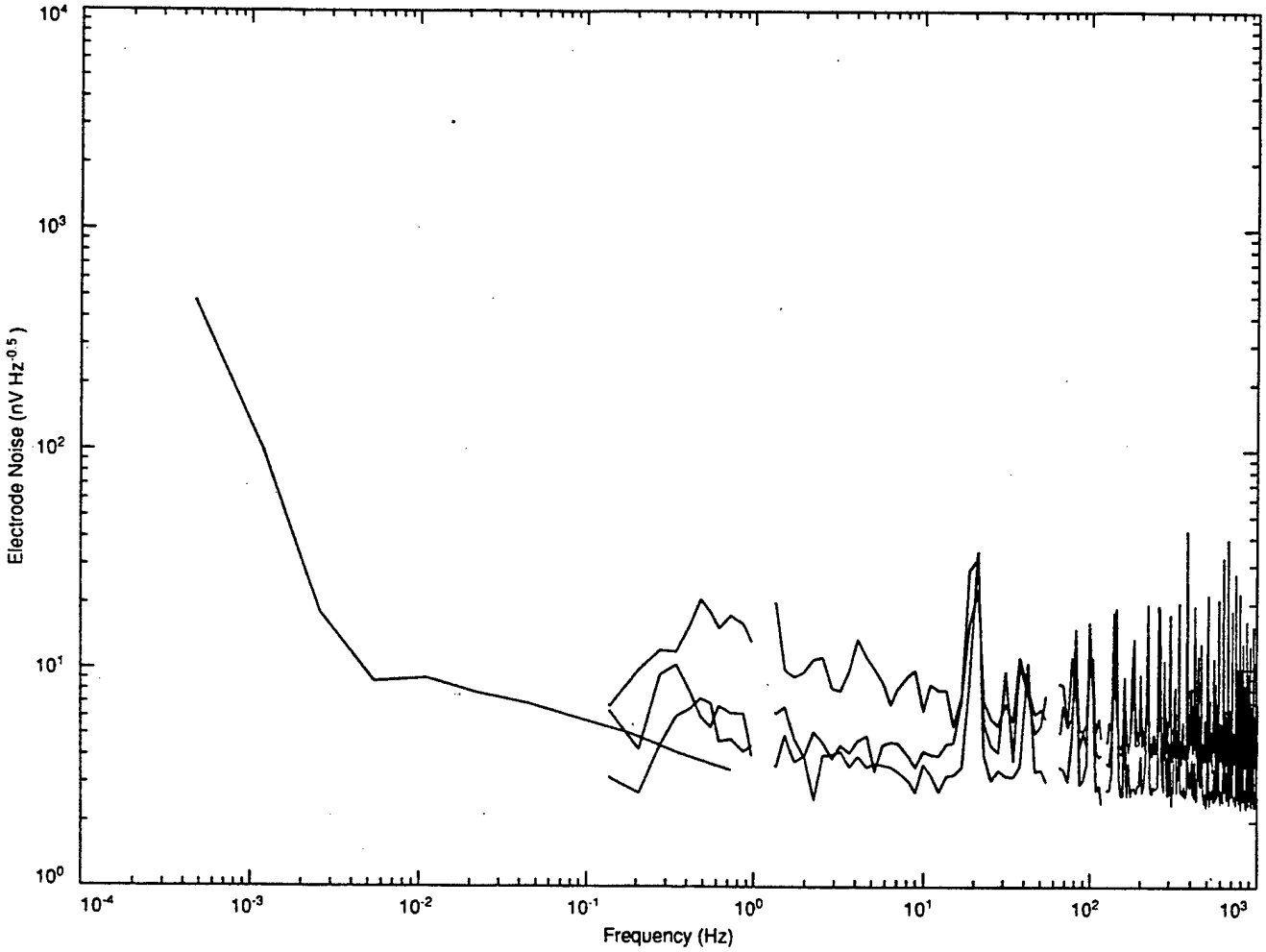

Figure D.6 Spectra from the SAIC system. The LF spectra are from samples of the SAIC system's LF output while the HF spectra are from three selected days of sampling the HF output. The HF spectra show the day to day noise level variability of the SAIC system.

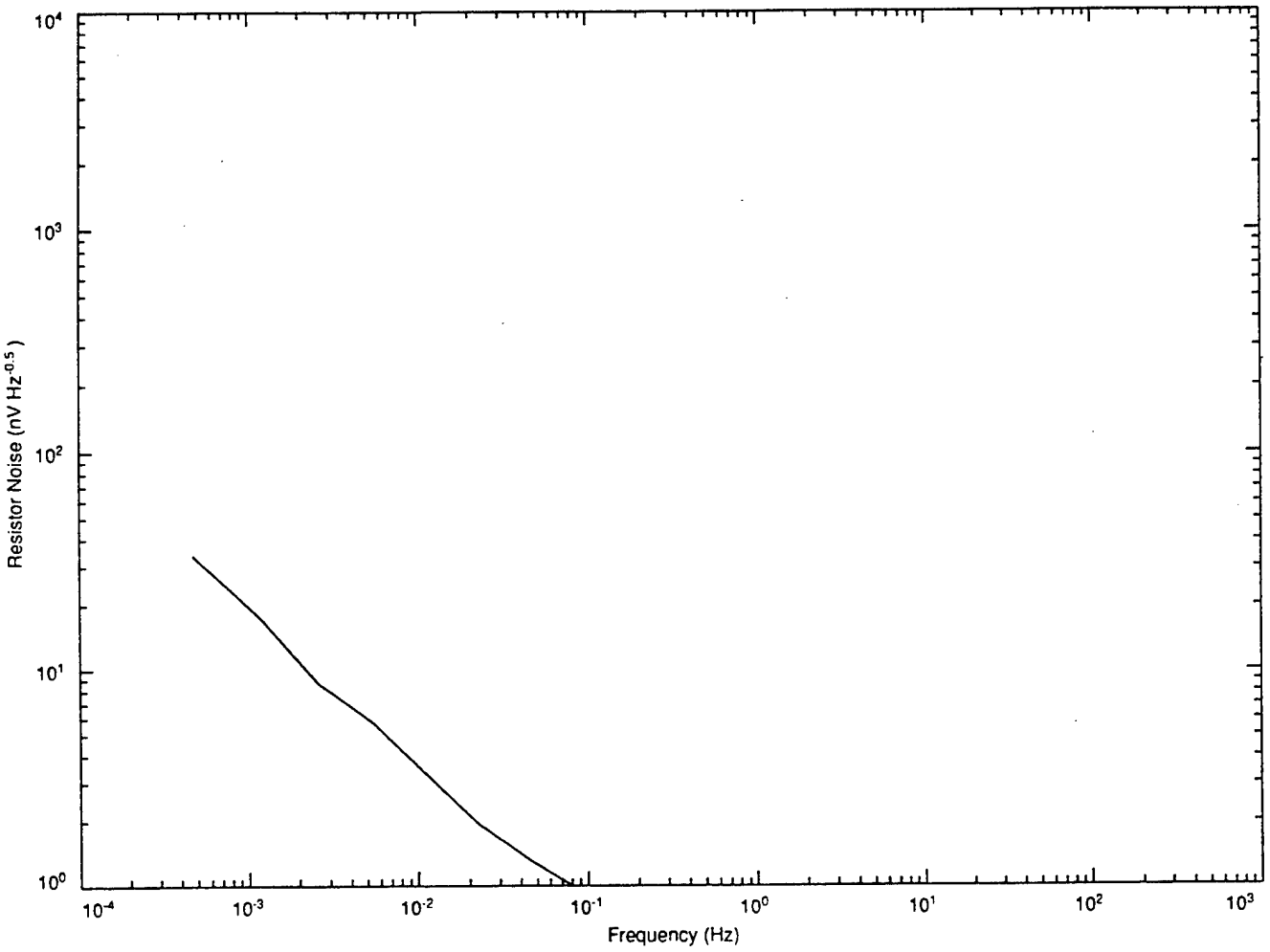

Figure D.7 Spectrum of the SAIC system with the input preamplifier turned off. All the rest of the system was operational. This shows that the measurement system was configured well enough so that the input preamplifier was the dominating influence in Figure D.6.

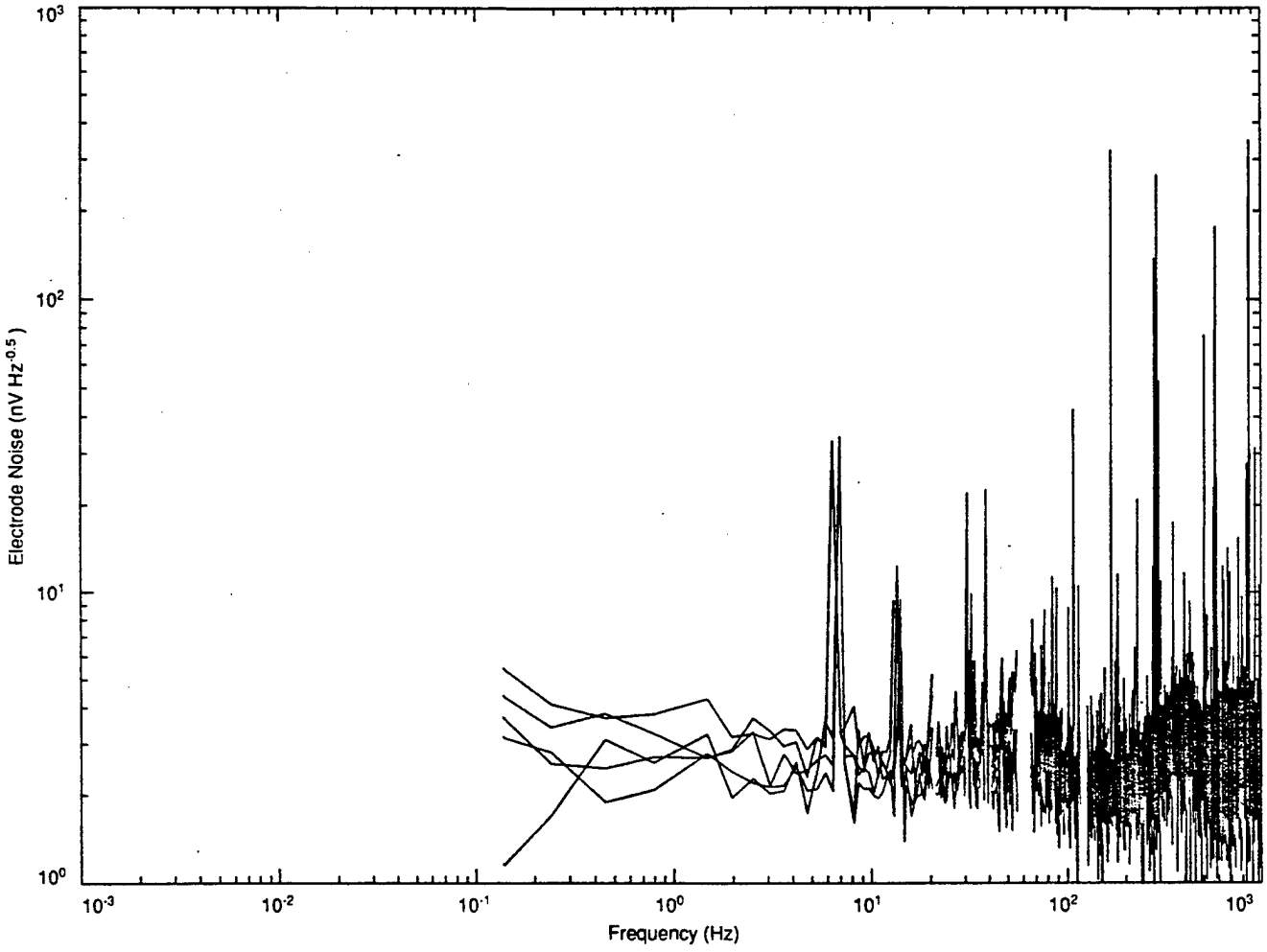

Figure D.8 High frequency spectra of APL sensor A3 in the salt water tank with a 100 Ω and 5 μF RC low pass filter on the input of the Keithley 1801 preamplifier. The corner frequency of the filter allowing for the salt bridge resistance is about 160 Hz. Note the many spurious responses of the Keithley 1801 preamplifier.

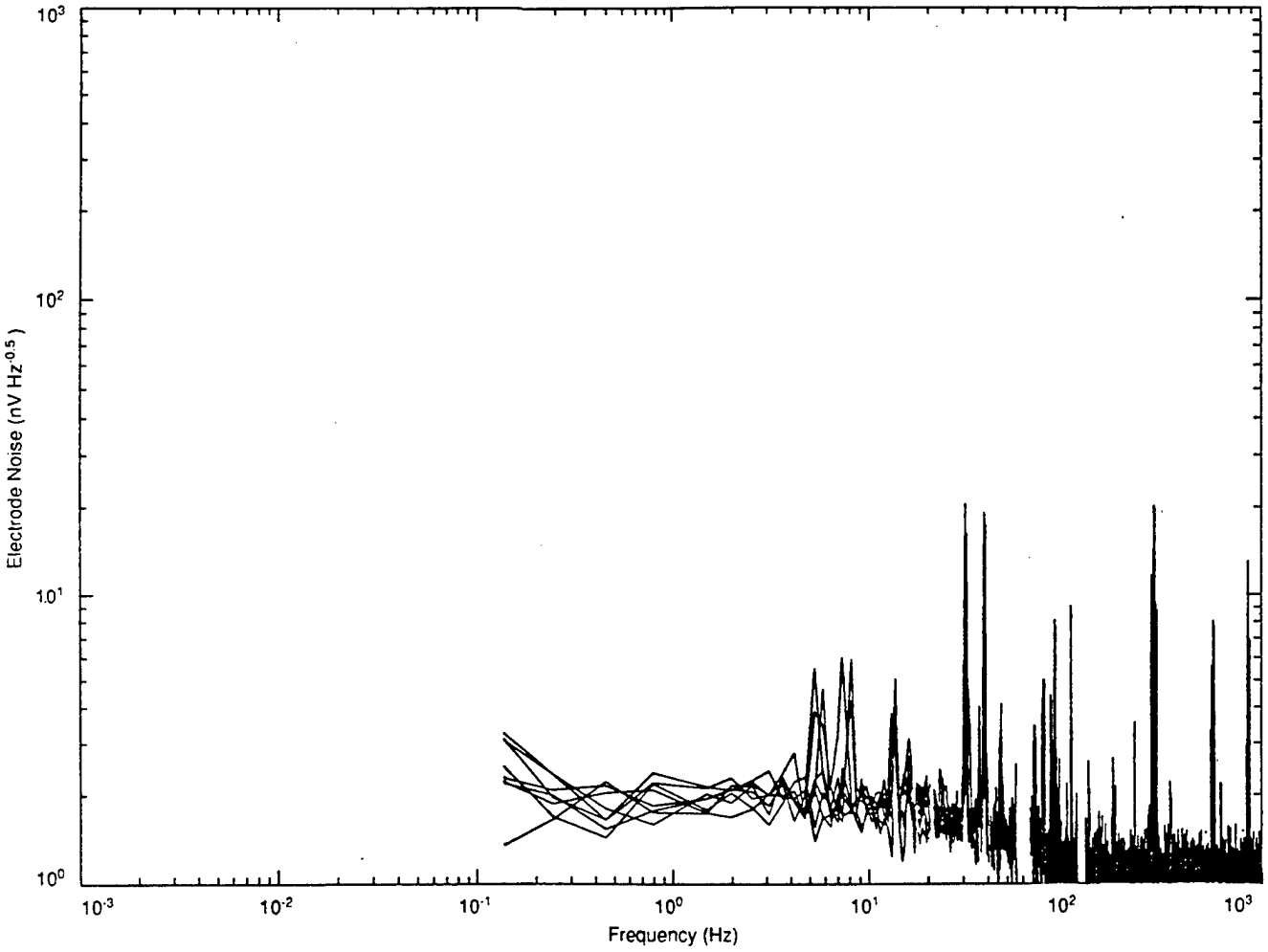

Figure D.9 High frequency spectra of APL sensor A3 in the salt water tank with a 20 Ω and 5 μF RC low pass filter on the input of the Keithley 1801 preamplifier. The corner frequency of the filter allowing for the salt bridge resistance is about 265 Hz. However, because of a programming error, the actual corner frequency, 32 Hz, is controlled by the 1801 preamplifier. Note the many spurious responses of the Keithley 1801 preamplifier.

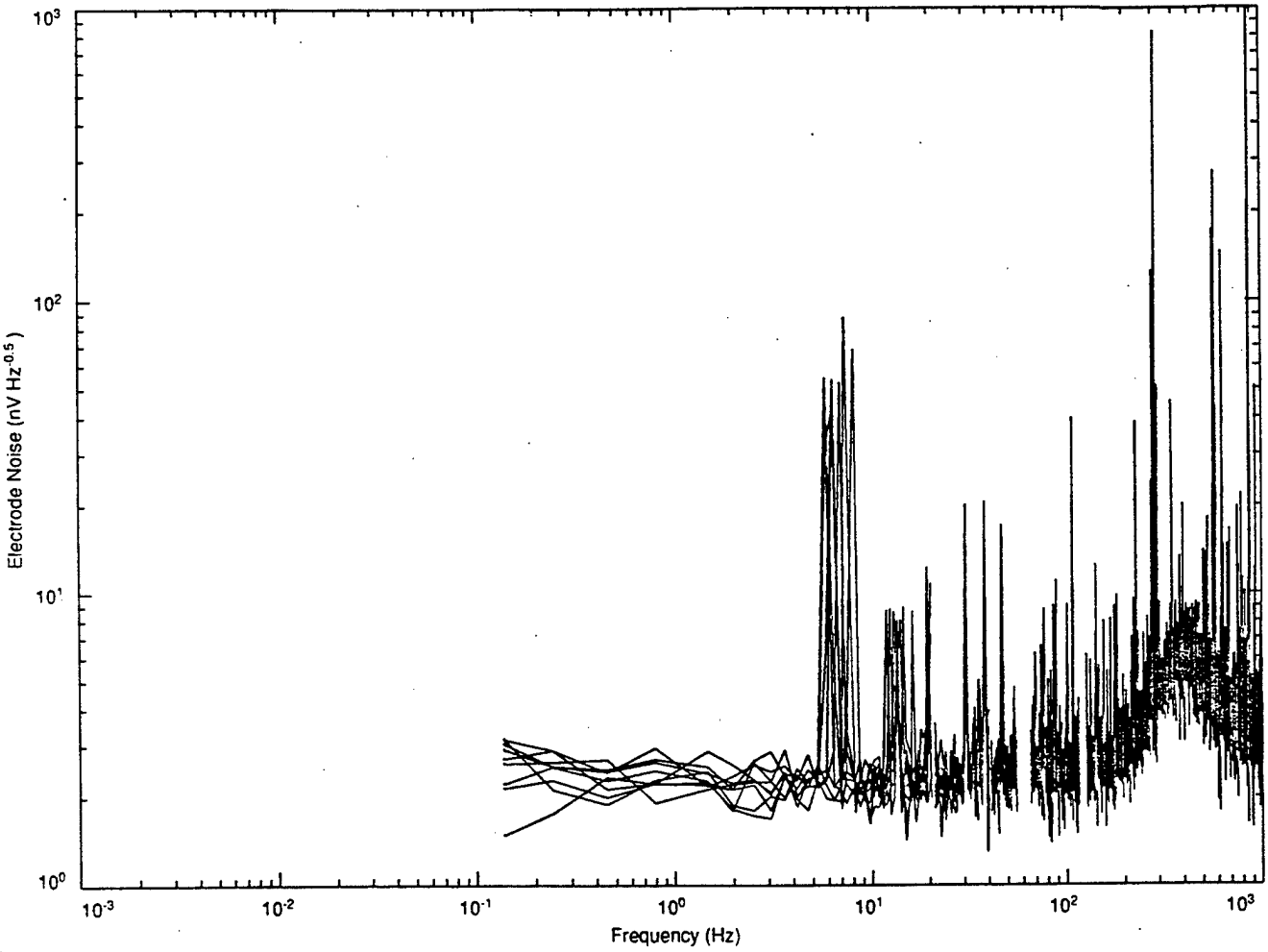

Figure D.10 High frequency spectra of APL sensor A3 in the salt water tank with a 20 Ω and 0.5 μF RC low pass filter on the input of the Keithley 1801 preamplifier. The corner frequency of the filter allowing for the salt bridge resistance is about 2650 Hz. Note the rise in the noise level between 300 and 500 Hz. This is an artifact of the 1801 preamplifier. Note the many spurious responses of the Keithley 1801 preamplifier.

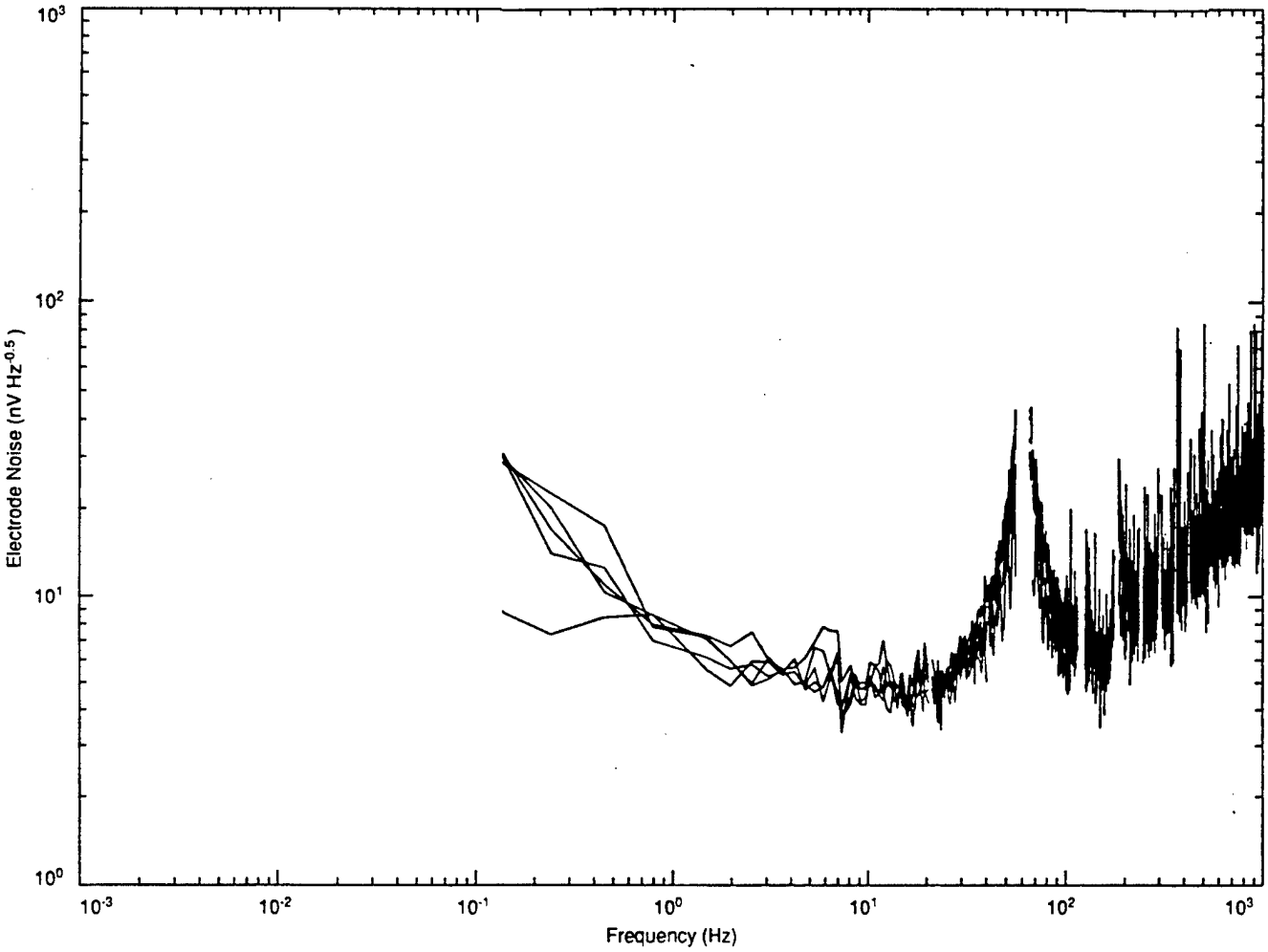

Figure D.11 High frequency spectra of NSWC system in the salt water tank. Note the wide skirts around the 60 Hz power line frequency. This was caused by a large loop in the electrode connections. The rise in noise level above 100 Hz is caused by increasing the plotted spectral values to allow for the 17 Hz corner frequency in the NSWC amplifier.

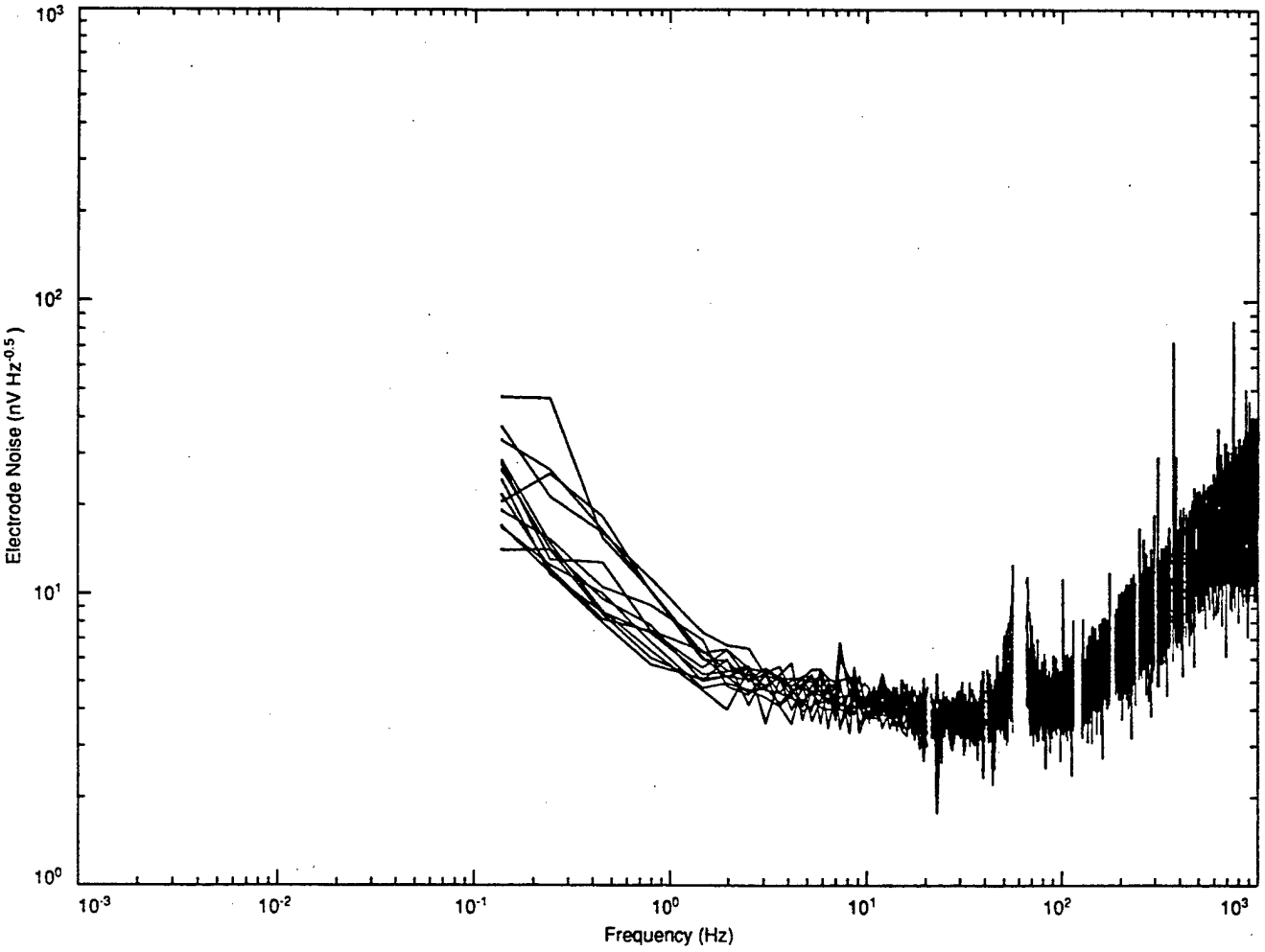

Figure D.12 High frequency spectra of NSWC system in the salt water tank. The loop in the electrode connections is reduced. Note the narrow skirts around the 60 Hz power line frequency as compared to the previous figure, D.11. The rise in noise level above 100 Hz is caused by increasing the plotted spectral values to allow for the 17 Hz corner frequency in the NSWC amplifier. Occasionally there is a spurious response at about 7 Hz. The NSWC system is very clean up to about 220 Hz. Its output drops into the noise at about 100 Hz because of the 17 Hz amplifier corner frequency.

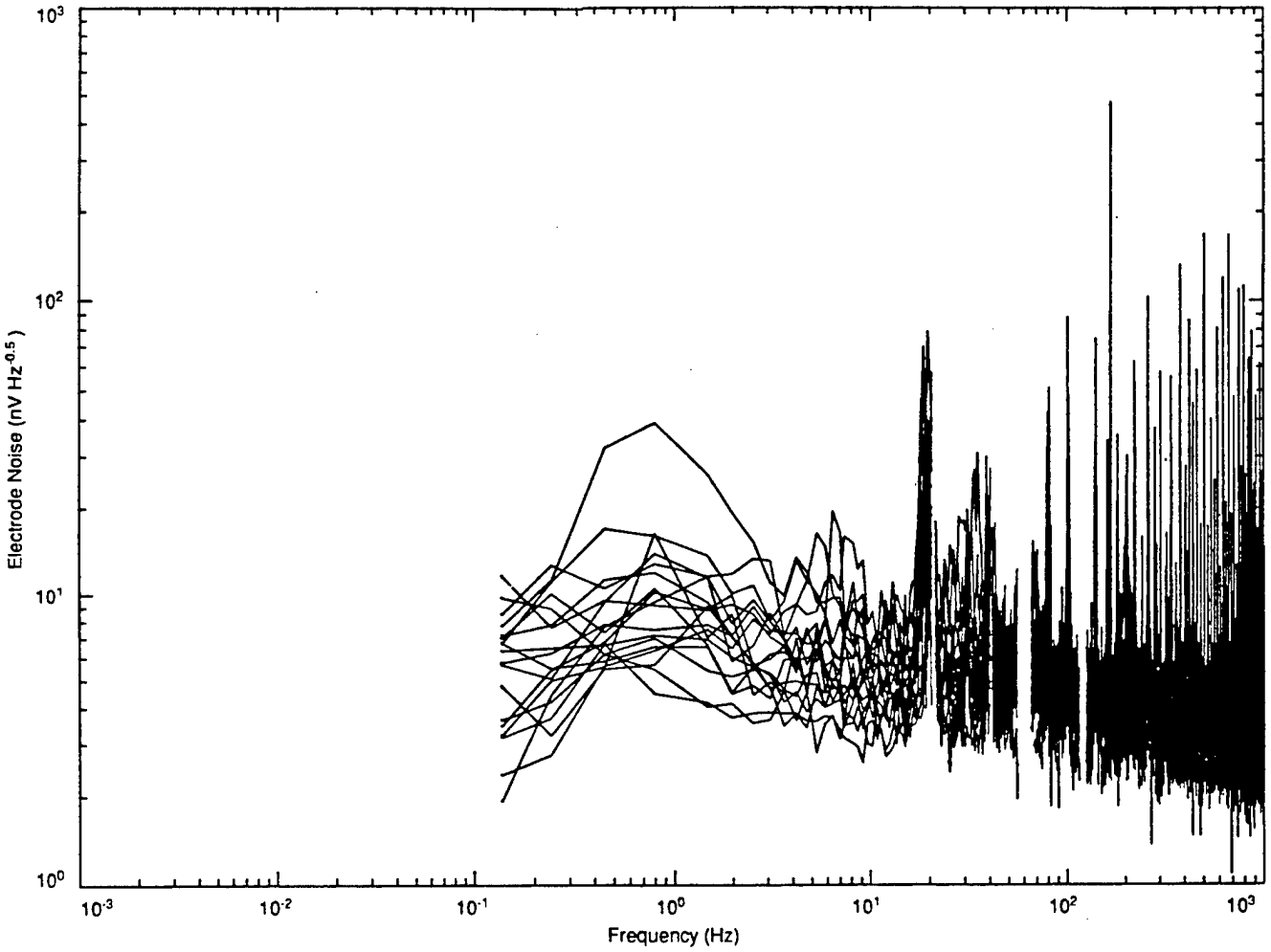

Figure D.13 High frequency spectra of SAIC system in the salt water tank. The high variability of the spectral levels was because the SAIC amplifier was unstable. Note that there is sometimes a spurious response at 7 Hz. The spurious response at 18 to 20 Hz is always present. There are other spurious responses near 30 Hz. There are many spurious responses above 60 Hz.

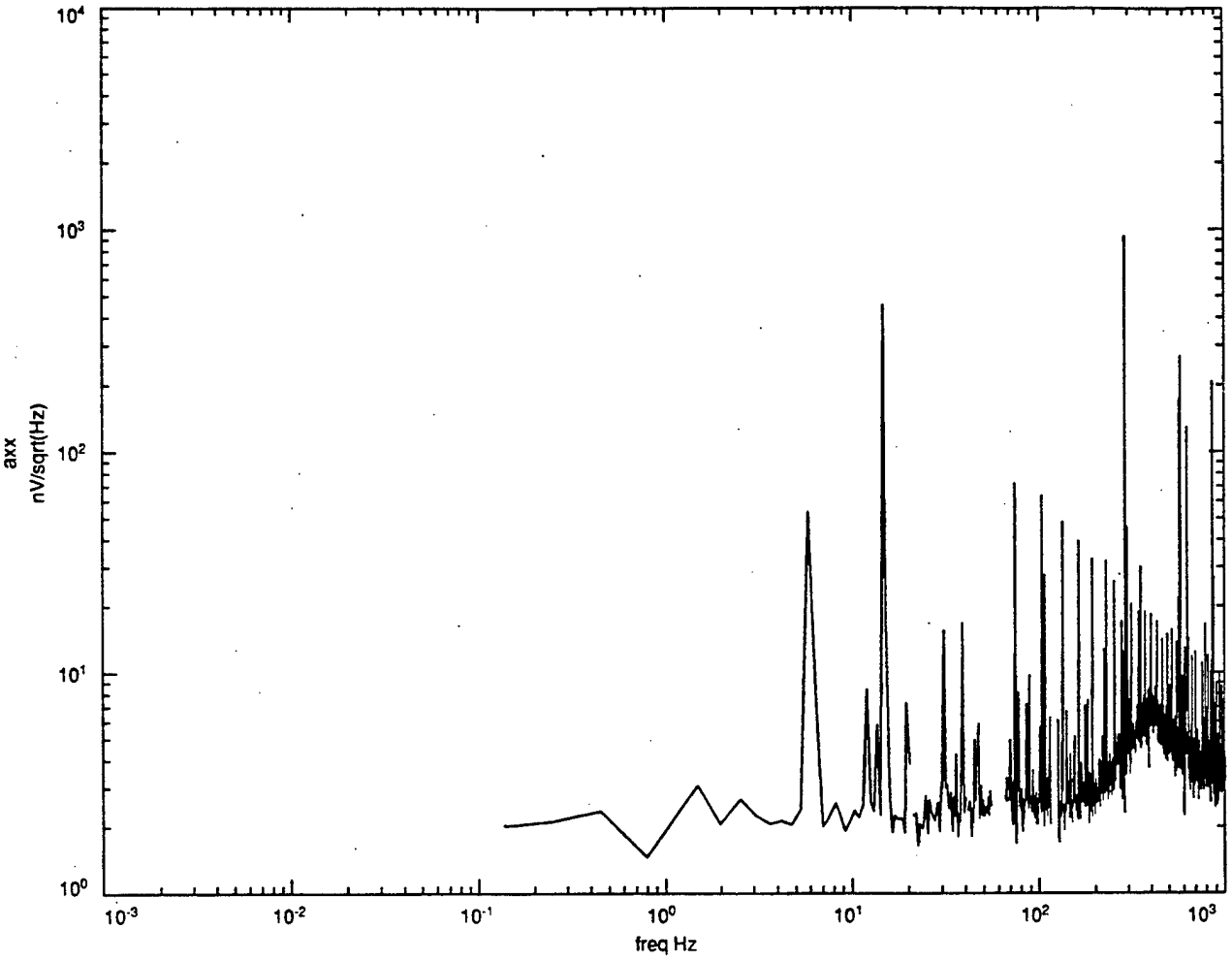

Figure D.14 Spectrum of the response of the APL sensor with Keithley 1801 preamplifier to a square wave signal in the tank. The fundamental frequency is 14.71 Hz. As expected, only odd harmonics appear. The amplitudes fall off as expected with frequency up to 1 kHz. The lump in the spectrum between 300 and 500 Hz is an artifact of the 1801 preamplifier

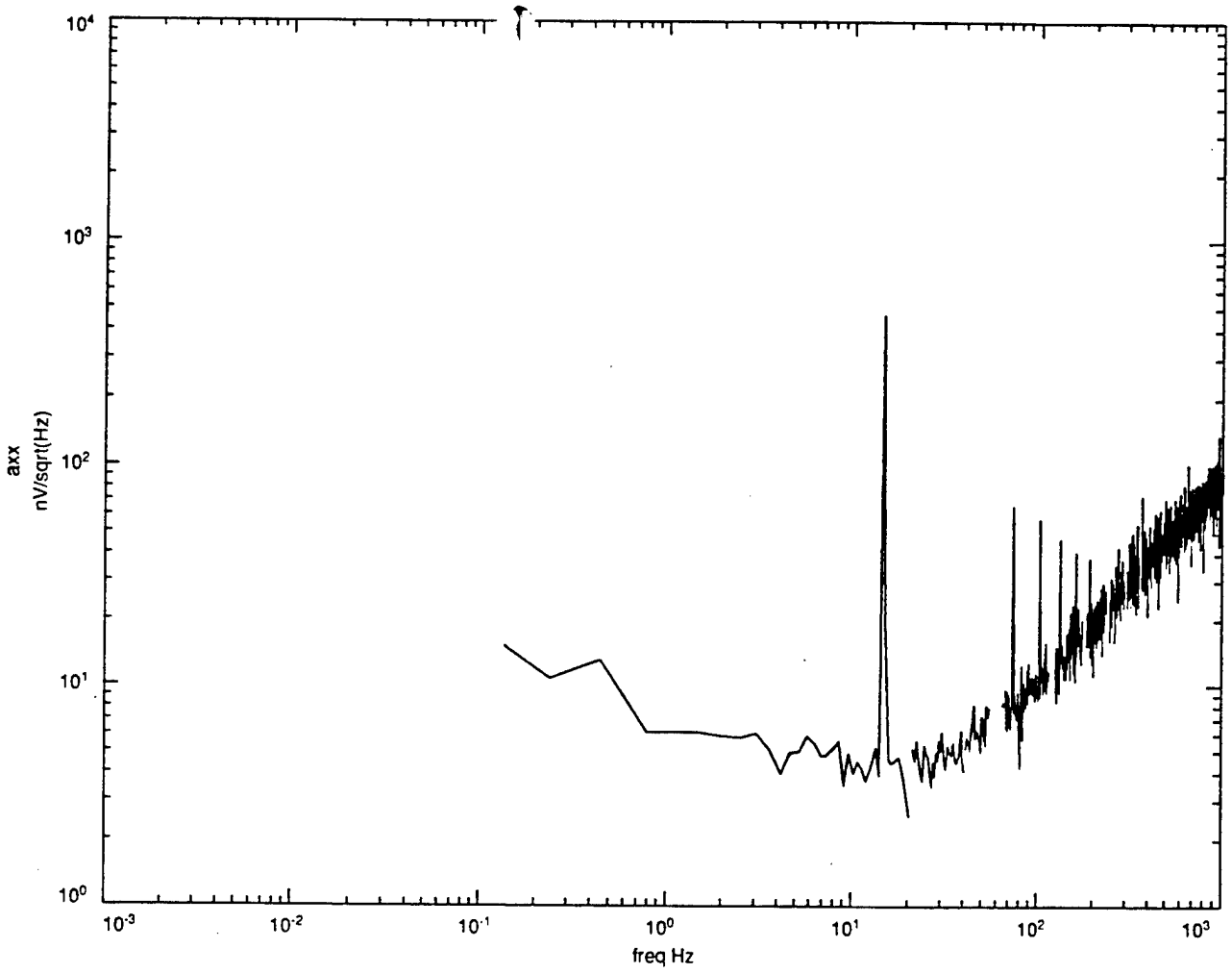

Figure D.15 Spectrum of the response of the NSWC system preamplifier to a square wave signal in the tank. The fundamental frequency is 14.71 Hz. As expected, only odd harmonics appear. The smooth comb of the amplitudes of the harmonics has the correct roll off for the impressed square wave. The harmonic signals fall below the noise above about 200 Hz. The spectrum has been adjusted to counteract the 17 Hz corner frequency of the NSWC amplifier.

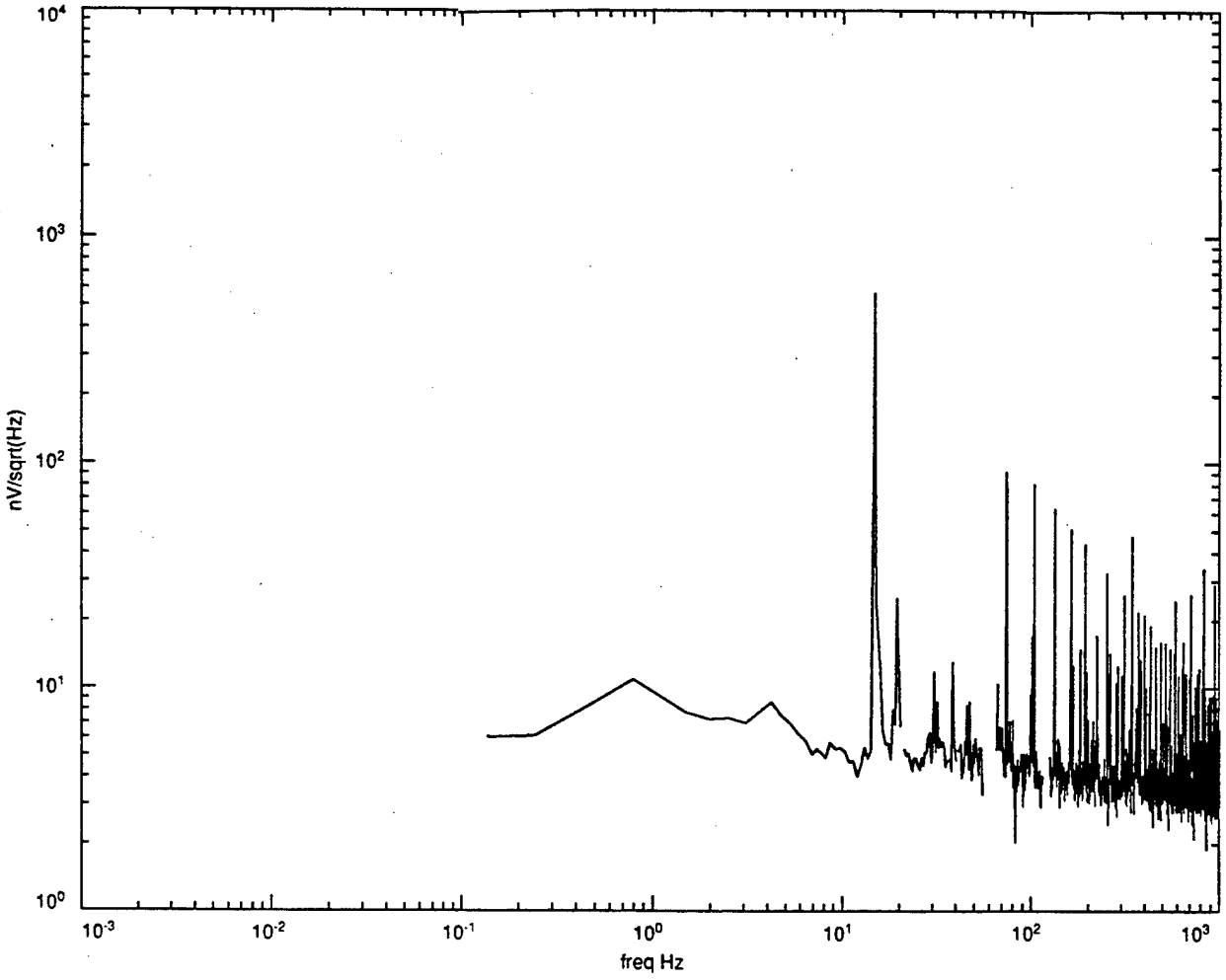

Figure D.16 Spectrum of the response of the SAIC system to a square wave signal in the tank. The fundamental frequency is 14.71 Hz. As expected only the odd harmonics appear. The smooth comb of amplitudes of the harmonics has the correct roll off out to 1 kHz.

REPORT DOCUMENTATION PAGE

Form Approved
OMB No. 0704-01-0188

PLEASE DO NOT RETURN YOUR FORM TO THE ABOVE ADDRESS.

1. REPORT DATE *(DD-MM-YYYY)*	2. REPORT TYPE	3. DATES COVERED *(From - To)*
09–2001	Final	

4. TITLE AND SUBTITLE
ELECTRODE AND ELECTRIC FIELD SENSOR EVALUATION

5a. CONTRACT NUMBER
N66001–92–D004

5b. GRANT NUMBER

5c. PROGRAM ELEMENT NUMBER
0603747N

6. AUTHORS
Applied Physics Laboratory
The University of Washington

5d. PROJECT NUMBER

5e. TASK NUMBER

5f. WORK UNIT NUMBER

7. PERFORMING ORGANIZATION NAME(S) AND ADDRESS(ES)
Applied Research Laboratories
The University of Washington
1013 N.E. 40th Street
Seattle, WA 98105–6698

8. PERFORMING ORGANIZATION REPORT NUMBER
TD 3124

9. SPONSORING/MONITORING AGENCY NAME(S) AND ADDRESS(ES)
SSC San Diego
San Diego, CA 92152–5001

10. SPONSOR/MONITOR'S ACRONYM(S)

11. SPONSOR/MONITOR'S REPORT NUMBER(S)

12. DISTRIBUTION/AVAILABILITY STATEMENT
Approved for public release; distribution is unlimited.

13. SUPPLEMENTARY NOTES

14. ABSTRACT
The measurement of ocean electric fields depends on electrodes to interface electronics to seawater and amplifiers to boost the weak signals to useful levels. This work evaluated the performance of certain commonly used electrodes and amplifiers.

15. SUBJECT TERMS
Mission Area: Surveillance
electric field measurement
sensor evaluation

16. SECURITY CLASSIFICATION OF:			17. LIMITATION OF ABSTRACT	18. NUMBER OF PAGES	19a. NAME OF RESPONSIBLE PERSON
a. REPORT	b. ABSTRACT	c. THIS PAGE			Tom Roy
U	U	U	UU	196	19B. TELEPHONE NUMBER *(Include area code)* (619) 553–3068

INITIAL DISTRIBUTION

D0012	Patent Counsel	(1)
D0271	Archive/Stock	(1)
D0274	Library	(2)
D714	T. Roy	(1)

Defense Technical Information Center
Fort Belvoir, VA 22060–6218